

**Signal Transduction Pathways Involved
In Inhibition Of Axonal Regeneration
After CNS Injury**

**Ezgi Ozturk
B. Biol. Sc. (Hons)**

Australian Regenerative Medicine Institute
Faculty of Medicine, Nursing and Health Sciences
Monash University
Melbourne, Australia

Submitted to Monash University in accordance with the
requirements for the degree of Doctor of Philosophy

August 2013

Chapter 1; page 8; subsection 1.3 Animal models of MS, as 3rd paragraph add: "Rodent models of SCI and EAE are commonly utilised to investigate signalling pathways of axonal degeneration and regeneration. However, the induction of these diseases is very different. Typically, SCI results from mechanical shearing of a specific region of the spinal cord, while MOG-EAE provokes a Th1/Th17-mediated autoimmune response in the CNS as a whole. Therefore the primary pathways, which instigate and promote neurodegeneration in these models are distinct. In SCI, a primary focus for clinical recovery is to prevent the processes of oligodendrocyte death and secondary demyelination that results from continuous inflammatory activity at the primary injury site and allow for regeneration to ensue. In the EAE model there are two major arms of investigation: dampening the autoimmune response and inhibiting neurodegeneration. A common factor in these models is the presence of myelin debris potentiating a non-permissive environment for recovery. Thus blocking specific signalling pathways, particularly those that mediate axon retraction and promote disassembly of the tubulin network, like that of ROCKII-dependent CRMP-2 phosphorylation, may promote regrowth of damaged axons in the CNS. Animal models of disease are extremely valuable as they can mimic many aspects of MS and SCI. However, no model can reproduce all the aspects of disease, resulting in studying a specific pathway in isolation. Animal models therefore lack the capacity to examine the interplay between these major signalling pathways and their effects on axonal regeneration collectively. This is a major confounder in the ability to translate successful rodent-based therapies to human patients. Indeed, there are currently no therapeutic treatments available for SCI patients, and there are only few approved drug treatments for MS sufferers."

Chapter 2; page 43; subsection 2.17 Immunofluorescence, last sentence, add: "All immunofluorescence (IF) -studies conducted in this thesis were only undertaken to detect the presence or absence in colocalisation of key molecules in the CNS. To that effect, representative sections were imaged at random and only high power images were taken at or near lesion sites."

Chapter 2; page 43 under subsection 2.19 Statistics, Paragraph 1, 2nd sentence, add: "This statistical package was used as it factors in group interactions and can compare the significance of the means between the 4 groups that are classified by treatment."

Chapter 2; page 43 under subsection 2.19 Statistics, Paragraph 1, 4th sentence, add: "This test was chosen as each subjects was scored once per day over 14 days. Only the LIF-treated group was compared with the MSA treated group. The sham groups were not assessed."

Chapter 2; page 43 under subsection 2.19 Statistics, Paragraph 2, 2nd sentence, add: "Comparisons were made between treatment groups and between time points."

Chapter 2; page 43 under subsection 2.19 Statistics, Paragraph 3, 4th sentence, add: "The Wilcoxon-Mann-Whitney comparison test is used as it is a non-parametric test which does not assume equal distribution between groups. Multiple comparisons were not conducted for this experiment."

Chapter 3; page 51; Figure 2.; Figure legend, add "E) Densitometric analysis of (A). A significant increase in GAP43 is observed in the SCI LIF treatment group ($^{\#}P<0.01$) compared to MSA treated groups. LIF treatment results in a significant decrease in the inhibitory GTP-RhoA at the second week time point compared to MSA treatment groups ($^{\#}P<0.01$); while total RhoA expression is not altered. The growth promoting GTP-Rac1 is significantly increased in the SCI

LIF 1 wk group, and total Rac1 remained unchanged ($n=3$ $^{\#}P<0.01$, $^{\&}P<0.001$ compared to SCI LIF 1wk group; $^{\%}P<0.01$, $^{\$}P<0.001$ compared to SCI LIF 2wk group; One-way ANOVA). F) Densitometric analysis of (B). There is a significant reduction in phospho-CRMP2 expression in the LIF treatment group 1 week post-SCI ($*P<0.05$) ($n=3$, one-way ANOVA)."

Chapter 3; pg 54; Figure 3.; Figure legend, last sentence, add: "($n=3$ per group; $*P<0.05$ 8-14 days Post-SCI)."

Chapter 4; page 65; Figure 1; Figure legend, A) last sentence add: "***** $P<0.0001$ 15-30dpi."

Chapter 4; page 77; Figure 6.; Figure legend, last sentence add: "**** $P<0.001$ between EAE and NogoA antibody treated groups at day 30; ** $P<0.01$ between IgG and NogoA antibody treated groups at day 30."

Chapter 5; page 90; Figure 2.; Figure legend, add: " B) Densitometric analysis of (A). PHF-tau (AT8) is significantly reduced in *ngR1*^{-/-} group at onset and chronic stages of EAE compared to their *ngR1*^{+/+} controls. Tau-5 expression is unchanged between groups. pSer199/202 tau is significantly decreased in *ngR1*^{-/-} group at onset of EAE when compared to their *ngR1*^{+/+} at onset of disease ($n=3$ per genotype, One-way ANOVA)."

Chapter 5; page 93; Figure 4.; Figure legend, 2nd sentence, add: "A reduction in PCRMP-2 expression is observed in *ngR1*^{-/-} mice at all time points compared to their respective *ngR1*^{+/+} controls."

Chapter 5; page 93; Figure 4.; Figure legend, 4th sentence, add: "($n=3$ per genotype per time point)."

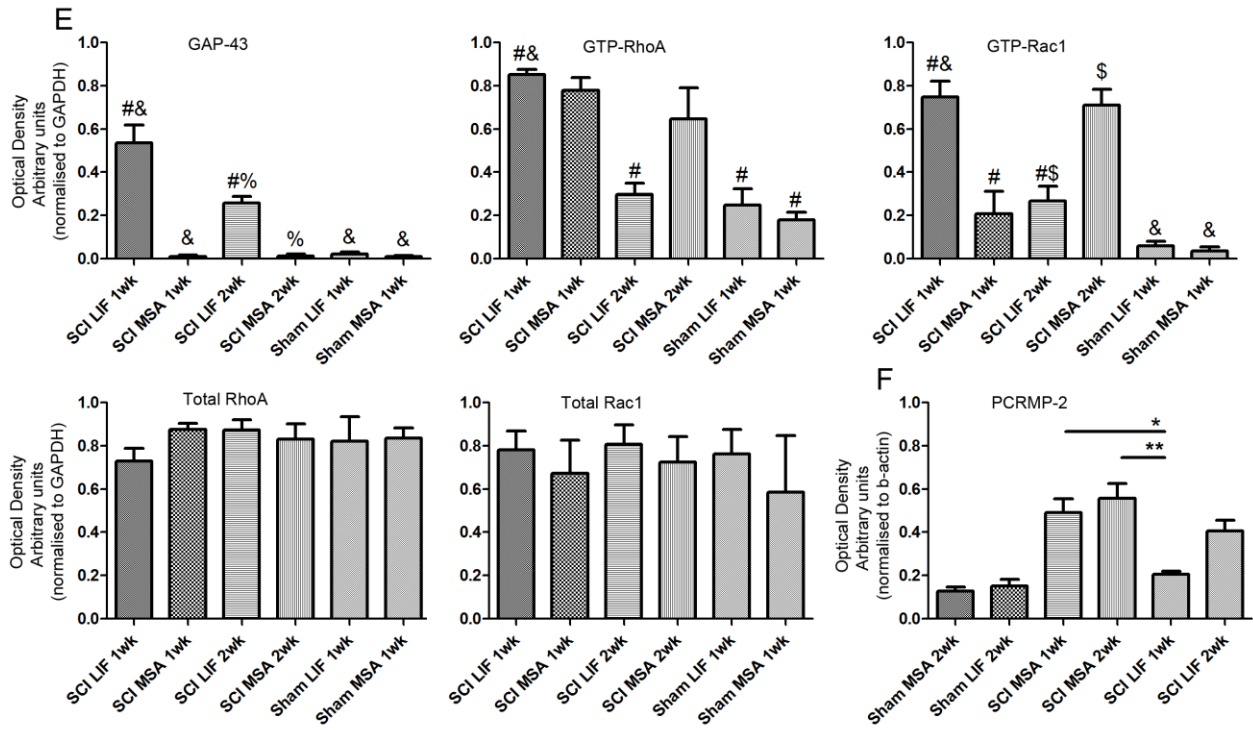
Chapter 5; page 105; Figure 8; Figure legend, last paragraph, add: "No statistically significant results were found in splenocyte response to MOG₃₅₋₅₅ in *ngR1*^{-/-} mice when compared to the respective *ngR1*^{+/+} controls."

Chapter 5; page 105; Figure 8.; Figure legend, B); last paragraph; add: "No statistically significant results were found in the cytokine profiles of *ngR1*^{-/-} mice when compared to the respective *ngR1*^{+/+} controls."

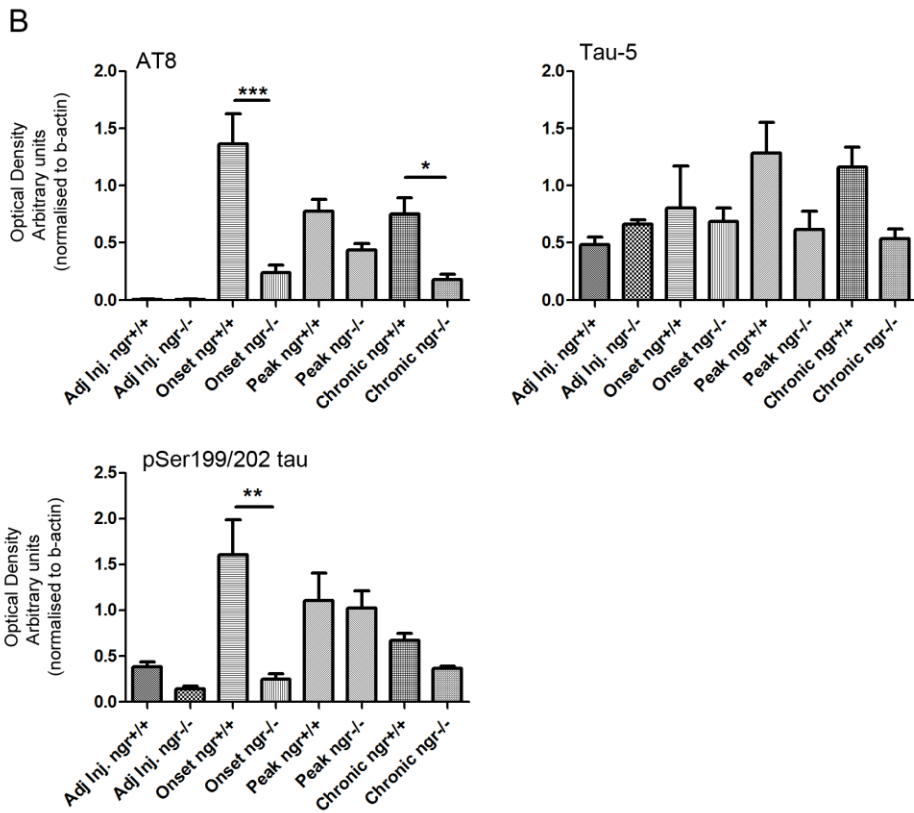
Chapter 5; page 108; Figure 10.; Figure legend, A), last paragraph add "**** $P<0.05$. Two-way ANOVA at days 14-18 post-induction."

Chapter 6; page 120; 2nd paragraph, add: "While this thesis encompasses novel findings and contributes to the pool of knowledge that is currently available today, it's relevance to the human conditions must be further validated. It would be interesting to conduct similar experiments of immunofluorescence co-localisation and western blot techniques using human post-mortem tissue. A comparative analysis of NgR1 signalling and its levels of activation within the 4 major MS subtypes would yield valuable information. Validating the localisation of PCRMP-2 in degenerating axons of MS tissue would be of particular interest."

Chapter 3; page 52; Figure 2. add to figure:

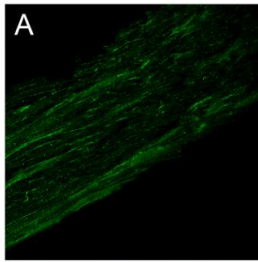


Chapter 5; page 90; Figure 2. add to figure:

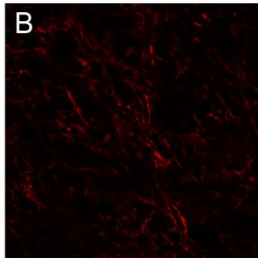


add:

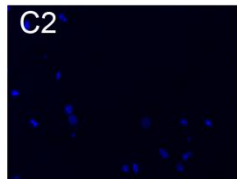
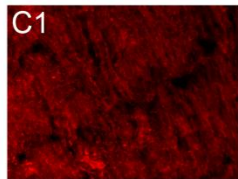
Appendix VII: Immunofluorescence staining - Negative controls.



A) Nogo-A negative control for Chapter 3 Figure 1B.
Secondary only (goat anti-rabbit Alexa Flour 488)

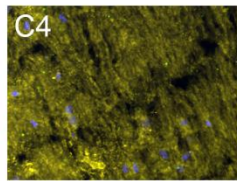
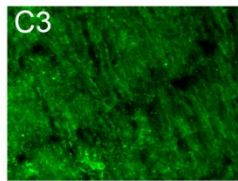


B) CRMP-2 negative control for Chapter 3 Figure 2CD.
Secondary only (goat anti-rabbit Alexa Flour 519)



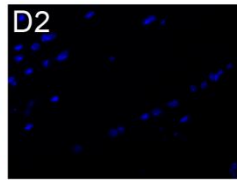
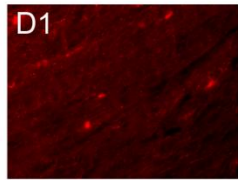
C1) CRMP-2 negative control for Chapter 4 Figure 5A.
Secondary only (goat anti-rabbit Alexa Flour 555)

C2) DAPI staining of same section Chapter 4 Figure 5A



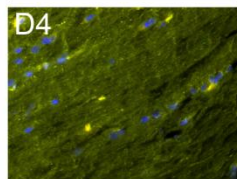
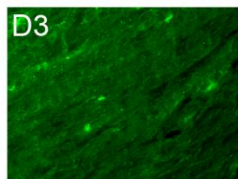
C3) BIII-tubulin negative control for Chapter 4 Figure 5A.
Secondary only (goat anti-mouse Alexa Flour 488)

C4) Merged image for Chapter 4 Figure 5A



D1) CRMP-2 negative control for Chapter 4 Figure 5B.
Secondary only (goat anti-rabbit Alexa Flour 555)

D2) DAPI staining of same section Chapter 4 Figure 5B



D3) SMI-31 negative control for Chapter 4 Figure 5B.
Secondary only (goat anti-mouse Alexa Flour 488)

D4) Merged image for Chapter 4 Figure 5B

This thesis is dedicated to my parents

Notice 1

Under the Copyright Act 1968, this thesis must be used only under the normal conditions of scholarly fair dealing. In particular no results or conclusions should be extracted from it, nor should it be copied or closely paraphrased in whole or in part without the written consent of the author. Proper written acknowledgement should be made for any assistance obtained from this thesis.

Notice 2

I certify that I have made all reasonable efforts to secure copyright permissions for third-party content included in this thesis and have not knowingly added copyright content to my work without the owner's permission.

TABLE OF CONTENTS

THESIS SUMMARY	i
GENERAL DECLARATION	iii
CONTRIBUTING AUTHOR CHAPTER DECLARATIONS	iv
RESEARCH DISSEMINATION	vii
ACKNOWLEDGEMENTS	x
ABBREVIATIONS	xi
CHAPTER 1: Literature review	1
1.1 Multiple sclerosis	2
1.1.1 Epidemiology of MS	2
1.1.2 Types of MS	3
1.2 Proposed mechanisms contributing to the manifestation of MS	3
1.2.1 The inflammatory response	3
1.2.2 Demyelination	5
1.3 Animal models of MS	6
1.4 Pathological features of MS lesions	8
1.5 Axonal injury and its implications in MS	8
1.6 MAIFs and their role in the CNS	9
1.6.1 OMgp	9
1.6.2 MAG	10
1.6.3 Nogo-A	11
1.7 The Nogo receptor complex	13
1.7.1 NgR1	13
1.7.2 LINGO-1	14
1.7.3 P75NTR	14
1.7.4 TROY/Taj	16
1.7.5 Rho-A	16
1.8 Targeting components of the NgR1 signalling to promote axonal regeneration .	17
1.8.1 Nogo-A	17
1.8.2 NgR1	18
1.8.3 LINGO-1	19
1.9 Modulation of cytoskeletal dynamics	20
1.10 Rho-A activation and neurodegeneration following NgR1 signalling	22
1.10.1 Rho-A/NgR1 interactions	22
1.10.2 Targeting Rho-A and its downstream mediators	23

1.11	Collapsin response mediator protein-2 (CRMP-2)	26
1.12	Conclusion and project aims	34

CHAPTER 2: Materials and methods 35

2.1	Animals	36
2.2	Spinal cord injury surgery and treatment	36
2.3	BMS behavioural analysis	36
2.4	EAE induction and clinical parameters	36
2.5	Histopathology: inflammation, demyelination and axonal degeneration/loss	37
2.6	Splenocyte proliferation assay and cytokine analysis	38
2.7	Isolation of mononuclear cells	38
2.8	Flow cytometric analysis	39
2.9	Antibodies and reagents	39
2.10	Production of anti-pThr555CRMP-2 polyclonal antibody	40
2.11	Rho/Rac activation assay	40
2.12	Preparation of tissue lysates for western blotting	40
2.13	Amyloid- β treatment human SY-SY5Y neuroblastoma cell culture, Tg2576 transgenic animals and Alzheimer's disease brain tissue	41
2.14	Sarcosyl gradient centrifugation	41
2.15	Western immunoblotting	41
2.16	Immunoprecipitation	42
2.17	Immunofluorescence	42
2.18	Therapeutic anti-Nogo(623-640) antibody treatment of EAE-induced mice	43
2.19	Statistics	43

CHAPTER 3: LIF-treatment reduces Nogo-A deposits in spinal cord injury modulating Rho-GTPase activity and CRMP-2 phosphorylation 44

3.1	Abstract	45
3.2	Introduction	46
3.3	Results	48
3.3.1	LIF-treatment reduces Nogo-A deposits in SCI	48
3.3.2	Exogenous LIF supports molecular signalling events promoting axonal regrowth	48
3.3.3	Systemically administered LIF promotes locomotor recovery following SCI in mice	53
3.4	Discussion	55

CHAPTER 4: ROCKII-dependent CRMP-2 phosphorylation is associated with EAE disease progression and chronic-progressive MS lesions.....	59
4.1 Abstract.....	60
4.2 Introduction	61
4.3 Results	63
4.3.1 Clinical and histological development of MOG-EAE	63
4.3.2 Expression profile of Nogo-A and CRMP-2 are altered in EAE.....	64
4.3.3 Generation of ROCKII specific P-CRMP-2 antibody	67
4.3.4 Disease severity correlates with increase in ROCKII phosphorylated CRMP-2	69
4.3.5 CRMP-2 is only phosphorylated in degenerating axons	72
4.3.6 Therapeutic administration of anti-Nogo-A antibodies prevents clinical progression, axonal degeneration and ROCKII-dependent CRMP-2 phosphorylation in EAE	75
4.4 Discussion.....	80
CHAPTER 5: Limiting axonopathy in EAE by blocking nogo receptor and CRMP-2 phosphorylation.....	84
5.1 Abstract.....	85
5.2 Introduction	86
5.3 Results	88
5.3.1 Deletion of the ngr1 allele (exon 2) limits the progression of EAE, axonal degeneration and phosphorylation of CRMP-2.....	88
5.3.2 Axonal damage and CRMP-2 phosphorylation in the optic nerve of EAE-induced mice	97
5.3.3 Immune activation following EAE-induction is unaltered in <i>ngr1</i> ^{-/-} mice.....	104
5.3.4 Phenotype of immune cells of naive and EAE-induced <i>ngr1</i> ^{-/-} mice....	106
5.4 Discussion.....	109
CHAPTER 6: GENERAL DISCUSSION	112
BIBLIOGRAPHY	121
APPENDICES.....	149
Appendix I	<i>Limiting multiple sclerosis related axonopathy by blocking Nogo receptor and CRMP-2 phosphorylation</i>
Appendix II	<i>Novel therapeutic targets for axonal degeneration in multiple sclerosis</i>

Appendix III *LIF-treatment reduces Nogo-A deposits in spinal cord injury modulating Rho GTPase activity and CRMP-2 phosphorylation*

Appendix IV *Nogo-Receptor 1 Deficiency has no Influence on Immune Cell repertoire or Function during Autoimmune Mediated Demyelination*

Appendix V *Mesenchymal stem cells for treatment of CNS injury*

Appendix VI *Leukemia inhibitory factor arrests oligodendrocyte death and demyelination in spinal cord injury*

ERRATUM.....

THESIS SUMMARY

SCI and MS are devastating conditions of the CNS that propagate neurological dysfunction with poor long term prognoses. In the past few decades, much effort has gone in to understanding mechanisms of neuroinflammation, demyelination and neurodegeneration that combined, drive the neurological deterioration observed in patients. However, currently available treatments are only effective in a small percentage of sufferers. Therefore there is an urgent need for the discovery of new and more effective therapies to dramatically improve patients quality of life. In recent years, a body of research has shifted towards discovering therapies that modulate mechanisms of neurodegeneration rather than immunomodulation. It is now evident that recurring axonal injury and eventual failure in regenerative compensatory mechanisms in the CNS are the major causes of irreversible neurological deficit observed in SCI and MS. The role of MAIFs and their potent capacity to drive neurodegeneration in damaged axons has been convincingly presented in the literature. Nogo-A, which signals through the NgR1 complex on axons, has been deemed the most potent inhibitor of regeneration.

The overall aim of this thesis was to investigate Nogo-A/NgR1 signalling and their downstream mediators in the context of neurodegeneration in SCI and in the animal model for MS, EAE. Furthermore, we explored the potential of therapeutic agents in reversing the affects of Nogo-A/NgR1 signalling in an attempt to hinder neurodegeneration in these models. The first part of this thesis assessed the deposition of Nogo-A and the ROCKII-dependent phosphorylation of its downstream mediator CRMP-2 in a mouse model of SCI with and without the therapeutic intervention of daily LIF administration following injury. LIF administration resulted in substantial improvements in functional locomotor recovery in treated animals. At the molecular level LIF treatment reduced Nogo-A deposition at the lesion site. Similarly, RhoA-GTP and PCRMP-2 molecules which negatively regulate the cytoskeleton showed diminished activity. In contrast, factors indicative of growth and regeneration such as Rac-1 and GAP-43 were elevated in animals receiving LIF. Therefore factors like LIF that limit Nogo-A deposition in the injured CNS could have therapeutic potential in SCI.

The second part of this thesis, a time-course evaluation of neurodegeneration in the MOG-induced EAE model was carried out, with a particular focus on the modulation of CRMP-2 in disease progression. CRMP-2 expression reached maximum levels at peak stage of EAE, however, its expression was evident as early as pre-onset stage of

disease. In addition, levels of PCRMP-2 was associated with and only activated in neurodegenerative axons. Furthermore, molecular transport of tubulin heterodimers by CRMP-2 to promote microtubule assembly was impeded. Moreover, therapeutic administration of the function blocking Nogo-A antibody in EAE animals reduced clinical severity and in parallel decreased PCRMP-2 expression. These data indicated that Nogo-A signalling could mediate axonal degeneration through post-translational modification of CRMP-2 by negatively regulating microtubule assembly.

Therefore, in the third part of this thesis, a direct relationship between NgR1 signalling and CRMP-2 phosphorylation and their role in mediating axonal degeneration in the progression of EAE was investigated. The clinical severity was significantly reduced in *ngr1^{-/-}* mice with EAE. Correspondingly, ROCKII-dependent CRMP-2 phosphorylation was also diminished at all time points. Furthermore CRMP-2 association with tubulin heterodimers was restored, allowing for positive microtubule assembly and therefore regeneration. Moreover, the immune capacity of naive and EAE-induced *ngr^{-/-}* mice remained unchanged, signifying that the observed alleviation in disease severity is due to alterations in mechanisms related to axonal injury and not mechanisms of immunomodulation.

Collectively, research conducted in this thesis describe a common mechanism of neurodegeneration that can be activated in both SCI and EAE. It was demonstrated that growth inhibition can be initiated by MAIFs such as Nogo-A through the NgR1 complex in axons. A direct consequence of this is the ROCKII-dependent phosphorylation of CRMP-2 which impedes CRMP-2 transport of tubulin, negatively regulating microtubule assembly. Of particular relevance is the capacity of the CNS to regenerate when this mechanism is hindered by way of therapeutic intervention. Therefore, it can be concluded that targeting the components of MAIF/NgR1 signalling following CNS injury may provide novel therapeutic avenues by which neurological decline observed in patients can be diminished.

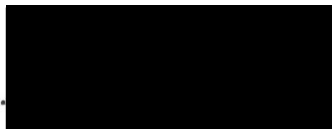
GENERAL DECLARATION

In accordance with Monash University Doctorate Regulation 17.2 Doctor of Philosophy and Research Master's regulations the following declarations are made:

I hereby declare that this thesis contains no material which has been accepted for the award of any other degree or diploma at any university or equivalent institution and that, to the best of my knowledge and belief, this thesis contains no material previously published or written by another person, except where due reference is made in the text of the thesis.

This thesis includes 3 original papers published in peer reviewed journals and 1 unpublished publications. The core theme of the thesis is the role of Nogo receptor signalling in promoting axonal degeneration following injury in the central nervous system. The ideas, development and writing up of all the papers in the thesis were the principal responsibility of myself, the candidate, working within the Australian Regenerative Medicine Institute under the supervision of Professor Claude Bernard. I have renumbered sections of submitted or published papers in order to generate a consistent presentation within the thesis. The inclusion of co-authors reflects the fact that the work came from active collaboration between researchers and acknowledges input into team-based research. A description of the nature of co-author contributions is provided in the declarations on the following pages. As per Monash University requirements for submission, percentage contribution is only provided for student co-authors.

Signed:



Date:

10.8.13

Ezgi Ozturk

Declaration for Thesis Chapter 3

Declaration by candidate

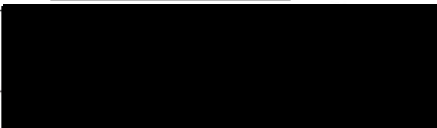
In the case of Chapter 3, the nature and extent of my contribution to the work was the following:

Nature of contribution	Extent of contribution (%)
Responsible for part of the design of the experiments and performed the experimental work with the exception of spinal cord injury in mice. This included processing of tissue, immunofluorescence and immunoblot experiments, analysis and interpretation of the data, and preparation of figures for the manuscript. I am a first co-author in this manuscript and was involved in the drafting, revising and editing of this manuscript. For this chapter, I have added additional work which was not part of the published manuscript.	70%

The following co-authors contributed to the work. If co-authors are students at Monash University, the extent of their contribution in percentage terms must be stated:

Name	Nature of contribution	Extent of contribution (%) for student co-authors only
Michael F Azari	Spinal cord injury and drafting of parts of the manuscript	
Christos Profyris	Initial spinal cord injury	
Shunhe Wang	Help with immunofluorescence	
David H Small	Intellectual input	
Claude CA Bernard	Intellectual input, revised manuscript	
Steven Petratos	Experimental design, Intellectual input, revised manuscript	

The undersigned hereby certify that the above declaration correctly reflects the nature and extent of the candidate's and co-authors' contributions to this work*.

Candidate's Signature		Date 10.8.13
Main Supervisor's Signature		Date 11/07/2013

*Note: Where the responsible author is not the candidate's main supervisor, the main supervisor should consult with the responsible author to agree on the respective contributions of the authors.

Declaration for Thesis Chapter 4

Declaration by candidate

In the case of Chapter 4, the nature and extent of my contribution to the work was the following:

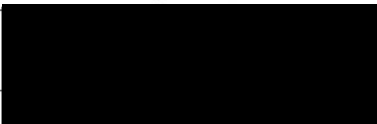
Nature of contribution	Extent of contribution (%)
Research of literature, experimental design, conducting of experiments, drafting of manuscript and preparation of all figures. This included induction of EAE in mice, Nogo-A peptide treatment, clinical scoring of disease progression in mice, collecting and processing of tissue, histological stains and analysis, immunofluorescence, immune blot and coimmunoprecipitation assays and quantification and analysis and interpretation of data generated and preparation of all figures. I am a first co-author in this manuscript and was involved in the drafting, revising and editing of this manuscript. This chapter includes published and unpublished data.	95%

The following co-authors contributed to the work. If co-authors are students at Monash University, the extent of their contribution in percentage terms must be stated:

Name	Nature of contribution	Extent of contribution (%) for student co-authors only
Michael F Azari	Participated in the induction of EAE and PCRMP-2 antibody characterisation experiments	
Claude CA Bernard	Intellectual input, experimental design and revision of manuscript	
Steven Petratos	Intellectual input, experimental design, histopathological scoring, drafting and revision of manuscript	

The undersigned hereby certify that the above declaration correctly reflects the nature and extent of the candidate's and co-authors' contributions to this work*.

Candidate's Signature  **Date** 10.8.13

Main Supervisor's Signature  **Date** 11/07/2013

*Note: Where the responsible author is not the candidate's main supervisor, the main supervisor should consult with the responsible author to agree on the respective contributions of the authors.

Declaration for Thesis Chapter 5

Declaration by candidate

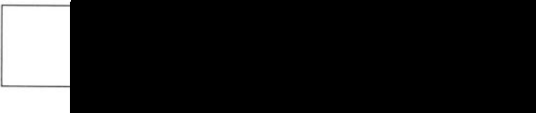
In the case of Chapter 5, the nature and extent of my contribution to the work was the following:

Nature of contribution	Extent of contribution (%)
Research of literature, experimental design, conducting of experiments, drafting of manuscript and preparation of all figures. This included induction of EAE in mice, clinical scoring of disease progression in mice, collecting and processing of tissue, histological stains and analysis, immunofluorescence, immune blot and co-immunoprecipitation assays, splenocyte proliferation, cytokine profiles and FACS experiments, processing mouse optic nerve tissue for electron microscopy and quantification and analysis and interpretation of data generated and preparation of all figures. I was also responsible for breeding, maintaining and genotyping of the NgR1 knock-out mouse colony. I am a first co-author in this manuscript and was involved in the drafting, revising and editing of this manuscript. This chapter includes published and unpublished data.	95%

The following co-authors contributed to the work. If co-authors are students at Monash University, the extent of their contribution in percentage terms must be stated:

Name	Nature of contribution	Extent of contribution (%) for student co-authors only
Michael F Azari	Participated in induction of EAE, imaging optic nerves	
Sara Litwak	Participated in induction of EAE, genotyping of NgR1 mice and immunophenotypic analysis	
Steven Petratos	Intellectual input, experimental design, histopathological scoring, drafting and revision of manuscript, corresponding author	
Claude CA Bernard	Intellectual input, experimental design and revision of manuscript	

The undersigned hereby certify that the above declaration correctly reflects the nature and extent of the candidate's and co-authors' contributions to this work*.

Candidate's Signature		Date 10.8.13
Main Supervisor's Signature		Date 11/07/2013

*Note: Where the responsible author is not the candidate's main supervisor, the main supervisor should consult with the responsible author to agree on the respective contributions of the authors.

RESEARCH DISSEMINATION

Publications

Petratos S*, **Ozturk E***, Azari MF, Kenny R, Lee JY, Magee KA, Harvey AR, McDonald C, Taghian K, Moussa L, Mun Aui P, Siatskas C, Litwak S, Fehlings MG, Strittmatter SM, Bernard CC. Limiting multiple sclerosis related axonopathy by blocking Nogo receptor and CRMP-2 phosphorylation. *Brain*. 2012;135(Pt 6):1794-818.

*These authors contributed evenly to this work.

Petratos S*, **Ozturk E***, Azari MF*, Papadopoulos R, Bernard CC. Novel therapeutic targets for axonal degeneration in multiple sclerosis. *J Neuropathol Exp Neurol*. 2010;69(4):323-34.

*These authors contributed evenly to this work.

Azari MF*, **Ozturk E***, Profyris C, Wang S, Small DH, Bernard CCA, Petratos S. LIF-treatment reduces Nogo-A deposits in spinal cord injury modulating Rho GTPase activity and CRMP-2 phosphorylation. *J Neurodegen Regen* 2008,1(1):23-29.

*These authors contributed evenly to this work.

Litwak SA, Campanale N, Ozturk E, Payne N, Petratos S, Siatskas C, Bernard C. Nogo-Receptor 1 Deficiency has no Influence on Immune Cell Repertoire or Function during Autoimmune Mediated Demyelination. Draft manuscript submitted to *J Neuropathol Exp Neurol*.

Azari MF, Mathias L, **Ozturk E**, Cram DS, Boyd RL, Petratos S. Mesenchymal stem cells for treatment of CNS injury. *Curr Neuropharmacol*. 2010; 8(4):316-23.

Azari MF, Profyris C, Karnezis T, Bernard CC, Small DH, Cheema SS, **Ozturk E**, Hatzinisiriou I, Petratos S. Leukemia inhibitory factor arrests oligodendrocyte death and demyelination in spinal cord injury. *J Neuropathol Exp Neurol*. 2006; 65(9):914-29.

Conference Podium Presentations

Petratos S*, **Ozturk E**, Azari MF, Kenny R, Strittmatter SM, Fehlings MG and Bernard CCA. Limiting nogo-a receptor 1-dependent Phosphorylation of crmp-2 reduces axonal Degeneration in EAE. Australian Neuroscience Society (ANS) Conference. Gold Coast, Australia, 2012.

*SP delivered this presentation.

Ozturk E, Azari MF, Bernard CCA and Petratos S.* Axonal degeneration in a model of multiple sclerosis is initiated through Nogo-A receptor signalling by phosphorylation of CRMP-2. International Symposium on Protein Phosphorylation in Neurodegenerative Diseases. Valencia, Spain, 2010.

*SP delivered this presentation.

Ozturk E, Azari M, Sun G, Wang S, Emerson-Webber A, Bernard C.C.A. and Petratos S. Nogo-A Modulates Rho-A & CRMP-2 in Experimental Autoimmune Encephalomyelitis. International Brain research Organisation (IBRO): Function of myelinated axons and glial-axonal signalling in the CNS: Basic aspects and clinical implications Satellite Symposium. Melbourne, Australia ,2007

Conference Poster Presentations

Petratos S.*, **Ozturk E**, Azari MF, Kenny R, Lee JY, Magee KA, Harvey AR, Aui PM, Fehlings MG, Strittmatter SM & Bernard CC. Limiting Nogo-A Receptor 1-Dependent Phosphorylation Of Crmp-2 Reduces Axonal Degeneration In EAE. 8th Forum of European Neuroscience (FENS). Barcelona, Spain, 2012.

*SP presented this poster

Ozturk E, Azari MF, Emerson-Webber A, Petratos S and Bernard CCA. Axonal degeneration in a model of multiple sclerosis is initiated through Nogo-A receptor signalling by phosphorylation of CRMP-2. International Symposium on Protein Phosphorylation in Neurodegenerative Diseases. Valencia, Spain, 2010.

Ozturk E, Azari MF, Sun G, Wang S, Emerson-Webber A, Petratos S and Bernard CCA. Inactivation of the Axonal Growth Promoter CRMP-2, in the Spinal Cord of Mice with Autoimmune Mediated Demyelination. Keystone Symposia: Multiple Sclerosis. New Mexico, USA, 2009. *Recipient of 1 of 10 travel grants awarded

Azari MF*, **Ozturk E**, Sun G, Wang S, Emerson-Webber A, Petratos S & Bernard CCA. Inactivation and degradation of the axonal growth promoter, CRMP-2, in the spinal cord in autoimmune demyelination. 6th Forum of European Neuroscience (FENS). Geneva, Switzerland, 2008. *MFA presented this poster

Ozturk E**, Azari MF, Sun G, Wang S, Emerson-Webber A, Petratos S & Bernard CCA*. Inactivation of the neurite growth promoter CRMP-2 in the spinal cord in autoimmune demyelination. The Brain Function and Repair Conference of the Asia Pacific

(BMAP) and Asia Pacific Symposium on Neurodegeneration (APSNR) organisations, Singapore, 2008. *CCAB presented this poster **Recipient of best poster prize

Ozturk E, Azari M, Sun G, Wang S, Emerson-Webber A, Bernard C.C.A. and Petratos S. Nogo-A Modulates RhoA & CRMP-2 in Experimental Autoimmune Encephalomyelitis. International Brain research Organisation (IBRO): Function of myelinated axons and glial-axonal signalling in the CNS: Basic aspects and clinical implications Satellite Symposium. Melbourne, Australia, 2007. *Awarded second prize

Ozturk E, Azari M, Sun G, Wang S, Emerson-Webber A, Bernard C.C.A. and Petratos S. Nogo-A Modulates RhoA & CRMP-2 in Experimental Autoimmune Encephalomyelitis. 7th IBRO World Congress of Neuroscience. Melbourne, Australia, 2007.

ACKNOWLEDGEMENTS

Firstly, I would like to thank my supervisor, Professor Claude Bernard. Your guidance and encouragement over the years has been invaluable to me. I very much appreciate all that you have done for me. I would like to thank all members of the Bernard lab, as one time or another we have leaned and depended on each other. A special thank you to Steven Petratos and Michael Azari, you were there for me every step of the way. I consider you to be not just my colleagues, but my friends. Thank you to Ashley Emerson-Webber and Dr Leon Moussa, you made the days interesting, filled with funny and exciting conversations. I would like to thank Courtney, Guizhi, Sara and Naomi for your help and friendship.

I would like to especially thank Dr Natalie Payne and Dr Sally Caine, you two were and still are my rocks. Nat, we met on our first day at La Trobe and Sally we met on our first year of PhDs here at Monash. I would like to thank you both for keeping me grounded and sane and for making this experience fun and enjoyable.

I would like to thank my parents who pushed me to achieve my goals. Without you, I would not be where I am today. I would also like to thank the rest of my family and friends for putting up with me through thick and thin. Last, I would like to thank my partner Marc. Your thoughtfulness, encouragement and continuous support made it possible for me to complete my PhD journey.

ABBREVIATIONS

A β	β -amyloid protein
AA	Amino acid
AD	Alzheimer's disease
AKD	Amino terminal kinase domain
APC	Antigen presenting cell
ATP	Adenosine triphosphate
BBB	Blood brain barrier
BMS	Basso Mouse Scale
CNP	Cyclic nucleotide phosphohydrolase
CNS	Central nervous system
CRMP	Collapsin response mediator protein
CST	Corticospinal tract
DRG	Dorsal root ganglion
dpi	Days post induction
EAE	Experimental autoimmune encephalomyelitis
EM	Electron microscopy
F-actin	Filamentous actin
GAP	GTPase-Activating Proteins
GDI	Guanine dissociation inhibitor
GDP	Guanosine diphosphate
GFP	Green fluorescent protein
GM-CSF	Granulocyte macrophage - colony stimulating factor
GPI	Glycosylphosphatidylinositol
GTP	Guanosine triphosphate
GTPase	Guanosine triphosphatase
H&E	Hemotoxylin and eosin
HD	Huntington's disease
HLA	Human leukocyte antigen
ICAM	Intercellular adhesion molecule
IFN	Interferon
Ig	Immunoglobulin
IL	Interleukin
IP	Intraperitoneal
IV	Intravenous
JAK/STAT	Janus Kinase/Signal transducer and activator of transcription
KO	Knock out

LINGO	Leucine-rich repeat Ig domain-containing NgR interacting protein
LFA	Lymphocyte function-associated antigen
LFB	Luxol fast blue
LIF	Leukemia inhibitory factor
LRR	Leucine-rich repeat
LRRCT	Cysteine-rich LRR
LPA	Lysophosphatidic acid
LV	Lentivirus
MAIF	Myelin associated inhibitory factor
MAG	Myelin-associated glycoprotein
MBP	Myelin basic protein
MHC	Major histocompatibility complex
MHV	Murine hepatitis virus
MLC	Myosin light chain
MOG	Myelin oligodendrocyte glycoprotein
mRNA	Messenger ribonucleic acid
MS	Multiple sclerosis
MSA	Mouse serum albumin
NGF	Nerve growth factor
NMW	Normal white matter
NgR	Nogo receptor
NS	Not significant
NTF	Neurotrophin factor
P75NTR	Low-affinity neurotrophin receptor
PAS	Periodic acid Schiff
Ph	Pleckstrin homology domain
PKA	Protein kinase A
PKC	Protein kinase C
PLP	Proteolipid protein
pNF-H	Phospho-neurafilament heavy
PP-MS	Primary-progressive MS
PR-MS	Primary relapsing MS
RB	Rho-binding domain
RGC	Retinal ganglion cell
RHD	Reticulon-homology domain
RNAi	RNA interference
ROCKII	Rho-associated, coiled-coil containing protein kinase 2

RR-MS	Relapsing-remitting MS
RST	Rubrospinal tract
SAH	Aneurysmal subarachnoid hemorrhage
SCI	Spinal cord injury
siRNA	Short interference RNA
SP-MS	Secondary-progressive MS
TAJ/TROY	TNF-Receptor Super family member 19
TCR	T cell receptor
TMEV	Theiler's murine encephalomyelitis virus
TNF	Tumour necrosis factor
VCAM	Vascular-cell adhesion molecule
VLA	Very late antigen
WT	Wild type

Chapter 1

LITERATURE REVIEW

1.1 Multiple sclerosis

Multiple Sclerosis (MS) is a chronic and disabling disease of the central nervous system (CNS) that results in irreversible neurological damage in the brain and spinal cord. The heterogeneity of the disease is marked by a multiple array of symptoms observed in patients including cognitive impairment, dysarthria, dysphagia, vertigo, sensory loss, ataxic tremors and spasticity (1).

1.1.1 Epidemiology of MS

Worldwide, approximately 2.5 million individuals suffer from MS, with the clinical onset of disease generally occurring between the ages of 20 and 50 years. Women are almost 3 times more likely to develop MS than men (2). It is generally believed that both genetic and environmental factors contribute to the prevalence of MS. The "latitude" effect of MS is well documented, showing that regions further away from the equator have higher incidence of this condition. While there are exceptions (Sardinia, South Europe), North America and North Europe are deemed to be high risk areas, southern regions of America and Europe are medium risk areas. South America, Asia and Africa are considered low risk regions for developing MS (3, 4). Vitamin D and exposure to sunlight and its role in MS has been studied extensively (5, 6). In other studies, a "continental" effect has been reported, with a higher incidence in Western Europe and North America compared to the Middle East, Asia, South America and Africa (7, 8).

Genetic analysis suggests that first degree relatives are more likely to be diagnosed with MS compared to the general population (9). Monozygotic twins show a concordance rate of 38%, while dizygotic twins have a less than 4% concordance (9). Investigation into genetic factors such as human leukocyte antigen (HLA)-polymorphisms indicate that some HLA haplotypes increase the risk of MS while others reduce the risk (10-13). In contrast, sharing the same or comparable environment does not increase the risk for MS in individuals without genetic links. These findings suggest that the onset of MS is multi-factorial and possibly triggered by the interaction between genes and the environment. It is widely speculated that MS is induced by a virus or another infectious agent (3, 5, 14), which then initiates a cascade of autoimmune responses. Despite the consensus however, scientist so far failed to find the mechanism behind this interplay.

1.1.2 Types of MS

No two patients with MS present with identical symptoms or disease progression, however generally speaking, prognosis of the disorder can be divided into four distinct groups [Fig. 1; (1, 15)].

1. Relapsing-Remitting MS (RR-MS) - RR-MS is present in more than 85% of patients initially diagnosed with MS. These patients exhibit oscillations between partial or full recovery of symptoms (remitting) and acute exacerbations (relapse) without progression of disability between relapses.

2. Secondary-Progressive MS (SP-MS) - 80% of patients with RR-MS progress into this stage, marked by progression of disability between episodes.

3. Primary-Progressive MS (PP-MS) - PP-MS is present in 10% of patients that show signs of severe progression of disability from onset of disease, separated by periods of dormancy with negligible improvements.

4. Primary-Relapsing MS (PR-MS) - PR-MS is present in less than 5% of patients that exhibit signs of severe progression of disability from onset of disease, with noticeable periods of neurological attacks with little to no improvements.

1.2 Proposed mechanisms contributing to the manifestation of MS

The major pathological hallmarks of MS in the CNS are inflammation, demyelination and axonal damage. The disease can be divided into two major components: the autoimmune component in which it is believed immune cell infiltration initiates inflammation; and the neurodegenerative component in which axonal damage eliciting progressive neurological deficit in MS patients. MS lesions in the CNS contain T lymphocytes, B lymphocytes and activated macrophages/microglia, which combined orchestrate the destruction of the myelin sheathing that insulate axons and cause subsequent axonal damage.

1.2.1 The inflammatory response

The CNS has long been considered to be an immunologically privileged site (16), with the endothelial blood-brain barrier (BBB) restricting the trafficking of naive T cells into the CNS parenchyma (17). However, activated T cells have been shown to traverse the BBB and gain access to the CNS; and is not dependent on antigen specificity (18). While the exact order of events involved in the pathology of MS is still unknown, the

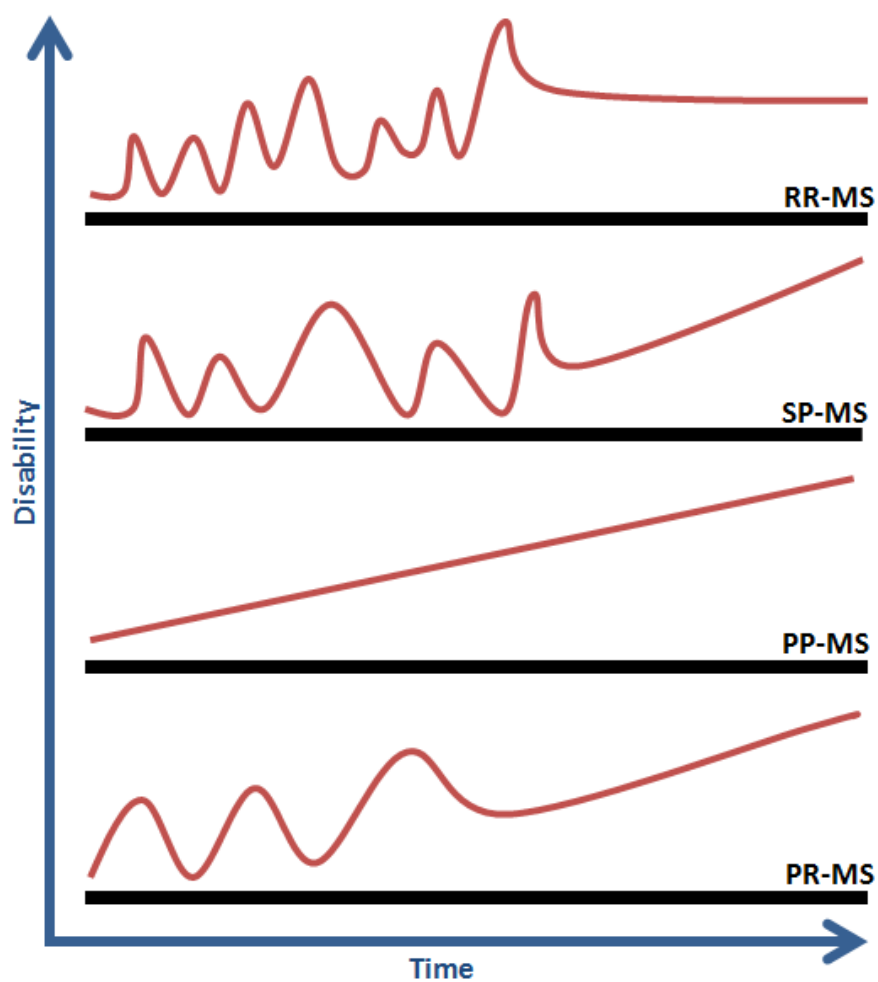


Figure 1. Most common forms of Multiple Sclerosis. Schematic diagram showing variation of clinical disability in the course of MS, divided into four main categories. RR: relapsing remitting; SP: secondary progressive; PP: primary progressive; PR: primary relapsing. Adapted from Lassmann, H. and J. van Horssen (2011) *FEBS Lett* **585**(23): 3715-3723.

initial stages of disease are thought to begin in the periphery, where naive T cells are activated against myelin and/or other CNS antigens. These autoreactive T cells then disrupt and transmigrate through the BBB via interactions between integrins expressed on the T cell surface (VCAM and ICAM) and endothelial cell adhesion molecules of the BBB (VLA-4 and LFA-1, respectively) (19).

In order to initiate an inflammatory cascade in the CNS, T cells need to be activated by a reactive stimulating antigen, most likely a component of myelin, but this could also include other molecules such as $\alpha\beta$ -crystallin, antigen presenting cells (APCs), perivascular monocytes, macrophages and microglia (20-23). Autoreactive T cells become reactivated in the CNS when a myelin epitope is presented to them by resident APCs. Disruption of the BBB and the influx of further autoreactive T cells among other blood cells cause changes in the local environment resulting in further upregulation of endothelial adhesion molecules and initiating additional T cell infiltrations into the CNS. APCs form a trimolecular complex of a T cell receptor (TCR), the antigen and either a class I or class II major-histocompatibility-complex (MHC) molecule (24, 25). MHC class I APCs activate Cytotoxic CD8⁺ T cells, while MHC class II APCs activate CD4⁺ T helper (Th) cells (26-28). There are two subsets of CD4⁺ Th cells; Th1 lymphocytes secrete proinflammatory cytokines such as interferon- γ (IFN- γ), tumour necrosis factor α (TNF- α) and interleukin 2 (IL-2), while Th2 lymphocytes secrete anti-inflammatory cytokines such as IL-4, IL-5, IL-6, IL-10, and IL-13 (24). Reactivated T cells produce proinflammatory cytokines that amplify the immune response by influencing the increase of MHC class II expression by APCs in the CNS. These events form a cycle in which reactivation of T helper cells escalates further expansion and influx of reactive T cells, B cells and macrophages in the CNS (25, 29).

1.2.2 Demyelination

It is believed that the inflammatory immune response initiated by myelin or CNS reactive T cells results in demyelination: the destruction of the myelin sheath. The myelin sheath are plasma membrane extensions of oligodendrocytes in the CNS (30, 31); they spiral around axons, forming several layers. A single oligodendrocyte is capable of myelinating several axons (32). The major proteins forming myelin are myelin basic protein (MBP) and proteolipid proteins (PLP), comprising 70-80% of the total protein. MBP functions mainly to compact the myelin sheath, while PLPs are important in the ultrastructure of the sheath. Other proteins making up myelin include 2',3'-Cyclic nucleotide-3'-phosphohydrolase (CNP), Myelin-associated glycoprotein (MAG), and myelin oligodendrocyte glycoprotein (MOG) comprising 4%, 1% and 0.05%

of total protein, respectively, as well as small basic proteins and other minor proteins, and oligodendrocyte/myelin enzymes (30, 33). MAG and MOG are integral membrane proteins while CNP is associated with signal transduction and post translational modifications (34). As such, investigations on the components of myelin that could be a potential target antigen in MS and T cell responses against these myelin antigens have been studied extensively (35).

1.3 Animal models of MS

Experimental autoimmune encephalomyelitis (EAE), an animal model for MS, has been priceless in the discovery of therapies targeting MS (36, 37). Although not without its limitations, EAE mimics the clinical course and pathological hallmarks of MS (Fig. 2). The principles behind approved MS therapies such as glatiramer acetate and natalizumab (antibody against $\alpha 4\beta 1$ integrin) were first established using the EAE model (38-42). EAE can be induced by several myelin derivatives in rodents and non-human primates, however immunisation with the myelin component MOG shows the most human-like characteristics of MS. Immunisation with MOG₃₅₋₅₅ peptide (a small fragment of the full length protein) in mice, mimics the Th2 CD4⁺ T cell activated inflammatory response as well as demyelination and axonal damage observed in MS patients (43). Use of MBP, PLP and other myelin components as modes of immunisation results in inflammation but has little effect on axonal damage (44, 45). C57BL/6 mice strains present the classical symptoms of MS and the severity of disease is similar to the progression observed in PP-MS patients. MOG-EAE on a C57BL/6 background portrays chronic-progressive forms of MS, and encompasses the pathological features of inflammation, demyelination and axonal damage.

When examining individual pathological aspects of MS such as demyelination, remyelination or the autoimmune response, other induction methods such as viral infection or toxin administration are utilised. Of the viruses, Theiler's murine encephalomyelitis virus (TMEV) and murine hepatitis virus (MHV) models are the most widely used (46-51). These models have been used to study epitope spreading of myelin autoepitopes, and axonal degeneration as axonal injury precedes demyelination in this model. On the other hand, toxins result in focal demyelination in the CNS. The most commonly used toxin is cuprizone. Complete demyelination of the white matter tracts of the corpus callosum is achieved in mice fed cuprizone-supplemented diet for 5-6 weeks (52). In the reverse, once cuprizone is excluded from their feed, these mice then undergo remyelination in the affected areas, allowing both processes to be studied in the same animals. Therefore the versatility of induction methods in animal

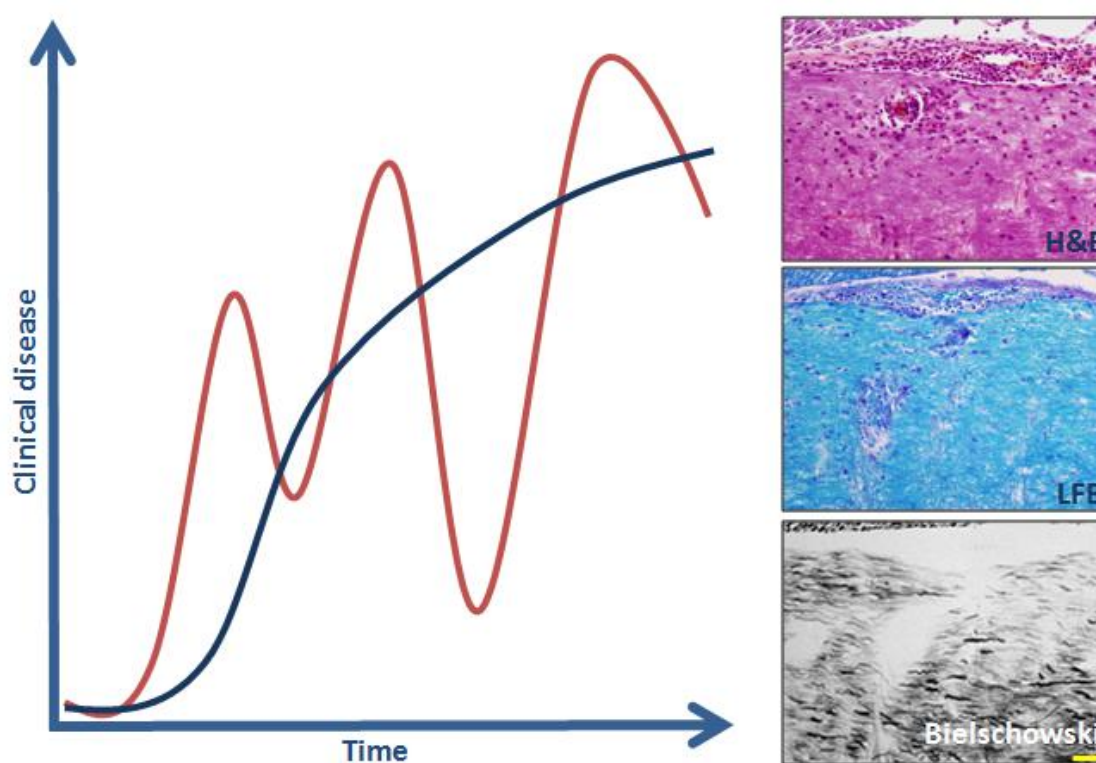


Figure 2. Clinical progression and histopathology in EAE. Typical clinical disease time course observed in primary progressive EAE (blue line) and relapsing-remitting EAE (red line). Representative histological serial sections of white matter tracts obtained from the lumbar cord of EAE-induced mice. Hematoxylin and eosin (H&E) stained section showing the influx of inflammatory infiltrates; Luxol fast blue (LFB) staining demonstrating demyelination; and Bielschowsky staining depicting axonal degeneration in EAE. Magnification bar 20 μ m.

models allows for the study of individual or multiple factors involved in the pathogenesis and or progression of MS-like diseases.

1.4 Pathological features of MS lesions

While the cause of MS is still unknown, the study of different types MS plaques and the molecular contents that reside therein have advanced our understanding of the disease process. Traditionally, MS lesions have been categorised as acute, chronic active and chronic silent plaques (53). Acute lesions encompass a repertoire of inflammatory cells (predominantly T cells), demyelination throughout with active stripping of myelin, and exhibit varying degrees of oligodendrocyte apoptosis (54), and axonal injury (55). Chronic active lesions have well defined edges with the active inflammatory cells surrounding the border including activated macrophages (53). There is also a prominent presence of antibodies and complement in these lesions (56-58). Chronic silent lesions are devoid of inflammatory activity. While inflammation and demyelination are major hallmarks of the MS plaque, the associated axonal injury and axonal loss is thought to determine the level of neurological deficit in MS patients (55, 59, 60). Bjartmar and colleagues (61) also confirmed this observation by studying 10 chronic inactive lesions obtained at autopsy from 5 long time suffering MS patients; these exhibited 68% axonal loss. Research into axonal injury has increased in recent years, aiming to prevent or impede axonal degeneration by developing novel therapeutic treatments.

1.5 Axonal injury and its implications in MS

MS is hypothesised to begin with an inflammatory response, followed by demyelination and subsequent axonal injury and loss. However, there is some debate as to the rigidity in the order of these events. A number of studies have suggested that axonal injury concomitantly occurs alongside demyelination (62-64). Trapp and colleagues (55) investigated axonal transection in the white matter of MS patients obtained from autopsies. The authors found that all 47 lesions (acute and chronic active) acquired post-mortem from 11 MS patients presented with transected axons demonstrated by the presence of terminal axonal ovoids and changes in axonal calibre that implicate axonopathy as a significant component of lesion formation. Furthermore, at the lesion site, the frequency of transected axons correlated with the levels of inflammatory activity, independent of disease duration. Similar conclusions have been drawn by other investigators (60, 65). These findings suggest that axonal injury is an early occurring event in MS. However, axonal injury generally does not present as a symptom in the initial phases of MS. This is due to other active compensatory

mechanisms, primarily the process of remyelination, that are sufficient to maintain axonal integrity. It is theorised that RR-MS patients progress to the SP-MS phase when the proportion of axonal injury exceeds the ability of the CNS to compensate (62). Current approved treatments of MS are generally aimed at decreasing the autoimmune inflammatory response in order to reduce subsequent demyelination. While this treatment has proved to be effective in delaying the disease progress in about 30% of MS patients (66), it is still far from a cure. Such therapies, when combined with newly discovered drugs that target axonal injury could prove more efficacious in combating MS pathology and clinical symptoms.

1.6 MAIFs and their role in the CNS

One factor enabling neurodegeneration is the inhibitory environment of the CNS under pathological conditions (67-69). The initial response to injury in the CNS is an attempt by the axon to regenerate by sprouting new extensions, called neurites. However in the inflamed CNS, neurites are unable to grow over long distances (70). In earlier studies, Schwab & Corroni (71) demonstrated that axonal regeneration was inhibited when exposed to components of CNS myelin. In a murine model of spinal cord injury (SCI; dorsal hemisection), pre-immunisation with purified CNS myelin resulted in significant axonal regeneration compared to non-immunised controls (72). Therefore, it has long been argued that myelin associated inhibitory factors (MAIFs) play a role in limiting neurite outgrowth and axonal regeneration, thus contributing to the neurological decline in MS and other CNS related conditions. To date, 5 MAIFs have been identified: MAG; Nogo-A; oligodendrocyte myelin glycoprotein (OMgp); Semaphorin-4D/CD100; and eprin-B3 (73-80). OMgp, MAG and Nogo-A are all expressed in the innermost lamella of the myelin sheath and physiologically function to inhibit unnecessary axonal sprouting via ligand-receptor interactions. This function is altered in the injured CNS, whereby deposition of myelin constituents on axons restricts the regenerative capacity of neurons (Fig. 3).

1.6.1 OMgp

OMgp is a glycoprotein of 120 kDa, consisting of five tandem leucine-rich repeats (LRR), anchored to the plasma membrane by a GPI linkage (78). OMgp which is highly expressed in oligodendrocytes, is localised on perinodal regions aiding in spacing of the nodes of ranvier (81), and function to inhibit unnecessary neuronal sprouting in this region (81, 82). OMgp is also expressed in motor neurons, but not in microglia or astrocytes (83). OMgp has inhibitory effects upon binding to the nogo receptor-1 (NgR1) (78), a receptor which is highly abundant in neurons (84).

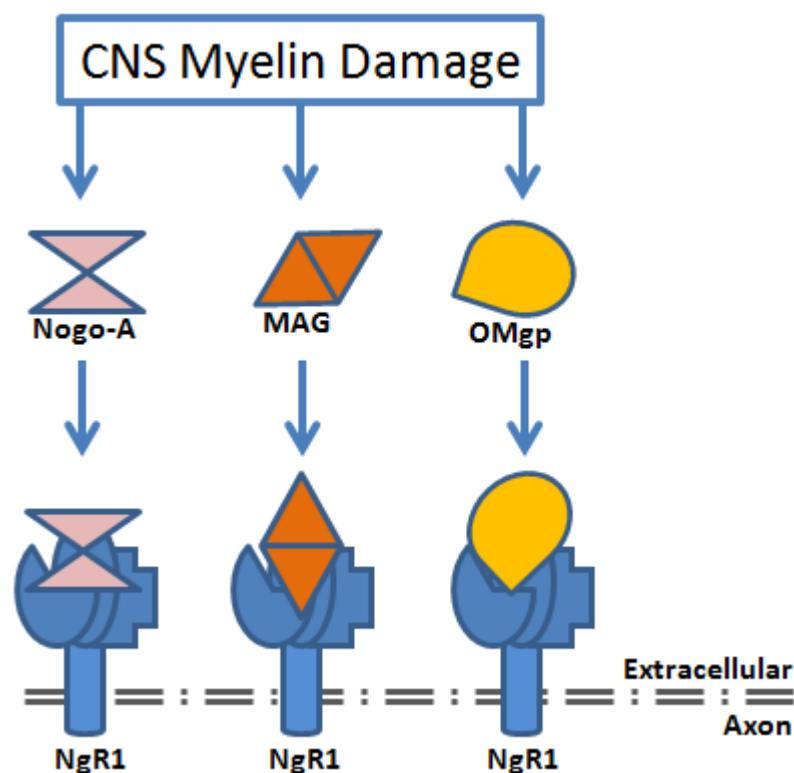


Figure 3. Nogo-A, MAG and OMgp are ligands for NgR1. Upon CNS myelin damage, MAIFs such as Nogo-A, MAG and OMgp are released into the extracellular environment and can bind to the NgR1 complex on axons to induce an intracellular signal leading to neurite outgrowth inhibition.

1.6.2 MAG

A member of the immunoglobulin superfamily, MAG is a transmembrane protein with an extracellular domain consisting of five immunoglobulin-like domains (85, 86). MAG, which is expressed on oligodendrocytes has been implicated in oligodendrocyte maturation, myelin sheath formation and maintenance (87). MAG has been shown to be an inhibitor of neurite outgrowth in neurons (73, 88, 89). It is thought that while MAG is involved in neurite outgrowth in the developing brain, it switches roles to become inhibitory in the adult CNS (73, 74). The inhibitory activity of MAG has been demonstrated by utilising neurite outgrowth assays on fractions of detergent-soluble myelin proteins collected by ion exchange (73). The authors found an increase in neurite outgrowth inhibition in the fractions containing MAG. MAG expression has also been shown to be upregulated upon axonal injury in the CNS (90). MAG binds NgR1 and NgR2 (88, 91, 92), as well as GT1a and GT1b receptors (93).

1.6.3 Nogo-A

While MAG and Nogo-A have been the most extensively studied MAIFs to date, in recent years Nogo-A has stimulated greater interest following the identification of two functional binding domains that can inhibit neurite outgrowth; Nogo-66 and Amino-Nogo, which may operate via independent mechanisms. Three isoforms of Nogo are present in the CNS due to the alternative transcription of the *nogo* gene (Fig. 4). These are Nogo A of 1192 amino acids, Nogo B of 373 amino acids, and Nogo C of 199 amino acid length. Nogo A, B and C are members of the Reticulon gene family, characterised by the homologous 188 aa carboxyl terminal termed reticulon-homology domain (RHD), and by definition are endoplasmic reticulum-associated proteins (77). All Nogo isoforms are deemed glycosylated integral membrane proteins due to the presence of two hydrophobic domains, and all three isoforms share the common Nogo-66 region. The topology of Nogo-A on the cell membrane has been demonstrated to vary in that the Nogo-66 region is always extracellular, while Amino-Nogo may be in an intracellular or an extracellular conformation (94). Nogo-A is expressed by oligodendrocytes and neurons, but not astrocytes (95). Nogo-A is highly expressed in motor neurons as well as sensory neurons as determined by mRNA expression levels (96). Satoh and colleagues (97) observed upregulation of Nogo-A on oligodendrocytes in tissue surrounding chronic active demyelinating MS lesions. Furthermore, in a rat spinal cord weight drop model, Nogo-A expression was increased in oligodendrocytes and neurons (98). The expression of Nogo-A in neurons may provide an intracellular regulatory mechanism by which aberrant axonal sprouting is inhibited during development. Similarly, its expression in oligodendrocytes may be an extracellular mechanism that might also inhibit axonal growth, through the interactions of the innermost lamella of the myelin sheath. Nogo-66 is located in the extracellular domain (loop) between the two transmembrane segments. Nogo-66 has been implicated as the region responsible for initiating axonal growth inhibition (77) through interactions with its cognate receptor, NgR1 (99, 100). Binding of Nogo-A to NgR1 involves the trivalent interaction of the Nogo-A domains (Nogo-66, Nogo-A-24 and Nogo-C39), with the concave LRR-filled binding site of NgR1 (101). The N-terminal domain of Nogo-A, Amino-Nogo, has been implicated in the inhibition of neurite outgrowth by an NgR1-independent mechanism (99, 102). Although Amino-Nogo does not interact with NgR1 directly, it increases the binding affinity of Nogo-66 to NgR1 (101). While a candidate receptor still remains elusive, Amino-Nogo has been shown to be inhibitory by its interactions with $\alpha 5$ and αv integrins (103).

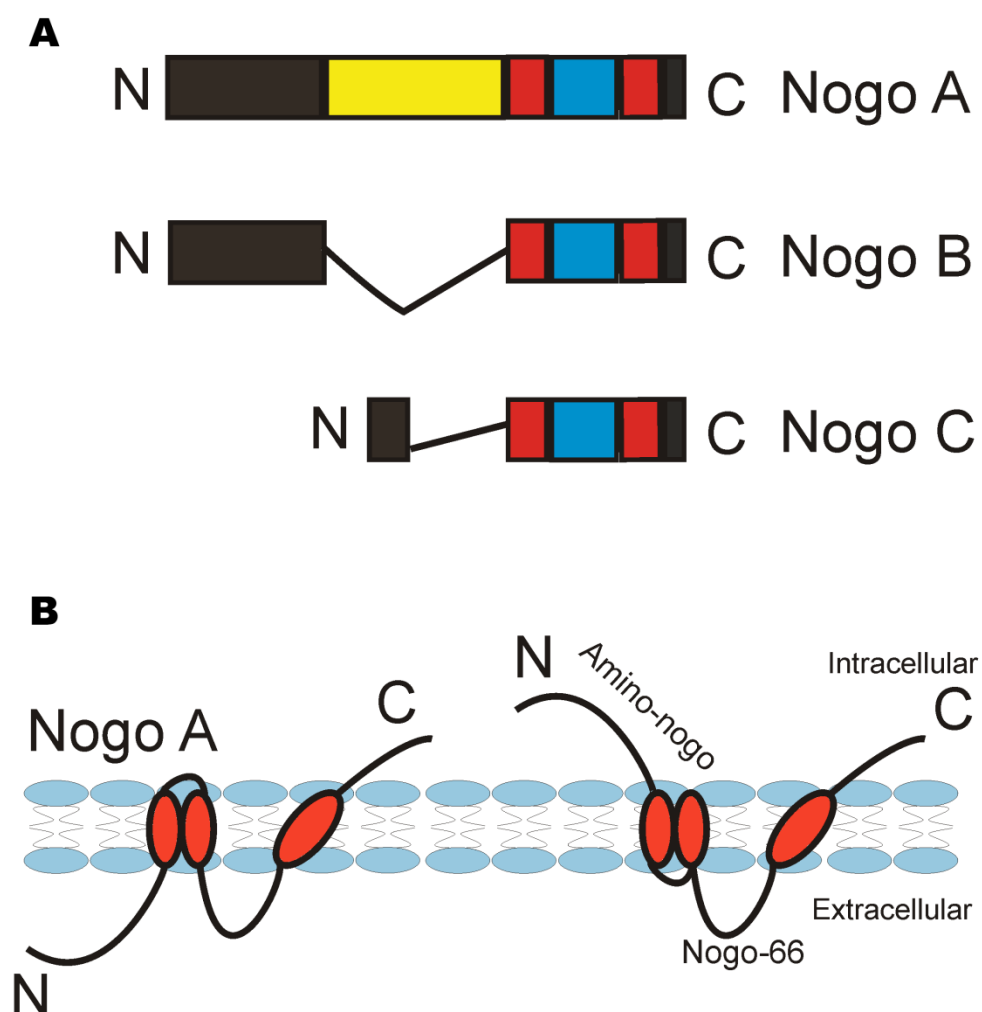


Figure 4. Structure and functional domains and conformation of Nogo isoforms.

A) Alternatively spliced isoforms of Nogo (Reticulon 4). Nogo-A is 200 kDa, Nogo-B is 55 kDa, and Nogo-C is 25 kDa. Despite the evolutionary conservation of the C-terminus among these isoforms consisting of two transmembrane domains (red) flanking the nogo-66 domain (ligand binding domain; blue), the N-terminus (black) is longer in Nogo-A than the other 2 isoforms. (B) Full-length Nogo-A is 1,192 amino acids (AA) in length and consists of 2 transmembrane domains, a C-terminus extracellular Nogo-66 domain, and 2 intracellular tails (one at the N-terminus, one at the C-terminus in the cis configuration). Nogo-A in the trans configuration has its N-terminus Amino-Nogo in the extracellular compartment is able to interact with integrin receptors. Published in Petratos, S. et al. (2010) *J Neuropathol Exp Neurol* **69**(4): 323-334 (Appendix II).

Several approaches such as vaccination with Nogo-A peptides, deletion of the Nogo A gene, or silencing Nogo-A by siRNA techniques can promote functional recovery in EAE mice (104, 105). Positive outcomes have been obtained using similar techniques in SCI and stroke models (106-108). Furthermore, administering antibodies directed against Nogo A (IN-1), resulted in regenerative sprouting and axonal growth in SCI models (109-114). Therefore, the development of therapies which target Nogo-A may be advantageous in conditions such as MS and SCI.

The effects of Nogo-A, OMgp and MAG in hindering the regeneration in the CNS in the context of MS and SCI as well as in their animal models has been well established. However, what is known of the functional relationships or redundancies between these inhibitory factors is limited. A direct approach to address these questions is the use of combinatory transgenic deletion mutant animal strains to evaluate neurite outgrowth *in vitro* and determine regenerative capacity after CNS insult *in vivo*. A recent study by Cafferty and colleagues (115) compared the inhibitory activity of myelin extracted from transgenic knock out (KO) mice with either the single deletion mutant Nogo-A/B^{-/-} (N⁻), the double deletion mutant MAG^{-/-}/OMgp^{-/-} (M⁻O⁻) or the triple mutant Nogo-A/B^{-/-}/MAG^{-/-}/OMgp^{-/-} (N⁻M⁻O⁻), against *NgR1* positive dorsal root ganglion (DRG) neurons *in vitro*. Of interest was the finding that while deletion of Nogo-A/B resulted in significant disinhibition of neurite outgrowth, this effect was enhanced when all three inhibitors (Nogo-A/B, MAG and OMgp) were deleted. The deletion of OMgp and MAG alone did not promote neurite outgrowth. Comparative results were obtained *in vivo* when the mutant mice were subjected to T8 dorsal hemisection injury (115). Regenerative capacity and recovery of motor function following SCI was more prominent in the triple mutant mice compared to the single Nogo-A/B mutant. These data not only implicate Nogo-A as the most potent non-redundant myelin associated inhibitor, but also reveal the possible synergistic effects of MAG and OMgp for Nogo-A in axonal degeneration.

1.7 The nogo receptor complex

1.7.1 NgR1

The NgR family of receptors consist of NgR1, NgR2 and NgR3. NgR1 was first documented as a receptor for Nogo-66 (99). Soon after, NgR2 and NgR3 were identified as structurally similar homologues of NgR1 with comparable expression patterns in the CNS (116, 117). While no binding partners have been elucidated for NgR3, MAG has been shown to bind NgR2, with even greater affinity than binding to NgR1 (92). NgR1, which lacks an intracellular signalling domain, forms a ternary complex with its co-receptors to induce the inhibitory signal initiated by binding of

Nogo-66, MAG or OMgp (Fig. 5). The co-receptors for NgR1 have been identified to be: 1) LINGO-1 "leucine-rich repeat and immunoglobulin [Ig] domain-containing Nogo-receptor interacting protein 1", and 2) neurotrophin receptor P75NTR (118) or 3) TAJ/TROY (TNF-Receptor Super family member 19) (67, 119). NgR1 is expressed in neurons and the axon cell surface (91, 117, 120), is of 473 aa length (64kDa) and consists of eight LRRs flanked by an amino terminal LRR domain (LRRNT) and a carboxyl terminal cysteine-rich LRR (LRRCT). A unique domain of 100 aa's links LRRCT to its GPI anchor (121, 122), resulting in NgR1 to accumulate in lipid rafts (99, 123). LRR domains are required for Nogo-66 binding, and the C-terminal domain is required for inhibitory signalling (121, 124). Interestingly, the C-terminal domain of NgR1 is essential for P75NTR binding (122).

1.7.2 LINGO-1

LINGO-1 is a transmembrane glycoprotein, and a member of the LRR family of proteins that are CNS-specific and is expressed on neurons as well as oligodendrocytes but not astrocytes in the adult CNS (118, 125). LINGO-1 and NgR1 have similar expression profiles of in the CNS (84, 118, 126). LINGO-1 consists of an extracellular domain of 12 LRR motifs, an Ig-domain, a transmembrane domain and a cytoplasmic tail (118). The intracellular domain of LINGO-1 is important in inducing neurite outgrowth inhibition. Mouse mutants lacking this domain fail to induce growth cone collapse *in vitro* (127). Furthermore, LINGO-1 has been implicated in having negative effects on oligodendrocyte differentiation and myelination (127).

1.7.3 P75NTR

P75NTR is a part of the TNF receptor family consisting of an extracellular domain of cysteine-rich motifs, a transmembrane domain and a cytoplasmic domain, that includes a death domain (128, 129). It is a trophin receptor that binds all neurotrophins and as such has multiple downstream effects depending on its binding partners including cell survival, apoptosis, axon growth cone collapse as well as neurite outgrowth, (130-132). In the CNS, physiological expression of P75NTR is restricted to the subventricular zone (SVZ), however its expression is upregulated in the white matter in EAE and MS (133, 134). In particular, post mortem MS brain tissue sections showed P75NTR expression in the periventricular chronic-active plaques but not in chronic-inactive plaques or in the normal white matter (NMW). Furthermore, in an animal model of SCI the expression levels of P75NTR was upregulated in injured axons and upregulated in the white matter as well as grey matter (135). P75NTR is expressed on dendrites and axons (136, 137)

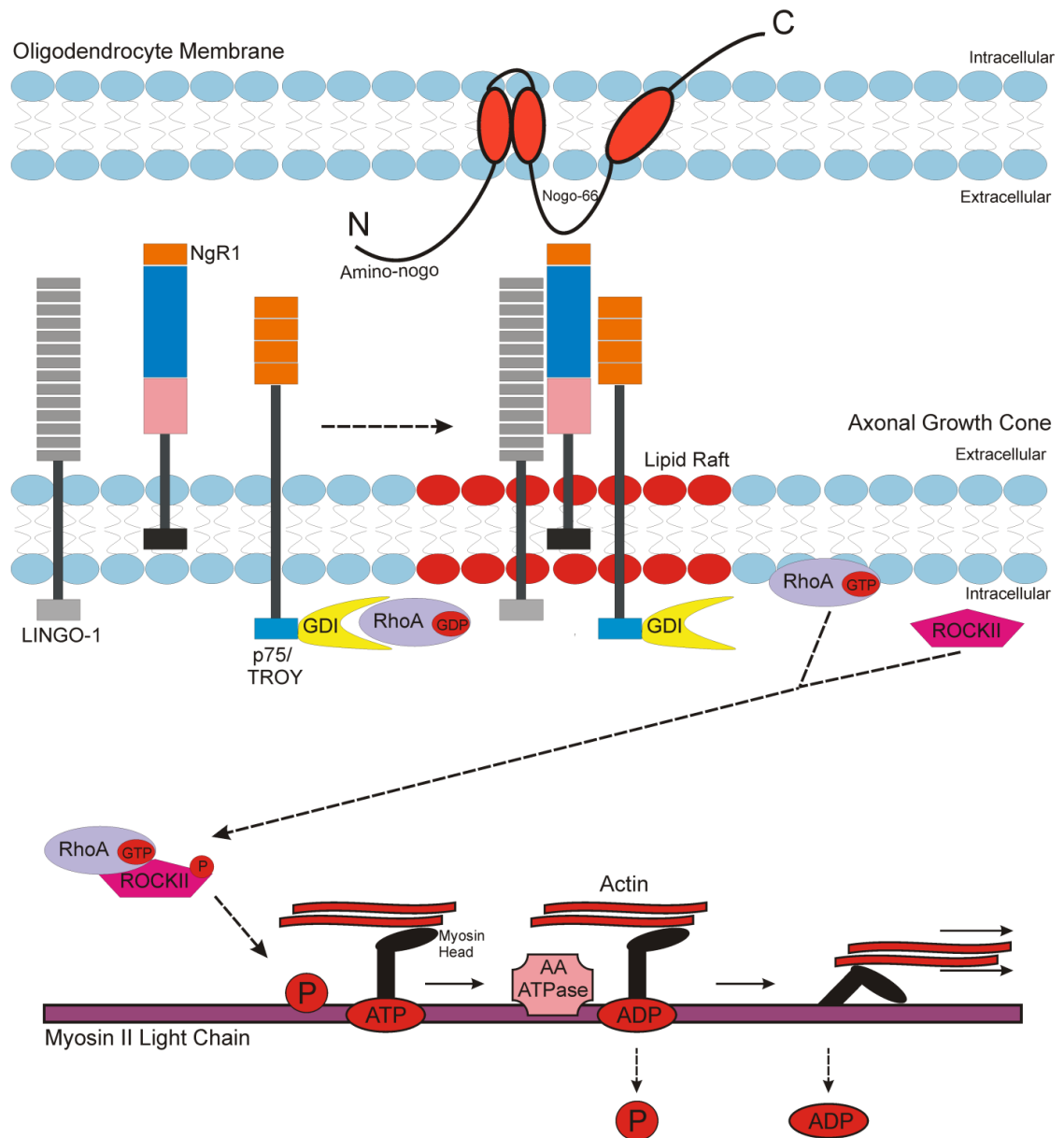


Figure 5. Oligodendrocyte myelin membrane localized Nogo-A and its interaction with its cognate receptors. A) The interaction of the Nogo-66 domain is a high affinity binding with the LRR ectodomain of NgR1 is at a nanomolar range. This produces conformational changes of the NgR1 co-receptors to signal downstream, modifying the axonal cytoskeleton and favoring retraction of the distal growth end of the injured axon. Microfilament and microtubule dynamics are modified through the activation of Rho-A (Rho-A-GTP) and its effector kinase, Rho kinase (ROCKII). GTP: guanine triphosphate GDI: guanine dissociation inhibitor; LINGO-1: LRR and immunoglobulin domain-containing Nogo receptor-interacting protein 1 receptor; p75: low-affinity neurotrophin receptor (P75NTR). Published in Petratos, S. et al. (2010) *J Neuropathol Exp Neurol* **69**(4): 323-334 (Appendix II).

and has been shown to be involved in the NgR1 complex, mediating neurite outgrowth *in vitro* (122, 138, 139). However, absence of P75NTR does not permit axonal regeneration after spinal cord injury. Mice with a mutation to the P75NTR gene did not result in enhanced axonal regeneration or improved motor recovery (140). Perhaps this finding is not surprising since the receptor component TROY can replace P75NTR and still induce NgR1 signalling.

1.7.4 TROY/Taj

TROY is a member of the TNF receptor family, and is highly expressed in adult CNS, including cerebral cortex, cerebellum, DRG and retinal ganglion neurons (RGCs) (119). Dominant-negative forms of TROY abolishes neurite growth inhibition (119). Soluble forms of TROY (TROY-Fc), an antagonist and a decoy co-receptor, also disinhibits neurite outgrowth in RGC neurons and DRG neurons *in vitro* (141). Furthermore, neurons from TROY/*taj*-deficient mice show reduced resistance to the inhibitory effects of MAIF substrates (141). Moreover, it has been demonstrated that the administration of soluble TROY resulted in similar effects *in vivo*. TROY/Taj is an alternative co-receptor to P75NTR, as a binding partner for NgR1. TROY may be a more dominant player in the NgR1 signalling than P75NTR because TROY is constitutively expressed in the postnatal and adult CNS (119, 141-143). The interchangeability between P75NTR and TROY in forming a functional NgR1 complex highlights the redundancy of this inhibitory mechanism in the CNS. Thus, a strategy whereby multiple components of the NgR1 complex are simultaneously inhibited may be a promising therapeutic approach for MS.

1.7.5 Rho-A

The binding of Nogo-A, MAG or OMgp to the NgR1 complex, activates the small guanosine triphosphatase (GTPase) Rho-A, a key downstream modulator of cytoskeleton dynamics. Therefore Rho-A activation is a molecular switch whereby neurite outgrowth is inhibited (67, 144, 145). Rho-A-GTP was found to inhibit neurite outgrowth in postnatal sensory neurons and cerebellar neurons by rigidifying the actin cytoskeleton (139). Furthermore, TROY and P75NTR can bind Rho-GDI, activating Rho-A. Moreover, addition of MAG or Nogo-A enhanced these interactions, while the introduction of a P75NTR peptide reversed the effects of P75NTR (146). Additionally, Mi et al. (118) demonstrated that LINGO-1/NgR1/P75NTR interaction was necessary for Rho-A activation in the presence of myelin inhibitory substrates, as LINGO-1/NgR1 alone was not able to induce Rho-A activation. Tight regulation of Rho-A, by upstream transducing signals is therefore central in modulating neurite outgrowth inhibition.

1.8 Targeting the components of NgR1 signalling to promote axonal regeneration

1.8.1 Nogo-A

There is now strong evidence demonstrating the potency of NgR1 inhibitory signalling pathway in limiting axonal regeneration in animal models of SCI and MS (115, 147, 148). As such, interactions between MAIFs and components of the NgR1 complex have been studied extensively. Karnezis and colleagues (104), showed that NogoA-deficient mice with MOG-EAE, displayed delayed onset of EAE and significant improvement in clinical outcome compared to controls. Histological analysis of CNS tissue taken from these mice revealed minimal inflammation, demyelination and axonal damage. Therefore lack of Nogo-A may limit the inhibitory effects of NgR1 signalling, promoting axonal integrity and functional recovery. Strategies including vaccination or treatment with Nogo-A peptides or specific antibodies support the idea that blocking NgR1 signalling in the CNS makes the immediate environment more permissive for regeneration in EAE and SCI models (104, 109-114). In a recent report, the systemic administration of siRNA directed against Nogo-A gene in MOG-EAE animals resulted in a significant reduction in incidence and severity of EAE (105). Along the same lines, experiments in non-human primate SCI models, anti-Nogo-A antibody (IN-1) treatment was shown to promote axonal regeneration and locomotor recovery, suggesting a pivotal role for Nogo-A in inhibition of axonal regeneration (149, 150). Of interest is the recently completed human phase I clinical trial performed in patients with complete SCI who received anti-Nogo-A antibody by continuous intrathecal infusion 4-14 days post injury which produced promising data (151). A phase II trial using the same experimental design was reported to commence in 2010 but no outcomes have yet been published.

Nogo KO animals used to dissect the axonal inhibitory properties of Nogo A in SCI models have produced conflicting results. Three independent investigations concluded that Nogo-A or Nogo-A/B KO animals with SCI (dorsal hemisection) exhibited enhanced regeneration in the corticospinal tract after insult compared to wild type controls (115, 152, 153). In another model of SCI, pyramidized *nogo-ab* and *ngr1^{-/-}* showed pronounced regeneration in the severed cord with return of preferred forelimb usage (154). Nogo-A/B and Nogo-A/B/C KO mice used by Zheng and colleagues (155) did not demonstrate any such regeneration in the CNS following injury. The differences in these findings may reflect the variation in genetic background when crossing 129X1/SvJ and C57BL/6 mouse strains used in these experiments. Indeed Dimou et al (156) had Nogo-A KO animals on a single genetic background (129X1/SvJ or C57BL/6), and showed enhancement of regeneration in either mouse strain after SCI.

Interestingly, the regenerative capacity of Nogo-A KO animals with 129X1/SvJ were observed to be 2-4 times that of the C57BL/6 background when analysing fiber numbers caudal to the lesion.

1.8.2 NgR1

Cleavage of NgR1 disinhibits growth cone collapse in neurites *in vitro* (157). Overexpression of NgR1 turns unresponsive neurons responsive to neurite outgrowth inhibition (158). Furthermore, silencing of NgR1 by RNA interference (RNAi) in a rat model of experimental stroke was effective in promoting axonal regeneration and improved behavioural outcomes in treated rats (147). Thus targeting NgR1 may prove most efficacious as this method has the potential to block inhibitory signalling of all three myelin ligands, Nogo-A, MAG and OMgp. In 2004, Li and colleagues generated the first neutralising monoclonal antibody directed against NgR1 specifically, 7E11, and characterised its properties *in vitro* (159). 7E11 directly interacts with the LRR3 domain of NgR1 to block the binding of Nogo-A, MAG and OMgp, promoting DRG neuron outgrowth on myelin inhibitory substrates. While the exact mechanism of action remains to be elucidated, it is likely that E711 antibody either induces conformational changes in NgR1, or interferes with the ligand-receptor interaction by steric effects (159). Similarly, the NgR1 antagonist peptide NEP1-40 corresponding to the Nogo-66 residues 1-40 has proved efficacious in enhancing locomotor recovery in SCI models. NEP1-40 competitively binds to NgR1 thereby blocking the inhibitory effects of only Nogo-A. Administration of NEP1-40 to rats subjected to mid-thoracic hemisection and lateral funiculus injury resulted in increased regenerative capacity in the corticospinal tract (CST) and rubrospinal tract (RST), respectively (106, 160, 161). Furthermore, generation of NgREcto, the truncated soluble NgR1 protein, was effective in promoting axon growth on myelin substrates *in vitro* (121). NgREcto is comprised of the first 310 aa's of NgR1, encompassing the N-terminal LLR-rich ligand binding domains and lacks the GPI anchor and C-terminal signalling domains. Transfected NgR1-sensitive COS7 cells underwent neurite extension when plated on Nogo or purified myelin substrates in the presence of NgREcto protein (121). This suggests that NgREcto is capable of disrupting ligand receptor interactions. In a rat model of SCI, intrathecal administration of the soluble NgR1 ectodomain fused to an antibody Fc region, NgR(310)-ecto-Fc (a functional blocker of Nogo-A, MAG and OMgp), after mid-thoracic dorsal hemisection, resulted in the sprouting of corticospinal and raphespinal fibers, improved locomotor recovery in treated rats compared to controls (160). Interestingly, it would appear that the improvements observed by NgR(310)-ecto-Fc administration outweighed that of the Nogo-66-specific NEP1-40 peptide treatments (106, 162), the former exhibiting

considerable axonal sprouting. These data support the idea that simultaneous hindrance of multiple ligand interactions is a more effective therapeutic approach to targeting single ligands.

While NgR(310)-ecto-Fc promotes greater sprouting of CST fibers and raphespinal axon growth than NEP1-40, perhaps due to its ability to block the effects of Nogo-A, MAG and OMgp, the two treatments produce similar levels of locomotor recovery in treated animals highlighting the potency of Nogo-A compared to other inhibitory ligands (160, 162). The efficacy of NgR(310)-ecto-Fc as a therapeutic agent was analysed with rat spinal contusion experiments comparing immediate versus delayed administration of this agent (163). Delayed therapeutic administration was just as affective in promoting locomotor recovery as the immediate therapy. Immediate and delayed therapy strategies resulted equally in axonal growth in the severed CST and raphespinal fibers (163). Similar findings were obtained in a mouse SCI model, where therapeutic administration of NEP1-40 one week after insult was just as affective in promoting functional recovery in treated animals (162).

1.8.3 LINGO-1

Investigations into LINGO-1 and its effects in the injured CNS has intensified in the last decade and produced positive results. A double negative truncated form of LINGO-1 which lacks the cytoplasmic signalling domain was found to form a complex with NgR1 or P75NTR, but was unable to inhibit neurite outgrowth in primary neuronal cultures when plated on inhibitory myelin substrates (Mi et al 2004). When LINGO-1 antagonist (LINGO-1-Fc) was administered in rats with spinal cord damage, improved functional recovery and neurite outgrowth was observed (164). In addition these authors found an increase in neuronal and oligodendrocyte cell survival. Complementary data have shown that blocking LINGO-1 function by administration of soluble LINGO-1-Fc in rats following ocular hypertension and optic nerve transection promoted RGC survival (165). In the context of EAE, Mi et al (166) found that interfering with LINGO-1 activity by means of *Lingo-1* KO or treatment with anti-LINGO-1 antibodies had profound effects on disease outcome. *Lingo-1* KO animals presented with significantly reduced EAE clinical scores compared to wild type controls (166). In a series of experiments, the authors ruled out the possibility that the improvement observed in *Lingo-1* KO animals was due to changes in the inflammatory response in the *Lingo-1* KO mice. Firstly, MOG-reactive T cells isolated from EAE induced *Lingo-1* KO mice had similar proliferative responses to various concentrations of MOG peptide, compared to controls. Secondly, adoptive transfer of MOG-immunized encephalogenic T cells

isolated from *Lingo-1* KO animals into naive wild type animals induced EAE in both groups, producing comparable EAE clinical scores. In the reverse experiment, adoptive transfer of MOG-immunized encephalogenic T cells isolated from wild type animals, into *Lingo-1* KO animals did not induced EAE in *Lingo-1* KO animals (166). These findings support the idea that LINGO-1 is not involved in modulating the inflammatory response, but rather that it plays an important role in remyelination and maintaining axonal integrity. Indeed, electron microscopy (EM) imaging of the lumbar spinal cord of *Lingo-1* KO mice showed processes of remyelination, an abundance of newly formed myelin sheaths, and significantly higher numbers of myelinated axons compared to controls (166). Control animals exhibited signs of demyelination, evident by the presence of loose myelin layers appearing in both the inner- and outermost lamellas.

In a therapeutic treatment paradigm, there were significant differences in animals treated with the antagonistic anti-LINGO-1 antibody after induction of EAE (166). This study employed two strategies. In the first, the antibody treatment was administered twice; at pre-onset and onset of EAE. In the second, the antibody was administered every 4 days starting at the onset phase of EAE, for the duration of the experiment. The second strategy was more effective in reducing EAE clinical scores. Complementary to these data, continuous focal administration of LINGO-1 antiserum via a mini-osmotic pump to rats immediately after dorsal hemisection to the spinal cord resulted in the recovery of some hind limb motor function (167). LINGO-1 antiserum blocks endogenous LINGO-1 signalling, increases neuronal survival and results in a significant reduction in Rho-A activity (167). The use of antibodies against NgR1 receptor signalling components as a means of ongoing therapy may be effective in reducing the neurological decline observed in patients with MS. Interestingly, the more recently developed anti-LINGO-1 antibody, BIIB033, is currently being tested in clinical trials for 42 patients with either relapsing-remitting or secondary-progressive MS. This is the first drug tested in MS that is not immunomodulatory, but rather targets myelin repair (ClinicalTrials.gov ID #NCT01244139).

1.9 Modulation of cytoskeletal dynamics

In neurons, directional growth and retraction of axons and dendrites is governed by members of the Rho family; Rho-A, Rac-1 and Cdc42 (168, 169),330). The relative activation states of these molecules modulate the assembly and disassembly of microtubules and microfilaments and therefore affect neurite outgrowth and inhibition. While Rac-1 and Cdc-42 promote neurite outgrowth by regulating lamellipodia and filopodia extension, Rho-A promotes inhibition by modulating contractility (170-172).

Intracellular signalling induced via NgR1 initiates an increase in Rho-A activation and therefore neurite outgrowth inhibition (146). As such, understanding the signalling pathways of NgR1 and Rho-A and their roles in promoting neurodegeneration could be critical in discovering new treatment methods for neurodegenerative diseases such as MS. Rho-A inactivation induces neurite outgrowth in several ways, all of which converge on the activation of Rho associated kinase-2 (ROCKII) by Rho-A. ROCKII, then further phosphorylates and activates other inhibitory molecules involved in several pathways. Rho-A/ROCKII activation results in rigidification of the cytoskeleton through alterations to the myosin II light chain (Fig. 5) (169). ROCKII phosphorylation of the downstream target LIMK-I and its subsequent target cofilin affects actin dynamics, while ROCKII mediated phosphorylation of CRMP-2, influences microtubule assembly and stability. Since NgR1 can activate Rho-A, and Rho-A can initiate a downstream signalling cascade which inhibits neurite outgrowth, it is conceivable that NgR1/Rho-A signalling also contributes to inhibition of axonal regeneration in conditions such as SCI and MS. The initiators and the effector molecules involved in NgR1 signalling pathway, and their implications in MS and SCI will be discussed in detail here.

The morphology of the developing neuron begins as a spherical cell body, which then produces small spiky structures (lamellipodia and filopodia) forming the growth cones that protrude and branch out from several locations around the cell body, called immature neurites. One of these neurites extends further, forming the axon. The remaining neurites mature into multiple branches called dendrites. Axonal guidance and dendrite formation is a result of the restructuring of the cytoskeleton and are mediated by the above-mentioned Rho family members (171). The dynamic rearrangement of the cytoskeleton is key to axon elongation (173). This is mainly mediated by the motility of the sensory growth cone present at the end of the axon. These molecules achieve this by altering microtubule and filamentous actin (F-actin) assembly and disassembly through actin polymerization or depolymerisation, branching, and contractility for actin transport within the growth cone (172, 174-176). There are 2 major components in the structure of the growth cone; microtubules and microfilaments (177). Microtubules are made up of α - and β -tubulin heterodimers and serve as structural elements and tracks for organelle traffic (178). Microfilaments, made up of F-actin and a complex set of actin binding proteins, are longer and more prominent in the growth cone than in any other region of the neuron (179). Stable microtubule bundles comprise the shaft of the axon, which extends to the growth cone by dynamic microtubule filaments (178, 180). F-actin bundles protrude out to multiple filopodia which are separated by a mesh of F-actin network. Actin microfilaments may

interact with axonal microtubules, especially the dynamic microtubule filaments which are unstable and probe the periphery of the growth cone (181). Dynamic microtubule filaments may be pulled toward the preferred direction of growth to interact with appropriate filopodium actin filaments through the guidance cues of Rho GTPases (172, 181). Axonal outgrowth involves actin polymerization at the extending end, followed by microtubule polymerization, bundle formation, capture and stabilization in the filopodium, which effectively dilates (182, 183). With these events, the growth cone turns towards an attractant signal while the most distant filopodia retract through repulsive signals (180). In the case of growth cone collapse, it is believed that repulsive signalling is first received by actin filaments that then begin the depolymerising process (173). The signal is then transmitted to microtubules that also depolymerise and rearrange their conformation.

1.10 Rho-A activation and neurodegeneration following nogo receptor signalling

1.10.1 Rho-A/NgR1 Interactions

In the adult CNS, Rho-A generally functions to inhibit aberrant sprouting of axons and dendrites. Rho-A is inactive in its guanosine diphosphate (GDP) bound form and becomes active in its GTP bound form (93, 184, 185). In the context of neurodegeneration, MAIFs released from damaged myelin sheaths bind and activate the NgR1 complex on neurons, resulting in intracellular activation of Rho-A and its effectors, inhibiting neuronal regeneration. Increase of MAIF ligands affects the signal transduction equilibrium from a proregenerative state to an antiregenerative state by modifying levels of the key molecules Rho-A, Rac1 and Cdc42, whereby Rho-A activation overwhelms the activities of the other two (93). The expression profile of Rho-A is altered in the CNS in response to injury. Under physiological conditions, Rho-A expression is observed in oligodendrocytes but not neurons or astrocytes (186). Following SCI, Rho-A expression is upregulated in reactive astrocytes and neurons around the site of injury some 7 days post injury, suggesting a pivotal role for Rho-A signalling in neurodegeneration. Upregulation of Rho-A could also be occurring in EAE and MS. Interestingly, the expression of Rho-A is long lasting, remaining at heightened levels three months after SCI (186), indicating that targeting Rho-A as a means of therapy may have prolonged beneficial effects in human conditions such as MS.

P75NTR and TROY/Taj have been implicated as the intracellular signalling components of the NgR1 complex in the injured CNS, by directly binding and activating Rho-A (141, 143). Shao and colleagues (97) employed *in vitro* transfection strategies to demonstrate that when plated on inhibitory MAIF substrates, NgR1/LINGO-1/P75NTR

or NgR1/LINGO-1/TROY complex formation is enough to induce inhibitory signalling, activating intracellular Rho-A. COS cells transfected with *Taj*, *NgR1* and *LINGO-1* had increased activation of Rho-A, while this effect was not evident in cells transfected with single constructs, suggesting all three components are required to induce NgR1 signalling (141). Furthermore, introduction of soluble TROY/TAJ as an antagonist or overexpression of dominant negative TROY reverses these effects (119, 141). Moreover, Nogo-66 and OMgp bind to NgR1, activating Rho-A, inducing growth cone collapse (139). By contrast, administration of LINGO-1 antagonist results in Rho-A inactivation (164).

SCI studies with P75NTR null mice have shown that Rho-A remained inactive for 72 hours post-injury while in control animals Rho-A was significantly active in both neurons and glial cells at these time points (187). It was further reported that in P75NTR KO mice, Rho-A activation was dependent on P75NTR in the initial phase after SCI (187). It is speculated that P75NTR interacts directly with Rho-A, releasing Rho-A from Rho-GDI in a spatially restricted manner (188). Moreover, siRNA targeted triple knockdown of NgR, P75NTR, and Rho-A disinhibits both DRG neurons and RGC neurite outgrowth in the presence of CNS myelin (189).

1.10.2 Targeting Rho-A and its Downstream Mediators

C3 transferase enzyme from *Clostridium botulinum* was found to be a Rho-A antagonist. *In vitro* studies demonstrated that the introduction of C3 transferase, which inhibits Rho-A downstream signalling, resulted in significant neurite outgrowth in primary retinal neurons plated on inhibitory myelin substrates (190). The same authors further showed *in vivo*, that administration of C3 transferase in a rat model of optic nerve crush, resulted in regeneration of injured axons that traversed lesioned areas. In rat SCI models topical application of C3 transferase at the lesion site resulted in regeneration of cortical neurons over long distances, and improvements in functional recovery (191). An analogue of C3 transferase, BA-210, was then developed that could more efficiently traverse cell membranes (192). The investigators reported that administration of BA-210 immediately or 24 hours following thoracic spinal cord contusion in rats was satisfactory in promoting axonal regeneration and functional recovery. In 2011, Fehlings and colleagues published their results from phase I/IIa clinical trials testing a Rho-A blocker BA-210, trademarked Cethrin, in acute SCI patients with either thoracic or cervical injury (193). As a recombinant variant of C3 transferase, BA-210 possesses more advanced properties that allow enhanced penetration of spinal cord dura and cell membranes. A single dose of BA-210 ranging

from 0.3mg to 9mg was administered extradurally at the site of spinal cord injury. While there were functional improvements in groups with cervical injuries, Cethrin was not an effective treatment for patients with injured thoracic cords. This is perhaps due to additional and severe trauma caused to the tissue surrounding the injury site. The most significant locomotor recovery was observed in the cervical injury group that received 3mg of the drug, 66% of these patients improved their American Spinal Injury Association Assessment (ASIA) from level A to level D. Deemed a promising therapeutic drug, next phase trials proving its efficacy are in the planning stages (193).

A downstream effector of Rho-A, is Rho associated kinases (ROCKs), a serine/threonine kinase of 160kDa (194, 195), involved in cytoskeleton reorganization (196). The general domain structure of ROCKs consist of an amino terminal kinase domain (AKD), and a carboxyl terminal made up of Rho-binding domain (RB) and pleckstrin homology domain (Ph) that have autoinhibitory effects on AKD, independent of each other (197, 198). Two isoforms of ROCK exist: ROCKI, which is predominantly expressed on non-neuronal cells, and ROCKII which is expressed on neuronal cells in the hippocampus, cerebral cortex and the purkinje cells of the cerebellum (199, 200). Rho-A activation of ROCKII in neurons results in growth arrest, neurite contraction and growth cone collapse (67). ROCKII activation also indirectly effects myosin light chain (MLC), which regulates actinomyosin contractility (Fig. 5) (201). Upon phosphorylation MLC is inactivated and causes actin filament cross-linking and therefore aids in cytoskeleton rigidification (202). By contrast, Rac1 can activate PAK which dephosphorylates MLC (203). Neurofilaments are also a substrate for ROCK and undergo depolymerisation upon phosphorylation (204).

The PC-12 cell line has been employed as an effective *in vitro* model in Rho-ROCK signalling pathways, as these cells can be manipulated to maintain growth arrest while undergoing neurite outgrowth when treated with nerve growth factor (NGF) (205). Direct Rho-A inhibition is also possible for this cell line using *Clostridium b. C-3* exoenzyme (190, 206). Y-27632, a selective inhibitor of ROCK, induces neurite outgrowth on a dose-dependent manner in PC-12 cells effective on 90% of cells subjected to increased concentrations of 25-100 μ M Y-27632 (197). Time course analyses found lamellipodia and filopodia formation within 10 minutes of exposure to 25 μ M Y-27632, neurite formation within 6 hours, and complete neurite extension within 24 hours in <85% of cells. Moreover, after ROCK inhibition with Y-27632, PC-12 cells showed increased concentration of F-actin along neuronal growth cones with β III-tubulin being concentrated along nascent neurites (197). Other experimental methods

have been used to dissect the role ROCKII in the CNS under pathophysiological conditions. Differentiated PC-12 cells or rat DRG neurons transfected with double negative (DN)ROCK overcome the inhibitory properties of myelin substrates, forming a greater number of growth cones and extending neurites further than untransfected controls (207). This data suggests a role for ROCKII in neurite outgrowth inhibition due to the presence MAIFs. In a rat model of unilateral cervical rubrospinal tract transection, rats injected with lentivirus (LV)DNROCK prior to injury exhibited enhanced axonal sprouting caudal to the lesion site, a finding in line with improved functional recovery in the affected limbs (208). Genetic investigation of ROCKII function *in vitro* and *in vivo* in the ROCKII^{-/-} transgenic mouse SCI models showed similar results (209). Indeed ROCKII^{-/-}-DRG neurons obtained from these mice plated on Nogo-22 peptide had significantly greater neurite outgrowth than ROCKII^{+/+} DRG neurons. Following dorsal hemisection, mice lacking ROCKII showed enhanced axonal regeneration, exhibiting sprouting of corticospinal tracts into the lesion site (209).

Thus, disinhibition of CNS axon regeneration may be induced by several experimental approaches. One approach is to create ROCK inhibitors, of which several have now been developed and vary in their selective inhibitory properties. The isoquinoline derivatives include fasudil, hydroxyfasudil, and dimethylfasudil (H-1152P), while 4-aminopyridine derivatives are Y-27632 and Y-39983. *In vitro* studies have been conducted to elucidate binding interactions and affinities for all ROCK inhibitors. For example, fasudil, inhibits both ROCKI and ROCKII by directly binding to the adenosine triphosphate (ATP) site located in the ROCK kinase domain, but also inhibits cAMP-dependent protein kinase A (PKA) and protein kinase C (PKC). H-1152P inhibits ROCK and PKA with greater affinity. Y-27632 inhibits ROCKI and ROCKII in the same manner with similar binding affinity. Y-27632 also inhibits citron kinase, PKA and PKC with lower binding affinity. Use of Rho-A and ROCK inhibitors indicate *in vitro* that neurite outgrowth inhibition can be disinhibited (191, 210). Several studies using murine SCI models have demonstrated axonal regeneration as well as locomotor recovery after inhibition of either RhoA or ROCK (190, 191, 210). For example, blocking activation of Rho-A or ROCK with the antagonists C3 transferase or Y-27632 on RGC neurons, respectively, enhanced neurotrophin factor (NTF)-stimulated axonal outgrowth on CNS myelin substrates *in vitro* and *in vivo* (189).

Several *in vivo* studies have employed ROCK inhibitors as a means to dampen the severity of various diseases, including animal models of Huntington's disease (HD), spinal muscular atrophy, neuropathic and nociceptive pain and SCI (211-215). More

recently, there have been several reports emphasising the beneficial effects of fasudil in EAE models. These reports collectively suggest various roles for ROCK inhibition. In the PLP-induced EAE model, orally or intraperitoneally (i.p.) injected fasudil resulted in amelioration of clinical signs, a decrease of inflammatory infiltrates in to the CNS, and increased axon preservation (216). Similar affects were obtained when fasudil was administered as a therapeutic at onset of PLP-EAE. Outcomes other than axonal maintenance have also been reported. In a rat EAE model provoked by immunisation with whole spinal cord, fasudil was shown to reduce BBB leakage (217). In another report using the MOG-EAE model, fasudil reduces inflammatory infiltrates in the CNS of EAE mice (218).

Of the ROCK inhibitors, fasudil has been the only derivative that has been tested in clinical trials for various human conditions. Fasudil was deemed to be safe and will now be used by Japanese patients with cerebral vasospasm following aneurismal subarachnoid hemorrhage (SAH) (219, 220). Also in clinical trials, fasudil has proved effective in acute ischemic stroke patients when administered 48 hours following stroke (221). Clinical trials investigating the efficacy of fasudil in other conditions such as carotid stenosis (NCT00670202) and atherosclerosis (NCT00120718) are underway. The intense testing of the applications of fasudil suggests that it is a "safe" drug as it does not cause adverse side effects in humans. Fasudil may indeed be a good candidate in treatments for conditions such as MS and SCI.

1.11 Collapsin response mediator protein-2 (CRMP-2)

Rho-A induces neurite outgrowth inhibition by causing retraction of microtubules and therefore facilitates growth cone collapse with the aid of key downstream modulatory molecules. One such molecule is collapsin response mediator protein-2 (CRMP-2) (222). CRMP-2 can have beneficial or detrimental effects on neurite outgrowth depending on its phosphorylation status or other post-translational modifications (Fig. 6). CRMP-2 is localized in the growth cone, the axon shaft and the cell body of neurons, and mediates neurite elongation, axonal growth and inhibition (222-224).

CRMPs are a family of cytosolic proteins present in developing and adult neurons, consisting of five members, CRMP1-5 (225-228). The CRMP family is also known as Unc-33-like proteins (Ulip), dihydropyrimidinase-related proteins (DRP), TUC (TOAD/Ulip/DRP), and dihydropyrimidinase-like (DPYSL) proteins (229). CRMPs are heavily involved in neuronal development, playing a role in mechanisms mediating cytoskeleton dynamics, including axonal guidance and axonal transport. The first

CRMP to be discovered was CRMP-2, which was found to be a part of the Semaphorin-3A-induced growth cone collapse of DRG neurons (230). CRMP-2 shares sequence homology with the Unc-33-like protein of *Caenorhabditis elegans* (230). Mutations in the *Unc-33* gene in *C. elegans* results in abnormal axonal and dendritic growth (231). The CRMPs are not only highly homologous to each other (50-75%), but are highly conserved throughout evolution, suggesting a critical role for these family members in neurons (232, 233). While all CRMPs are expressed during neuronal development, CRMP-2 remains the most abundant isoform in the adult CNS, while the expression of CRMP-1/3/4/5 are significantly downregulated (227).

The full length CRMP-2 consists of 571 amino acids, consisting of an N-terminal domain, a dihydropyrimidinase domain, a tubulin binding domain, and a C-terminal domain that can be hyperphosphorylated by various kinases (Fig. 6). CRMP-2 plays a critical role in axonal guidance, axonal elongation, neuronal polarity, axonal growth, growth cone collapse, endocytosis and vesicular transport (177, 223, 227, 230, 232, 234-239). Expression levels of CRMP-2 directly correlate with neurite outgrowth, whereby deletion of the gene in a dominant negative manner, abrogates axonal elongation (240, 241). Deletion of the CRMP-2 gene by way of siRNA also resulted in inhibition of neurite outgrowth. The C-terminal region of CRMP-2 can be phosphorylated by various kinases to modulate its activity (Fig. 6). The most studied activity of CRMP-2 phosphorylation has been its effects on growth cone dynamics by modulation of tubulin dimers or microtubules. Phosphorylation of CRMP-2 by GSK-3 β at Thr509/Thr514/Ser518 and subsequent phosphorylation by Cdk5 at Ser522 initiates regulation of cell polarity by lowering CRMP-2 binding affinity to tubulin, through the Sema-3A-induced pathway (242-244). Phosphorylation of CRMP-2 at Thr555 by ROCKII or Ca²⁺/calmodulin-dependent protein kinase II (CaMKII) also alters CRMP-2 binding affinity towards tubulin resulting in growth cone collapse (245, 246). ROCKII induced CRMP-2 phosphorylation can be triggered by either occur through MAIFs or Eph-A5 signalling. There is accumulating evidence that suggest calpain cleavage of CRMP-2 at the C-terminus can also modulate CRMP-2 activity in neurons (Fig. 6). Several studies have shown the presence of cleaved CRMP-2 product by western blot analysis (247-250). The putative calpain cleavage sites are thought to be between residues 486 and 559, the same region encompassing majority of the phosphorylation sites. Collectively these data suggest that while full length CRMP-2 mediates neurite outgrowth, post-translational modifications such as phosphorylation or cleavage of the C-terminus can change the primary function of CRMP-2 to neurite outgrowth inhibition.

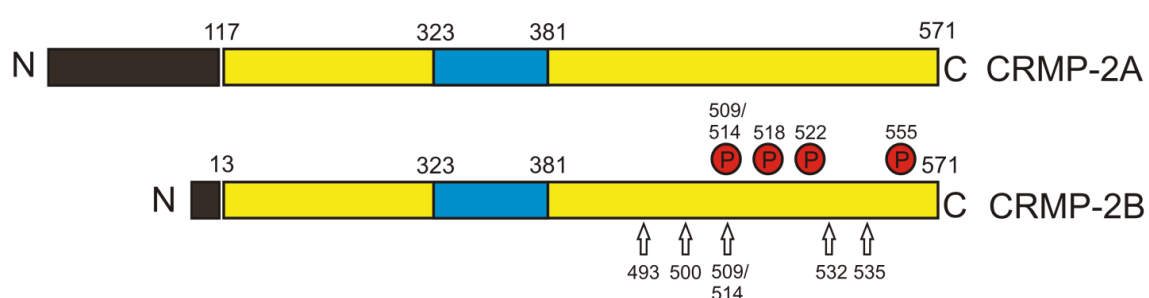


Figure 6. Structure and functional domains of CRMP-2. The alternatively spliced variants of CRMP-2 are CRMP-2A (75 kd) and CRMP-2B (62 kd). Full-length CRMP-2 is 571 amino acids in length with a dihydropyrimidinase domain and a tubulin-binding domain 323 to 381 amino acids. The CRMP-2 can be phosphorylated by specific kinases that regulate microtubule dynamics within the growing axon. The priming kinase for CRMP-2 is cyclin-dependent kinase 5 at Ser522 followed by glycogen synthase kinase 3 β (GSK-3 β) at Thr509/514 and experimentally at Ser518. The CRMP-2 can also be phosphorylated independently by Rho kinase (ROCKII) at Thr555. The CRMP-2 activity can be modulated by calpain cleavage of the C-terminus domain (calpain cleavage sites denoted by red arrows). Published in Petratos, S. et al. (2010) *J Neuropathol Exp Neurol* **69**(4): 323-334 (Appendix II).

Yuasa-Kawada et al., (2003) found that there were 2 isoforms of CRMP-2 due to alternative N-terminal splicing of the gene, producing the full length CRMP-2A of 75kDa, and CRMP-2B of 62kDa, both possessing differential expression patterns in neurons (Fig. 6). CRMP-2B expression is present in dendrites and axons, while CRMP-2A expression is axon-specific (251). This suggests the presence of an axon transport signal at the N-terminus of CRMP-2A, that is absent in CRMP-2B. The authors found differential roles of the two subtypes in neuronal morphology. Overexpression of CRMP-2B in cultured DRG neurons resulted in increased axonal branching while axonal elongation was inhibited. Co-overexpression of CRMP-2A and CRMP-2B produced the opposite effect, whereby axonal branching was inhibited and axonal elongation was induced through restructuring of microtubule dynamics. The association between CRMP-2 and tubulin have been studied extensively *in vitro*, to decipher the exact mechanism by which CRMP-2 interacts with cytoskeletal microtubules and tubulin (Fig. 7). The first line of evidence of indicating a role for CRMP-2 in microtubule dynamics was demonstrated by Gu and colleagues (252), who observed that mitotic N2a cells overexpressing CRMP-2, had strong immunoreactivity to CRMP-2 in microtubule bundles formed during mitosis. Inagaki et al (241) found that overexpression of CRMP-2 in cultured hippocampal neurons resulted in the formation of multiple axons. Furthermore, time-lapse fluorescence microscopy demonstrated that increased expression of CRMP-2 in these cells turned established dendrites in to axons, indicating a role for CRMP-2 in microtubule reorganisation. This ability was abolished in cells expressing the C-terminally truncated form Δ C548-CRMP-2 (241). Δ C381-CRMP-2 and Δ C350-CRMP-2 transfected cells exhibited shortened axons or no axons, effectively abolishing the activity of endogenous CRMP-2. These results imply that the C-terminal region of CRMP-2 may be autoinhibitory. Similar conclusions have been drawn by other authors, who demonstrated that the Δ 323-381 fragment of CRMP-2 was sufficient in suppressing microtubule assembly induced by full length CRMP-2 (222). Furthermore, residues 150-299 of CRMP-2 may also have inhibitory effects on neurite outgrowth, whereby deletion of 150-299 increase microtubule assembly *in vitro* (253). Binding assays showed that the CRMP-2(150-299) fragment had a great binding affinity to CRMP-2(450-572), indicating a possible mechanism by which CRMP-2 could modulate its own activity in microtubule assembly.

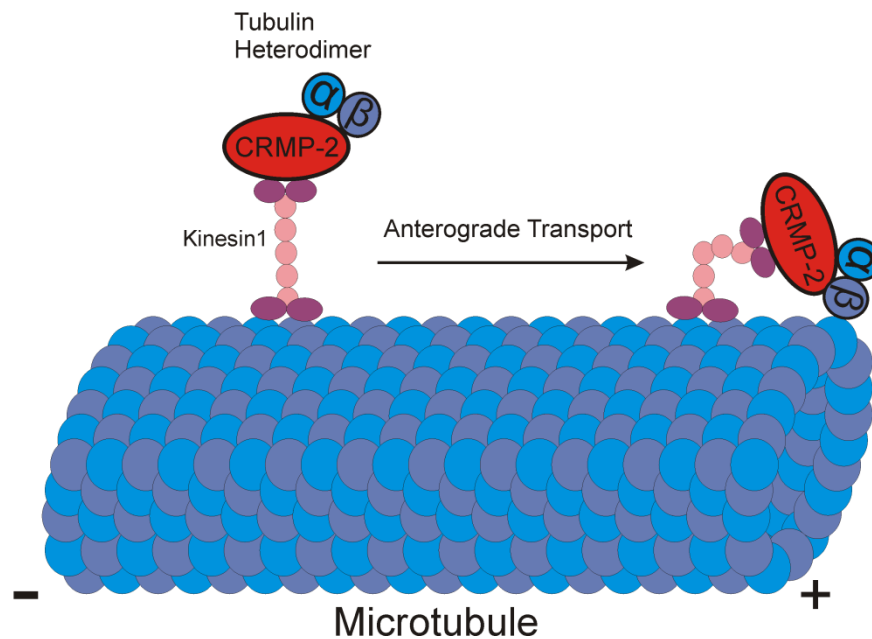


Figure 7. CRMP- 2 and its role in the axonal cytoskeleton. Anterograde transport of cargo (tubulin heterodimers) along the microtubule by CRMP-2 through interactions with kinesin-1, the primary anterograde transport protein. Published in Petratos, S. et al. (2010) *J Neuropathol Exp Neurol* **69**(4): 323-334 (Appendix II).

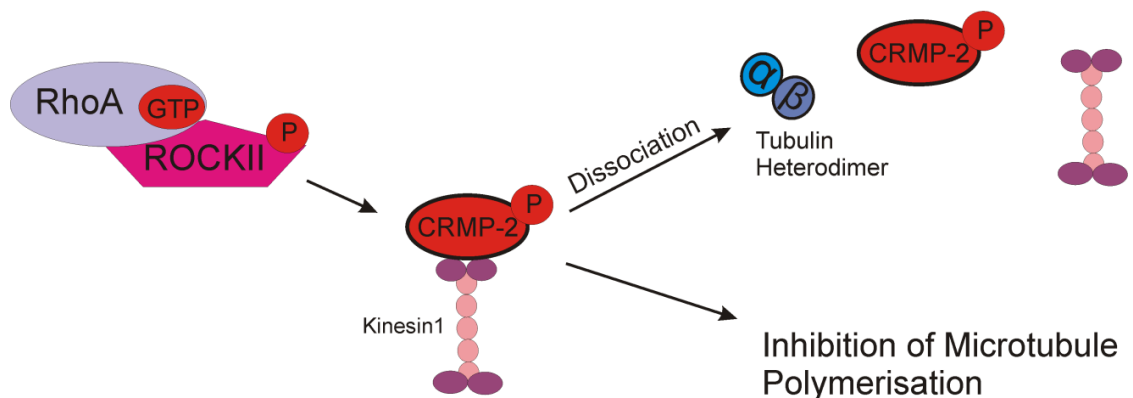


Figure 8. ROCKII modulation of CRMP-2 disrupts anterograde transport of molecular cargo. ROCKII phosphorylation of CRMP-2 at Thr555 may affect the binding of CRMP-2 to kinesin-1. Phosphorylation of CRMP-2 produces dissociation of kinesin-1 and of the α - and β -tubulin heterodimers, preventing their transport to growth ends of microtubules. This blockade of molecular cargo transported down the axonal microtubules limits the growth of the axon. Published in Petratos, S. et al. (2010) *J Neuropathol Exp Neurol* **69**(4): 323-334 (Appendix II).

In 2002, Fukata *et al.*, provided critical *in vitro* evidence that CRMP-2 binds tubulin heterodimers and promotes microtubule assembly. They incubated purified tubulin with several CRMP-2 deletion mutant constructs and observed their effects on microtubule assembly under dark field microscopy (222). While full length CRMP-2 and the N-terminally deleted CRMP-2 mutant promoted microtubule assembly, the deletion mutant lacking the C-terminal portion of CRMP-2 had no activity towards microtubule formation. Further dissection of the CRMP-2 C-terminus indicated that CRMP-2 residues 323-381 were relevant in promoting microtubule assembly, suggesting that these residues associate with tubulin. Additional analysis of CRMP-2-tubulin interactions, implicated CRMP-2 as a GTPase activating protein (GAP) for tubulin GTPase activity in differentiated PC12 cells (253). Hydrolysis of GTP by tubulin is essential for microtubule assembly (254). By using CRMP-2 deletion GST-fusion proteins, the region responsible for GAP activity towards tubulin on CRMP-2 was found to be residues 480 to 509 as determined by GTP hydrolysis assays. These data suggest that while GAP activity of CRMP-2(480-509) promotes neurite outgrowth, CRMP-2(323-381) is also capable of promoting microtubule assembly in a GTPase-independent manner. Furthermore CRMP-2 was found to influence pre-assembled microtubules, increasing the growth rate at the plus ends of microtubules. CRMP-2 is thought to function as a transporter of tubulin heterodimers as the native protein, delivering them to the assembly plus ends of nucleating sites or microtubules (Fig. 7) (222). These authors also determined that CRMP-2 had a greater affinity towards tubulin heterodimers than microtubules by a factor of 10, and proposed that CRMP-2 forms a trimeric complex with tubulin heterodimers, transporting them to plus ends of microtubules to promote microtubule assembly (222). Similar findings were also reported by Arimura and colleagues (246) who found that CRMP-2 directly binds microtubules, mediating microtubule assembly, and was observed concentrated at ends of growing axons. They too concluded that CRMP-2 had a greater affinity for tubulin heterodimers than for microtubules (246). These findings are in line with the idea that CRMP-2 can function as a transport molecule, delivering cargo to distal parts of the axon. Indeed, immunofluorescence experiments following the distribution of CRMP-2 in cultured hippocampal neurons showed CRMP-2 was preferentially expressed in the longest neurite, and support the notion that CRMP-2 is involved in axonal protein trafficking (222).

While CRMP-2 promotes neurite outgrowth in its natural active form, post translational modifications such as phosphorylation of CRMP-2 or cleavage of CRMP-2 can influence CRMP-2 activity from a growth promoting protein to a growth inhibitory

protein *in vitro* and *in vivo*. One such post translational modification is the phosphorylation of CRMP-2 at threonine-555 (Thr555) by ROCKII, transforming CRMP-2 in to a potent inhibitor of neurite outgrowth (Fig. 8) (173). Phosphorylation of CRMP-2 by ROCKII modulates CRMP-2 binding activity towards tubulin heterodimers and microtubules, but does not alter its binding capacity to actin filaments (246). Electron microscopy studies indicate that while CRMP-2 interacted with both microtubules and actin filaments around the growth cone, phosphorylated CRMP-2 lost the ability to bind microtubules (246). CRMP-2 was first identified as a substrate for ROCKII by Arimura and colleagues (240) who generated an antibody which only recognises the ROCKII phosphorylated CRMP-2 at Thr555. They further demonstrated *in vitro* that ROCKII phosphorylated CRMP-2 downstream of Rho-A in COS7 cells and chick DRG during lysophosphatidic acid (LPA)-induced growth cone collapse (240). Administration of rock inhibitors HA1077 or Y-32855 were sufficient to reverse the effects of LPA, demonstrating that ROCKII directly interacts with CRMP-2 (240). Furthermore, N1E-115 neuroblastoma cells transfected with the CRMP-2(T555A) construct had an increased tendency to transform into neurite forming cells (246). DRG neurons transfected with the same construct exhibited an increase in axon elongation (246). These data suggest that limiting ROCKII phosphorylation of CRMP-2 at Thr-555 permits neurite outgrowth.

The Rho-A/ROCKII pathway has been implicated in playing a role in inhibiting axonal regeneration in several neuropathological conditions including SCI, MS and Alzheimer's disease (AD) (216, 218, 255-257). It is therefore conceivable that ROCKII-dependent modulation of CRMP-2 via phosphorylation could be an event contributing to neurological disability for such medical conditions. While there have been a multitude of studies exploring CRMP-2 phosphorylation by GSK-3 β and Cdk5 *in vivo*, there exists only two publications that have investigated the role of CRMP-2 phosphorylation by ROCKII under neuropathophysiological conditions (173, 258), emphasising the urgency for further study in this field. In the first study, Mimura et al (173) demonstrated that addition of a Nogo-66-Fc or MAG-Fc peptide resulted in ROCKII-dependent phosphorylation of CRMP-2 in cerebellar granule neurons in a concentration-dependent manner. Introduction of ROCK inhibitors, Fasudil and Y-27632 reversed these effects, indicating that the MAIFs Nogo-66 and MAG can cause CRMP-2 phosphorylation by activating ROCKII downstream signalling (173). Transfection of cerebellar neurons with a mutant form of CRMP-2 with a single point mutation at T555A, rendered the molecule incapable of being phosphorylated by ROCKII (173). In the rat model, Mimura and colleagues showed an increase in Rho-A

activation around lesions two hours post-SCI of rats with thoracic transection injury, along with reduced polymerized levels of tubulin in areas adjacent to the lesion site (173). These findings also correlated with an increase in phosphorylated CRMP-2, two hours after SCI in the caudal and rostral regions of the injury site (173). A recovery of polymerized tubulin was observed when the site of injury was treated with Y-27632 following axotomy. The results suggest that *in vivo*, activation of Rho-A and ROCKII are activated at the site of CNS injury, whereby phosphorylation of CRMP-2 impacts on microtubule organisation and stability.

The second study investigating ROCKII-mediated CRMP-2 phosphorylation used the mouse model for Alzheimer's disease (258) triggered by administration of the β -amyloid protein ($A\beta$). First, the authors showed *in vitro* that, administration of $A\beta$ increased Rho-A activation and decreased Rac1 activation in a concentration dependent manner in human neuroblastoma SH-SY5Y cells. CRMP-2A and CRMP-2B levels increased dependent on $A\beta$ concentration. The axonal specific CRMP-2A was inhibited when Y-27632 was introduced, and its expression levels could not be recovered by addition of $A\beta$. Furthermore, they demonstrated that the increase in CRMP-2A phospho-threonine levels in $A\beta$ treated cells was not mediated by GSK-3 β , but rather by ROCKII. This effect could be reversed in the presence of Y-27632 (258). These observations correlated with a reduction in CRMP-2 binding to tubulin heterodimers, suggesting that $A\beta$ -induced CRMP-2 phosphorylation is dependent on ROCKII and affects microtubule assembly by inhibiting CRMP-2 interactions with tubulin heterodimers. In the transgenic Tg2576 mouse model of AD, Rho-A and CRMP-2 levels remained unchanged in the preclinical 6 month old mice, while post-onset at 12 and 18 months of age, there was a significant increase in Rho-A activation and CRMP-2A/B (258). CRMP-2A and CRMP-2B were also phosphorylated at 12 and 18 months age and this correlated with the reduced binding capacity of CRMP-2 with tubulin heterodimers. Collectively these studies provide a convincing argument that ROCKII mediated CRMP-2 phosphorylation may play a critical role in neurodegeneration. It is conceivable that the ROCKII/CRMP-2 pathway is activated in conditions such as SCI and MS and that this may be facilitated by MAIFs binding to the NgR1 complex, and further studies are required to test this hypothesis.

1.12 Conclusion and project aims

From decades of research, there are now four approved immunomodulatory drugs for the treatment of MS, albeit with benefits to a small percentage of patients. With less success, of the five therapeutic agents tested in phase III clinical trials for the treatment of acute SCI, only methylprednisolone has shown some neurological improvement in a subset of SCI patients. Nonetheless, this agent is still not considered to be the gold standard for acute SCI treatment, remaining controversial due to its adverse side effects. Therefore further exploration is paramount to either increase the efficacy of what is currently available or to discover new therapies that potentiate considerably improved neurological outcomes. Furthermore, it is becoming more apparent that in combination with immunomodulatory and immunosuppressive therapies, there is a need for administration of neuroprotective and neuroregenerative agents for the complete restoration of the CNS. This chapter has focused on a body of evidence which implicate MAIFs and their signalling partners as a major mechanism limiting the potential neuroregenerative capacity of the injured CNS.

Therefore the first overall aim of this thesis was to understand the mechanism of Nogo-A/NgR1 signalling, its downstream mediators and their role in neurodegeneration in SCI and EAE models. The second aim was to explore the potential of blocking Nogo-A signalling by administering therapeutic agents in SCI and EAE in promoting regeneration. In the first experimental chapter, the levels of Nogo-A deposition and ROCKII-mediated CRMP-2 phosphorylation was assessed following injury in a mouse model of SCI. Furthermore, the efficacy of LIF administration in these animals in enhancing locomotor recovery and changes in the expression of growth inhibitory or growth promoting molecules including CRMP-2 were investigated. In the second experimental chapter, whether ROCKII-dependent CRMP-2 phosphorylation is associated with EAE disease progression was examined. The expression patterns and localisation of PCRMP-2 along with its ability to transport tubulin was evaluated. In addition, function blocking Nogo-A antibody was administered to a cohort of EAE-induced animals to assess whether these changes were governed by Nogo-A/NgR1 signalling resulting in improved outcome. Nogo-A/NgR1 signalling was further characterised in the third experimental chapter by inducing EAE in NgR1 KO mice. The effects of blocking NgR1 signalling in alleviating EAE disease progression was assessed in the context of axonal injury, with a particular focus on the modulation of CRMP-2. Furthermore, to rule out the possibility of immune dysregulation in NgR1 KO mice a series of experiments were conducted to obtain an immune profile of naive and EAE-induced NgR1 KO mice, which was then compared to that of wild type controls.

Chapter 2

MATERIALS AND METHODS

2.1 Animals

Female C57BL/6 mice (aged 10-16 weeks) were bred and maintained at Monash University Animal House. Female *ngr1*^{-/-} mice on a C57BL/6 background were kindly donated and generated by Professor Strittmatter as described (259), and used throughout this study at 8-16 weeks of age. In the *ngr1*^{-/-} animals, the exon 2 of the *ngr1* gene was replaced with the NeoR cassette. Wild type littermates (*ngr1*^{+/+}) were used as controls. For routine genotype assessment, tail genomic DNA was extracted using Puregene® DNA Purification reagents (Qiagen) and PCR performed with specific primers as described in Kim et al. (259). Experiments were performed in accordance with the Australian code of practice for the care and use of animals for scientific purposes, approved by the Monash University Animal Ethics Committee and Office of the Gene Technology Regulator of Australia.

2.2 Spinal cord injury surgery and treatment

Spinal cord overhemisection surgery was done as previously described (260, 261). Briefly, a laminectomy followed by an overhemisection SCI lesion at T12 cord level, was made in C57BL/6 mice. Sham operations of animals consisted of laminectomy alone. Animals received recombinant murine LIF (AMRAD Operations) diluted in surgical saline containing 0.1% mouse serum albumin (MSA) (Sigma-Aldrich) at a daily intraperitoneal (i.p.) dose of 25 µg/kg of body weight as previously described (99, 260-262). Control animals received 0.1% MSA. LIF or MSA administration started within 2 hours following surgery.

2.3 BMS Behavioural Analysis

Mice were scored prior to surgery, and every day following spinal cord injury for two weeks (n=3 animals per treatment group), in an open-field manner using the Basso Mouse Scale (BMS) for locomotion (263).

2.4 EAE induction and Clinical parameters

To induce EAE, a total of 200µg of the encephalitogenic peptide, MOG₃₅₋₅₅ (GenScript) emulsified in 200 µl of complete Freund's Adjuvant (Sigma-Aldrich), supplemented with 4 µg/ml Mycobacterium tuberculosis was injected subcutaneously into the lower flanks, then followed with an intraperitoneal injection of 350 ng pertussis toxin (Sigma-Aldrich). Mice were injected with a second dose of pertussis toxin 48h later (104). Mice were graded daily post-MOG₃₅₋₅₅ injection (days post-injection) for disease progression (Bernard et al., 1997) corresponding to pre-onset (7 days post-injection), onset (12

days post-injection), peak (18 days post-injection) and chronic (30 days post-injection) stages of disease (in wild-type C57BL/6 mice, n = 53), respectively. Mice were monitored daily and scored clinically according to the following scale: 0, asymptomatic; 1, loss of tail tone; 2, hind limb weakness; 3, complete hind limb paralysis; 4, forelimb weakness; 5, moribund. Severely paralysed mice (Score 3–4) were killed with CO₂ inhalation; serum and tissues were then collected.

2.5 Histopathology: inflammation, demyelination and axonal degeneration/loss

For histological experiments, the animals were initially transcardially perfused with 0.1M phosphate buffered saline (pH 7.4), followed with 4% paraformaldehyde. The tissue was dehydrated in 30% sucrose for 48h. Histological evaluation was performed on 4% paraformaldehyde-fixed, O.C.T-embedded 10µm sections of cerebellum, optic nerve and spinal cord. Sections were stained using Luxol fast blue and Periodic acid Schiff (to demonstrate demyelination and inflammatory cell infiltration, respectively) and Bielschowsky silver stains (to demonstrate axonal degeneration/loss). A trained histopathologist semiquantitatively scored more than three sections per mouse, per genotype or per antibody-treated group [see anti-Nogo(623–640) antibody treatment section below] in a blinded manner. The following criteria were used to define histopathological inflammation and demyelination events respectively: 0, no inflammation; 1, cellular infiltrate only in the perivascular areas and meninges; 2, mild cellular infiltrate in parenchyma; 3, moderate cellular infiltrate in parenchyma; and 4, severe cellular infiltrate in parenchyma. The myelin breakdown was assessed by pale staining with Luxol fast blue (no evidence of remyelination) and scored in a blind fashion as follows: 0, no demyelination; 1, mild demyelination; 2, moderate demyelination and 3, severe demyelination. Images were captured in bright-field under a UPlanApo x40 1.20 NA objective lens of an Olympus Provis Ax70 microscope. The captured 16-bit images were then converted to TIFF files and the images were assembled and formatted using Adobe Photoshop vCS3 software.

For ultrastructural analysis, mice were perfused with 2.5% glutaraldehyde and 4% paraformaldehyde, dissected and the optic nerves and lumbosacral spinal cords were post-fixed. Optic nerves were embedded in resin and prepared for ultrastructural analysis of demyelination by calculating G-ratios, which is the ratio of axon diameter over the diameter of the axon and myelin sheath. Toluidine blue staining was performed and photomicrographs were then obtained from these regions using a light dotSlide™ BX51 microscope (Olympus) with a digital camera (2.3.0, RT Slider, Diagnostic Instruments, Inc.). Thickness of axons and their surrounding myelin were

measured using the MetaMorph software. At least 300 axons were measured from serial sections ($n = 3$ sections per animal and $n = 3$ animals per group) at a distance of 100 μm apart, with values expressed as mean \pm SEM. Percentage of demyelination in the optic nerve was calculated from the G-ratio data by converting the basal level of the mean ratio in the adjuvant injected *ngr1^{+/+}* control to 100%, then converting the EAE-induced mouse optic nerve ratios to a percentage relative to that basal level (260).

2.6 Splenocyte proliferation assay and cytokine analysis

MOG₃₅₋₅₅ peptide (5 $\mu\text{g}/\text{ml}$, 10 $\mu\text{g}/\text{ml}$, 20 $\mu\text{g}/\text{ml}$ concentrations respectively), CD3/CD28 and PMA/I (at 10 $\mu\text{g}/\text{ml}$ each) were coated on 24 and 96 well plates overnight. Freshly dissected spleens were cut into smaller pieces, mashed through a 70 μm mesh and the cells re-suspended in RPMI medium supplemented with 10% heat inactivated Fetal Calf Serum (JRH), 1% Sodium Pyruvate (Sigma, 100mM), 1% Penicillin/Streptomycin (Invitrogen, 10000 U/ml), 1% L-Glutamine (Invitrogen, 200 mM) and 278 μl of 0.1M β -mercaptoethanol. The spleen cells were spun at 300 rcf for 5 min at 4°C, and the supernatant aspirated. Cells were treated with Red Blood Cell Lysis buffer (0.83%NH₄Cl, 0.1% KHCO₃, 0.003% EDTA) for 3 min, spun and washed. For the 96 well plates, 0.5×10^6 splenocytes were added to each well (in triplicate), and 2.5×10^6 splenocytes were added to each well in the 24 well plate. Cytokine levels generated by splenocytes in culture derived from both female *ngr1^{-/-}* ($n=22$) and *ngr1^{+/+}* ($n=14$) mice 18 days post-MOG₃₅₋₅₅ injection, were performed by using the cytometric bead array (Th1/Th2/Th17) cytokine kit according to the company's protocols (BD Biosciences).

2.7 Isolation of mononuclear cells

Single cell suspensions of inguinal and axillary lymph nodes, thymus and spleen were prepared by gentle dissociation into sterile fluorescence-activated cell sorting (FACS) buffer (PBS/2% BSA/0.02% azide) using a 70 μm filter. Spleen cells were incubated with sterile red cell lysis buffer (Sigma-Aldrich) for 1 min and washed twice in FACS buffer (PBS supplemented with 1% FBS, 5mM EDTA, and 0.02% sodium azide) as described previously (264). Bone marrow (BM) cells were obtained by flushing tibiae and femurs with FACS buffer and a 27-gauge needle. CNS infiltrating mononuclear cells were isolated as previously described (265). Briefly, the completely dissected CNS tissue was cut to small pieces in 2ml digestion buffer (1mg/ml Collagenase D [Roche], 25ng/ml DNaseI [Qiagen]), and incubated for 1hr at room temperature. Digestion was halted with the addition of PBS. Tissue was filtered through a 70 μm mesh in FACS buffer, followed by centrifugation at 2000 rpm for 5 min at 4°C. The pellet was resuspended in 8ml 40% Percoll (Sigma), and gently layered on top of 70%

Percoll, and centrifuged at 2000 rpm for 25 minutes without break at room temperature. The mononuclear cells present at the 40%-70% percoll gradient interface were collected, washed in PBS and pelleted by centrifugation at 1500 rpm at 4°C for 5 min.

2.8 Flow cytometric analysis

For flow cytometric analysis, 1×10^6 cells were incubated with cocktails of the following primary antibodies or isotype-matched controls: FITC-anti-CD3 (145-2C11), Percp-anti-CD4 (RM4-5), PE-anti-CD8 (53-6.7), Percp-anti-B220 (RA3-6B2), FITC-anti-Gr1 (RB6-8C5), PE-anti-CD11c (HL3), APC-anti-NK1.1 (PK136) (all from BD Biosciences) and APC-anti-F4/80 (BM8) (eBioscience). All samples were analyzed using a FACS Canto flow cytometer (BD Biosciences). Post-acquisition analysis was performed using FACSDiva software. Live cell gates were estimated using 7-AAD (eBioscience) as recommended by the manufacturer.

2.9 Antibodies and reagents

The following primary antibodies were used: rabbit polyclonal anti-pThr555CRMP-2 affinity purified (generated by the authors), mouse monoclonal anti-CRMP-2 affinity purified clone (Immuno- Biological Laboratories Co. Ltd.), rabbit polyclonal anti-pThr514CRMP-2 (Cell Signalling Technology), mouse monoclonal anti-tau-5 (Calbiochem), mouse monoclonal anti-hyperphosphorylated-tau (clone AT8; Pierce-Thermo Scientific), rabbit polyclonal anti-pSer199/202-tau (Biosource), mouse monoclonal anti-NF200 (Sigma-Aldrich), mouse monoclonal anti- β III-tubulin (clone Tuj-1; Millipore-Chemicon), rat monoclonal anti- α -tubulin (Millipore-Chemicon), mouse monoclonal anti- β -actin (Sigma-Aldrich), mouse anti-human CD3 (BD Pharmingen), mouse monoclonal anti-glyceraldehyde-3-phosphate dehydrogenase (GAPDH; Sigma-Aldrich), anti-GAP-43, mouse monoclonal anti-RhoA (Millipore), mouse monoclonal anti-Rac1 antibodies (Millipore), rabbit polyclonal anti-Nogo-A antibody (Millipore), rabbit polyclonal anti-RhoA (Abcam) and mouse monoclonal SMI-31 (Covance). The following secondary antibodies were used: sheep polyclonal anti-mouse horseradish peroxidase (HRP)-conjugated affinity purified IgG, goat polyclonal anti-rabbit HRP-conjugated affinity purified IgG, goat polyclonal anti-mouse Alexa Fluor 555 affinity purified IgG, goat polyclonal anti-rabbit Alexa Fluor 488 affinity purified IgG (Molecular Probes). For immunoprecipitation experiments, the control peptides included full-length CRMP-2 and the pThr555CRMP-2 peptide (Millipore).

2.10 Production of anti-pThr555CRMP-2 polyclonal antibody

A rabbit polyclonal antibody was generated against the pThr555CRMP-2 peptide sequence [Cys-Ile550-Pro-Arg-Arg-Thr-Thr(P)-Gln-Arg-Ile-Val-Ala560] as previously reported (Arimura et al., 2000). Characterization of anti-pThr555CRMP-2 antibody was by enzyme-linked immunosorbent assay, demonstrating phospho-peptide reactivity with the affinity purified polyclonal antibody. Immunoreactivity was at 1:10 000 dilution of the anti-pThr555CRMP-2 antibody using 5 µg of the pThr555CRMP-2 peptide (Millipore) as substrate. Mouse spinal cord lysates reacted with the anti-pThr555CRMP-2 antibody by western blot showing a 62 kDa band, which was subsequently demonstrated to be CRMP-2 by mass spectrometry. The 62 kDa band immunoreactivity was blocked by preincubation of the antibody with the pThr555CRMP-2 peptide (20µg). Preincubation with the same CRMP-2 peptide without phosphorylation produced the same immunoreactive 62 kDa band demonstrating the phospho-specificity of the antibody. Incubation with the pre-bleed antiserum showed no reactivity with the 62 kDa band.

2.11 Rho/Rac Activation Assay

Assays for GTP-RhoA and GTP-Rac1 were performed using commercially available kits (Rho activation assay kit and Rac/Cdc42 activation assay kit; Millipore) according to manufacturer's instructions, and as previously described (258). Briefly, to measure activated RhoA and Rac1, tissue samples were incubated with either GTP γ S (positive control), or GDP (negative control). The lysates were then incubated with Rhotekin RBD-agarose slurry (Rho-A) or PAK-1 PBD agarose slurry (Rac-1), the beads pelleted and the resulting lysate was run on 12% SDS agarose gel. Total RhoA and Rac1 levels were measured using 5µg of tissue lysate. Samples were pooled spinal cord lysates from 3 animals per treatment group.

2.12 Preparation of tissue lysates for western blotting

The brain (including optic nerves) and spinal cord were removed and immediately snap frozen in tubes using liquid nitrogen. Spinal cord and optic nerve tissues were ground and lysed using RIPA buffer (25mM Tris•HCl pH 7.6, 150mM NaCl, 1% NP-40, 1% sodium deoxycholate, 0.1% SDS; 10%w/v) supplemented with protease inhibitor (Sigma-Aldrich) and PhosSTOP phosphatase inhibitor cocktail (Roche Applied Science) in a dounce homogenizer. Homogenates were centrifuged at 13 000 rpm for 20 min and protein concentrations of the supernatants determined using the bicinchoninic acid protein assay reagent kit (Pierce).

2.13 Amyloid- β treated human SH-SY5Y neuroblastoma cell culture, Tg2576 transgenic animals and Alzheimer's disease brain tissue

SH-SY5Y cells were cultured and differentiated with retinoic acid as previously described (258). Cells were treated with the 10 μ M amyloid- β peptide diluted in Dulbecco's modified Eagle medium: nutrient mixture F-12 (Invitrogen) for 24h. The cells were then lysed using cell lysis buffer and then run on a 12% sodium dodecyl sulphate polyacrylamide gel. Transgenic Tg2576 female mice at 18 months of age, along with human Alzheimer's disease frontotemporal brain tissue were used as positive controls for the tau phosphorylation and hyperphosphorylation western blot studies. Sarcosyl-insoluble tau preparations were prepared as previously described (266, 267).

2.14 Sarcosyl gradient centrifugation

Sarcosyl-insoluble tau preparation was done as previously described (266, 267) Briefly, lumbosacral spinal cords were homogenized in a 10x volume of high salt buffer of 10mM Tris (pH 7.4), 0.8M sodium chloride, 1mM EGTA, 10% sucrose (w/v). The extracts were centrifuged at 45000g for 30 min, supernatants collected and pooled, then subjected to another extraction with a 5x volume of the same buffer. The pooled supernatant fraction was incubated with 1% sarcosyl for 1h then centrifuged at 260000g for 1h at 4°C. The resulting pellet represented the sarcosyl insoluble tau preparation.

2.15 Western immunoblotting

We loaded and ran 5 μ g of protein on a 4–12% graded SDS polyacrylamide gel (Invitrogen). Proteins were then electrophoretically transferred onto polyvinylidene fluoride membranes (Millipore). The membranes were blocked with 5% skimmed milk powder and the primary antibodies diluted in this blocking buffer (polyclonal anti-pThr555CRMP-2, 1:1000; monoclonal anti-CRMP-2, 1:1000; anti- α -tubulin, 1:1000; anti- β -actin, 1:5000; anti-pThr514CRMP- 2, 1:1000; anti-tau5, 1:1000) were incubated overnight at 4°C. After washing the membranes in 0.1% v/v Tris-buffered saline-Tween, the secondary anti-rabbit (1:1000), anti-sheep (1:1000), anti-mouse (1:1000) or anti-rat (1:1000) HRP-conjugated antibodies were incubated for 2h at room temperature. Immunoreactive proteins were detected using an ECL PlusTM chemiluminescence method (Amersham). The level of immunostaining was determined by image analysis after scanning the exposed films using AlphaImager (Alpha Innotech) and then processing the 16-bit monochrome images through the ImageQuant TLTM v2003

software (Nonlinear Dynamics, Ltd.) to measure pixel intensity relative to background. The level of staining was normalized with β -actin or α -tubulin and expressed as arbitrary units. Percentages of band levels were also derived by setting the controls as 100% and the test samples were determined to be elevated or reduced from this basal level. All protein bands were analysed from at least four separate samples and statistics then performed (as described below).

2.16 Immunoprecipitation

To measure the level of total CRMP-2 or α -tubulin prior to immunoprecipitation of CRMP-2, 5% of the starting amount was run on a 4–12% graded SDS polyacrylamide gel. Protein A-Sepharose beads (Millipore) and Protein G Sepharose beads (Millipore) were blocked using PBS-BSA buffer (1% w/v) overnight with at 4°C using a rotator. All immunoprecipitation assays were performed from samples containing 100 μ g of total protein in 1 ml of lysate buffer. Immunoprecipitation was facilitated by adding 2 μ g of polyclonal anti-pThr555CRMP-2 or monoclonal anti-CRMP-2 (IBL) capture antibody to each sample. Rabbit IgG or mouse IgG was used as negative controls and the positive control included pThr555CRMP-2 peptide with the anti-pThr555CRMP-2 antibody. Samples were incubated overnight at 4°C followed by the addition of 70 ml of a 50% slurry of Protein A-Sepharose beads (Millipore) for incubations with polyclonal anti-pThr555CRMP-2 antibody or 70 ml of 50% Protein G Sepharose beads (Millipore) for incubations with monoclonal anti-CRMP-2 antibody. The samples were then washed with RIPA buffer and centrifuged 4x at 10000g, 4°C for 5 minutes and the supernatant was removed after each repeat. Following the last wash, 25 μ l of 2x SDS loading sample buffer was added to each sample and incubated at 95°C for 5 minutes to dissociate the beads. Samples were loaded onto a 4–12% SDS polyacrylamide gel and then transferred onto a polyvinylidene fluoride membrane for immunoblotting.

2.17 Immunofluorescence

Mouse cryostat sections following transcardial perfusion of the mice with 4% paraformaldehyde, the lumbar enlargements of the spinal cords were removed and embedded in O.C.T (Tissue-Tek® Sakura Finetek Inc.). Serial 10 μ m thick longitudinal sections were then cut on a cryostat (CM 1900, Leica Microsystems) and mounted on Superfrost Plus® slides (Menzel-Glaser). The tissue was initially incubated with blocking buffer (phosphate-buffered saline supplemented with 3% goat serum, 3% mouse serum and 0.3% Triton X-100) for 2h at room temperature. The sections were incubated with primary antibodies in blocking buffer overnight at 4°C. The samples were washed three times in phosphate-buffered saline (pH 7.4) for 10 min, followed by

2h incubation with secondary antibodies (goat anti-mouse Alexa Fluor 488, goat anti-rabbit Alexa Fluor 555; Invitrogen) at room temperature. After three washes with phosphate-buffered saline, the sections were stained with 40,6-diamidino-2-phenylindole (DAPI; Molecular Probes) for 10 min, washed and cover-slipped using fluorescent mounting medium (Dako). Primary antibodies used were mouse anti- β III-tubulin (1:500), mouse anti-NF200 (1:200), rabbit anti-pThr555CRMP-2 (1:200), rabbit anti-Nogo-A antibody (1:200), rabbit anti-RhoA (1:200) and SMI-31 (1/100). Images were captured by fluorescence with an UPlanApo x40 1.20 NA objective lens of an Olympus Provis Ax70 microscope.

2.18 Therapeutic anti-Nogo(623-640) antibody treatment of EAE-induced mice

Anti-Nogo(623–640) affinity purified antibody was produced as described previously (104) and concentrated at 1 μ g in 0.2 ml for in vivo use. Three intravenous administrations of this antibody at Days 8, 11 and 14, and two intraperitoneal injections on Days 9 and 16 were performed in post-MOG_{35–55} EAE-induction in adult C57Bl/6 mice (n = 4). A control administration of non-specific affinity purified rabbit IgG was also performed at the same time-points and routes of administration (n = 4) as the anti-Nogo(623–640) antibody-treated group. Another group received no antibody administration (n = 4). Clinical progression data are expressed as mean \pm SEM.

2.19 Statistics

For the spinal cord injury study, one-Way ANOVA and Tukey's post-hoc tests were used to analyse differences in optical densities between groups for western blots as determined by ImageQuant software. A One-Way Repeated-Measures ANOVA was done to analyse differences in clinical scores between the two groups. The *P* value of 0.05 was set as the threshold for significance.

For studies conducted using the EAE model, data were analysed using Graph Pad Prism v3.02 software. A one-tailed Student's t-test or a one-way ANOVA with Tukey's post hoc test was used to determine statistical significance ($P < 0.05$) at a 95% confidence level for optical density levels obtained from immunoblot analysis.

For flow cytometry analysis, all values are expressed as mean \pm standard error of the mean (SEM). Statistical analysis was performed using Prism 5.04 GraphPad Software. Unless otherwise specified, statistical comparison between genotypes was performed using a Wilcoxon-Mann-Whitney comparison test. A *P* value less than 0.05 was considered statistically significant.

Chapter 3

LIF-TREATMENT REDUCES NOGO-A DEPOSITS IN SPINAL CORD INJURY MODULATING RHO GTPASE ACTIVITY AND CRMP-2 PHOSPHORYLATION

3.1 Abstract

We have previously shown that systemically administered leukaemia inhibitory factor (LIF) following overhemisection SCI in the mouse, prevents oligodendrocyte death and secondary demyelination. Here we report that prevention of oligodendrocyte death by LIF-treatment reduces Nogo-A deposits above and below the transection site. This finding is associated with modulation of Nogo-A-dependent signalling whereby active Rho-A (GTP-Rho-A) is decreased and the levels of its downstream target, the phospho-Thr555-collapsin response mediator protein-2 (pThr555CRMP-2), are reduced in the white matter in axons near the lesion. The potential for axonal growth in LIF-treated animals is enhanced through upregulation of the neurite growth-related molecules GAP-43 and GTP-Rac1. These findings suggest a mechanism by which exogenous LIF can promote axonal growth in the mammalian spinal cord following injury, by providing a permissive tissue environment for endogenous regrowth.

3.2 Introduction

A contributor of the poor regenerative capacity of the adult CNS following injury is the presence of factors in the extracellular environment that inhibit neurite growth (69). These factors include an important component of myelin, Nogo-A, which has been most widely studied as an inhibitor of axonal regrowth (77, 268). Specific domains of Nogo-A are believed to mediate its inhibitory effects on neurite outgrowth. These are the extracellular Nogo-66 domain (77), and the amino-Nogo domain that can also be located extracellularly (146, 154, 269). The strong inhibitory effect of Nogo-A is demonstrated by the finding that Nogo-A/B mutant mice, following hemisection SCI, exhibit: heavy sprouting rostral to the lesion site; regenerating fibres through the lesion; and recovery of locomotor function, compared to their wild type counterparts (77, 270). Furthermore, Nogo-A inhibition by the use of either the IN-1 antibody or monoclonal IgG antibodies have been reported to promote axonal regeneration in animal models of SCI and stroke respectively (271, 272). Inhibition of the Nogo receptor 1 (NgR1) can also increase regeneration/sprouting of corticospinal tract fibres following pyridotomy (154). Thus it would seem that Nogo-A signalling has detrimental downstream effects under neuropathological conditions in the CNS.

Nogo-A signals through a tripartite receptor complex (273), the stimulation of which leads to activation of Rho-A (146). Active, or GTP-bound Rho-A (GTP-Rho-A) then activates ROCKII (194), which induces depolymerisation of actin (270) and actin-myosin contractility promoting neurite collapse (271). Another Rho GTPase, Rac1 (272), opposes GTP-Rho-A, inducing neurite extension (273). Rho GTPases, in addition to modulating the actin microfilaments at the growth cone, can also modulate tubulin assembly in the core region of the outgrowing neurite (100). CRMP-2 is an important phosphoprotein governing microtubule dynamics (252) and mediating axonal extension (225). ROCKII is known to phosphorylate CRMP-2 at the threonine 555 residue, thereby inactivating this molecule, disabling its capacity to bind tubulin heterodimers, and contributing to growth cone collapse (100). Mimura and co-workers have recently reported that in spinal cord injury, MAG, another inhibitory myelin protein that signals through NgR, predominantly NgR2, can activate ROCKII and induce phosphorylation of CRMP-2 in axons (92, 173). Therefore, preventing CRMP-2 phosphorylation by ROCKII could be an avenue by which regeneration is encouraged.

Following the primary spinal cord injury, the ensuing pathophysiological changes at and around the lesion site cause progressive secondary injury, whereby loss of oligodendrocytes and subsequent deposition of myelin debris further escalate the

neurodegenerative response (268, 274, 275). Oligodendrocyte apoptosis and axonal loss, as well as diminished axo-glia trophic support must be overturned in order to limit demyelination and promote regeneration. Leukemia inhibitory factor (LIF) is a neuroregulatory cytokine which has been shown to have neuroprotective properties. Binding of LIF to its cognate LIF receptor β complex activates JAK/STAT pathways, which in turn promote transcription of prosurvival molecules (276-279). LIF has recently been shown to induce increased uptake of myelin debris by macrophages in the injured CNS via the activation of the JAK/STAT pathway (279). Furthermore, therapeutic administration of LIF in a mouse model of SCI promotes oligodendrocyte survival (280). Moreover, our laboratory has previously reported that systemic administration of LIF following overhemisection SCI in the mouse, prevents the secondary wave of oligodendrocyte apoptosis, via the Akt/cIAP2 pathway (260). LIF administration resulted in an overall preservation of mature oligodendrocytes and minimised the spreading of demyelination during secondary injury. As a consequence, deposition and accumulation of myelin debris were also reduced in LIF treated animals (260), suggesting that an environment with increased regenerative capacity is achieved and this is in part modulated by LIF following SCI. As such, it is feasible that LIF administration may hinder the effects of myelin inhibitory proteins such as Nogo-A by promoting the clearance of myelin debris from the CNS, thus reducing Nogo-A/NGR1-induced axonal degeneration. Therefore, we investigated the molecular events driving axonal changes in our T12 overhemisection model of SCI and whether the administration of the cytokine, LIF, can alter the downstream signalling occurring after injury. In this study, we report that oligodendrocyte survival, and hence preservation of myelin, following SCI reduces Nogo-A deposits in LIF-treated spinal cords, which correlates with the upregulation of active Rac1 and downregulation of GTP-Rho-A levels. Furthermore, we show that phosphorylation of CRMP-2, a downstream target of Rho-A and the critical determinant of tubulin assembly at the growth cone (100, 139), is downregulated as a result of LIF-treatment in mammalian SCI.

3.3 Results

3.3.1 LIF-treatment reduces Nogo-A deposits in SCI

Nogo-A is an integral oligodendrocyte and myelin protein that is acutely upregulated at the lesion site and exerts strong inhibitory effects on regeneration following SCI (100, 152). We investigated levels of Nogo-A in spinal cords of transected animals with and without LIF administration by immunohistochemistry and western blot analysis. We found that in contrast to the LIF-treated group, MSA-treated animals had extensive Nogo-A deposits 1 week after SCI, particularly at the lesion site but also rostral and caudal to it (Fig. 1AB). At the two-week time point, the reduction in Nogo-A deposition by exogenous LIF was not as marked. To quantitate the levels of Nogo-A in the different treatment groups, western blots of spinal cord lysates were probed with an anti-Nogo(623-640) polyclonal antibody generated by us (104) (Fig. 1CD). The reduction of Nogo-A expression in the spinal cord by LIF-treatment at the 1 week time-point was found to be statistically significant both caudal and rostral to the lesion site ($*P < 0.01$), comparable with the sham treated groups. These results indicate that administration of LIF following SCI decreased the abundance of Nogo-A deposits that are otherwise the result of oligodendrocyte death and demyelination.

3.3.2 Exogenous LIF supports molecular signalling events promoting axonal regrowth

Since LIF decreased myelin deposits after SCI, we investigated the potential for neurite regeneration. The GTPase-related, growth associated protein (GAP)-43 is a protein that is acutely upregulated upon axonal growth cone extension (281). We found that GAP-43 was increased in the spinal cord in LIF- compared to the MSA-treated groups at both 1 and 2 weeks following SCI (Fig. 2A). To specify this regenerative response with LIF-treatment, we investigated the levels of the Rho family of small GTPases which can be activated downstream of NgR/P75NTR/LINGO-1 (139). We found that levels of GTP-Rho-A were reduced in the LIF-treated group at the 1 and 2 week time-points (Fig. 2A). Furthermore, the activity of Rac1, that can potentiate neurite outgrowth through actin polymerisation 1, was increased in LIF-treated animals 1 week, but not at 2 weeks post-SCI (Fig. 2A). To directly investigate ROCKII mediated phosphorylation of CRMP-2 we probed for phospho-Thr555-CRMP-2 on western immunoblots. CRMP-2 was phosphorylated at the Thr555 residue (the ROCKII site) in response to injury, but this phosphorylation was significantly reduced by LIF-treatment 1 week, but not 2 weeks, following SCI (Fig. 2B).

Figure 1. LIF-treatment following SCI decreases Nogo-A deposition and acutely down-regulates its expression. A) Illustration which shows the grey matter (GM) and the white matter (WM) and the proximity of the lesion site to the areas imaged. B) Expression of Nogo-A in the spinal cord, as demonstrated by immunofluorescence using an amino-Nogo-A antibody, was significantly reduced in LIF-treated animals particularly at the 1 week time-point following SCI both rostral (R) and caudal (C) to the lesion. This difference was particularly marked at the lesion site and in the segment rostral to the lesion site. Magnification bar = 50 μ m. Arrows denote strongest immunostaining of Nogo-A deposits. Asterix denotes cavity-filled cysts appearing in MSA-treated animals at the injury site, at 2 weeks post-SCI. C) Representative immunoblot showing the expression of Nogo-A in the treatment groups showing a marked reduction in Nogo-A in lysates of both rostral and caudal segments of the spinal cord 1 week post-injury. D) Densitometric analysis of C) demonstrating a significant decrease in Nogo-A expression in the LIF treated 1 week group, at both caudal and rostral to the lesion site, compared to the MSA treated groups at the same time point (n=3, * P < 0.01). Published in Azari, M. et al. (2008) JNDR **135**: 1794-1818 (Appendix III).

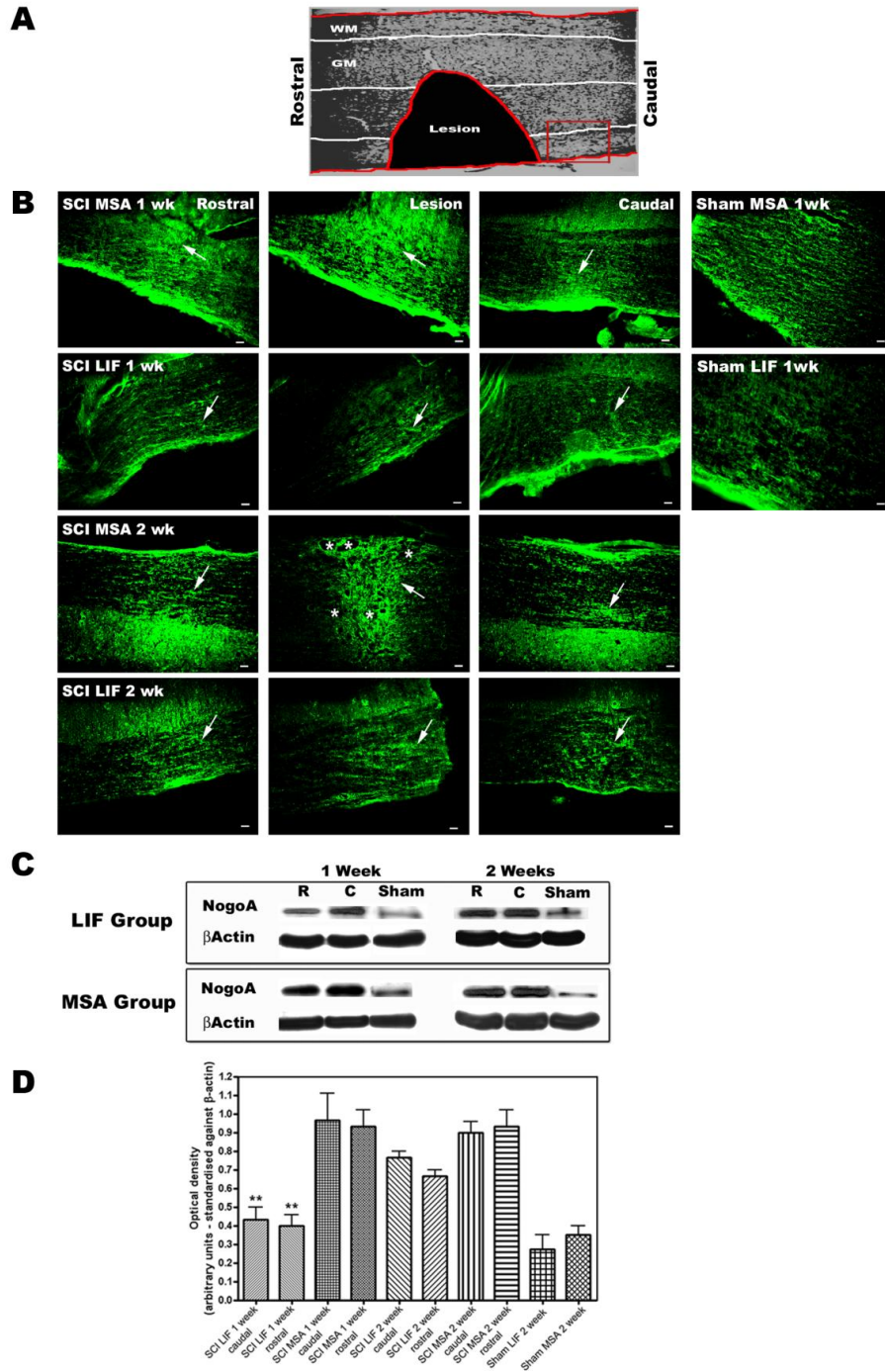
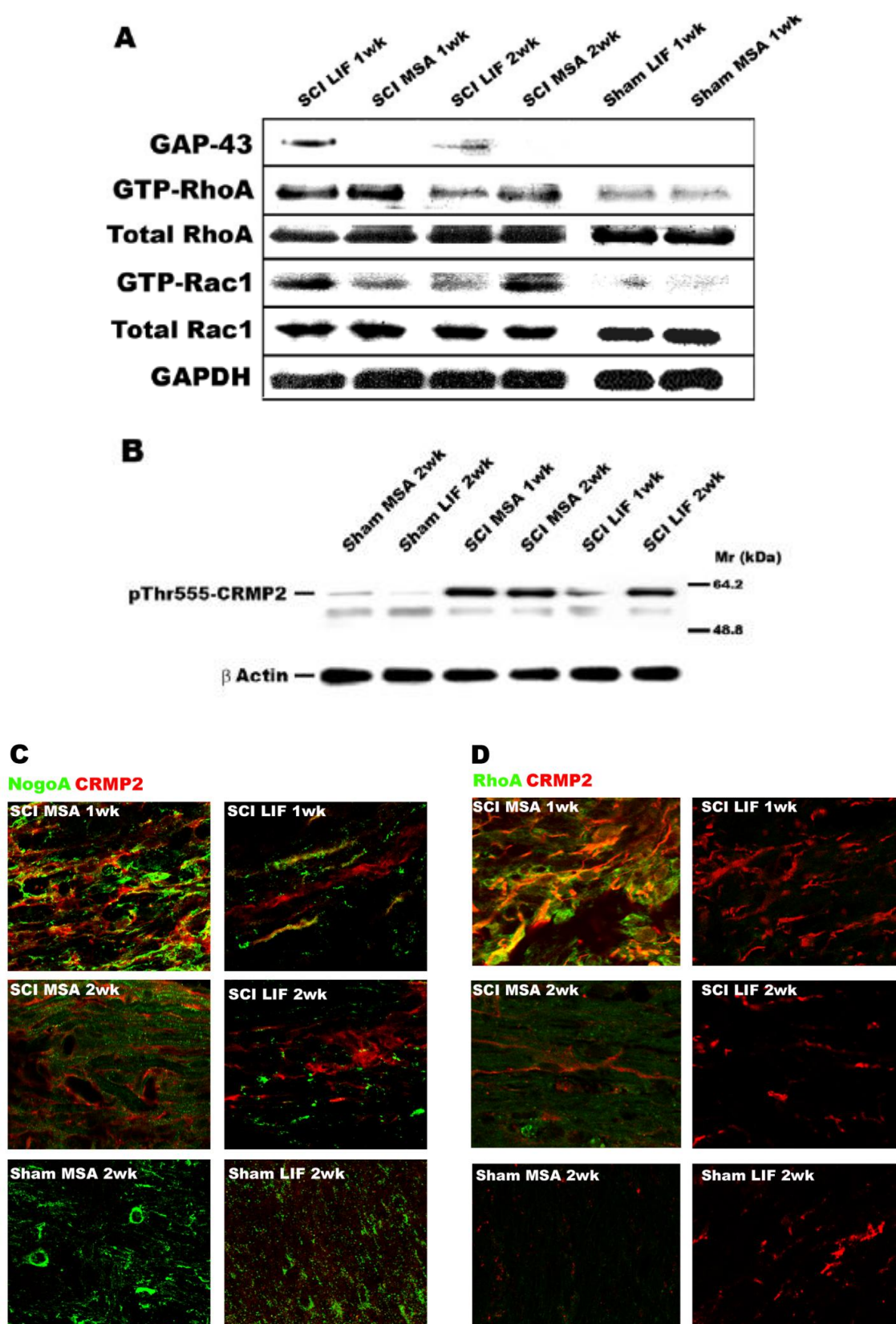


Figure 2. Modulation of GAP-43 expression, Rho-A activation, and CRMP-2 phosphorylation by exogenous LIF in SCI. A) Expression levels of GAP-43 were increased at 1 and 2 weeks post SCI as a result of LIF treatment in the spinal cord. LIF-treatment also decreased levels of active (GTP-bound) Rho-A while increasing levels of GTP-Rac1 at the 1 week time-point (A). Interestingly, at the 2 week time-point, LIF-treated animals showed decreased Rho-A activation while Rac1 activation was also found to be decreased. B) The 62 kDa splice variant of CRMP-2 was found to be phosphorylated as a result of injury by western blot analysis using a phosphospecific antibody that recognised the residue phosphorylated by ROCKII (Thr555). This phosphorylation event was acutely reduced one week following SCI. C) CRMP-2 expression was increased at the site of the lesion, where Nogo-A deposits were imaged, in the MSA group, while administration of LIF reduced these levels. D) Expression of Rho-A, and its target CRMP-2, was increased as a result of injury around the site of the lesion, as demonstrated by immunohistochemistry. However, exogenous LIF reduced these levels, predominantly at the 1 week time-point. Moreover, the cellular localisation of CRMP-2 changed with LIF-treatment. The expression pattern in MSA-treated mice was diffusely cytoplasmic whereas in LIF-treated mice, it was more punctate, resembling endosomal localisation. n=3 per group; magnification bar = 20 μ m. Published in Azari, M. et al. (2008) JNDR **135**: 1794-1818 (Appendix III).



To determine the cell specific effects of LIF-treatment on the putative downstream targets of Nogo-A signalling, Rho-A and CRMP-2, we probed spinal cord sections with Nogo-A and either Rho-A or CRMP-2 antibody by immunofluorescence. There was a reduction in the levels of CRMP-2 near the lesion site in LIF-treated animals compared to the MSA-treated group (Fig. 2C and 2D). We also found that increased Rho-A immunofluorescence was greatly reduced in LIF-treated animals (Fig. 2D). Taken together, these data suggest that molecular markers of axonal regeneration are acutely upregulated with LIF-treatment in the spinal cord following injury.

3.3.3 Systemically administered LIF promotes locomotor recovery following SCI in mice

To determine whether LIF-mediated modulation of molecular markers of axonal regeneration were associated with improved locomotor recovery from SCI, we scored mice according to the BMS scale (263). We show that in contrast to the vehicle-treated group, the LIF-treated mice continued to improve following the first week post-SCI. Using a repeated measures ANOVA, the locomotor difference between the LIF-treated and MSA-treated groups was found to be statistically significant ($*P < 0.05$). These data, together with our previous published data (260), suggest that LIF promotes locomotor recovery in SCI by preventing oligodendrocyte death and demyelination, thereby regulating molecular mechanisms that promote axonal regrowth.

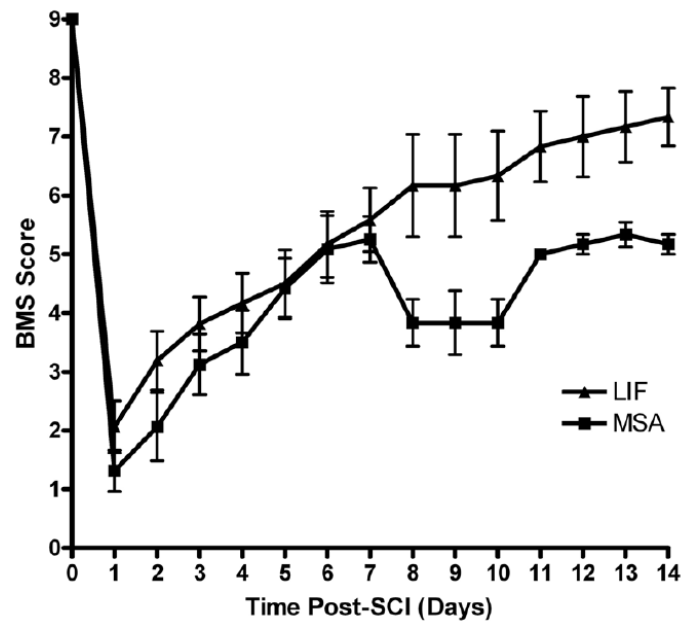


Figure 3. Exogenous LIF enhances locomotor recovery from SCI in mice. Locomotor status of mice was rated in an open-field set-up according to the Basso Mouse Scale (BMS). In contrast to vehicle-treated mice, the locomotor recovery of mice treated with LIF continued beyond the first week following SCI. (n=3 per group; * $P < 0.05$). Published in Azari, M. et al. (2008) *JNDR* **135**: 1794-1818 (Appendix III).

3.4 Discussion

As a consequence of mature oligodendrocyte death in injury and disease models, degraded myelin proteins are deposited throughout the primary and secondary injury sites (69, 260). Deposition of these proteins forms a barrier and aborts regeneration of transected neurites (69). We have previously reported that LIF-treatment decreases demyelination in SCI by reducing the death of oligodendrocytes (260). Furthermore, in a mouse model of MS, EAE, it has been shown that endogenous LIF mRNA expression is increased during acute inflammatory demyelination (282). This study further demonstrated that anti-LIF antibody administration which blocks endogenous LIF in two models of EAE resulted in a significant increase in disease severity, marked by a two-fold increase in oligodendrocyte apoptosis (282). These data indicate a role for LIF in preserving oligodendrocyte survival in CNS injury. However, in culture, LIF has been shown to promote the survival of oligodendrocytes and neurons (283-285). Furthermore, LIF has been demonstrated to rescue motor neurons following axotomy *in vivo* (286, 287). Recent emerging data by Gresle and colleagues (288) provided strong evidence that endogenous LIF protects axons in acute EAE. The authors found that following induction of EAE in LIF/CNTF double KO mice on a C57Bl/6 background resulted in increased EAE severity, reduced axonal integrity in the optic nerve, and decreased axon densities in the spinal cord, which was accompanied by detection of increased phospho-neurofilament (pNF-H) in the serum, a well known marker for axonal degeneration (288, 289). Collectively, these data suggest an equally important role for LIF in oligodendrocyte survival and axonal integrity in the CNS under pathophysiological conditions (Fig. 4A). We have previously reported reduced MBP deposits in mice receiving systemic LIF after being subject to overhemisection SCI (260). In line with these findings, here, we show that in SCI exogenous LIF prevents deposition of myelin proteins, particularly Nogo-A in the initial phase of injury. This suggests that LIF administration may limit the amount of secondary damage occurring at and around the lesion site and thereby creating an extracellular environment that may be more permissive to axonal regrowth (Fig.4).

The receptor required to signal Nogo-A-dependent neurite collapse is NgR1, which binds the C-terminal extracellular domain of Nogo-A known as Nogo-66 at nanomolar concentrations (99). This interaction leads to reciprocal activation of the small GTPases Rho-A and Rac1 which modulate the actin-myosin interaction of growth cone microfilaments governing neurite extension and/or collapse (69). In this study, LIF-treatment of animals following SCI caused an increase in GAP-43 in the spinal cord, a molecule known to be in abundance in extending growth cones of regenerating axons

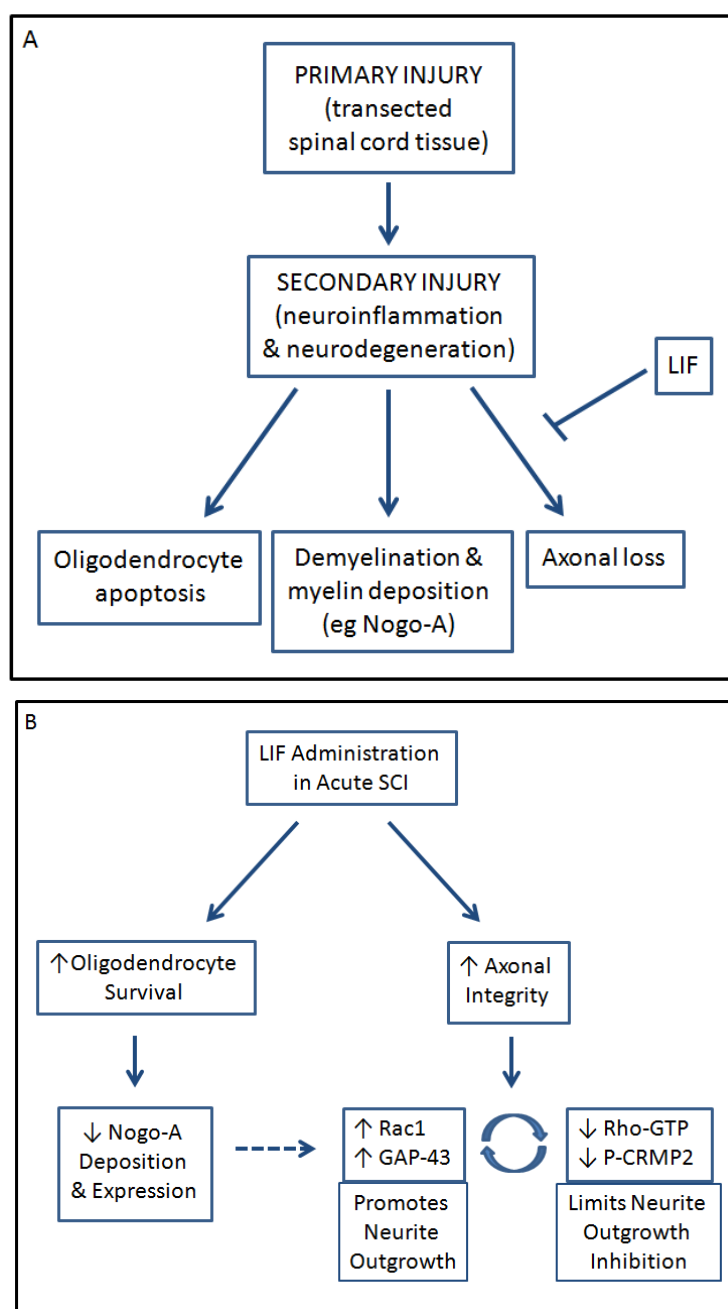


Figure 4. Concept mechanism of action of exogenous LIF in acute SCI. A)

Flow diagram depicting the outcomes of primary and secondary SCI under pathophysiological conditions. LIF treatment can inhibit these outcomes. B) In acute SCI, exogenous LIF results in increased oligodendrocyte survival and therefore reduced myelin debris (eg. Nogo-A). This positively affects axonal integrity whereby growth promoting Rac1 is activated and its growth inhibitory counterpart Rho-GTP is inactivated. This provides an environment where neuroregeneration can occur.

(281, 290). Furthermore, our observation that LIF decreased GTP-Rho-A and at the same time increased GTP-Rac1, at the 1 week time-point in the spinal cord advocates that LIF can promote neurite extension following SCI.

We also report that LIF-treatment acutely reduces ROCKII-mediated phosphorylation of CRMP-2 (i.e. PThr555-CRMP-2, a key mediator of neurite retraction events (241, 261)), at 1 week but not 2 weeks post-SCI. These data correlate with our previous study, which showed a reduced pro-survival effect of LIF in oligodendrocytes 2 weeks post-injury, and our current finding of increased Nogo-A deposits at this time point. The reduction in ROCK II-mediated phosphorylation of CRMP-2 in the first week following SCI together with reduced Nogo-A deposition, may allow for enough time to promote regrowth of axons in the spinal cord. LIF-treatment has been reported to result in improved locomotor recovery from SCI in mice (261). Consistent with these findings, we also observed that LIF-treatment promoted locomotor recovery as measured by BMS scores. These data suggest that preservation of oligodendrocytes immediately after primary SCI by LIF-administration may result in a window of opportunity for activation of regenerative mechanisms, and in parallel, inhibition of degenerative mechanisms whereby improved locomotor recovery by LIF-treatment is the result. While both LIF- and MSA-treated groups showed improved locomotor function in the first week post-SCI, the LIF-treated animals recovering abilities well surpassed that of MSA-treated animals in the second week post-SCI. In line with this theory, we found reduced Nogo-A deposits as well as reduced GTP-Rho-A activity and downstream to these molecules, inhibition of ROCKII-dependent CRMP-2 phosphorylation in LIF-treated animals at 1 week post-SCI. This correlated with Rac1 activation and increased GAP-43 expression both of which are known to promote regeneration. While most of these effects were diminished at 2 weeks post-SCI, GAP-43 expression was still upregulated in the LIF-treated animals, suggesting a sustained relationship between regeneration and improved locomotor recovery in these mice.

Collectively, our data are consistent with the notion that exogenous LIF promotes axonal regeneration in the mammalian spinal cord after injury. LIF decreases myelin debris and as such Nogo-A deposits at the site of the lesion, thereby reducing the potential for Nogo-A signalling in the spinal cord. In particular, we have shown that LIF-treatment has the capacity to modulate Rho GTPase activity, and prevent the inactivation by phosphorylation of CRMP-2, an important molecule governing tubulin dynamics in regenerating axons. These changes in the tissue milieu are likely to result in an environment that is more permissive to endogenous axonal regrowth in the initial

phases of injury. We therefore propose a function and mechanism of action for exogenous LIF in acute SCI (Fig. 4B). Systemic administration of LIF following SCI promotes oligodendrocyte survival, and consequently a reduction in myelin debris. This may have a negative impact on myelin derived inhibitory signalling whereby growth promoting molecules such as Rac1 and GAP-34 are activated. In contrast, the activity of inhibitory molecules such as Rho-GTP and PCRMP-2 are diminished. The acute effects of LIF-administration could therefore be utilized in a therapeutic setting and therefore warrants further investigation.

Chapter 4

ROCKII-DEPENDENT CRMP-2 PHOSPHORYLATION IS ASSOCIATED WITH EAE DISEASE PROGRESSION

4.1 Abstract

Axonal degeneration is considered to be a major contributor of the neurological deficit experienced by MS patients. However, little is known of the signal transduction pathways involved in neurodegenerative mechanisms governing neurological decline. We explored the involvement of CRMP-2, a regulator of axonal growth, in axonal degeneration in MS and its animal model, EAE. We found that CRMP-2 was altered by way of phosphorylation in EAE and MS tissue compared to respective controls. Here, we show for the first time that CRMP-2 is phosphorylated by ROCKII in EAE and MS, and is localised to neurodegenerative axons at lesion sites. Furthermore, we blocked CRMP-2 phosphorylation in EAE with therapeutic administration of Nogo A antibodies. These data suggest that Nogo-A can promote neurodegeneration in EAE by signalling through phosphorylation of CRMP-2.

4.2 Introduction

As discussed in the literature review, the molecular mechanisms governing axonal loss in MS are not well defined. An animal model of MS, EAE, has been extensively studied to understand the pathological and neurological aspects contributing to disease severity and outcome. In particular, the MOG₃₅₋₅₅ peptide-induced EAE mouse model display the pathological hallmarks of MS, evidenced by gradual ascending paralysis. Pathological analysis of post-mortem MS lesions by Trapp and colleagues (55) indicated the presence of transected axons in acute and chronic active lesions, demonstrating that axonopathy is an early event in MS. Similarly, findings from our laboratory have indicated axonal changes prior to onset of disease in the MOG-EAE model (104, 291). Therefore axonal injury contributes to neurological deficit in MS patients. However, neurological decline is generally not observed in patients in the initial stages of disease. This is due to the presence of compensatory regenerative mechanisms that are in play, such as aberrant sprouting and remyelination of denuded axons. Overtime, these mechanisms are overpowered by an increase in disease severity resulting in observable deterioration as axonal integrity is compromised.

NgR1 inhibitory signalling and its key downstream components may be pivotal in understanding axonal degeneration and neurological decline in EAE, and by implication in MS. One such molecule downstream of NgR1 is CRMP-2. Under physiological conditions, CRMP-2 has been shown to promote neurite outgrowth in vitro in hippocampal neurons (222). Studies have clearly defined this mechanism and found CRMP-2 to be a transporter molecule of tubulin heterodimers in the direction of plus ends of microtubules, which promotes microtubule assembly and neurite outgrowth (222, 252). Upon NgR1 signalling, phosphorylation of CRMP-2 by ROCKII at the Thr-555 residue, blocks CRMP-2 mediated microtubule assembly inhibiting neurite outgrowth.

In chapter 3, we demonstrated that LIF treatment alleviates the severity of SCI, resulting in decreased Nogo-A deposition, and thus reducing ROCKII mediated CRMP-2 phosphorylation. The role of CRMP-2 phosphorylation through activation of NgR1 signalling by MAIFs in the EAE model, however, has not yet been explored. We hypothesised that one degenerative mechanism contributing to the development of EAE may involve the phosphorylation of CRMP-2 by ROCKII, blocking tubulin transport by CRMP-2. We generated a polyclonal P-Thr-555-CRMP-2 (PCRMP-2) antibody that specifically recognises the ROCKII phosphorylated isoform of CRMP-2. We found increased expression of PCRMP-2 in injured axons in EAE animals compared to

controls at all sampled disease time points. CRMP-2 phosphorylation was most prominent at peak stage of disease. This correlated with a decrease in tubulin-bound CRMP-2 in the spinal cord lysates of these animals. Furthermore, we demonstrate that administration of an anti-Nogo antibody as a therapeutic means ameliorated disease severity and correlated with a reduction in ROCKII mediated CRMP-2 phosphorylation and increased CRMP-2 binding to tubulin. These results indicate a role for CRMP-2 in axonal degeneration in EAE and MS, providing a link between MAIFs and their mediation of CRMP-2 activity.

4.3 Results

4.3.1 Clinical and histological development of MOG-EAE

Clinical course of EAE was determined by injecting mice with MOG₃₅₋₅₅ peptide in CFA and clinical severity was monitored and recorded daily for 30 days using well established score criteria (Fig. 1). Animals which scored 3.5 or higher were euthanized. The EAE clinical course in this cohort was typical to what has been reported previously (104, 166). The animals were sacrificed at four stages of disease; preonset, onset, peak and chronic (Fig. 1A; Table 1.). Analyses of the clinical scores obtained from EAE induced animals indicated a high disease prevalence rate of $\geq 85\%$ at onset, peak and chronic stages, confirming the efficient pathogenicity of the MOG₃₅₋₅₅ immunogen in the induction of EAE in this cohort (Table 1.). The mean clinical score was greatest at peak stage of EAE (mean clinical score 3.11). By the chronic stage EAE mice displayed some clinical recovery, with a reduced mean clinical score of 2.71. We then characterised the histopathological manifestations of EAE progression in these mice (Table 1.). Semiquantitative evaluation of inflammation and demyelination was performed by staining 10 μ m thick longitudinal sections with Luxol fast blue and Periodic acid Schiff (LFB/PAS), a stain which reveals inflammatory demyelination, of the cerebellum and three regions of the spinal cord (cervical, thoracic and lumbosacral), scoring according to stringent histological criteria in a blinded fashion. The cerebellum was less affected by EAE than the spinal cord, demonstrating equal or lower inflammation and demyelination from onset to chronic stages of disease, attributable to the nature of EAE (also a limitation) as a disease of ascending paralysis. Also in line with this result, the lumbosacral cord provided with intensive pathophysiological manifestation when compared to the upper thoracic and cervical regions of the cord, showing signs of inflammation even as early as preonset stage of EAE.

To observe the pathological hallmarks individually, histological staining of longitudinal sections for the lumbar cord of control and EAE mice with LFB/PAS and Bielschowsky Silver stain was performed (Fig. 1B). The gradual loss of LFB staining indicated progressive demyelination, and correlated with increased PAS staining demonstrating accumulation of inflammatory infiltrate with disease severity. Significant/extensive axonal degeneration and axonal loss was observed at peak and chronic stages of EAE, however, axonal swelling was evident as early as onset of EAE. Loss of the bielschowsky silver staining indicative of the dysregulation of axons of the white matter correlated with inflammatory demyelination.

Table 1: Clinical and histopathological scores in adult female C57BL/6 EAE mice.

Post-induction MOG ₃₅₋₅₅ EAE	Prevalence	Mean Clinical Score	Histopathological parameter	Lumbosacral spinal cord	Thoracic spinal cord	Cervical spinal cord	Cerebellum
Adjuvant-Injected Control	0/16	0 ± 0	<i>I</i>	0 ± 0	0 ± 0	0 ± 0	0 ± 0
			<i>D</i>	0 ± 0	0 ± 0	0 ± 0	0 ± 0
Pre-onset	0/53	0 ± 0	<i>I</i>	0.25 ± 0.20	0 ± 0	0 ± 0	0 ± 0
			<i>D</i>	0 ± 0	0 ± 0	0 ± 0	0 ± 0
Onset	37/43	0.79 ± 0.08	<i>I</i>	1.5 ± 0.33	1.25 ± 0.29	1 ± 0	1 ± 0
			<i>D</i>	0.5 ± 0.33	0.25 ± 0.29	0 ± 0	0 ± 0
Peak	26/29	3.11 ± 0.11	<i>I</i>	2.5 ± 0.26	2 ± 0	1.25 ± 0.22	1.25 ± 0.22
			<i>D</i>	1.25 ± 0.22	1 ± 0	0.25 ± 0.22	0.25 ± 0.22
Chronic	12/14	2.71 ± 0.33	<i>I</i>	2.75 ± 0.43	2.75 ± 0.22	2.25 ± 0.43	1.5 ± 0.26
			<i>D</i>	2.0 ± 0.37	1.75 ± 0.22	1.25 ± 0.43	0.5 ± 0.26

I: inflammation; D: demyelination. Published in Petratos, S. et al. (2012) *Brain* **135**: 1794-1818 (Appendix I).

4.3.2 Expression profile of Nogo-A and CRMP-2 are altered in EAE

It has previously been reported that Nogo-A expression is increased in oligodendrocytes surrounding MS lesions (97). Therefore we investigated whether Nogo-A expression was modified at onset, peak and chronic stages in EAE. 10µm thick longitudinal sections of the lumbar spinal cord of control and EAE mice were immunostained with anti-Nogo-A antibodies and visualised under a fluorescence microscope (Fig. 2A). Fluorescence immunoreactivity for Nogo-A increased in parallel with development of EAE. Predominant expression of Nogo-A was observed in what morphologically appeared to be oligodendrocyte cell bodies. These findings give rise to the possibility that some of the Nogo-A-positive staining may be attributable to the accumulation of Nogo-A deposits in the spinal cord. Next we investigated the possible changes in the expression profile of total CRMP-2 and Rho-A in the cerebellum of EAE induced mice at the peak stage of disease by immunofluorescence studies (Fig. 2B). 10µm cross sections of cerebellum from EAE induced animals at the peak stage and corresponding control animals were immunostained with monoclonal pan-CRMP-2 and polyclonal Rho-A antibodies and visualised under a confocal microscope. Peak stage was chosen to get a measure of events occurring during the height of the disease clinical symptoms. In the adjuvant injected controls, Rho-A was predominantly expressed by granule cells in the nuclear layer, while the purkinje cells of the molecular layer showed high expression of CRMP-2 in the cell body and dendrites, appearing as

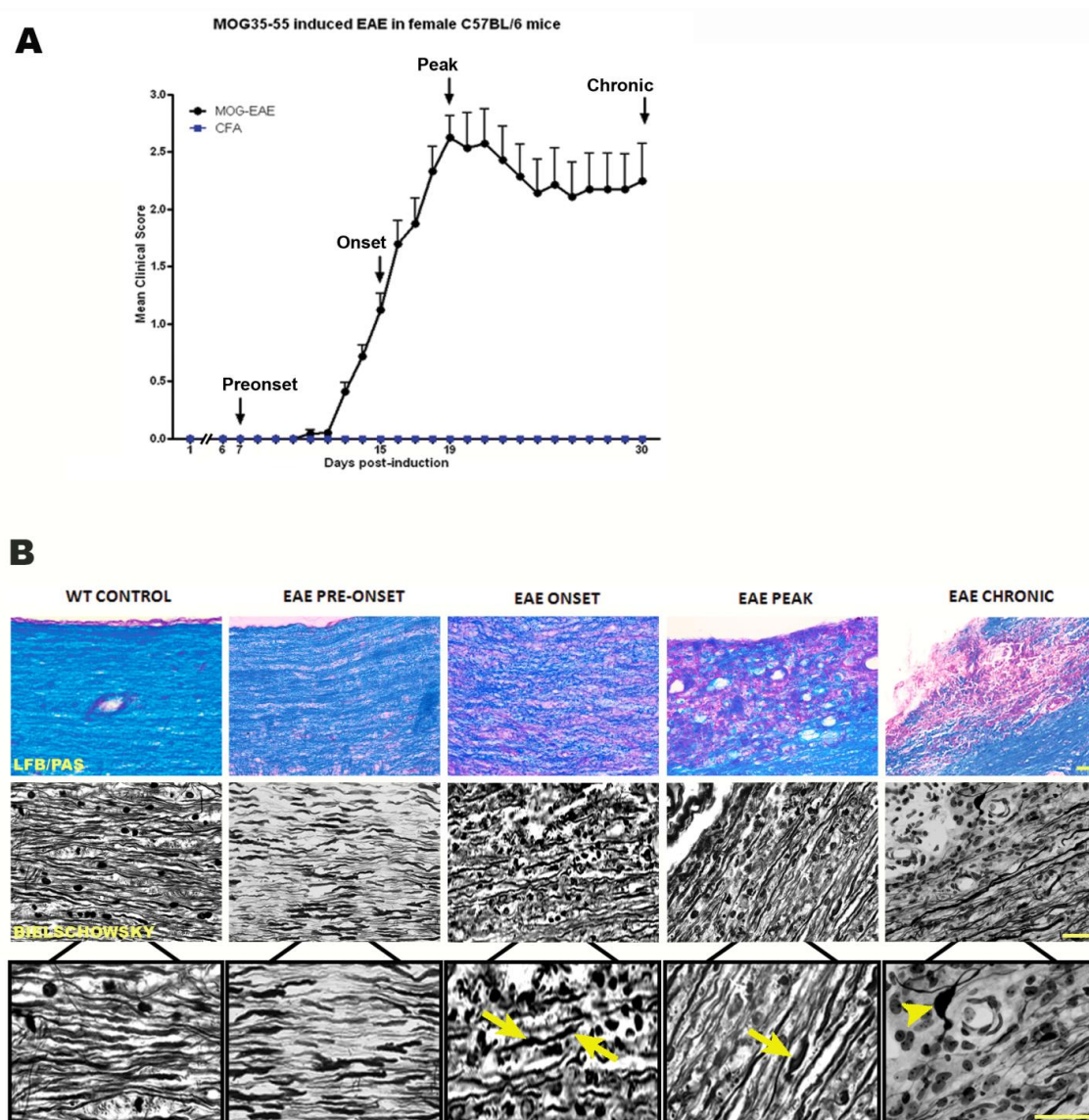


Figure 1. Clinical and histological progression of EAE disease after MOG₃₅₋₅₅-induction. A) Progression of EAE disease after MOG₃₅₋₅₅-induction represented with increasing mean clinical score of C57BL/6 female mice. Specific time-points of pathological progression are shown on the graph (black line), as pre-onset (7 days post-induction [dpi]; n=53 mice), onset (12-15 dpi; n=43 mice), peak (18 dpi; n=29 mice) and chronic (30 dpi; n=14 mice) stages of disease, respectively (arrows). Control mice included those injected with adjuvant alone (blue line). B) Histopathological progression of EAE at pre-onset, onset, peak and chronic stages of disease. LFB/PAS stain demonstrates inflammatory demyelination and Bielschowsky silver stain demonstrates axonal degeneration/loss (arrows show axonal swelling; arrow head shows an axonal retraction bulb). n=3 per group. Magnification bar=20 μ m. Published in Petratos, S. et al. (2012) *Brain* **135**: 1794-1818 (Appendix I).

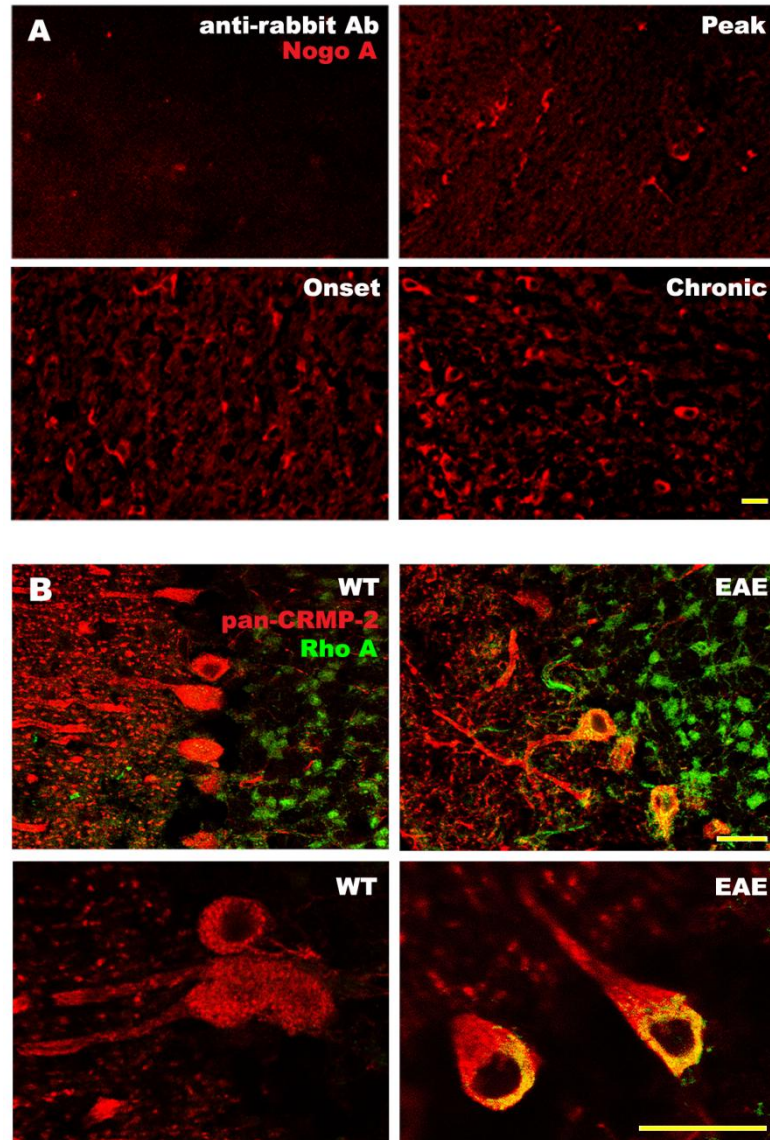


Figure 2. Expression profile of Nogo-A, Rho-A and CRMP-2 are altered in EAE. A) Time course immunoreactivity of polyclonal Nogo-A antibody in 10 μ m lumbar spinal cord sections of EAE mice at onset, peak and chronic stage of disease. B) 10 μ m cerebellar sections from WT and EAE mice counterstained with pan-CRMP-2 (red) and Rho-A (green) at peak stage of disease. n=3 per group; Magnification bar = 20 μ m.

punctate or clumped structures. In the peak EAE animals, the expression profile of CRMP-2 and Rho-A are altered in the cerebellum. CRMP-2 appeared to have a more diffuse profile and is co-expressed with Rho-A around the cell body. These results indicate that Rho-A is activated in purkinje cells and that the expression profile of CRMP-2 is modified in the purkinje cell body in EAE. Perhaps an increase in CRMP-2 expression results in CRMP-2 to appear diffuse.

Granule cells do not appear to constitutively express CRMP-2 in EAE or control animals. While granule cells do express Rho-A, this expression appears to be upregulated in EAE animals compared to controls in peak EAE.

4.3.3 Generation of ROCK-II specific P-CRMP-2 antibody

Observing an increase in Nogo-A expression in the spinal cord of EAE animals, as well as changes in the expression profiles of CRMP-2 and Rho-A in the cerebellum at peak EAE raised the question whether these events were constituents of the NgR1 signalling pathway. One such connection could be made if the level of ROCKII dependent phosphorylation at Thr-555 of CRMP-2 can be determined in EAE animals, since ROCKII activation can be initiated by NgR1. Since Thr-555-P-CRMP-2 (PCRMP-2) antibodies were not commercially available, we generated our own affinity purified rabbit polyclonal anti-Thr-555-P-CRMP-2 antibody against the PCRMP-2 peptide sequence [Cys-Ile550-Pro-Arg-Arg-Thr-Thr(P)-Gln-Arg-Ile-Val-Ala560] as previously reported (240). We characterised the anti-PCRMP-2 antibody by enzyme-linked immunosorbent assay (ELISA) and western blot analysis (Fig. 3). First, the immunoreactivity of the generated PCRMP-2 antibody against the phospho-Thr-555-CRMP-2 peptide was tested by ELISA. The level of antibody binding was determined by titrating the antibody against increased concentrations of PCRMP-2 peptide (0-4µg) (Fig. 3A). At higher concentrations (1:100 - 1:1000) the PCRMP-2 antibody immunoreactivity was very high and was somewhat maintained even at 1:10000 dilution. However, the antibody showed negligible immunoreactivity to pan-CRMP-2 peptide, even at high concentrations of 1:100 (Fig. 3B), indicating the specificity of the PCRMP-2 antibody. We characterised the antibody further by Western immunoblot analysis (Fig. 3C). 10µg of total protein from C57BL/6 wild type spinal cord lysates are probed with PCRMP-2 antibody. Anti-PCRMP-2 antibody recognised two bands around 62 kDa, corresponding to CRMP-2B. To determine the specificity of the antibody, preincubation of the antibody with the PCRMP-2 peptide abolished immunoreactivity, while this could not be demonstrated with anti-PCRMP-2 antibody preincubation with pan-CRMP-2 peptide, confirming the specificity of our PCRMP-2 antibody in only

recognising the ROCKII phosphorylated form of CRMP-2. As further controls we tested prebleed rabbit IgG with and without PCRMP-2 peptide preincubation, which also did not produce immunoreactivity, further confirming antibody specificity.

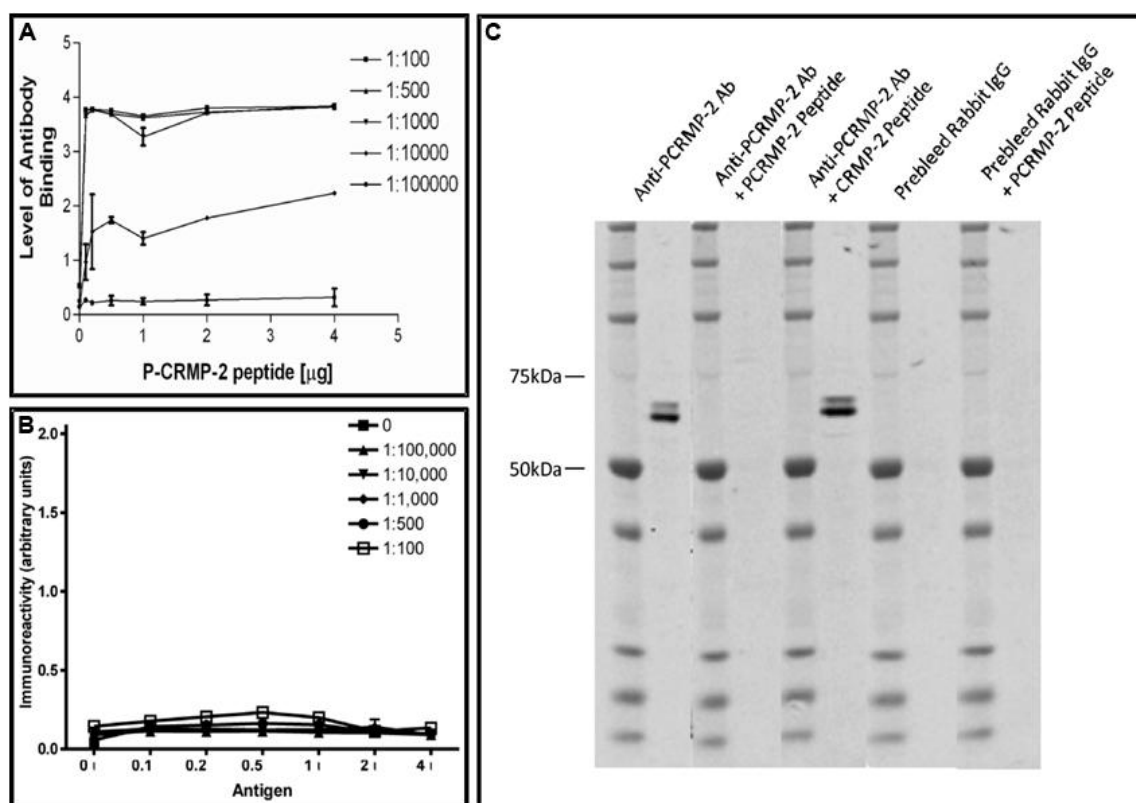


Figure 3. Characterisation of polyclonal pThr555CRMP-2 Antibody. A-B) Immunoreactivity and specificity of the PCRMP-2 antibody against increasing concentrations of the A) PCRMP-2 peptide and; B) pan-CRMP-2 peptide as determined by ELISA. C) Western immunoblot showing reactivity of PCRMP-2 antibody in spinal cord lysates. PCRMP-2 immunoreactivity is blocked in the presence of antibody specific PCRMP-2 peptide, which cannot be demonstrated using the pan-CRMP-2 peptide. n=3 per group

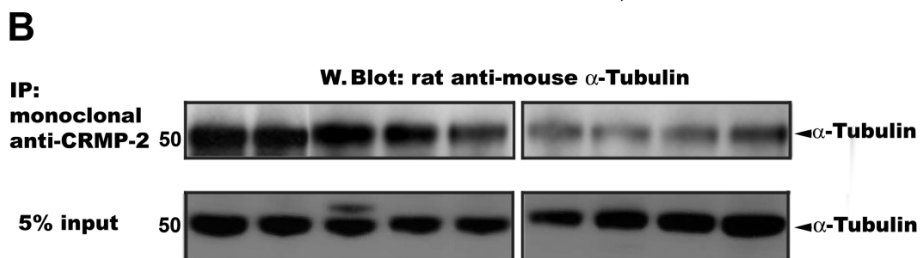
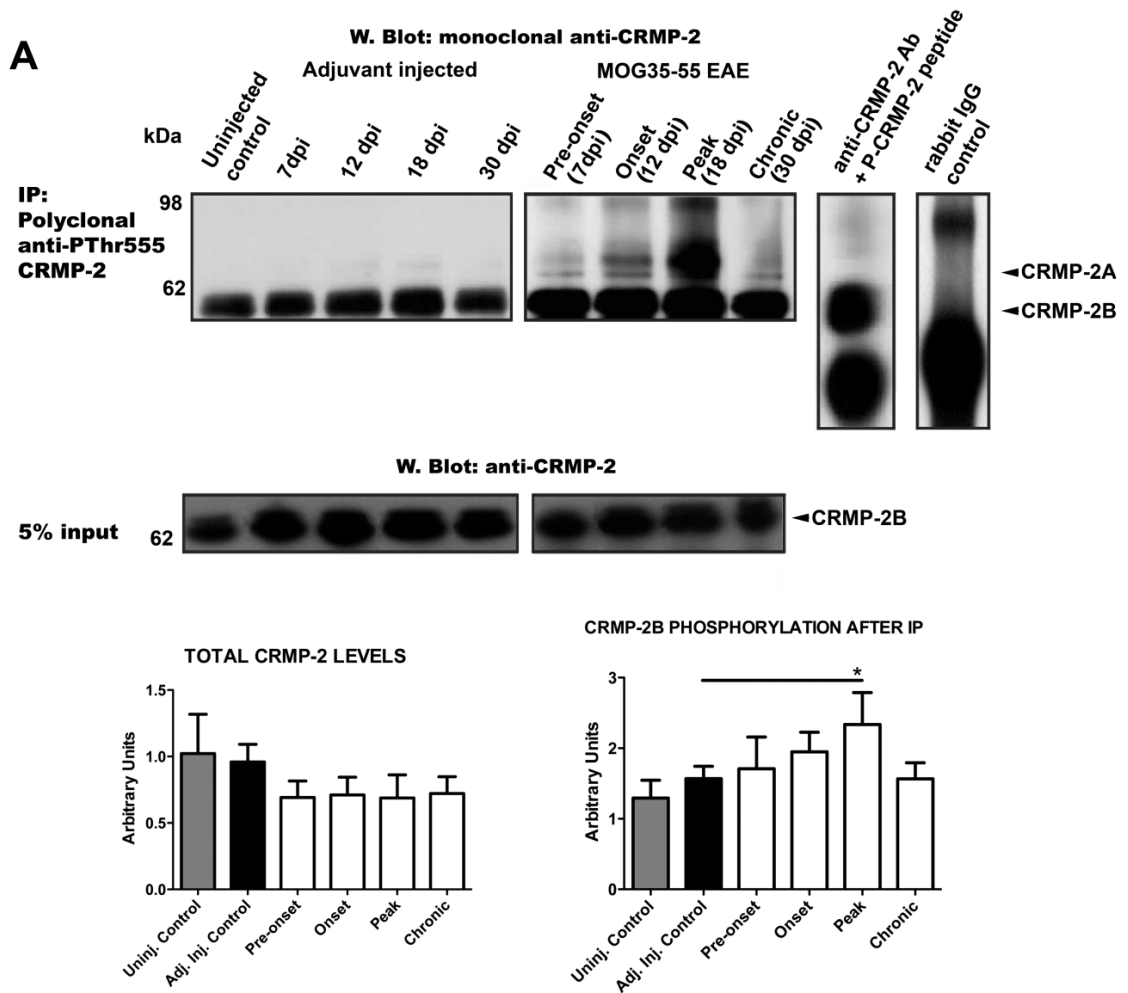
4.3.4 Disease Severity Correlates with increase in ROCKII phosphorylated CRMP-2

An increase in ROCKII dependent CRMP-2 phosphorylation was previously reported to be associated with axonal degeneration following SCI (173). We hypothesised that the same molecular mechanisms may also play a role in EAE induced axonal degeneration. We chose to investigate the lumbosacral region of the spinal cord as this region displayed the highest histopathological scores for inflammation and demyelination. Lumbosacral spinal cord tissue lysates from EAE induced, adjuvant injected and uninjected controls were prepared and used in immunoprecipitation assays (Fig. 4). To determine CRMP-2 phosphorylation, PCRMP-2 was immunoprecipitated using our generated polyclonal PCRMP-2 antibody. These samples were then probed with monoclonal pan-CRMP-2 by western immunoblot to compare differences in phosphorylation status of CRMP-2 between EAE and control groups at the determined time points. To confirm specificity of the PCRMP-2 antibody we used rabbit IgG, and anti-pan-CRMP-2 antibody spiked with PCRMP-2 peptide as negative and positive controls, respectively. The uninjected control and adjuvant injected control lysates tested had similar levels of ROCKII dependent CRMP phosphorylation, which suggests that the adjuvant alone has no effect on CRMP-2 phosphorylation (Fig. 4A) .

Following EAE induction, there was an increase of PCRMP-2B in spinal cord lysates when compared with adjuvant-injected controls (Fig. 4A). We found an incremental increase in CRMP-2 phosphorylation in EAE animals from preonset to peak stages with a drop in phosphorylation at chronic stage of disease. CRMP-2B phosphorylation was significantly higher at peak EAE compared to adjuvant injected controls ($*P < 0.05$ one way ANOVA). Interestingly levels of CRMP-2 phosphorylation mimicked the mean clinical scores obtained for each stage of EAE in these animals. Furthermore, we found an increase in the level of the axonally specific pThr555 N-terminal variant of CRMP-2, i.e. CRMP-2A, in EAE-induced mice that could not be demonstrated in the adjuvant injected controls (Fig. 4A). pThr555CRMP-2A expression pattern was similar to that of CRMP-2B. CRMP-2A phosphorylation was most prominent in peak EAE, the time point which presents with most severe clinical symptoms. 5% input samples, which were taken pre-immunoprecipitation were probed with monoclonal pan-CRMP-2 to determine total CRMP-2 levels. Total CRMP-2B levels were reduced in EAE animals at all time points, however this was not found to be statistically significant (Fig. 4A). These results collectively suggest an association of CRMP-2 phosphorylation with disease progression and axonal degeneration.

Figure 4: Phosphorylation of CRMP-2 correlates with axonal degeneration in EAE.

A) Immuno-precipitation of PCRMP-2 using our polyclonal anti-pThr555-CRMP-2 antibody, of lumbosacral spinal cord lysates, dissected from wild-type MOG₃₅₋₅₅-induced EAE, uninjected control or adjuvant injected alone control mice, followed by western immunoblot analysis using the monoclonal anti-CRMP-2 antibody. Control wells include non-specific rabbit IgG polyclonal antibody and pThr555 CRMP-2 (20 µg) peptide spiked in lysate buffer alone. The membranes were then reprobed using the monoclonal anti-CRMP-2 antibody. Western immunoblot for CRMP-2 from spinal cord lysate samples loaded pre-immunoprecipitation (5% input of immunoprecipitation sample) using the monoclonal anti-CRMP-2 antibody. Densitometric quantification (AU) of total CRMP-2 and pThr555 CRMP-2B (after immunoprecipitation) from spinal cord lysates of control and EAE-induced mice (n = 4 mice per group and per time-point; * $P > 0.05$ one-way ANOVA). B) Co-immunoprecipitation of CRMP-2-associated tubulin was performed from control and EAE-induced spinal cord lysates using monoclonal anti-CRMP-2 antibody followed by western immunoblotting with rat anti-mouse α -tubulin. Total loading levels of tubulin for each spinal cord sample pre-immunoprecipitation were demonstrated by loading 5% input of total protein (from the same samples illustrated in this figure pre-immunoprecipitation) and then probing the western transfer membrane with the rat anti-mouse α -tubulin monoclonal antibody. Published in Petratos, S. et al. (2012) Brain **135**: 1794-1818 (Appendix I).



In vitro studies have demonstrated that CRMP-2 can bind tubulin heterodimers, transporting them to plus ends of microtubules during neurite outgrowth (222, 252), and this interaction was inhibited after ROCKII phosphorylation of CRMP-2 (240). We therefore explored the idea that CRMP-2 phosphorylation may contribute to disease progression by limiting tubulin transport and thereby limiting axonal regeneration in EAE. Using lumbosacral spinal cord lysates from control and EAE animals, we coimmunoprecipitated CRMP-2 bound tubulin using monoclonal pan-CRMP-2 antibody and analysed by western immunoblot using rat anti- α -tubulin antibody (Fig. 4B). 5% input samples, which were taken pre-coimmunoprecipitation were probed with anti- α -tubulin antibody to determine total tubulin levels were similar between control and EAE spinal cord samples. CRMP-2 bound tubulin levels were decreased at all stages of disease compared to controls. Taken together, these results indicate that an increase in ROCKII dependent CRMP-2 phosphorylation which correlates with disease progression may exert its effects on axonal degeneration by limiting transport of tubulin heterodimers, which would be required for axon cytoskeletal reorganisation and positive growth.

4.3.5 CRMP-2 is only phosphorylated in degenerating axons

Our results so far suggested a possible role for CRMP-2 phosphorylation in the progression of EAE by promoting axonal degeneration. These results raised the question whether phosphorylation occurred in all axons or a subset of axons which may be doing through the process of axonal degeneration. To precisely localise PCRMP-2 in EAE, we conducted immunofluorescence experiments whereby 10 μ m thick longitudinal sections of the lumbar spinal cord of control and EAE mice were coimmunostained with anti-PCRMP-2 and β III-tubulin antibodies, and counterstained with DAPI to detect areas of hypercellularity, indicative of lesion sites, and visualised under a fluorescence microscope (Fig. 5A). β III-tubulin is a neuron-specific marker of disassembled, monomeric tubulin, which is also indicative of axonal degeneration. Co-expression of PCRMP-2 with β -III-tubulin was not found in adjuvant injected control animals. PCRMP-2 and β III-tubulin immunoreactivity was present at all stages of EAE. Moreover, there was an incremental increase in PCRMP-2 immunoreactivity and β III-tubulin reactivity with increasing disease severity. Minimal levels of β III-tubulin was detected at preonset stage of EAE, there was only partial co-expression of PCRMP-2 in β III-tubulin positive axons, suggesting that mechanisms governing ROCK-II dependent CRMP-2 phosphorylation are activated before clinical symptoms of EAE manifest. At onset stage of EAE a greater majority of β III-tubulin positive axons also co-expressed PCRMP-2. Co-expression was most intense at peak stage of EAE,

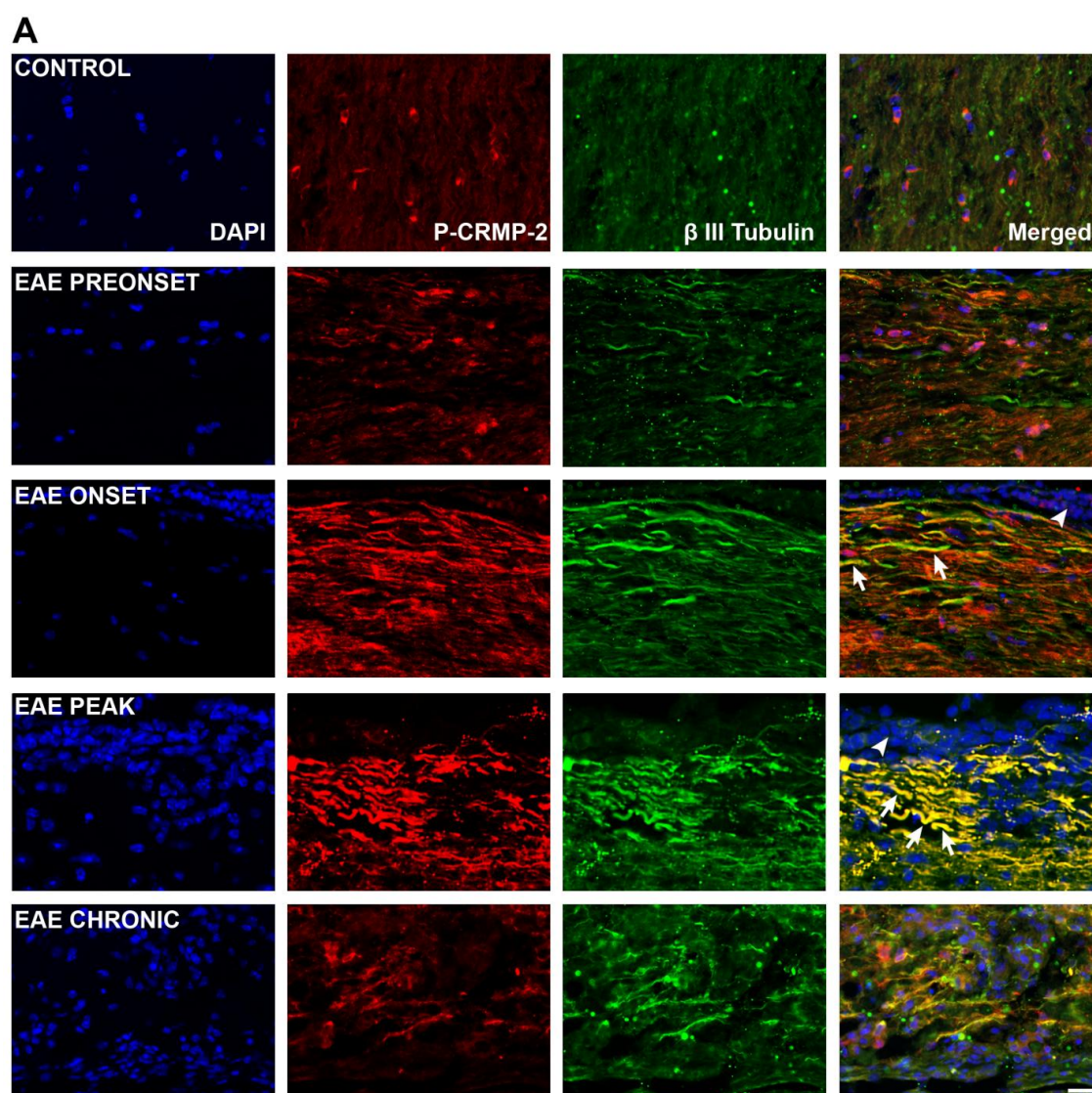


Figure 5. Phosphorylation of CRMP-2 is increased in EAE and is co-localised in degenerating axons. A) Polyclonal anti-pThr555 CRMP-2 antibody reactivity was demonstrated by double immunofluorescence staining on 10 μm cryostat sections showing co-localization with degenerating spinal cord axons from EAE-induced mice immunostained with the monoclonal β III-tubulin antibody (disassembled, monomeric tubulin; arrows) in axons. DAPI stain shows mononuclear cell infiltrate surrounding lesion (arrowheads). $n=3$ per group; magnification bar = 20 μm . Published in Petratos, S. et al. (2012) *Brain* **135**: 1794-1818 (Appendix I).

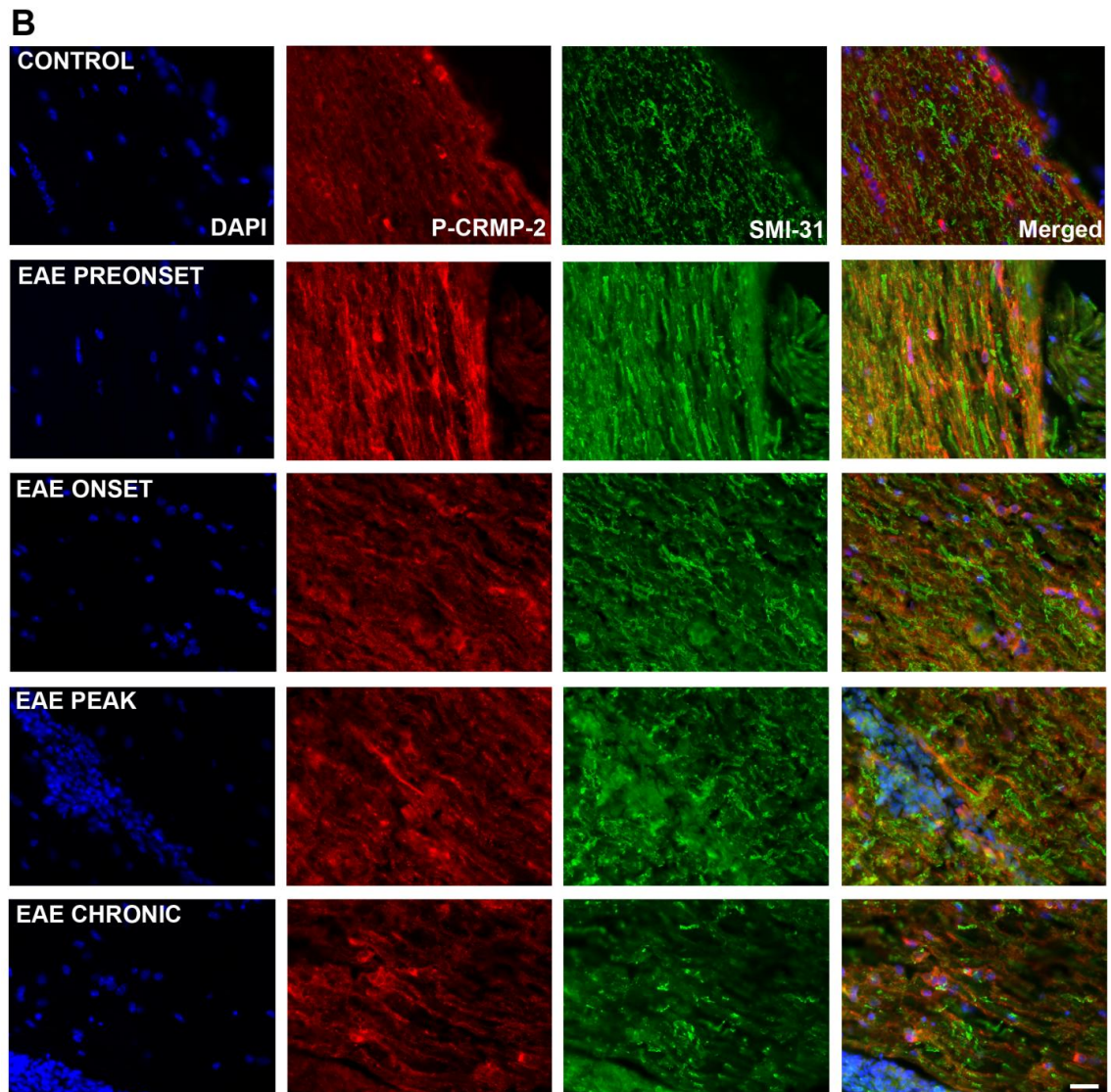


Figure 5. Phosphorylation of CRMP-2 is increased in EAE and is co-localised in degenerating axons. B) Double immunostaining of P-CRMP-2 with SMI-32 (hypophosphorylated neurofilament; a marker for normal appearing axons) showing no colocalisation in the spinal cord of EAE mice at any disease time point. n=3 per group; magnification bar = 20 μ m.

particularly evident on axons at and around lesion sites, suggesting P-CRMP-2 involvement in axonal degeneration.

To rule out the possibility that CRMP-2 was phosphorylated in axons not yet undergoing neurodegeneration, we performed a similar immunofluorescence experiment, and determined the localisation of Thr-555-P-CRMP-2 and SMI-32-reactive neurons in lumbosacral spinal cord sections obtained from control and EAE animals (Fig. 5B). SMI-32 is a marker of hypophosphorylated neurofilaments found in normal axons, and therefore a loss of SMI-32 staining indicates an increase in axonal pathology. We failed to find any PCRMP-2 and SMI-32 positive axons at any stage of disease. These results confirm that CRMP-2 phosphorylation is associated with axonal degeneration in EAE mice.

4.3.6 Therapeutic administration of anti-Nogo-A antibodies prevents clinical progression, axonal degeneration and ROCKII-dependent CRMP-2 phosphorylation in EAE

Our previous work has supported the notion that inhibition of Nogo-A in EAE limits axonal degeneration and disease progression (104). Therefore, we next ascertained whether the mechanism governing the limitation of axonal degeneration in Nogo-A passively vaccinated EAE-induced mice (104) was because of a limitation in phosphorylation of CRMP-2. We performed the therapeutic administration of the anti-Nogo(623–640) antibody in female wild-type mice following the induction of MOG_{35–55}-EAE (Fig. 6A). The antibody was administered i.v. or i.p. at 7, 9, 11, 14 and 16 dpi. As a control, a second cohort of animals were treated with control IgG. A significant delay in the onset of EAE clinical signs could be demonstrated in the anti-Nogo(623–640) antibody treated mice (at 21 dpi.) when compared with EAE-mice that were treated with a non-specific IgG isotype control or without any treatment (Fig. 6A). Furthermore, the severity of EAE was significantly blunted after continuous treatment with anti-Nogo(623–640) antibody (average clinical score of 0.6 ± 0.6 by 25 dpi.) compared to the EAE mice treated with the IgG control antibody (1.8 ± 0.5 by 25 dpi.) or without treatment (2.4 ± 0.5 by 25 dpi; Table 2A). In addition, histopathological scoring in several regions of the CNS demonstrated decreased axonal degeneration and reduced demyelination in anti-Nogo(623–640) antibody-treated mice (Table 2B).

Histological analysis showed reduced inflammation and increased preservation of axons in the spinal cords of Nogo(623-640) antibodies compared to IgG treated or untreated groups (Fig. 6B). Moreover, the abrogation of neurological decline and axonal degeneration demonstrated in the anti-Nogo(623–640) antibody-treated mice correlated with a significant reduction in the level of PCRMP-2 in the spinal cord (Fig. 6C and D). The decrease in the levels of PCRMP-2 correlated with a replenished level of tubulin association with CRMP-2 (Fig. 6C and D). Collectively, these data suggest that the reduction in the neurological decline and associated axonal pathology exhibited by the anti-Nogo(623–640) antibody treatment of EAE-induced mice may be related to a decrease in the phosphorylation status of CRMP-2.

Table 2A: Clinical scores of adult female C57BL/6 MOG-35-55 EAE mice.

Treatment	Clinical Parameter	Preonset	Onset	Peak	Chronic
None	Prevalence	0/5	3/5	5/5	5/5
	Mean Score	0 ± 0	1.22 ± 0.55	2.4 ± 0.4	2.3 ± 0.46
	Median Score	0	1	3	2.5
IgG	Prevalence	0/5	2/5	3/5	4/5
	Mean Score	0 ± 0	1.1 ± 0.68	1.2 ± 0.58	1.8 ± 0.49
	Median Score	0	0	1	2
Anti-Nogo-A Antibody	Prevalence	0/5	0/5	0/5	0/5
	Mean Score	0 ± 0	0 ± 0	0 ± 0	0 ± 0
	Median Score	0	0	0	0

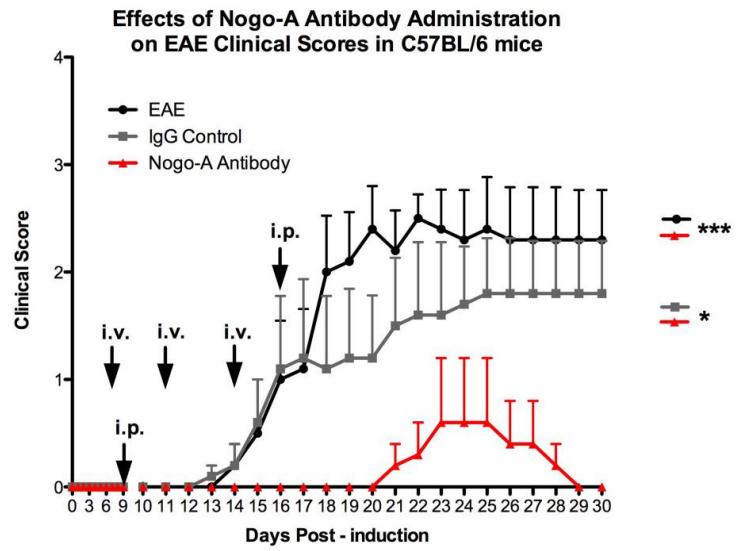
Table 2B: Histopathological score for inflammation & demyelination in adult female C57BL/6 EAE mice.

Treatment	Clinical Score	Day 30 Chronic EAE	Lumbo-sacral spinal cord	Thoracic spinal cord	Cervical spinal cord	Cerebellum
None	2.3 ± 0.46	I	4 ± 0	3.75 ± 0.25	2.25 ± 0.48	1.75 ± 0.25
		D	3 ± 0	2.75 ± 0.5	1.5 ± 0.5	0.75 ± 0.25
IgG	1.8 ± 0.49	I	3.5 ± 0.24	3.25 ± 0.39	2.75 ± 0.61	1 ± 0
		D	2.5 ± 0.24	2.75 ± 0.2	2.25 ± 0.39	0 ± 0
Anti-Nogo-A Antibody	0 ± 0	I	1.5 ± 0.75	1.25 ± 0.55	1 ± 0.47	0 ± 0
		D	1.25 ± 0.87	1 ± 0.67	0.5 ± 0.33	0 ± 0

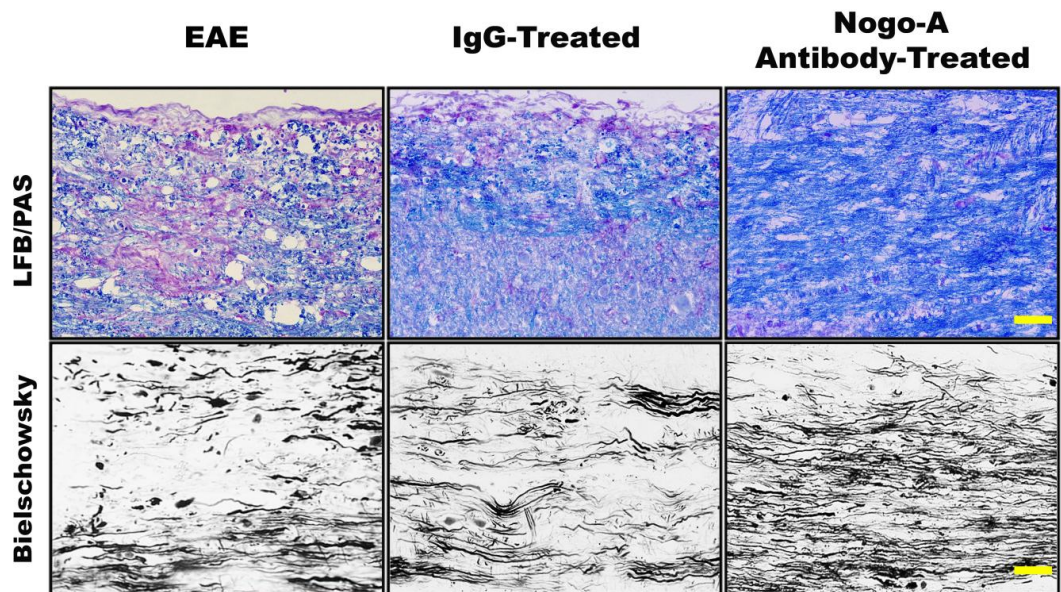
I: Inflammation; D: Demyelination. Published in Petratos, S. et al. (2012) *Brain* **135**: 1794-1818 (Appendix I).

Figure 6. Therapeutic administration of anti-Nogo-A antibodies prevents clinical progression, axonal degeneration and CRMP-2 phosphorylation in EAE. A) Combination of intravenous (Days 8, 11 and 14) and intraperitoneal (Days 9 and 16) administration of anti-Nogo(623-640) antibody (1mg per injection), non-specific IgG control antibody or no injection in EAE-induced mice (n = 8 mice per group, *** $P < 0.001$, * $P < 0.05$ analysed by Friedman's non-parametric repeated measures). B) Histopathological analysis of inflammatory demyelination (LFB/PAS stain) and axonal degeneration (Bielschowsky silver stain) at chronic stage of EAE after either, no treatment regime, IgG or anti-Nogo(623–640) antibody treatment. Staining with Luxol fast blue and Periodic acid Schiff highlights significant sparing of myelin in the Nogo(623–640) antibody treated spinal cord white matter tracts compared to the demyelination in EAE-induced mice with non-specific IgG or without treatment. Importantly, axonal degeneration is also substantially reduced in the Nogo(623–640) antibody treated group. n=3 per group; magnification bar = 20 μ m. Published in Petratos, S. et al. (2012) Brain **135**: 1794-1818 (Appendix I).

A



B



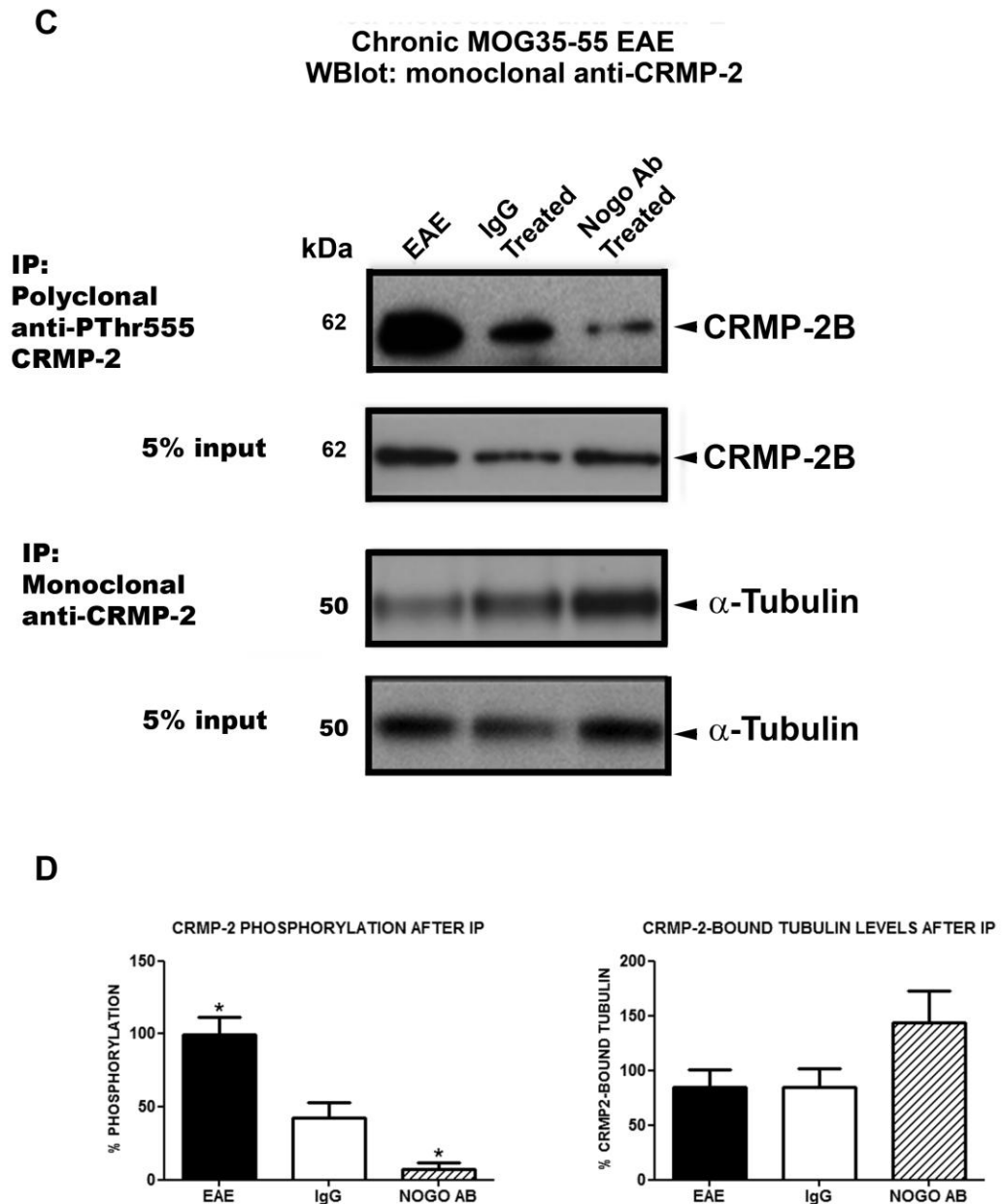


Figure 8. Therapeutic administration of anti-Nogo-A antibodies prevents clinical progression, axonal degeneration and CRMP-2 phosphorylation in EAE. C) Immunoprecipitation of PCRMP-2, demonstrating increased levels in spinal cord lysates from EAE mice without treatment or treated with IgG antibody. However, substantial reduction is evident following Nogo(623–640) antibody treatment. Co-immunoprecipitation of CRMP-2 shows reduced association of tubulin to CRMP-2 in EAE-induced mice treated with non-specific IgG or without treatment, but CRMP-2-bound tubulin levels are higher in the Nogo(623–640) antibody treatment group. D) Optical density measurements of protein levels show a significant reduction in PCRMP-2 (* $P < 0.05$) that correlate with an increase in tubulin association to CRMP-2 in the Nogo(623–640) antibody treatment group (n = 8 mice per group). Published in Petratos, S. et al. (2012) *Brain* **135**: 1794-1818 (Appendix I).

4.4 Discussion

A central hindrance in achieving axon regeneration in the injured CNS is the presence of inhibitory MAIFs. As such many studies have concentrated on identifying MAIFs and their downstream signalling molecules, and thus the underlying mechanisms involved in neurodegeneration are being progressively elucidated. Under pathophysiological conditions, Nogo-A has been shown to signal through NgR1, whereby activation in Rho-A inhibitory signalling results in neurite outgrowth inhibition (99, 106, 139, 159, 160, 162, 163). CRMP-2 was identified as a key effector molecule downstream of Rho-A, by which phosphorylation of CRMP-2 by ROCKII impedes tubulin binding and microtubule assembly *in vitro* (222, 246). Furthermore, Nogo-66 and MAG-Fc can induce CRMP-2 phosphorylation (173). While the effects of Nogo-A has been studied in EAE models, little is known about the involvement of the associated activity of CRMP-2 in this disease model. We hypothesised that NgR1 signalling triggered by MAIFs such as Nogo-A, would result in altered CRMP-2 expression and ROCKII dependent phosphorylation facilitating in EAE progression.

We found elevated levels of Nogo-A in the lumbar spinal cords of EAE animals. This finding is in line with previous reports demonstrating increased expression of Nogo-A in oligodendrocytes in animal SCI models, and in MS post mortem tissue (97, 98). Furthermore we observed changes in Rho-A and total CRMP-2 expression in the cerebellum of EAE animals compared to controls. Erschbamer and colleagues (186), found upregulation of Rho-A mRNA in oligodendrocytes and neurons following SCI. Similarly, we observed increased Rho-A expression in the purkinje cells and granule cells at peak stage of EAE. In addition, the punctate expression pattern of CRMP-2 observed in the purkinje cells of the control animals became more diffuse in tissue obtained from EAE animals at peak stage of disease. These data provide preliminary evidence that CRMP-2 may play a role in promoting neurodegeneration in EAE. Substantial research in to the effects of post translational modifications such as phosphorylation or cleavage of CRMP-2 has concluded that these events modify the physiological function of CRMP-2 (236, 238, 239, 246, 292, 293). Anterograde axonal transport of molecular cargo by CRMP-2 is disrupted and axonal retraction proceeds resulting in growth cone collapse, and ensuing neurodegeneration.

CRMP-2 was shown to be phosphorylated by ROCKII during LPA-induced growth cone collapse in dorsal root ganglion cells by using an antibody that specifically detects P-Thr555-CRMP-2 (240). This study demonstrated that CRMP-2 phosphorylation could be reversed by the introduction of ROCKII inhibitors. The same group further reported

in vitro that ROCKII phosphorylation of CRMP-2 limits its binding capacity to tubulin heterodimers and microtubules (246). These studies were the first to provide sound evidence that growth cone collapse could be induced by phosphorylation of CRMP-2 by a Rho-dependent mechanism in neurons. The same mechanism has since, also been validated in rodent *in vivo* models of SCI and AD (173, 258). However, the question remains as to whether these events can be initiated during neuroinflammatory diseases such as EAE and multiple sclerosis.

In this study we report for the first time that CRMP-2 plays an active role in promoting neurodegeneration in EAE, an animal model for MS. By performing co-immunoprecipitation assays, we illustrated that ROCKII dependent phosphorylation of CRMP-2 is increased in lumbar spinal cord lysates of EAE animals compared to controls. It has been previously reported that the two splice variants, CRMP-2A (75 kDa) and CRMP-2 B (62 kDa) have opposing effects on neurite outgrowth (251, 294). Furthermore, CRMP-2A expression is restricted to axons while the more abundant CRMP-2B is primarily expressed in dendrites (251, 294). In our study we found that both the axon-specific PCRMP-2A, and non-specific PCRMP-2B isoforms were significantly increased at peak stage in EAE-induced animals compared to controls, correlating with maximum clinical severity. We further illustrate that phosphorylation of CRMP-2 hinders CRMP-2 association with tubulin heterodimers in EAE animals. These data support the hypothesis that MOG-induced EAE promotes neurodegeneration by activating ROCKII signalling, inhibiting microtubule assembly through direct phosphorylation of CRMP-2 thus reducing its ability to bind and transport tubulin heterodimers. Nevertheless, we observed a reduction CRMP-2 phosphorylation at chronic stage of EAE. While at this stage the animals do enter a remitting phase, the progress of neurodegeneration is still present and active. One such possible explanation of this outcome may be the cleavage of CRMP-2 by calpains upon activation (295). Indeed, Zhang and colleagues (249) demonstrated calpain cleavage of CRMP-2 in the cortex lysates of rats which had incurred traumatic brain injury (controlled cortical impact), which could be reversed by administering calpain inhibitors. Therefore it is feasible that CRMP-2 phosphorylation plays a dominant role in promoting neurodegeneration in the acute progressive phase of the disease, followed by a switch in inhibitory mechanisms in chronic stages of disease whereby cleavage of CRMP-2 takes precedence in maintaining further neurodegenerative activity.

Mimura et al (173) found increased levels of ROCKII phosphorylated CRMP-2 in *tuj-1* expressing neurons in the dorsal column of rats that had undergone SCI, which was

not evident in control spinal cords. Similarly, we observed an increase CRMP-2 phosphorylation in β III-tubulin (*tuj-1*) positive axons in the lumbar spinal cord white matter tracts of MOG-induced EAE animals that was absent in adjuvant-injected controls. Heightened PCRMP-2 expression was observed around lesions sites presenting with inflammatory influx. Furthermore, we observed no co-localisation of PCRMP-2 with hypophosphorylated neurofilament indicating that normal appearing axons do not express PCRMP-2. This suggests that ROCKII mediated CRMP-2 phosphorylation is a mechanism that is activated only in degenerating axons, resulting in depolymerisation of microtubules.

We detected upregulation in CRMP-2 phosphorylation in the spinal cords of EAE animals at pre onset stage of disease, suggesting that Rho-A signalling is activated before clinical signs manifest. This finding further confirms previous reports from our laboratory which have provided evidence of axonal injury in EAE-induced animals preceding clinical deterioration (291). Our data provide additional validation to the hypothesis that inflammation, demyelination and axonal loss can all occur concomitantly. As microtubule formation is essential for neurite extension, it is conceivable that inhibitory CNS ligands such as Nogo-A could initiate axon outgrowth inhibition in the injured CNS through NgR1 signalling in neurons, by phosphorylation of CRMP-2, bringing tubulin transport and therefore the ability for regeneration to a halt. Indeed Mimura et al (173) found that administration of the ROCKII inhibitor Y-27632 at the site of lesion following SCI resulted in a recovery of polymerised tubulin. These data together point to potentially a common mechanism of axonal degeneration in SCI and EAE.

Current evidence defines pharmacological blockade of myelin associated inhibitory factors as a means of enhancing regeneration in the CNS (68, 151). Blocking the signalling of Nogo-A in CNS disease and injury has been well studied and includes EAE (104, 166). In this study, we used the anti-Nogo(623–640) antibody, previously demonstrated to promote axon outgrowth in the presence of the Nogo peptide, as well as the prevention of neurological decline when injected intravenously over the course of EAE (104). We showed that after four injections of anti-Nogo(623–640) antibodies, the decreased severity of EAE correlated with a decreased amount of axonal degeneration. Importantly, reduced levels of PCRMP-2 in these animals corresponded with replenished tubulin association. Function-blocking antibodies of Nogo-A have been successfully used in preclinical experiments enhancing locomotor performance in neurotrauma paradigms in rodents and adult monkeys (111, 150), improving manual

dexterity after cervical SCI in the latter (150). Over the space of two decades, these significant studies advocating therapeutic targeting of Nogo-A in neurotrauma have encouraged the Phase I clinical trials of anti-human Nogo-A antibody (ATI 355) by Novartis (296). With 45 patients enrolled in this study, intrathecal administration of the antibody in these patients has shown remarkable tolerance with no side-effects manifest in this group (296). With a Phase II trial currently underway, we now propose that one of the major mechanisms by which anti-Nogo-A antibody treatment is clinically effective may well be through the eventual decrease of the phosphorylated levels of CRMP-2 limiting NgR1-dependent axonal degeneration. Interestingly, other pharmacological studies using the ectodomain of NgR1 and co-receptors such as Lingo-1 have recently shown enhanced neurological improvement in injury and disease models of the CNS by blocking the binding of the myelin associated inhibitory factors (108, 160, 163). It is tantalizing to suggest that similar therapeutic effects could be met in the treatment of multiple sclerosis.

Whether the anti-Nogo(623–640) antibody used in the current study directly blocks Nogo-66 interaction with the NgR1 complex, or whether it achieves this indirectly through modulation receptor signalling by impacting the binding affinity between receptor and ligand still remains to be elucidated. Nevertheless our studies implicate the involvement of a ROCKII mediated mechanism, whereby the consequential CRMP-2 phosphorylation impacts the severity of failed regeneration which can be alleviated by therapeutically targeting Nogo-A. We therefore must consider the possibility that CRMP-2 phosphorylation is a result of neurodegenerative mechanism initiated by MAIFs and NgR1. Investigation of CRMP-2 phosphorylation in NgR1 null mice challenged with MOG-induced EAE could further strengthen this hypothesis.

Chapter 5

LIMITING AXONOPATHY IN EAE BY BLOCKING NOGO RECEPTOR AND CRMP-2 PHOSPHORYLATION

5.1 Abstract

Multiple sclerosis involves demyelination and axonal degeneration of the central nervous system. The molecular mechanisms of axonal degeneration are relatively unexplored in both multiple sclerosis and its mouse model, EAE. Here we show that the collapsin response mediator protein 2 (CRMP-2), an important tubulin-associated protein that regulates axonal growth, is phosphorylated and hence inhibited during the progression of EAE in degenerating axons. Specifically, pThr555CRMP-2 is implicated to be Nogo-66 receptor 1 (NgR1)-dependent, since MOG₃₅₋₅₅-induced NgR1 knock-out (*ngR1*^{-/-}) mice display a reduced EAE disease progression, without a deregulation of *ngR1*^{-/-} MOG₃₅₋₅₅-reactive lymphocytes and monocytes. Furthermore, we show that NgR1-deficient mice present an immune profile comparable to their WT counterparts under both naive and pathological conditions. The limitation of axonal degeneration/loss in EAE-induced *ngR1*^{-/-} mice is associated with lower levels of CRMP-2 in the spinal cord and optic nerve during EAE. We conclude that phosphorylation of CRMP-2 may be downstream of NgR1 activation and play a role in axonal degeneration in EAE. Blockade of Nogo-A/NgR1 interaction may serve as a viable therapeutic target in multiple sclerosis.

5.2 Introduction

Multiple sclerosis is a severe neurological disorder that involves inflammation in the brain and spinal cord, axonal damage and demyelination. Experimental autoimmune encephalomyelitis (EAE) is an animal model that mimics many of the pathophysiological hallmarks of multiple sclerosis. The induction of EAE by immunization with the myelin oligodendrocyte glycoprotein (MOG) peptide encompassing the 35–55 amino acid sequence (MOG_{35–55}) is a commonly used animal model for the neurodegenerative changes observed in multiple sclerosis (43). It has long been believed that axonal damage, degeneration and loss are secondary to demyelination. However, data from our laboratory have demonstrated that axonal degeneration can precede demyelination in EAE (291). Notably, Trapp et al. (55) have reported the appearance of newly transected axons in active and hypocellular chronic-active multiple sclerosis lesions from brains obtained at autopsy, suggesting a relationship between axonal damage and permanent neurological deficits. It is likely that multiple sclerosis may display similar pathogenic mechanisms and features as observed in spinal cord injury, whereby degenerating axons may attempt regeneration, but fail due to the inhibitory environmental cues (297). The factors in the adult CNS that inhibit these compensatory regenerative responses include myelin proteins and extracellular matrix constituents (69). Chief among these factors are integral components of myelin known as the myelin-associated inhibitory factors (MAIFs), such as the potent inhibitor of neurite outgrowth, Nogo-A (77, 99). Expression of Nogo-A in oligodendrocytes has been reported to be upregulated in active demyelinating lesions of multiple sclerosis (97). In addition, our laboratory has demonstrated that immunization against Nogo-A or deletion of the nogo gene ameliorates the effects of EAE (104). While Nogo-A is known to be a potent inhibitor of axonal regrowth, a direct relationship with bona fide axonal pathology, an important feature of both EAE and multiple sclerosis lesions (55, 291), is as yet undefined.

Although it has been demonstrated that deletion of the co-receptor for Nogo-A, LINGO-1, improves axonal integrity and protects against neurological decline in MOG-induced EAE (166), the mechanism by which this eventuates is not known. Furthermore, small interfering RNA silencing of Nogo-A in both MOG_{35–55}⁻ and myelin basic protein-induced EAE models has been shown to limit the clinical severity of the disease and promote repair (105) but again it is unclear how this therapeutic effect is achieved. This raises the question of whether in EAE and multiple sclerosis, Nogo-A can signal axonal degeneration through its axonally localized cognate receptors. In this study, we show that phosphorylated CRMP-2 (pThr555CRMP-2, a key molecule that regulates

microtubule assembly) is abundant in degenerating spinal cord neurons and their axons of EAE-induced mice. We are able to define further that the increase in axonally specific PCRMP-2 is limited in EAE-induced *ngr1*^{-/-} mice, thereby preventing significant axonal and myelin degeneration characteristic of MOG₃₅₋₅₅ EAE. Thus, reducing the NgR1- dependent signalling capacity during EAE may limit the activation of the phosphorylation of CRMP-2, preventing axonal degeneration and neurological decline.

5.3 Results

5.3.1 Deletion of the *ngr1* allele (exon 2) limits the progression of EAE, axonal degeneration and phosphorylation of CRMP-2

We investigated the possibility that limiting the phosphorylation of CRMP-2 during EAE will limit the progressive neurodegenerative changes that occur in *ngr1*^{-/-} mice. We first demonstrated that following EAE-induction, the *ngr1*^{-/-} mice displayed a shift in the time-point of disease onset when compared with the *ngr1*^{+/+} mice (Fig. 1A and B; Table 1A). The *ngr1*^{-/-} mice showed induction of disease by 15–16 days post-MOG_{35–55} immunization compared with the *ngr1*^{+/+} mice, which displayed onset of EAE by 12–13 dpi. (Fig. 1A and Table 1). Importantly, the majority of the *ngr1*^{+/+} mice manifested significant disease (12 of 14 mice) by 18 dpi, corresponding to peak neurological deficit with a clinical score of 1.93 ± 0.23 (Fig. 1A and Table 1). However, of the *ngr1*^{-/-} EAE-immunized mice, only 6 of the 16 mice displayed disease symptoms. Moreover, peak severity of the clinical signs occurred at clinical score 1.0 ± 0.34 by 19 days post-injection (Fig. 1A and Table 1). This was associated with a reduction in the histopathological parameters for the *ngr1*^{-/-} mice, which coincided with the progressive neurological decline post-MOG_{35–55}-immunization (Fig. 1B and Table 1B). Notably, there was a reduction in the score for inflammatory cell infiltrates, demyelination and axonal degeneration in the EAE-induced *ngr1*^{-/-} mice (Fig. 1B and Table 1). These parameters were associated with a reduction in the molecular marker of axonal degeneration, abnormally phosphorylated tau (hyperphosphorylated tau, AT8; Fig. 2). Moreover, following the isolation of the insoluble proteins from spinal cord lysates of EAE-immunized mice (266), by western blot analysis we found that the MOG_{35–55}-induced *ngr1*^{-/-} mice had reduced levels of sarcosyl-insoluble AT8-positive tau, as compared with the EAE-induced *ngr1*^{+/+} mice (Fig. 2). These findings were associated with an increase in the soluble forms of tau in the *ngr1*^{+/+} compared with the *ngr1*^{-/-} mice, immunostained with tau-5 (for total tau levels) and normal phosphorylated tau stained with an anti-pSer199/202 tau antibody (Fig. 2). Thus it would appear that in *ngr1*^{-/-} mice, a modest increase in the phosphorylated and hyperphosphorylated forms of tau correlates with axonal degeneration and disease progression.

To further assess the extent of axonal degeneration, we performed ultrastructural analysis on lumbosacral spinal cords of both *ngr1*^{-/-} and *ngr1*^{+/+} mice. As illustrated in Fig. 3, lesions appearing in the white matter tracts of the spinal cord of *ngr1*^{+/+} mice showed significant axonal degeneration and demyelination with inflammatory infiltrates (Fig. 3). However, in the spinal cord white matter tracts of *ngr1*^{-/-} mice, there was preservation in axo-myelin integrity along with limited inflammatory infiltrates (Fig. 3).

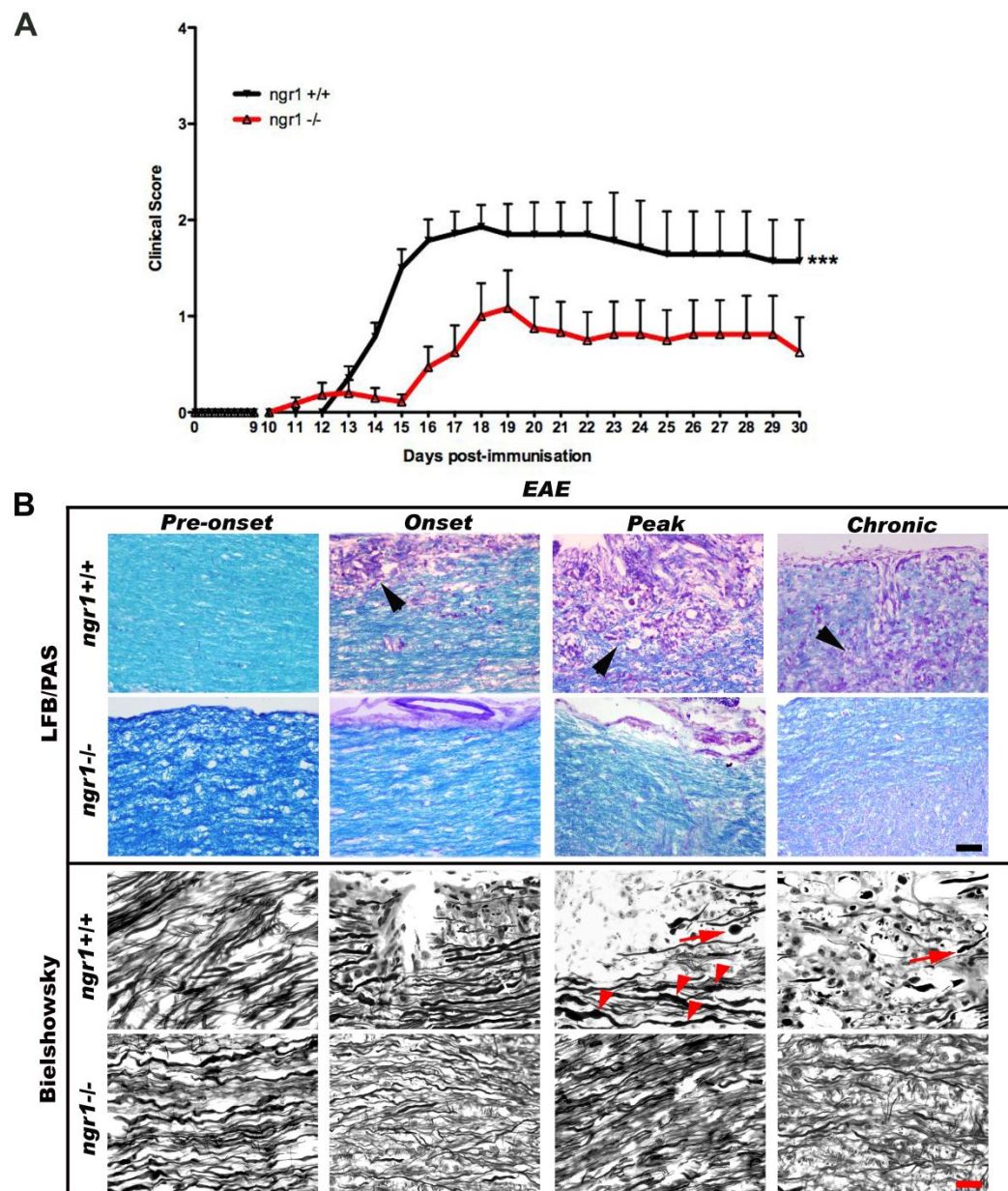


Figure 1. Reduction in EAE disease, inflammatory demyelination and axonal degeneration in *ngr1*^{-/-} mice. (A) EAE clinical scores after MOG₃₅₋₅₅-induction in female C57Bl/6 wild-type littermate (*ngr1*^{+/+}, n = 21, black line) and *ngr1*^{-/-} mice (n = 14 *ngr1*^{-/-}, red line; ****P*<0.001 repeated measures ANOVA). (B) Histopathology of EAE in *ngr1*^{+/+} and *ngr1*^{-/-} mice at pre-onset, onset, peak and chronic stages. Luxol fast blue (LFB) and Periodic acid Schiff (PAS) stain showing inflammatory demyelination and Bielschowsky stain to demonstrate axonal degeneration/loss. Arrows show axonal swelling; arrowhead shows an axonal retraction bulb; scale bar = 20 μm; n=3 per group. Published in Petratos, S. et al. (2012) *Brain* **135**: 1794-1818 (Appendix I).

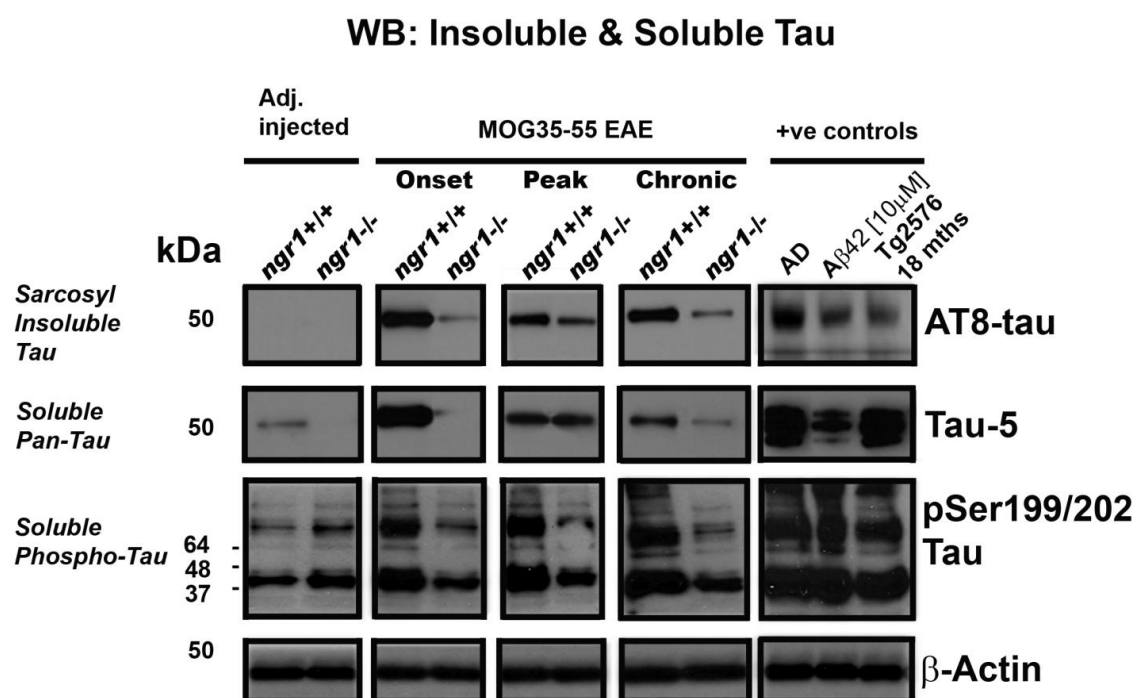


Figure 2. Hyperphosphorylated Tau is decreased in EAE-induced *ngr1*^{+/+} and *ngr1*^{-/-} mice. Western immunoblotting of soluble and insoluble hyperphosphorylated tau in spinal cord lysates from *ngr1*^{+/+} and *ngr1*^{-/-} mice during EAE. Insoluble PHF-phospho-tau from spinal cord lysates extracted by sarcosyl gradient centrifugation show increased AT8-positive protein levels in *ngr1*^{+/+} mice throughout EAE when compared with *ngr1*^{-/-} mice; n=3 per genotype. Controls include adjuvant injected animals alone, human AD fronto-temporal lobe brain lysates, 18 month-old Tg2576 mouse brain lysates, and Aβ42-treated [10 μM] SH-SY5Y cell lysates. Pan-tau and normal phosphorylated tau, demonstrated by monoclonal Tau-5 and polyclonal pSer199/202 antibodies respectively, also show increases in the *ngr1*^{+/+} mice throughout EAE. Loading control shown by β-actin monoclonal antibody detection. Published in Petratos, S. et al. (2012) *Brain* **135**: 1794-1818 (Appendix I).

The reduced axonal degeneration together with the abrogated neurological decline in the *ngr1*^{-/-} mice following EAE-induction, prompted us to investigate whether spinal cord axons in these mice displayed a reduced propensity to initiate phosphorylation of CRMP-2. Immunofluorescence analysis showed that in the *ngr1*^{-/-} mice there were reduced levels of pThr555CRMP-2 in axons in the longitudinal white matter tracts during EAE (Fig. 4). We showed that neurofilament NF200-positive axons (particularly those showing axonal-spheroids) co-localized significantly with PCRMP-2 immunofluorescence at peak and chronic stages of EAE in *ngr1*^{+/+} mice (Fig. 4). These data suggest that during the progression of EAE there are greater levels of PCRMP-2 in degenerative axons in the spinal cords of *ngr1*^{+/+} compared with *ngr1*^{-/-} mice. In order to quantitate these changes, we performed co-immunoprecipitation and western blotting from spinal cord lysates of *ngr1*^{+/+} and *ngr1*^{-/-} mice during EAE. We found that the *ngr1*^{+/+} mice had an incremental increase in PCRMP-2 levels, compared with *ngr1*^{-/-} mice during the progression of EAE (Fig. 5A and B). This increase was also evident in the 75 kDa N-terminal variant of the protein, which did not appear in the *ngr1*^{-/-} mice during EAE (Fig. 5A). Importantly, the levels of CRMP-2-associated tubulin were reduced in the *ngr1*^{+/+} but not in the *ngr1*^{-/-} mice during EAE (Fig. 5C and D). The data can be interpreted as increased dissociation of monomeric tubulin from CRMP-2 in the *ngr1*^{+/+} [from 19.75 ± 2.83% at pre-onset ($P < 0.001$) to 33.77 ± 3.187% at peak ($P < 0.001$); Fig. 5D] as the levels of CRMP-2 phosphorylation increase during the progression of EAE disease [from 39.16 ± 49.62% in adjuvant injected *ngr1*^{+/+} mice to 382 ± 94.41% at peak ($P < 0.05$); Fig. 5B]. However, deletion of the *ngr1* gene limits the EAE-dependent phosphorylation (Fig. 5C and D), replenishing the tubulin association levels (Fig. 5C and D).

Table 1A: Clinical scores of adult female *ngr1*^{-/-} and *ngr1*^{+/+} MOG-35-55 EAE mice.

	Preonset	Onset	Peak	Chronic
Prevalence <i>ngr</i> +/+	0/14	0/14	12/14	5/7
Prevalence <i>ngr</i> -/-	0/22	2/22	6/16	4/8
Mean Score <i>ngr</i> +/+	0 ± 0	0 ± 0	1.93 ± 0.23	1.57 ± 0.43
Mean Score <i>ngr</i> -/-	0 ± 0	0.18 ± 0.13	1 ± 0.34	0.63 ± 0.36
Median Score <i>ngr</i> +/+	0	0	2	2
Median Score <i>ngr</i> -/-	0	0	0	0.25

Table 2B: Histopathological score for inflammation & demyelination in adult female *ngr1*^{-/-} and *ngr1*^{+/+} MOG-35-55 EAE mice.

Day 30 Chronic EAE	Female mice	<i>Clinical Score</i>	<i>Lumbo- sacral spinal cord</i>	<i>Thoracic spinal cord</i>	<i>Cervical spinal cord</i>	<i>Cere- bellum</i>	<i>Optic Nerve</i>
<i>I</i>	<i>ngr1</i> ^{+/+}	1.57 ± 0.43	3.0 ± 1.0	2.33 ± 1.53	3.0 ± 1.0	1.33 ± 0.58	3 ± 1.73
	<i>ngr1</i> ^{-/-}	0.63 ± 0.36	1.75 ± 0.96	1.5 ± 0.58	1.25 ± 1.26	0.25 ± 0.5	1 ± 1
<i>D</i>	<i>ngr1</i> ^{+/+}	1.57 ± 0.43	2.0 ± 1.0	1.33 ± 1.53	1.67 ± 1.15	0.33 ± 0.58	2.33 ± 1.15
	<i>ngr1</i> ^{-/-}	0.63 ± 0.36	0.75 ± 0.5	0.75 ± 0.5	0.75 ± 1.5	0.25 ± 0.5	0.33 ± 0.58

I: inflammation; D: demyelination. Published in Petratos, S. et al. (2012) Brain **135**: 1794-1818 (Appendix I).

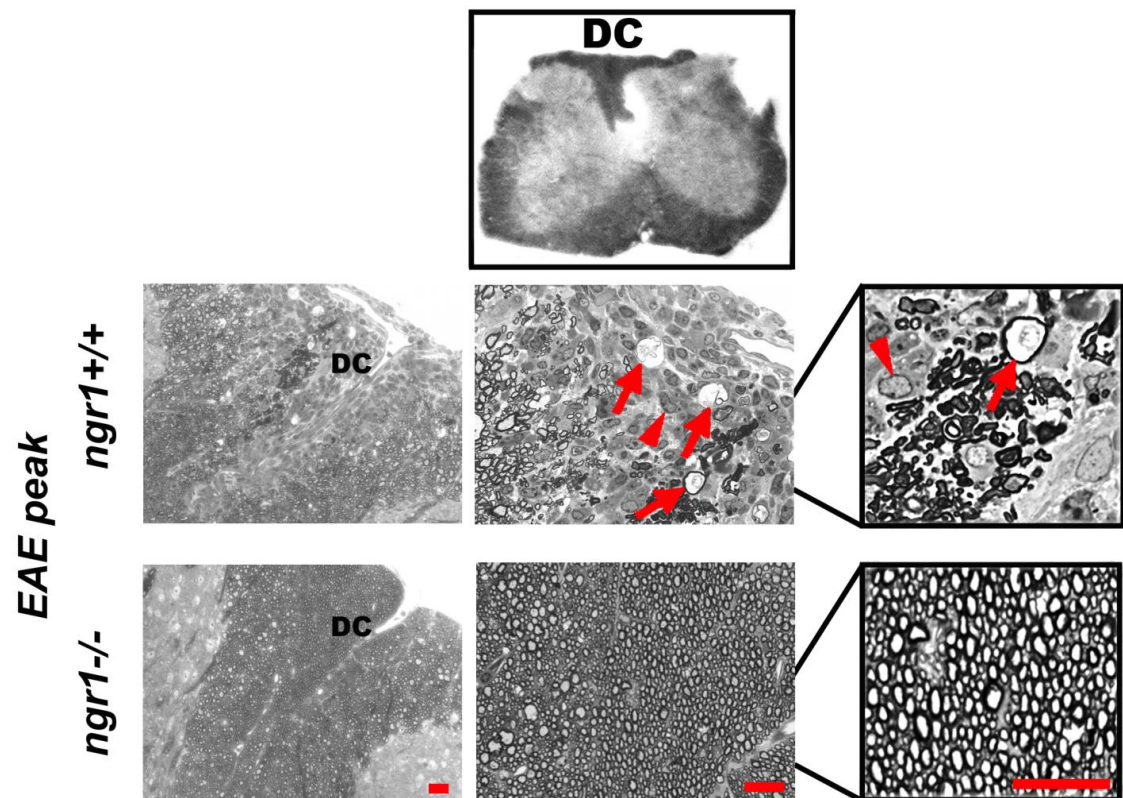


Figure 3. Axonal degeneration in EAE-induced *ngr1*^{+/+} and *ngr1*^{-/-} mice. Representative semi-thin (1 μ m) lumbosacral spinal cord sections from EAE-induced *ngr1*^{+/+} and *ngr1*^{-/-} mice demonstrating significant axonal degeneration in the dorsal column (DC) white matter tracts of *ngr1*^{+/+} mice (arrows) at peak of disease. Inflammatory cells are also present in *ngr1*^{+/+} mice (arrowheads). Magnification bar = 50 μ m. Published in Petratos, S. et al. (2012) Brain **135**: 1794-1818 (Appendix I).

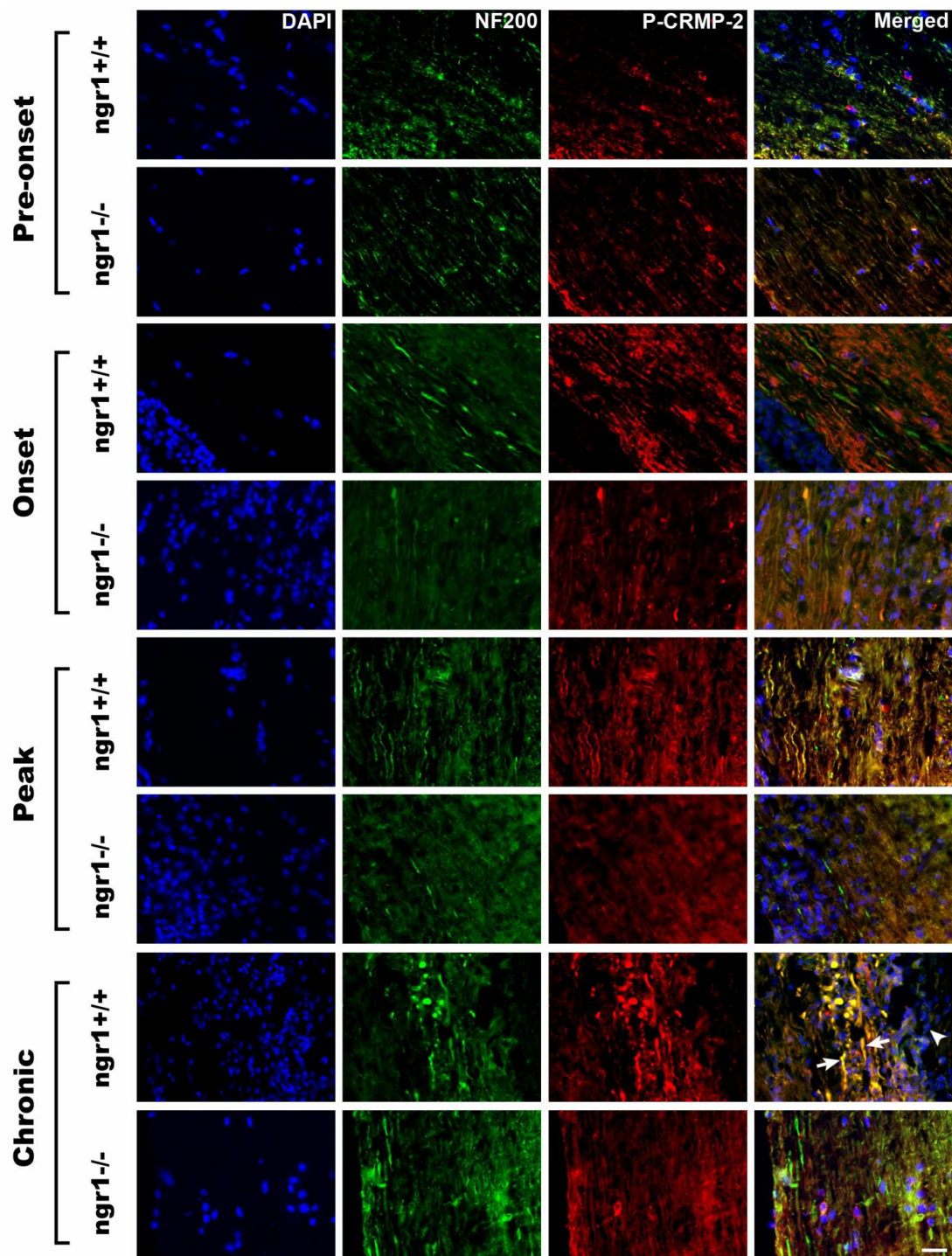
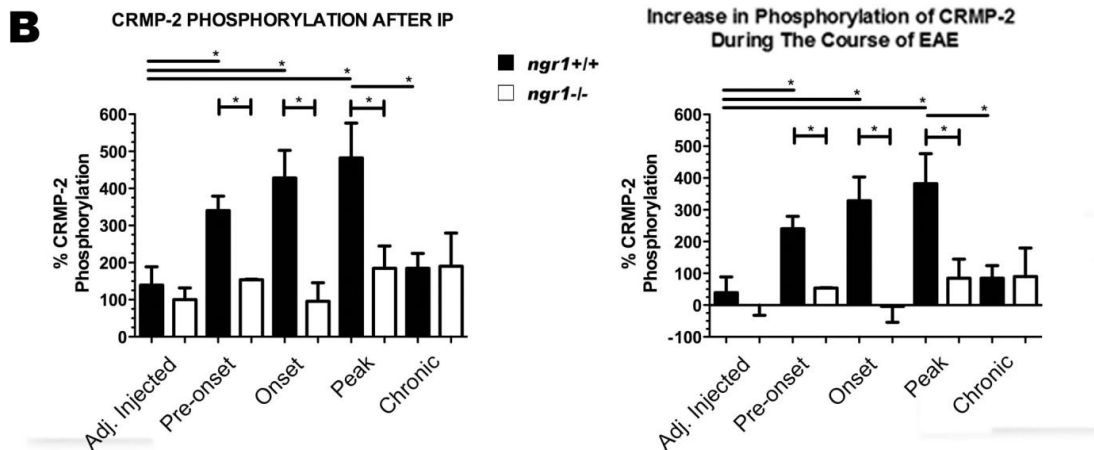
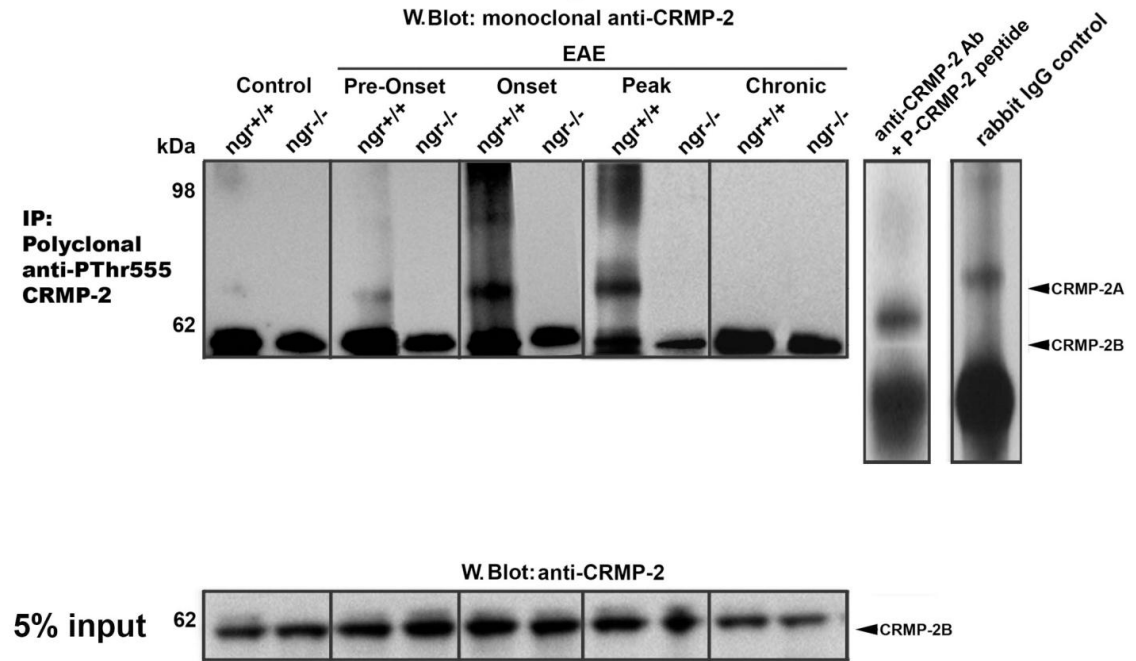


Figure 4. Reduction of phosphorylation of CRMP-2 in *ngr1*^{+/+} and *ngr1*^{-/-} mice in the clinical course of EAE. Polyclonal anti-pThr555CRMP-2 antibody reactivity, in spinal cord sections of EAE-immunized *ngr1*^{+/+} and *ngr1*^{-/-} mice, showing co-localization with degenerating axons in *ngr1*^{+/+} mice at peak and chronic stages of disease as indicated by NF200 immunostaining (phosphorylated neurofilament heavy chain; arrows). DAPI staining showing inflammatory cell infiltrates (arrow head). Magnification bar=50 μ m. Published in Petratos, S. et al. (2012) *Brain* **135**: 1794-1818 (Appendix I).

Figure 5. CRMP-2 phosphorylation is decreased and its association with tubulin is increased in EAE-induced in *ngr1*^{-/-} mice. A) Immunoprecipitation (IP) of pThr555CRMP-2 of spinal cord lysates from EAE-induced *ngr1*^{+/+} and *ngr1*^{-/-} mice, followed by reprobing of the membranes with the monoclonal anti-CRMP-2 antibody. There is an increase in PCRMP-2 of both the CRMP-2A and CRMP-2B variants in EAE-immunized *ngr1*^{+/+} mice from pre-onset to peak of disease. No such changes occurred in the *ngr1*^{-/-} mice at the same time-points after MOG_{35–55} challenge. Control lanes include non-specific rabbit IgG polyclonal antibody and pThr555 CRMP-2 (20 µg) peptide spiked in lysate buffer alone. A pre-immunoprecipitation 5% input of protein from spinal cord lysates show no discernible difference in total levels of CRMP-2. B) Densitometric quantification of total CRMP-2 and pThr555 CRMP-2B (after IP) from spinal cord lysates of control, *ngr1*^{+/+} and *ngr1*^{-/-} EAE-induced mice, represented as a percentage of basal levels (control uninjected *ngr1*^{-/-} mice; n = 4 mice per group and per time-point; **P*<0.05 one-way ANOVA). Representation of the percentage change in the levels of PCRMP-2 demonstrates up to a 4-fold increase occurring in *ngr1*^{+/+} EAE-induced mice when compared with *ngr1*^{-/-} mice at peak stage of disease. Published in Petratos, S. et al. (2012) Brain **135**: 1794-1818 (Appendix I).

A LumboSacral Spinal Cord



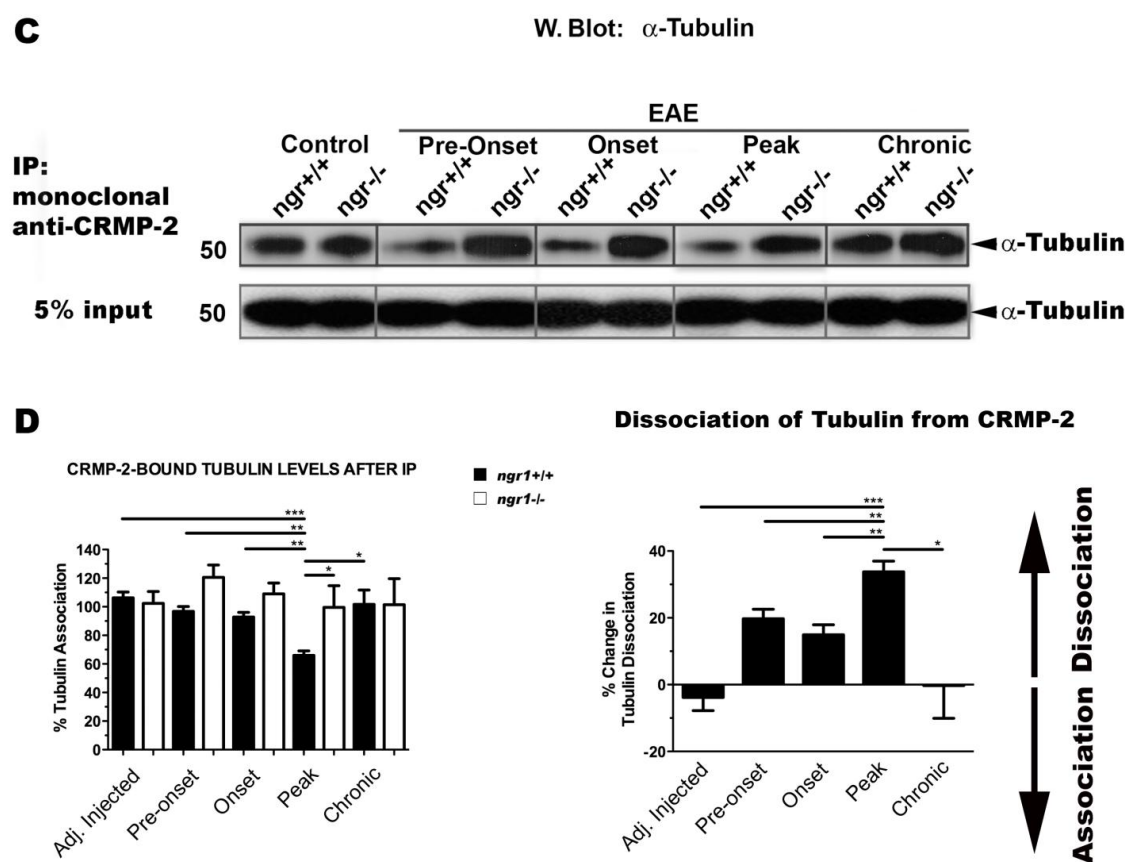


Figure 5. CRMP-2 phosphorylation is decreased and its association with tubulin is increased in EAE-induced in *ngr1*^{-/-} mice. C) Co-immunoprecipitation of CRMP-2 from spinal cord lysates of control, *ngr1*^{+/+} and *ngr1*^{-/-} EAE-induced mice, showed a decreased association with tubulin in the *ngr1*^{+/+} mice from pre-onset until peak stage of EAE. This finding was not replicated in the *ngr1*^{-/-} EAE-induced mice. D) Densitometric quantification of the levels of CRMP-2-associated tubulin (after immunoprecipitation) from spinal cord lysates of control, *ngr1*^{+/+} and *ngr1*^{-/-} EAE-induced mice, represented as a percentage of basal levels (n = 4 mice per group and per time-point; **P*<0.05 one-way ANOVA). Representation of the percentage change in the levels of CRMP-2-bound tubulin, demonstrates up to a 3-fold increase in the dissociation of tubulin from CRMP-2 in *ngr1*^{+/+} when compared with *ngr1*^{-/-} EAE-induced mice at peak stage of disease (**P*<0.05). Published in Petratos, S. et al. (2012) Brain **135**: 1794-1818 (Appendix I).

5.3.2 Axonal damage and CRMP-2 phosphorylation in the optic nerve of EAE-induced mice

To obtain a direct and quantitative measurement of demyelination and axonal pathology, we stained semi-thin optic nerve cross-sections with toluidine blue and assessed both axon/myelinated fibre diameter and degeneration/loss, between EAE-induced *ngr1*^{-/-} and *ngr1*^{+/+} mice. Toluidine blue staining clearly demonstrated axo-myelin degeneration in a number of axons from pre-onset and onset stages of EAE in the *ngr1*^{+/+} but not in the *ngr1*^{-/-} mice (Fig. 6A and Fig. 6B). As indicated by the most severe axonal degeneration/loss, the greatest ultrastructural abnormalities were found at peak and chronic stages of EAE, in *ngr1*^{+/+} mice (Fig. 6A). Optic nerve cross-sections were also investigated for lamellated myelin structure, relative to ensheathed large and small calibre axons, by calculating G-ratios (Fig. 6C). There was a significant, incremental increase in the optic nerve G-ratios of EAE-induced *ngr1*^{+/+} mice with disease progression (from 0.768 ± 0.004 at pre-onset to 0.799 ± 0.004 at peak; Fig. 6C). In *ngr1*^{-/-} mice, there was a moderate but comparable increase in the G-ratio at pre-onset of disease (from 0.761 ± 0.003 at pre-onset), but neared basal levels by peak (0.705 ± 0.003 ; Fig. 6C). The overall increase in demyelination was $11.43 \pm 0.597\%$ in adjuvant injected controls (basal level) from the optic nerves of EAE-induced *ngr1*^{+/+} mice by peak of disease, compared with a $-1.651 \pm 0.472\%$ change in demyelination in EAE-induced *ngr1*^{-/-} mice at the same time-point (Fig. 6C). Interestingly, there was demonstrable demyelination in the optic nerves of *ngr1*^{-/-} mice at the earliest investigated time-point (Day 7 post-EAE induction), resembling that seen in the *ngr1*^{+/+} mice ($6.123 \pm 0.437\%$ versus $7.096 \pm 0.490\%$, respectively). Interpretation of the data would be that there is an initial thinning of lamellated myelin surrounding axons in the optic nerves in both genotypes that is eventually repaired in the *ngr1*^{-/-} mice by Days 12 to 18 (onset and peak, respectively).

However, we did find an increase in the axonal diameter without compensatory increases in the thickness of myelin that normally occurs during development, with larger calibre axons (298). To exclude the possibility that the optic nerves of *ngr1*^{-/-} mice exhibited thinly myelinated but larger calibre axons, we plotted the axonal diameter measurements during EAE, of the *ngr1*^{+/+} and *ngr1*^{-/-} mice (Fig. 6C). We found that in *ngr1*^{-/-} mice, the axonal calibre was at basal levels at Day 7, post-EAE-induction (Fig. 6C). Thus it would appear that the increase in G-ratio in the *ngr1*^{-/-} mice at this early time-point of EAE is related to myelin thinning of axons but is then repaired by 12–18 days post-injection (Fig. 6C). There was an incremental rise in the axonal diameter in the *ngr1*^{+/+} mice as EAE progressed, with a sharp rise by peak of disease

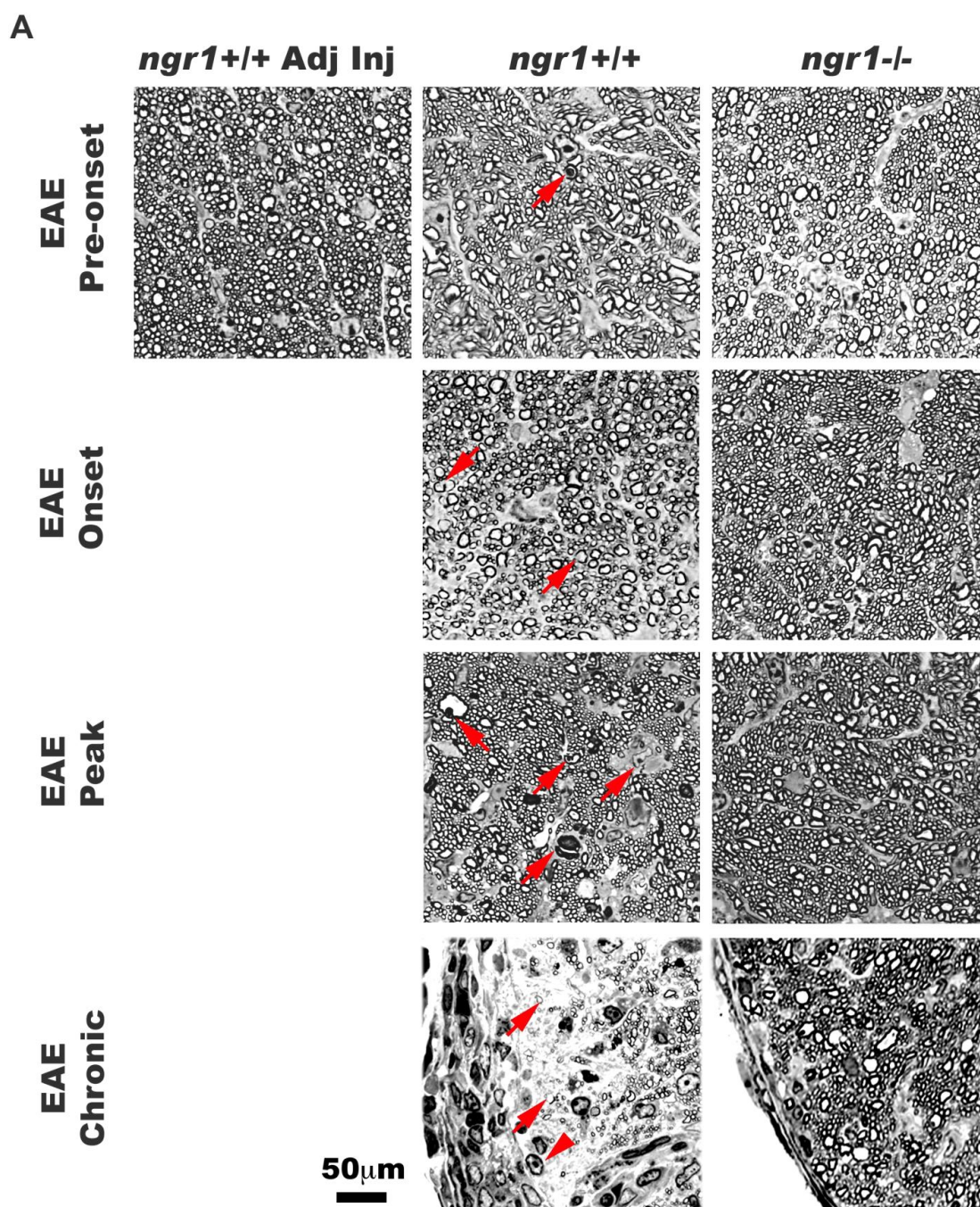


Figure 6. Axonal and myelin damage in the optic nerve of EAE-induced *ngr1*^{-/-} mice is reduced and corresponds with abrogated CRMP-2 phosphorylation. A) Semi-thin (1 µm) optic nerve sections of *ngr1*^{+/+} and *ngr1*^{-/-} mice at pre-onset, onset, peak and chronic stages of EAE or adjuvant only injected control mice. Axonal degeneration and demyelination in the *ngr1*^{+/+} EAE-induced mice are present throughout disease, becoming more prevalent at peak (arrows), with significant axonal loss at chronic stage. Perineurial inflammatory infiltrates are a ubiquitous finding in the optic nerves of *ngr1*^{+/+} EAE-mice (arrowhead). These pathological findings are not as evident in the *ngr1*^{-/-} mice. n=3 per genotype; magnification bar = 50 µm. Published in Petratos, S. et al. (2012) *Brain* **135**: 1794-1818 (Appendix I).

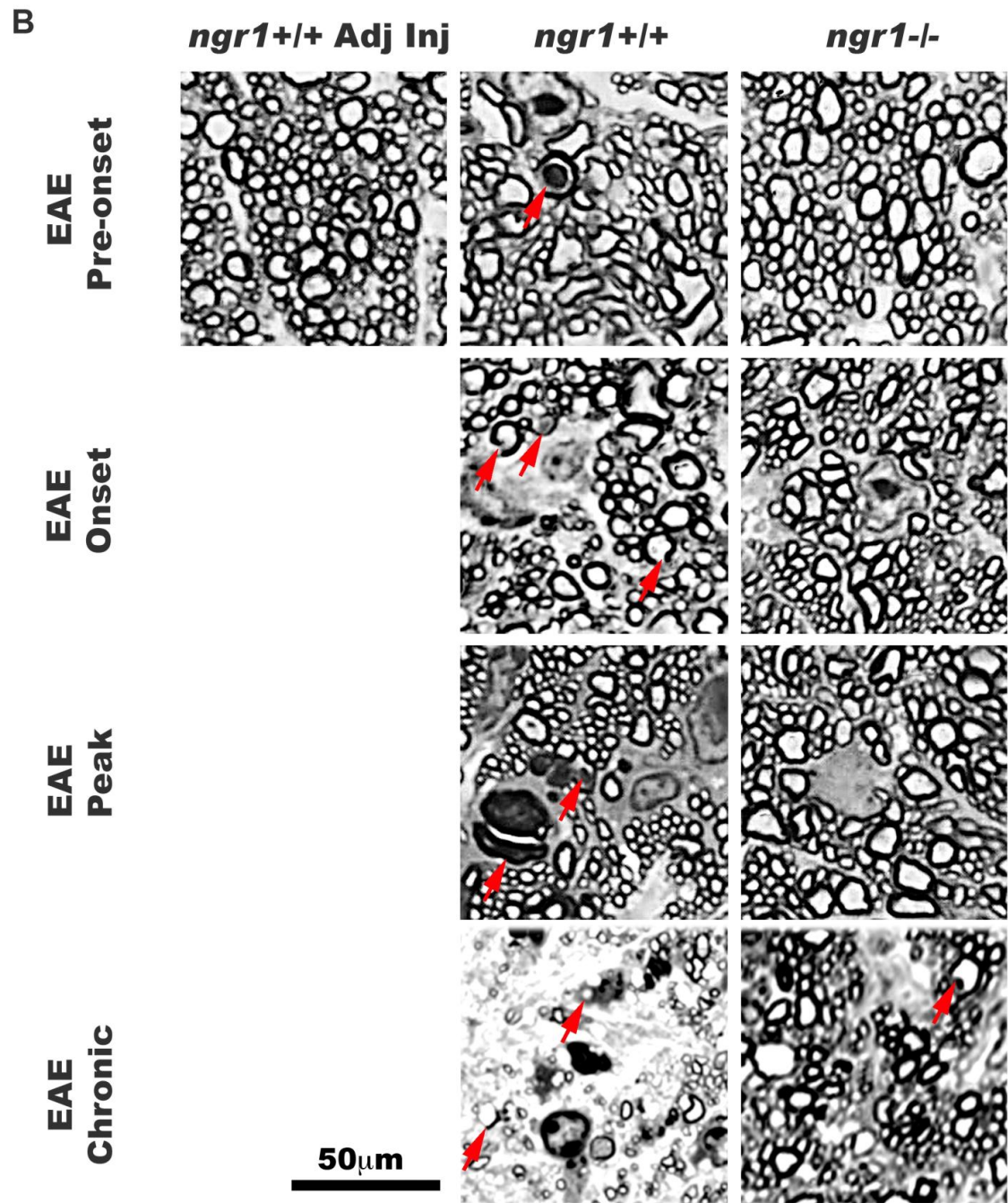


Figure 6. Axonal and myelin damage in the optic nerve of EAE-induced *ngr1*^{-/-} mice is reduced and corresponds with abrogated CRMP-2 phosphorylation. B) 6A visualised under higher magnification. Magnification bar=50 µm. Published in Petratos, S. et al. (2012) *Brain* 135: 1794-1818 (Appendix I).

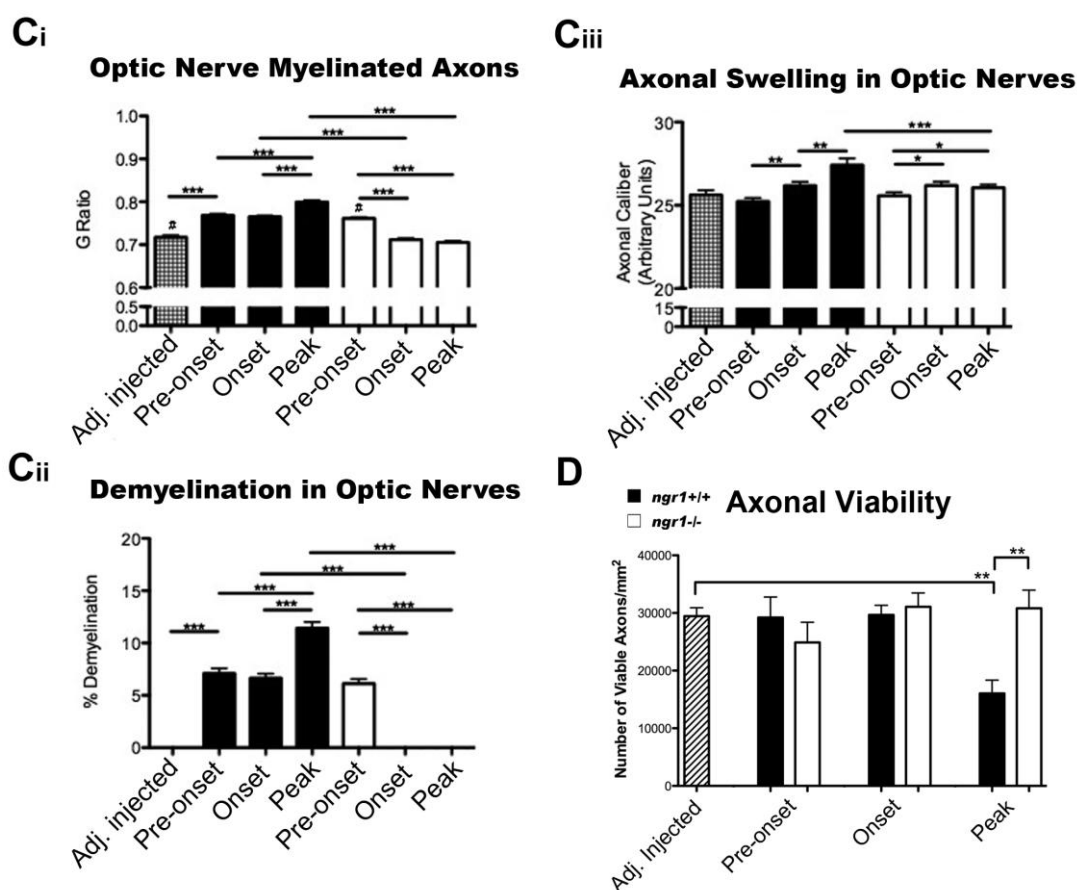
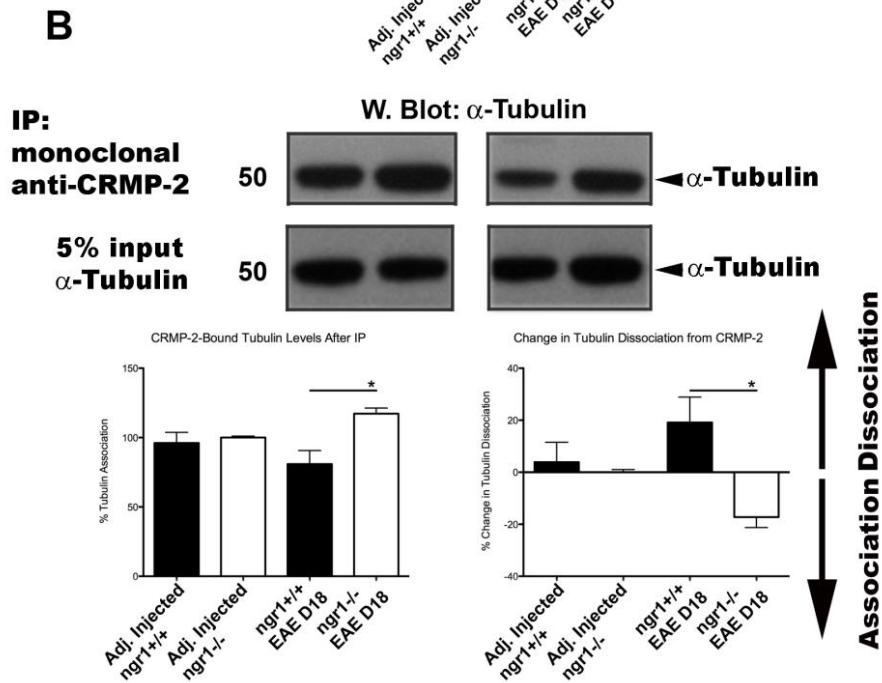
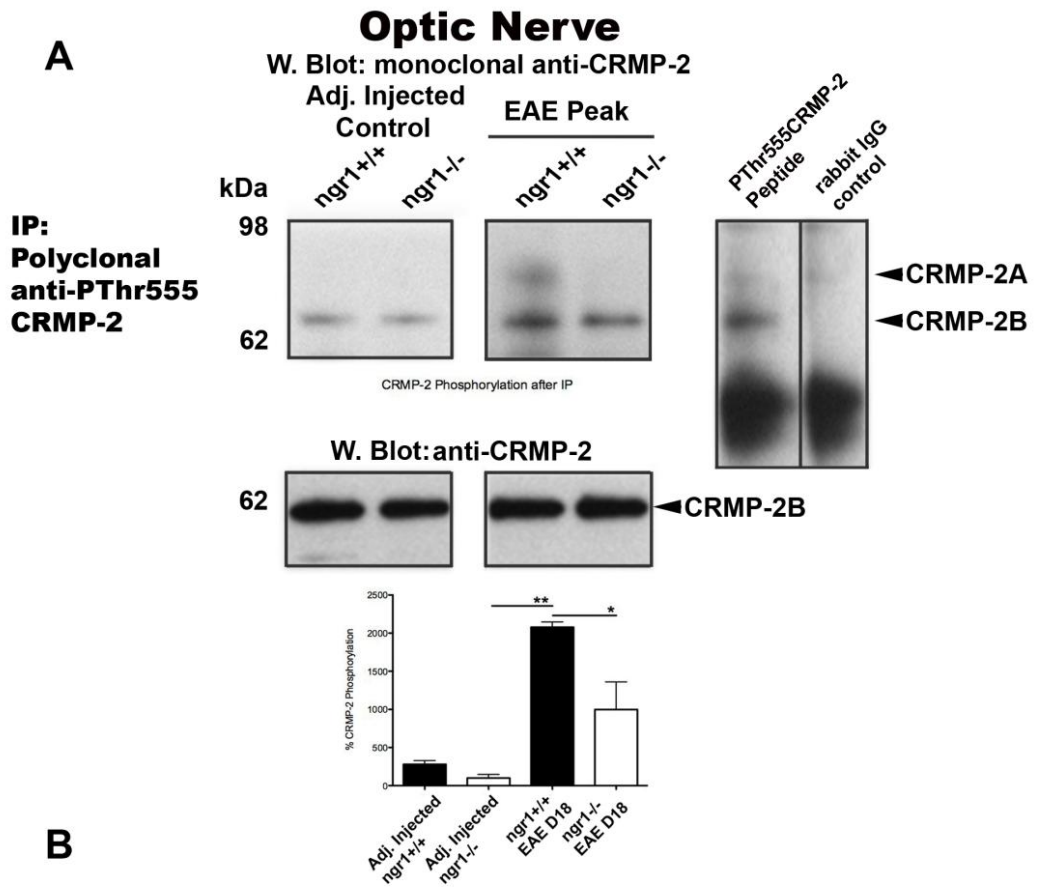


Figure 6. Axonal and myelin damage in the optic nerve of EAE-induced *ngr1^{-/-}* mice is reduced and corresponds with abrogated CRMP-2 phosphorylation. C) Increased demyelination of optic nerves in *ngr1^{+/+}* mice during the course of EAE as determined by G-ratios. At pre-onset and onset of EAE, respectively in *ngr1^{-/-}* mice (n = 3 mice per genotype, per disease stage and per animal), there is a reduction nearing basal levels (adjuvant injected controls). By peak stage of EAE, there is an increase in the G-ratios (i.e. axonal degeneration/demyelination) of *ngr1^{+/+}* mice. The percentage of demyelination is significantly reduced in the *ngr1^{-/-}* after EAE-induction, except at pre-onset stage of disease. Axonal diameters in the optic nerves are increased in *ngr1^{+/+}* mice following EAE-induction. The greatest axonal diameter was demonstrated by peak stage of EAE in *ngr1^{+/+}* mice. In the *ngr1^{-/-}* mice, axonal calibre remains relatively unaltered, with only a modest increase in the axonal diameter by peak stage of disease (**P<0.001, **P<0.01 and *P<0.05 for *ngr1^{+/+}* versus *ngr1^{-/-}* at all time points, analysed by ANOVA with Tukey's post hoc test). D) Number of viable myelinated axons in optic nerve semi-thin sections from *ngr1^{+/+}* and *ngr1^{-/-}* mice during the course of EAE (n = 3 mice per genotype, per disease stage and per animal). A significant reduction in axonal viability is demonstrated in the *ngr1^{+/+}* by peak stage of EAE (**P<0.01, analysed by one-tailed student's t-test). Published in Petratos, S. et al. (2012) *Brain* **135**: 1794-1818 (Appendix I).

(from 25.23 ± 0.21 (Arbitrary Units) at Day 7 to 27.42 ± 0.41 by Day 18 post-EAE induction; Fig. 6C). However, in the optic nerves of *ngr1*^{-/-} mice, there was only a modest increase in axonal diameters by peak stage of EAE, which was just above baseline (26.06 ± 0.19 (Arbitrary Units); Fig. 6C). These data suggest limited axonal swelling in the optic nerves of the *ngr1*^{-/-} mice during EAE. Highlighting the neurobiological role of the *ngr1* gene, there was an enhanced viability of axons in the optic nerves of *ngr1*^{-/-} mice during EAE (Fig. 6D). We showed that there were no differences in axonal loss in the optic nerves of *ngr1*^{+/+} and *ngr1*^{-/-} mice during the pre-onset and onset stages of EAE (Fig. 6D), although axons had swollen in the *ngr1*^{+/+} EAE-mice (Fig. 6C). However, by peak stage of EAE, we saw a dramatic drop-out of optic nerve axons in the *ngr1*^{+/+} mice (16048 ± 2316 myelinated axons per square millimetre) that was not replicated in the *ngr1*^{-/-} mice (30818 ± 3141 myelinated axons per square millimetre, $P < 0.01$; Fig. 6D). Thus we can conclude that there is a preservation of axons in the *ngr1*^{-/-} mice at the peak stage of EAE, correlating with myelin maintenance and a decrease in axonal swelling (Fig. 6C). We further demonstrated that there was an increase in the phosphorylation of CRMP-2 in the optic nerves of *ngr1*^{+/+} mice by peak stage of EAE (Fig. 7A). These data correlated with significant levels of axo-myelin degeneration and loss in the *ngr1*^{+/+} mice (Fig. 6C and D), showing approximately a 2-fold increase of CRMP-2 phosphorylation when compared to the *ngr1*^{-/-} mice at peak stage of EAE as determined by western blotting (Fig. 7A). The emergence of the 75 kDa PCRMP-2A band in the *ngr1*^{+/+} optic nerves was again present with EAE-induction but absent in *ngr1*^{-/-} mice (Fig. 7A). The levels of tubulin association with CRMP-2 were also reduced in the optic nerves of the *ngr1*^{+/+} mice, correlating with the phosphorylation status of CRMP-2 (Fig. 7B), mimicking what was observed in the lumbar cord of these mice (Fig. 5). These data implicate the phosphorylation of CRMP-2 with axonal degeneration during the progression of EAE in the optic nerve of *ngr1*^{+/+} mice and suggest that deletion of the *ngr1* gene limits this molecular mechanism of axo-myelin degeneration from ensuing, in the context of neuroinflammation.

Figure 7. Axonal and myelin damage in EAE-induced *ngr1*^{-/-} mice is reduced and corresponds with abrogated CRMP-2 phosphorylation. A) Immunoprecipitation of pThr555CRMP-2 of pooled optic nerve lysates from EAE-induced *ngr1*^{+/+} and *ngr1*^{-/-} mice (n = 6 per group), followed by reprobing of the membranes with the monoclonal anti-CRMP-2 antibody. There is an increase in pThr555 CRMP-2 of both the CRMP-2A and CRMP-2B variants in EAE-immunized *ngr1*^{+/+} mice at peak of disease. No such changes occurred in the *ngr1*^{-/-} mice at the same time-points after MOG₃₅₋₅₅ challenge. Control lanes include non-specific rabbit IgG polyclonal antibody and PCRMP-2 (20 mg) peptide spiked in lysate buffer alone. A pre-immunoprecipitation, 5% input of protein from spinal cord lysates show no discernible difference in total levels of CRMP-2. Densitometric quantification of total CRMP-2 and PCRMP-2B (after IP) from optic nerve lysates of control, *ngr1*^{+/+} and *ngr1*^{-/-} EAE-induced mice, represented as a percentage of basal levels (control uninjected *ngr1*^{-/-} mice; n = 6 mice per group; **P*<0.05 one-way ANOVA, ***P*<0.01). Representation of the percentage change in the levels of PCRMP-2 demonstrates up to a 2-fold increase occurring in *ngr1*^{+/+} EAE-induced mice when compared with *ngr1*^{-/-} mice at peak stage of disease. B, top) Co-immunoprecipitation of CRMP-2 from optic nerve lysates of control, *ngr1*^{+/+} and *ngr1*^{-/-} EAE-induced mice, showed a decreased association with tubulin in the *ngr1*^{+/+} mice at peak stage of EAE. This finding was not replicated in the *ngr1*^{-/-} EAE-induced mice. B Left) Densitometric quantification of the levels of CRMP-2-associated tubulin (after IP) from spinal cord lysates of control, *ngr1*^{+/+} and *ngr1*^{-/-} EAE-induced mice, represented as a percentage of basal levels (n = 6 mice per group; **P*<0.05 one-way ANOVA). B Right) Representation of the percentage change in the levels of CRMP-2-bound tubulin, demonstrates an increase in the dissociation of tubulin from CRMP-2 in *ngr1*^{+/+} when compared with *ngr1*^{-/-} EAE-induced mice at peak stage of disease (**P*<0.05). Published in Petratos, S. et al. (2012) *Brain* **135**: 1794-1818 (Appendix I).



5.3.3 Immune activation following EAE-induction is unaltered in *ngr1*^{-/-} mice

Having demonstrated a direct correlation between the limitation of axonal degeneration and the abrogation of NgR1-signalling through phosphorylation of CRMP-2, we next asked whether the deletion of the *ngr1* gene related to the inability of these mice to mount an appropriate autoreactive immune response. Since recent reports have implicated the involvement of NgR1-signalling in the efflux of activated macrophages from injured peripheral nerves (299), and that monocytes, T and B cells isolated from patients with MS show a significant expression of NgR1 (300), we further analysed the activity of *ngr1*^{-/-} mice to mount appropriate T cell responses to MOG. To that effect we analysed the peripheral immune response of EAE-induced *ngr1*^{+/+} and *ngr1*^{-/-} mice. We found no relative differences in the proliferative responses of T cells to MOG₃₅₋₅₅ from *ngr1*^{-/-} and *ngr1*^{+/+} mice, quantified from stimulated splenocyte cultures with MOG₃₅₋₅₅ peptide at 5, 10 and 20 µg/ml (Fig. 12A). The average stimulation indices (SI) for these time-points were 7 ± 4 , 8 ± 5 and 10 ± 6 AU for *ngr1*^{+/+} and *ngr1*^{-/-}, respectively (Fig. 8A). As for the auto-reactive T cell studies, cytokine assays were performed from the supernatant of splenocyte cultures using the Cytokine Bead Array system (BD Biosciences) and revealed no differences between *ngr1*^{-/-} and *ngr1*^{+/+} mice (12 and 18 dpi) following MOG₃₅₋₅₅-induction (Fig. 8B). There was no significant difference found in the cytokine levels derived from splenocyte cultures at the peak stage of EAE between the *ngr1*^{-/-} and *ngr1*^{+/+} mice. The pro-inflammatory cytokines IFN- γ , TNF, IL-2, IL-17A and IL-1 β were shown to be at similar levels and there was no difference in the acute-phase cytokine IL-6 (Fig. 12B). These data suggest that both pro- and anti-inflammatory reactions are intact in the *ngr1*^{-/-} mice. Similarly, Th2-dependent cytokine levels in splenocyte cultures isolated at day 18 post-EAE-induction from *ngr1*^{-/-} mice, such as IL-4, were not different when compared with *ngr1*^{+/+} mice (Fig. 8B). In keeping with these data, levels of the anti-inflammatory cytokine IL-10, were similar between the two genotypes (Fig. 8B). To determine whether there exists a perturbation in the granulocyte/monocytic cell differentiation capacity in the *ngr1*^{-/-} mice, we measured the levels of GM-CSF and found no differences in the levels being generated from the splenocyte cultures of these mice (Fig. 8B). This suggests that the potential for immune-mediated induction of disease is not altered in the *ngr1*^{-/-} mice. On the basis of these findings it is likely that the limitation in the neurological decline exhibited by the *ngr1*^{-/-} mice, relates to an altered neurobiological mechanism.

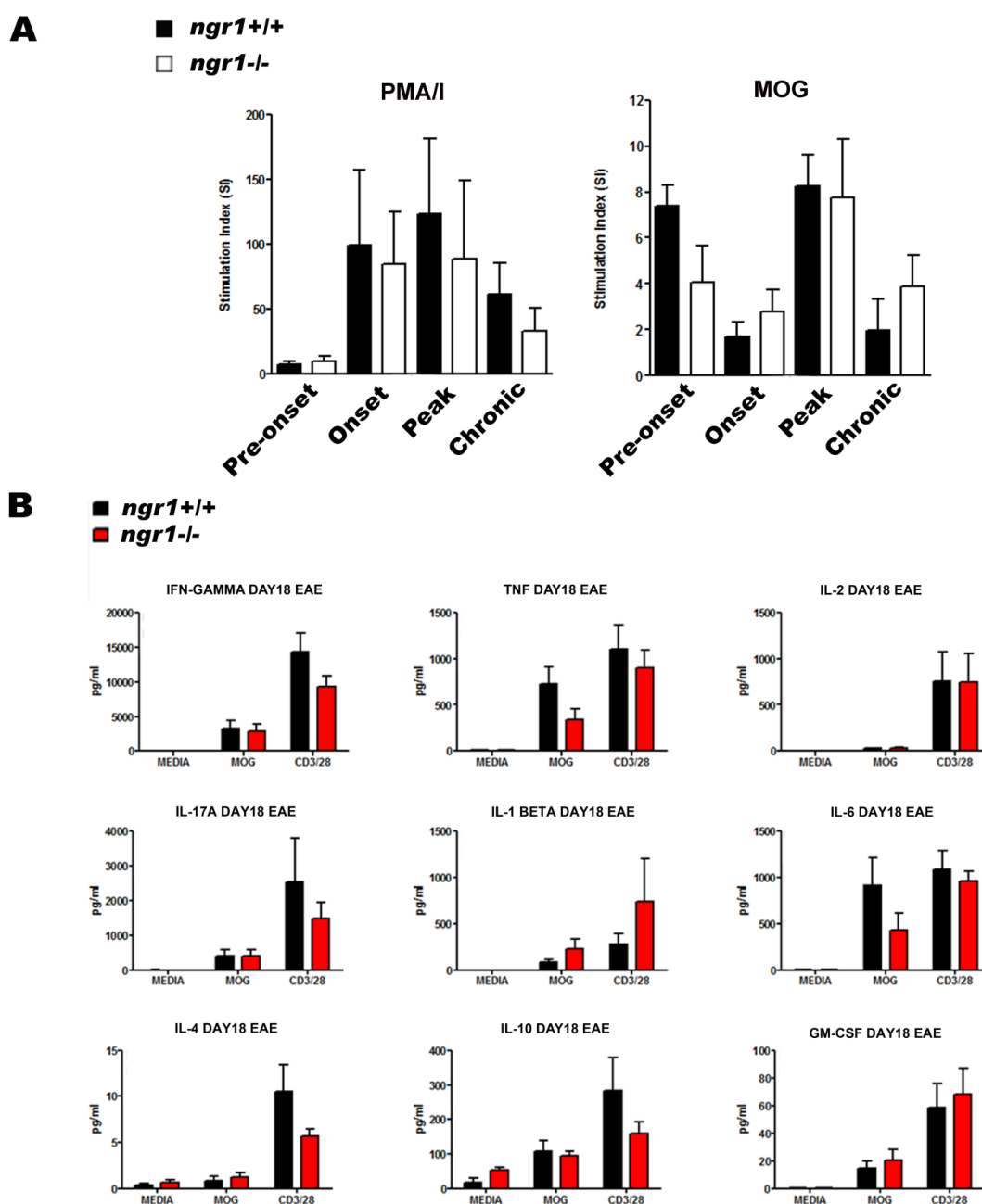


Figure 8. Immune activation following EAE-induction is not different in *ngr1*^{-/-} mice. A) Proliferation responses (stimulation index, SI) of splenocytes isolated from *ngr1*^{+/+} and *ngr1*^{-/-} EAE-induced mice, treated in culture with either non-specific phorbol myristate acetate and ionomycin (PMA/I, [200 ng/ml and 8 µg/ml, respectively]), or MOG₃₅₋₅₅ [20 µg] (n=3 per group; mean of triplicate measurements ± SEM). B) Generation of the following cytokines: INF-γ, TNF, IL-2 IL-17A, IL-1β, IL-6, IL-4, IL-10 and GM-CSF (represented as pg/ml), following the stimulation of the splenocytes from *ngr1*^{+/+} and *ngr1*^{-/-} EAE-induced mice at peak stage of disease with either medium alone, MOG₃₅₋₅₅ [20 µg] or non-specific stimulation of CD3/28 receptors (n=3 per group; mean of triplicate measurements ± SEM). Published in Petratos, S. et al. (2012) *Brain* **135**: 1794-1818 (Appendix I).

5.3.4 Phenotype of immune cells of naïve and EAE-induced *ngr1*^{-/-} mice.

The presence of NgR1 and its reported role on the migration of particular leukocyte subsets (301) suggest that NgR1 could potentially influence the behavior of immune cells during the initial events leading to CNS autoimmunity. As a preliminary step towards understanding the impact of NgR1 on the development of EAE, we first investigated the proportion and total number of various immune cell subsets in primary and secondary lymphoid tissues as well as the CNS and blood of naïve *ngr1*^{-/-} mice and their WT littermates. Specific markers were used to define each population, namely, CD4/CD3 and CD8/CD3 for assessing T lymphocytes, B220 for B lymphocytes, NK1.1 for natural killer cells, and Gr-1/F4/80 for granulocytes and monocytes/macrophages. Figure 9 shows the proportion and number of CD3+, B220+, Gr1+ and Gr-1+ and F4/80+ cells in all six organs analyzed. Overall the immune phenotype of *ngr1*^{-/-} was comparable to that of the *ngr1*^{+/+} mice, however, a slight but significant decrease in the proportion of CD3+ cells was observed in the *ngr1*^{-/-} spleens (*ngr1*^{-/-} 37.0±1.6% vs. *ngr1*^{+/+} 44.1±2.7%; *P*=0.04, *n*=8). Compared to the BM compartment of *ngr1*^{+/+} mice, *ngr1*^{-/-} mice showed an increase in the number of B220+ cells (*ngr1*^{-/-} 271.0 ± 29.4x10⁴ vs. *ngr1*^{+/+} 159.0 ± 22.6x10⁴; *P*=0.02, *n*=5), Gr-1+ cells (*ngr1*^{-/-} 504.5 ± 53.2x10⁴ vs. *ngr1*^{+/+} 355.9 ± 31.2 x 10⁴, NS, *n*=5) and F4/80 (*ngr1*^{-/-} 318.6 ± 34.6 x10⁴ vs. *ngr1*^{+/+} 236.6 ± 11.5 x 10⁴ , NS, *n*=5). There was also a significant increase in the number of single positive thymocytes detected in the thymus of *ngr1*^{-/-} mice, for both the CD4+ (*ngr1*^{-/-} 1319.9 ± 243.6x10⁵ vs. *ngr1*^{+/+} 626.1 ± 77.2x10⁵; *P*=0.03, *n*=5) and CD8+ (*ngr1*^{-/-} 833.9 ± 159.6x10⁵ vs. *ngr1*^{+/+} 341.5 ± 54.0x10⁵; *P*=0.02, *n*=5) subsets. No statistically significant difference in the proportion or number of immune cell subsets was found in the blood or lymph nodes. Since no major differences in immune cell subsets were identified between naïve *ngr1*^{-/-} and *ngr1*^{+/+} animals, we next sought to determine whether the lack of NgR1 could impact on the trafficking of leukocytes to the CNS, thereby affecting the development of EAE, provoked by MOG₃₅₋₅₅. To this effect, we first compared the development and severity of EAE in *ngr1*^{-/-} and *ngr1*^{+/+} mice up to peak stage of disease. There was a small but significant delay in the onset of disease in *ngr1*^{-/-} mice compared to WT (*ngr1*^{-/-} day 10.5 ± 0.3 vs. *ngr1*^{+/+} day 11.9 ± 0.5; *P*=0.02, *n*=11-13) (Fig. 10A). To determine if the composition of immune cells differed between *ngr1*^{-/-} and *ngr1*^{+/+} mice during the course of EAE, the proportion and total number of CD3+, B220+, Gr-1+ and Gr-1loF4/80+ cells present in the spleen and CNS of these mice were analyzed by flow cytometry at 18 dpi. As indicated in Figure 10B, no significant differences in the number and proportion of T cells, B cells or granulocytes/monocytes were found between *ngr1*^{-/-} and *ngr1*^{+/+} at this time point. On the basis of these findings, it would appear that under inflammatory

conditions, the presence of NgR1 on immune cells has little or no influence on their migratory behavior in the CNS.

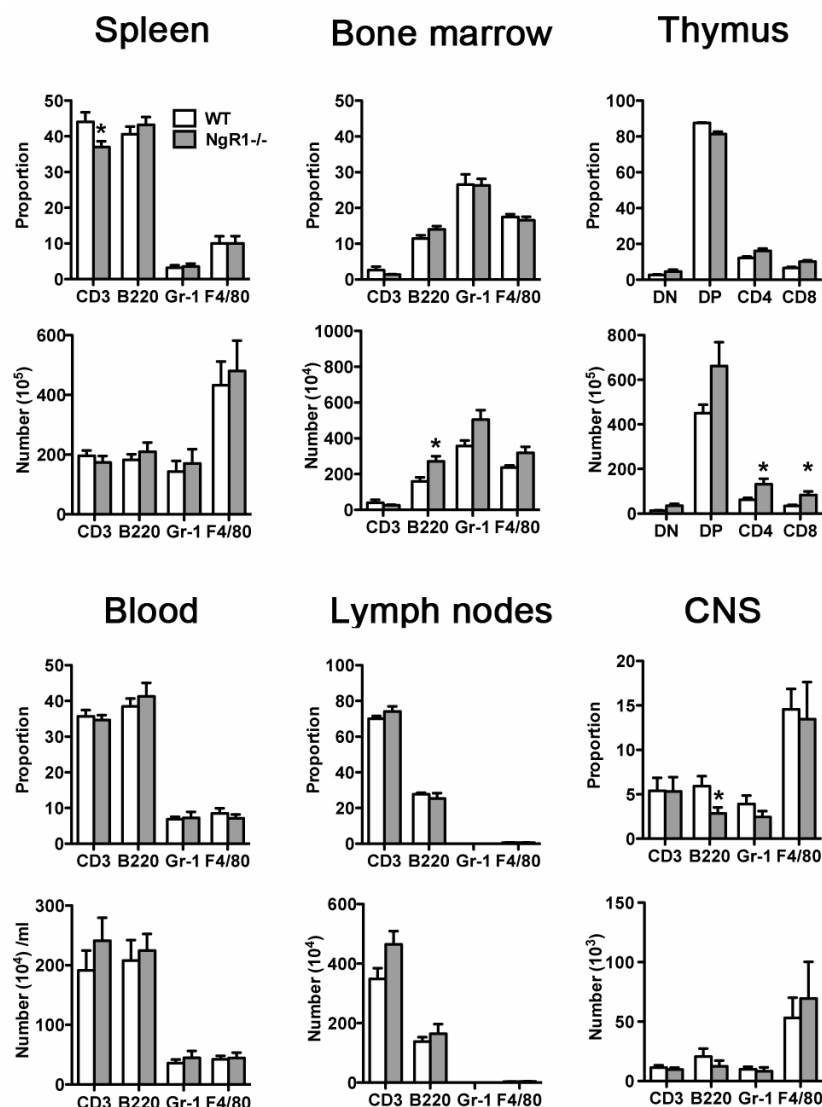


Figure 9. Immune-phenotype and bone marrow progenitor status of naïve *ngr1*^{-/-} and WT mice. Comparative flow cytometric analysis of single cell suspension from spleen, BM, thymus, blood, lymph nodes and central nervous system (CNS) associated mononuclear cells. Proportion and total number of subsets positive for lymphoid CD3+CD8+, CD3+CD4+ and CD3+NK1.1+, pooled under CD3, and for B220 membrane markers, granulocytic Gr-1 and monocyte/macrophage F4/80 (Gr-1^{lo}F4/80⁺) cells are shown. *ngr1*^{-/-} mice presented a decreased CD3+ cell proportion in their spleen, and increased B220+ and Gr-1+ cell number in their BM. A decreased B220+ cell proportion in the CNS and an increased number of CD4+ and CD8+ cells in the thymus were observed. Bars represent mean \pm SEM. * $P < 0.05$ Mann-Whitney test. (n=8-11). Unpublished manuscript (Appendix IV).

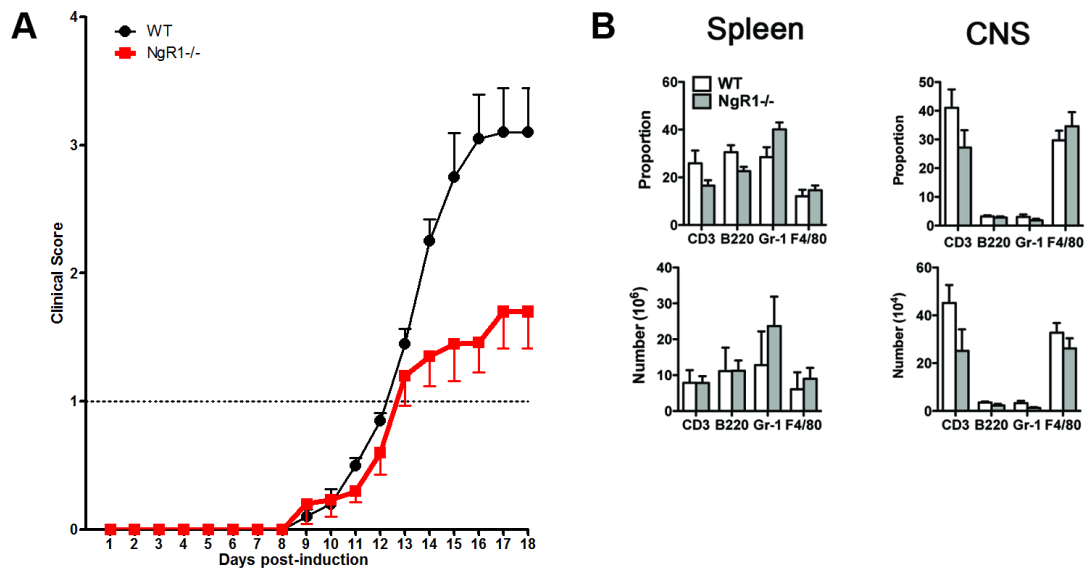


Figure 10. Reduced severity of MOG35-55 peptide-EAE in *ngr1*^{-/-} mice. (A) EAE was induced by immunization with MOG₃₅₋₅₅ peptide and animals were scored daily for disease clinical manifestations. NgR1 deficient animals presented a less severe clinical disease than the WT group. Data (mean ± SEM) pooled from 2 independent experiments (n=11-13). ****P*<0.05. Two-way ANOVA. (B C) Flow cytometric analysis of spleen and Central Nervous System (CNS) mononuclear cells. At day 18 post-MOG₃₅₋₅₅ immunization, single cell suspensions were prepared and analyzed for their immune-profile by Flow cytometry as above. The proportion and number of immune markers analyzed did not reach significant different values between the NgR^{-/-} and the WT. Bars represent mean ± SEM (n=3-5). Unpublished manuscript (Appendix IV).

5.4 Discussion

Despite the numerous investigative reports of NgR1 signalling in the CNS during disease and injury, there exists debate as to whether the limitation in axonal damage or enhanced regrowth potential is regulated through this mechanism. The current study supports the contention that limiting NgR1-dependent phosphorylation of CRMP-2 (which normally functions to regulate axonal microtubule assembly), axonal degeneration and hence neurological impairment can be halted in EAE. Our study advocates that targeting NgR1-signalling in EAE, and by extension multiple sclerosis, may be a feasible therapeutic approach to limit the neurodegenerative effects of these conditions. Current therapeutics in multiple sclerosis target the inflammatory nature of the disease in an attempt to limit the 'autoimmune attack' on CNS myelin and, as a consequence, reduce the devastating neurological complications that characterize this disease. However, comprehensive neuropathological investigations from a vast array of multiple sclerosis brain samples suggest a degree of heterogeneity in the pathogenesis, with some lesions showing tangible neurobiological origins (302). Both the 'outside-in' and 'inside-out' hypotheses of demyelination and axonal degeneration involve dysregulation of axo-glial signalling, driving axonal degeneration potentiating neurological decline and establishing disability.

Using the exon 2 nogo receptor null mutant mice bred on a C57BL/6 background (259), we report that the signalling mechanism that is operative during the neurodegenerative phase of EAE relies on NgR1-dependent phosphorylation of CRMP-2. A significant increase in the phosphorylation of CRMP-2 at the Thr555 site, specific for ROCKII (173, 240, 292), was demonstrated to be operative in EAE. This mechanism has been previously identified to be important in neurite/axon retraction events in culture (240, 292). Similarly, pThr555-CRMP-2 has been demonstrated to be responsible for axonal degeneration in an acute model of SCI (173). Our finding that levels of PCRMP-2 in the spinal cord and optic nerve of *ngr1^{+/+}* but not *ngr1^{-/-}* mice, incrementally increased during the clinical and pathological progression of EAE, is critical in defining a neurobiological basis for this signalling cascade during neuroinflammatory-mediated degeneration.

There is strong evidence that phosphorylation of CRMP-2, either by GSK-3 β , Cdk-5 or ROCKII, inactivates the normal physiological functions of CRMP-2. Physiologically, CRMP-2 can associate with α - and β -tubulin heterodimers (246, 292), kinesin-1 motor proteins (238), TrkB and the Sra/WAVE1 complex, to facilitate anterograde axonal transport, and thereby growth, repair, maintenance and communication (236, 239).

Disruption of transport of this molecular cargo is integral for the interruption in the maintenance of the axonal terminal and by extension, synaptic connectivity (238, 239, 246, 303). The consequential loss of axo-dendritic connectivity, mediated through various negative signal transduction events, leads to actin and tubulin depolymerisation and eventual axonal retraction (293). The CNS tissue milieu during injury or disease is rich in axonal outgrowth inhibitors such as Nogo-A, potentiating axonal retraction events and blocking regeneration (69). However, the question remains as to whether these events can be initiated during neuroinflammatory diseases such as EAE and multiple sclerosis. Our data suggest that pThr555CRMP-2 is involved as a neurodegenerative molecule of axons and neurons in EAE and that this signal can be limited by ablation of the NgR1 gene during acute neuroinflammation, without any immune-dependent mechanisms being directly responsible for this signalling. However, we did observe that the phosphorylation of CRMP-2 was reduced at the chronic stage of EAE, a stage where neurodegeneration continues to progress, and this warrants further investigation. However, one line of investigation may derive from data that show that CRMP-2 is cleaved by calpain during overt neurodegeneration, forming a 55 kDa truncated form (295). Such forms of CRMP-2 have been linked to neuronal cell death in various models of neurodegeneration (295).

It was recently discovered that the co-receptor of NgR1, LINGO-1, can promote demyelination in the MOG₃₅₋₅₅ EAE murine model (166). These investigators showed that in MOG₃₅₋₅₅-induced *lingo-1*^{-/-} mice or wild-type EAE-induced mice treated with a function-blocking anti-Lingo-1 antibody, demyelination was limited thereby blunting the neurological decline. Although these findings implicate the NgR1 signalling complex in the promotion of demyelination during neuroinflammation, our data suggest that targeting the NgR1 high-affinity receptor for myelin associated inhibitory factor-binding limits axonal degeneration during the onset and peak stages of EAE. Interestingly, at the early pre-onset stage of EAE, we found an equivalent proportion of demyelination in the optic nerves of both the *ngr1*^{-/-} and wild-type littermate mice. However, this initial thinning of myelin (increasing G-ratio) does not persist with progression of disease in the *ngr1*^{-/-} mice, suggesting that possible remyelination may in fact be preserving axons at the early stage of neuroinflammation (304). These data demonstrate that inhibition of the phosphorylation of CRMP-2 can prevent neuroinflammatory-mediated axonal degeneration.

Given the recent implication that NgR1 is involved in the efflux of activated macrophages from injured peripheral nerves (299), we wanted to investigate the

possibility of a putative immune role for NgR1 during CNS inflammation. We found no discernible difference in the proliferation response of T cells isolated from *ngr1^{-/-}* and *ngr1^{+/+}* mice at pre-onset, peak and chronic stages of EAE (7, 18 and 30 days post-injection) in response to the MOG_{35–55} peptide (Fig. 12). Furthermore, we were unable to demonstrate differences in cytokine profiles from EAE-induced *ngr1^{-/-}* (12 and 18 days post-injection) compared with *ngr1^{+/+}* mice. The inference would therefore be that the potential for immune-mediated induction of disease is not altered in the *ngr1^{-/-}* mice. Thus, it would appear that the limitation of the neurological decline in the *ngr1^{-/-}* mice is dependent on a neurobiological mechanism. Despite this, recent data show that monocytes, T and B cells isolated from patients with multiple sclerosis express NgR1 (300). Given that stimulation of immune cells with Nogo led to an alteration of their adhesion properties, it is possible that in immune cells, NgR1 signalling regulates their cytoskeletal dynamics through Rho-A activation (300). Therefore, further investigation is required to implicate or exclude a role of NgR1 in immune cell activation and migration in multiple sclerosis. In order to further assess the relevance of NgR1 in the development of encephalitogenic and pathogenic immune responses, we undertook a comprehensive phenotypic characterization of immune cells present in primary and secondary lymphoid organs of NgR1 deficient mice before and after MOG₃₅₋₅₅ stimulation. We report here that the lack of NgR1 has no significant impact on the phenotype of peripheral immune cells both, before or after antigenic stimulation, or on cells trafficking to the CNS.

This study has provided new insights into the molecular mechanisms that govern axonal degeneration during inflammatory demyelination of the CNS as occurs in EAE. Since myelin damage is a dominant event in neurodegeneration, the work presented here may provide novel therapeutic avenues to attenuate axonal abnormalities, which accompany demyelination in a variety of disorders such as spinal cord and brain injury, stroke and MS. We suggest that blockade of NgR1 signalling and reduction of CRMP-2 phosphorylation limits axonal degeneration in EAE, allowing for the normal physiological function of CRMP-2 to ensue, and by virtue, limiting the axonal degeneration and alleviating clinical symptoms of EAE.

Chapter 6

GENERAL DISCUSSION

MS and SCI are debilitating conditions that greatly impact quality of life. Current treatment strategies available are not very effective, yielding minimal functional recovery in long term sufferers. 2.5 million individuals have been diagnosed with MS globally, while for spinal cord injury, the estimated global incident rate is around 180000 cases per year (2, 305). These alarming statistics highlight the urgency as well as a need for discovering more effective therapeutic drugs that elicit significant recovery of motor function in those individuals affected by such disorders. In SCI, following primary insult, a secondary phase of injury ensues. At the primary site of injury resident cells become activated and initiate a neuroinflammatory response, recruiting inflammatory cells such as lymphocytes and activating microglia in the affected area (306). Prolonged and continuous inflammatory activity propagates neurodegeneration, resulting in additional cell damage and cell death at the primary lesion site, along with delayed neuronal cell death in nearby CNS tissue. In MS, the leakage of the BBB and the influx of autoreactive T cells into the CNS initiates an inflammatory cascade that perpetuates a cycle of neurodegeneration by demyelination, axonal damage and neuronal loss. Therefore it is plausible that similar mechanisms of neurodegeneration play a part in the acute and chronic stages of MS and SCI. One such common feature of neurodegeneration between MS and SCI is that both are governed by a non-permissive extracellular growth environment. Understanding the molecular mechanisms leading to axonal degeneration is of critical importance for the development of novel therapeutic strategies aimed at limiting the neurological decline observed in MS and SCI patients.

The action of the MAIFs on severed axons attempting regeneration after injury or disease has been determined to be one of the most critical inhibitory events that limits CNS repair. The molecular interaction of the MAIFs with NgR1 is a high-affinity ligand-receptor interaction that initiates intracellular signalling in affected neurons, converging on the Rho-GTPases to inhibit axonal regrowth. The downstream effectors of Nogo-A/NgR1 signalling are RhoA-GTP and CRMP-2 that regulate actin and tubulin dynamics after injury (173). The CRMPs regulate microtubule assembly as well as anterograde vesicular transport of important growth-related molecular cargo along neuronal microtubules (222). The CRMPs, particularly CRMP-2, are involved in the formation, outgrowth, and guidance of neurites. CRMP-2 is phosphorylated by cyclin-dependent kinase 5 at serine 522 (242, 244), glycogen synthase kinase 3A at threonine 509/514, serine 518 (223, 307), and also ROCKII at threonine 555 (240, 246); all of these can mediate neurite retraction. Such phosphorylation disrupts the association of CRMP-2 with tubulin heterodimers so that tubulin cannot be transported

to the plus ends of microtubules for assembly, thereby impeding directional growth of the neurite (222). Importantly, CRMP-2 phosphorylation also reduces its binding to the microtubule-related motor protein kinesin 1, which is involved in anterograde vesicular axonal transport of molecules that regulate synaptic integrity and plasticity to the distal ends of axons (239). Therefore, preventing the activation of these mechanisms is an avenue by which endogenous regrowth can be promoted.

Several pharmacological agents have been developed to target MAIFs in the context of injury, particularly those aimed at blocking the binding of Nogo-A to NgR1 (106, 150, 151, 160, 162, 163, 308-312). NgR(310)ecto-Fc is a soluble protein that encompasses the whole NgR1 ligand-binding domain which can competitively bind Nogo-A, OMgp and MAG and diminish their interactions with endogenous NgR1. Intrathecal or intracerebroventricular administration of NgR(310)ecto-Fc immediately or 3 days following spinal cord contusion injury in rats, continuously for a period of 28 days, resulted in very significant improvement of BBB locomotor scores in these cohorts, regardless of the therapy approach (163). Similarly, administration of anti-Nogo-A antibodies to treat spinal cord injury has been just as successful in rats and non-human primates (149, 150, 308-310, 312). Adult macaque monkeys subjected to unilateral SCI, which severely impairs hand function, showed improved manual dexterity after receiving intrathecal anti-Nogo-A antibody treatment for four weeks following injury (310). Furthermore, at the lesion site, corticospinal axons presenting with terminal retraction bulbs (a clear sign for neurodegeneration) were decreased and corticospinal axonal sprouting enhanced (310). These significant findings position NgR1 signalling as the driving force behind neurodegeneration in the injured CNS and highlights the therapeutic potential of blocking this inhibitory pathway. A phase I clinical trial using human anti-human Nogo-A antibody (ATI355, Novartis) in paraplegic and tetraplegic patients with acute SCI has recently been completed with great success (www.clinicaltrials.gov, NCT00406016; Abel et al., 2011). The anti-Nogo-A antibody was administered as a continuous intrathecal infusion (4 groups with varied antibody dose) up to 4 weeks, or as a repeated manual intrathecal bolus injection (2 groups, 6 injections, varied antibody dose per group) in patients with acute SCI, within 4-28 days post injury. While no adverse side effects were reported in either method of delivery, the intrathecal bolus injections were considered to improve treatment safety and minimise possible infection and surgical complications. We now await the results from phase II clinical trials.

Upon injury, the axo-glial unit is compromised; loss of trophic support and severing of axons elicit neuroinflammation and oligodendrocyte apoptosis in both acute and chronic phases of injury. The death of one myelinating oligodendrocyte can affect and denude multiple axons simultaneously (32). Therefore, therapies that limit oligodendrocyte death and subsequent deposition of MAIFs at the sites of injury is another avenue by which axonal regrowth can be encouraged. LIF has been shown to promote oligodendrocyte survival in a mouse model of SCI (280). In another report, LIF administration after SCI in mice resulted in significant recovery in hind limb locomotor function and an increase in the number of myelinated axons around the lesion site (261). These findings were attributed to the capacity of LIF to potentiate myelination of new axons. Complementary to this data, we have previously shown that LIF administration in a rodent model of spinal cord hemisection prevented oligodendrocyte apoptosis contralateral to the spinal cord lesion and preserved myelination in viable axons (260). Collectively these findings suggest that administration of LIF may enhance regeneration in the injured CNS by limiting axonal injury through preservation of myelinated axons and consequently allowing growth promoting mechanisms to ensue.

In a therapeutic paradigm, we hypothesized that by reducing the capacity of the myelin-derived deposits to signal through their cognate receptors following SCI by way of LIF administration, it may be possible to limit the activation of the RhoA/PCRMP-2 pathway in axons, thereby limiting degeneration. As reported in Chapter 3, we further characterised the implications of LIF therapy in altering the deposition of the MAIF, Nogo-A, and in the activation of molecules downstream of NgR1 signalling including RhoA and PThr555CRMP-2 using the hemisection SCI model (260). Functionally, animals undergoing LIF treatment exhibited continuous and significantly enhanced locomotor recovery compared to the MSA-treated control group, as determined by BMS scores. Spinal cord tissue obtained from LIF-treated animals presented with reduced Nogo-A deposits both caudal and rostral to the lesion site, and this was highly significant at the one week time point. Furthermore, we found increased expression of the growth associated molecules GAP-43 and Rac1-GTP at one week post-SCI. Correspondingly, a decrease was observed in the expression of RhoA and PCRMP-2, the molecules associated with growth inhibition. These findings indicate that exogenous LIF treatment can promote the activation of regenerative mechanisms in the acute phase of SCI. Therefore we conclude that LIF administration aids in improved locomotor function by limiting the deposition of myelin debris at lesion sites thereby reducing the activation of endogenous inhibitory axonal NgR1 signalling. Thus,

therapeutic strategies limiting deposition of MAIFs like Nogo-A could be ideal candidates to bring forth into human clinical trials.

An important observation generated from control SCI mice pertains to the considerable Nogo-A deposition not only seen at the lesion site but also in areas rostral and caudal to the lesion. Complementary to this, RhoA-GTP activation was most pronounced at the site of injury and this correlated with an increase in the levels of ROCKII-phosphorylated CRMP-2 at the same time point. These data imply that Nogo-A/RhoA/PCRMP-2 signalling is a major contributor to the non-permissive environment milieu surrounding CNS lesions. Furthermore, we did not detect upregulation of growth promoting molecules such as GAP-43 and GTP-Rac1 (active Rac1) in these animals at this time point, contrary to what was observed in the LIF treatment group, suggesting a failure in the activation of regenerative mechanisms. These findings suggest that an increase in extracellular MAIF deposition after CNS injury can signal CRMP-2 phosphorylation, possibly limiting microtubule assembly and therefore axonal regrowth. We did however, find an increase in GTP-Rac1 but not GAP-43 and a subsequent decrease in RhoA-GTP in the MSA treated groups two weeks post-SCI. While an explanation for this finding remains elusive, it must be noted that the BMS scores in these animals had shown some improvement of locomotor function at the two week time point. Therefore one could speculate that NgR1 signalling plays a more prominent role in the acute phases of SCI. However, further elucidation of these mechanisms are required. Perhaps, a similar investigation of LIF treatment in NgR1 KO mice with SCI would assess this contention.

The histopathological patterns of MS have been well characterized, with much emphasis on the destructive immunologic component of the disease in the brain and spinal cord (302). Currently, the mechanisms underlying axonal damage in MS are being defined. Axonal damage can either develop secondary to white matter damage, or, as recently postulated, may be a primary or precipitating event in MS. A more plausible scenario would be that axonal degeneration occurs concomitantly with demyelination (62). Trapp et al (55) reported the common appearance of newly transected axons in active and hypocellular chronic active MS brain lesions obtained at autopsy, corroborating such a hypothesis. Importantly, it is now recognized that permanent neurological impairment is a consequence of the level of axonal loss in MS (62). It is now evident that blockade of NgR1 signalling via ligand-receptor interactions or inhibition of activated downstream mediators promotes regeneration and axonal growth in the lesioned CNS (151). However at present, our knowledge of MAIF induced

axonal degeneration by way of the NgR1/Rho-A/PCRMP-2 signalling pathway in animal disease and injury models is very limited. There exists only one publication that focuses on ROCKII dependent CRMP-2 phosphorylation in a rat model of SCI (173). Our findings in Chapter 3 support and validate the view that axonal degeneration as a consequence of SCI is in part driven by RhoA activation and ROCKII-dependent phosphorylation of CRMP-2. These intriguing data raise the question as to whether Nogo-A can signal axonal degeneration in EAE and in MS and whether this leads to downstream modification and phosphorylation of CRMP-2.

This prompted the research reported in Chapter 4. More specifically, we followed the progression of MOG-induced EAE (over 30 days), and investigated the localisation and expression of PThr555CRMP-2 and its ability to bind and transport tubulin in the context of axonal injury. We found that the levels of PCRMP-2 correlated with axonal degeneration in EAE. In the lumbar cords of EAE animals, PCRMP-2 expression was restricted to *tuj-1* positive axons undergoing neurodegeneration at all time points examined, which was most marked at peak stage of disease. Interestingly, PCRMP-2 was detected as early as the pre-onset stage of EAE, supporting the idea that axonal degeneration and demyelination occur concomitantly (55, 62). Furthermore, while CRMP-2 association with tubulin heterodimers was hindered in EAE animals, this could not be demonstrated in adjuvant-injected controls. These data strongly advocate for the first time, that ROCKII-mediated CRMP-2 phosphorylation is a mechanism which promotes neurodegeneration in autoimmune-mediated demyelination. Similarly, Mimura and colleagues found upregulation of PCRMP-2 and downregulation of polymerised tubulin in the white matter tracts of rats 2 hours post-SCI. This could be reversed by administration of the ROCK-inhibitor, Y-27632, at the site of injury (173). Experiments presented in chapter 3 indicate that PCRMP-2 levels can remain heightened in animals for up to 14 days post-SCI. We furthermore demonstrated in chapter 4 that ROCKII-mediated CRMP-2 phosphorylation (particularly the axon-specific PCRMP-2A) is increased in the MOG-EAE model. Collectively these results strongly suggest that RhoA/PCRMP-2 activation is a common mechanism which propagates neurodegeneration in the injured CNS.

The role of Nogo-A in perpetuating neurodegeneration has predominantly come from data obtained from SCI models (115, 153, 160, 306, 310, 312-316). Interestingly, similar conclusions have been drawn from a number of studies performed both in EAE and MS (97, 104, 105, 297, 317-322). Some of these are outlined below. Nogo-A has been shown to be upregulated in oligodendrocytes bordering chronic active

demyelinating MS lesions (97). In addition, Nogo-A has been suggested to be a biomarker for MS (297). Indeed, CSF obtained from 114 patients with RR-MS, 96% were found positive for the 20kDa product of soluble Nogo-A. In EAE, peptides encoding Nogo-66 are encephalitogenic and can induce a similar clinical outcome to that of MOG-induced EAE (319). On the other hand, Bourquin *et al.*, (317) found DNA vaccination against Nogo-A ameliorated EAE. Mice that were vaccinated with a plasmid expression vector encoding Nogo-A prior to induction of PLP-EAE, displayed increased antibody production against Nogo-A and did not exhibit exacerbation of disease (317). Similarly, silencing Nogo-A by systemic administration of siRNA at onset and 2 weeks post-EAE induction resulted in a reduction in disease severity (105). Not only was Nogo-A expression suppressed, but the neurite growth promoting protein GAP-43 was increased in such treated animals.

Previous work from our laboratory have demonstrated the relevance of Nogo-A in neuroinflammation by its direct role in the pathogenesis of EAE (104). Furthermore, immunization against Nogo-A ameliorated EAE in mice and prevented axonal injury (104). We hypothesised that the observed attenuation of EAE was due to the suppression of Nogo-A to signal through NgR1, thereby inhibiting downstream events such as ROCKII-dependent phosphorylation of CRMP-2, allowing regeneration to ensue. In chapter 4, we investigated the effects of Nogo-A antibody treatment on CRMP-2 phosphorylation and axonal injury in EAE. Therapeutic administration of Nogo-A antibodies prevented EAE clinical progression, providing evidence that Nogo-A can indeed induce the signal for axonal degeneration through the NgR1 complex. As predicted, Nogo-A treatment moreover resulted in a decrease in ROCKII-dependent phosphorylation of CRMP-2. Complementary to these data, we found elevated levels of CRMP-2-bound tubulin. These results imply that when NgR1/Nogo-A interactions are impeded a permissive environment for anterograde transport of molecular cargo and hence regrowth can be achieved. These data strongly advocate the notion that the Nogo-A/NgR1/ROCKII/PCRMP-2 pathway is a major mechanism driving neurodegeneration in EAE. There is no doubt that defining and elucidating the signalling pathways elicited during the onset and progression of MS will provide novel therapeutic strategies to limit axonal degeneration in the acute and hopefully the chronic phases of the disease.

In this context it is noteworthy that robust evidence supporting the Nogo-A signalling pathway regulating axonal injury in EAE, has been obtained from recent studies showing that deletion of the co-receptor for Nogo-A, LINGO-1 (which can signal

through RhoA-GTP), improves axonal integrity and protects against neurological decline in MOG-induced EAE mice (166). Indeed, the protein BIIB033 (anti-LINGO antibody), a drug which functionally blocks LINGO-1, is currently undergoing safety clinical phase I trials in two separate studies; IV administration in healthy individuals, or MS patients with relapsing-remitting disease (clinical trials.gov.au, trials NCT01052506 and NCT01244139, respectively). In chapter 5, we therefore explored the possibility that abrogation of Nogo-A signalling by genetic deletion of another cognate receptor for Nogo-A, NgR1, may also provide resistance to EAE. For this, EAE was induced in NgR1 KO mice and the activation levels of the Rho-A/ROCKII/PCRM-2 pathway, its relationship to NgR1 signalling and axonal degeneration was assessed. In EAE-induced *ngr1*^{-/-} mice, a significant reduction in clinical severity and histopathology was observed compared to *ngr1*^{+/+} mice, and this correlated with reduced CRMP-2 phosphorylation and co-localisation with degenerating axons. At the molecular level, *ngr1*^{-/-} mice had increased interactions between CRMP-2 and tubulin heterodimers, providing evidence that regenerative mechanisms are promoted when inhibitory signals such as NgR1 are prevented. Examination of the axonal pathology in the optic nerve of EAE-induced *ngr1*^{+/+} mice showed signs of axo-myelin degeneration in the pre-onset and onset stages of EAE, while this could not be demonstrated in *ngr1*^{-/-} mice at these time points. Deletion of the *ngr1* gene therefore results in the preservation of axons, myelin maintenance and decreased axonal swelling. In line with the data obtained from the lumbar cord, optic nerves obtained from *ngr1*^{-/-} mice exhibited decreased PCRMP-2 and an increase in CRMP-2 association with tubulin. This provides for the first time, evidence that the activation of the NgR1 complex in axons promotes neurodegeneration by modulating microtubule dynamics, in particular hindering a tubulin transport mechanism required for regrowth by increasing the phosphorylation of CRMP-2. These data implicate MAIFs-NgR1 interactions to be a major determinant of neurodegeneration in EAE.

The possibility that attenuation of EAE in NgR1 KO mice was due to a defective immune response was ruled out by a number of studies aimed at assessing the immunological status of these mice. Firstly, no differences in the proliferative T cell responses to the MOG₃₅₋₅₅ antigen, or in their pro- or anti-inflammatory cytokines between the EAE-induced *ngr1*^{-/-} and *ngr1*^{+/+} mice were found. Secondly, phenotypic analysis of the immune subsets obtained from naive and EAE-induced *ngr1*^{-/-} mice revealed no significant differences, suggesting that NgR1 does not influence the migratory behaviour of immune cells. These data confirm that deletion of NgR1 has no influence on the immune response to the encephalitogen MOG, but rather has

significant implications in mechanisms of axonal injury and axonal preservation through modulation of CRMP-2. Therefore, the precise dissection of the NgR1 signalling pathways eliciting axonal degeneration during neuroinflammatory diseases such as MS, will we believe, open novel avenues for therapeutic intervention to limit the neurological decline that accompanies the various stages of this severe debilitating disease.

In conclusion, it is evident that multiple sclerosis is a complex and heterogeneous disease of the central nervous system. Patients diagnosed with MS experience a diverse range of clinical symptoms, rates of disease progression and episodes of recovery. Histopathologically, MS lesions present with varied levels of immune infiltrates, demyelination and axonal degeneration (25). MS has primarily been defined as a demyelinating autoimmune disease, and as such much research has been conducted in this field. Consequent to this research, there are now 4 major approved therapies employed in the treatment of MS: interferon- β 1a, glatiramer acetate, mitoxantrone, and natalizumab (323, 324). All four drugs are immunomodulatory in nature, aimed at dampening the autoimmune response, predominantly benefiting patients with RR-MS resulting in reduction in episodes of relapse. Overall, these drugs are effective only in 30% of cases, highlighting the necessity in further drug discovery. It is now evident that axonal loss and the failure of compensatory regenerative mechanisms in their ability to maintain axonal integrity are the major players in permanent neurological deficit incurred in MS (62, 325-329). Therefore the use of immunomodulatory drugs in combination with new therapies that directly target axonal integrity is critical in improving clinical outcomes. Our data suggest that a promising target candidate is the inhibition of Nogo-A/NgR1/RhoA/PCRM-2 signalling. Considering the physiological relevance of CRMP-2 in the regulation of axonal growth, part of this thesis demonstrates an increase in the levels of ROCKII-phosphorylated CRMP-2 after axonal transection following SCI. We furthermore illustrated that the same phosphorylation events occur in the progression of disease in an MS-like disease in mice. Moreover, by utilising mice with a genetic deletion of the NgR1 receptor in conjunction with EAE, we have convincingly established that ROCKII-dependent phosphorylation of CRMP-2 is dependent on MAIF/NgR1 signalling. On the basis of these findings, we advocate the notion that the use of currently available drugs in tandem with blockers of Nogo-A or its downstream mediators could be the combinatory therapy which may dramatically enhance the effectiveness of the current treatment of MS and other CNS conditions.

BIBLIOGRAPHY

1. DeLuca, J., and Nocentini, U. (2011) Neuropsychological, medical and rehabilitative management of persons with multiple sclerosis, *NeuroRehabilitation* 29, 197-219.
2. Langer-Gould, A., Popat, R. A., Huang, S. M., Cobb, K., Fontoura, P., Gould, M. K., and Nelson, L. M. (2006) Clinical and demographic predictors of long-term disability in patients with relapsing-remitting multiple sclerosis: a systematic review, *Archives of neurology* 63, 1686-1691.
3. Kurtzke, J. F. (2000) Multiple sclerosis in time and space--geographic clues to cause, *J Neurovirol* 6 Suppl 2, S134-140.
4. Pugliatti, M., Cossu, P., Sotgiu, S., Rosati, G., and Riise, T. (2009) Clustering of multiple sclerosis, age of onset and gender in Sardinia, *Journal of the neurological sciences* 286, 6-13.
5. Ascherio, A., and Munger, K. L. (2007) Environmental risk factors for multiple sclerosis. Part II: Noninfectious factors, *Annals of neurology* 61, 504-513.
6. Zivadinov, R., Treu, C. N., Weinstock-Guttman, B., Turner, C., Bergsland, N., O'Connor, K., Dwyer, M. G., Carl, E., Ramasamy, D. P., Qu, J., and Ramanathan, M. (2013) Interdependence and contributions of sun exposure and vitamin D to MRI measures in multiple sclerosis, *Journal of neurology, neurosurgery, and psychiatry*.
7. Zivadinov, R., Iona, L., Monti-Bragadin, L., Bosco, A., Jurjevic, A., Taus, C., Cazzato, G., and Zorzon, M. (2003) The use of standardized incidence and prevalence rates in epidemiological studies on multiple sclerosis. A meta-analysis study, *Neuroepidemiology* 22, 65-74.
8. Koch-Henriksen, N., and Sorensen, P. S. (2010) The changing demographic pattern of multiple sclerosis epidemiology, *Lancet Neurol* 9, 520-532.
9. Ebers, G. C. (2008) Environmental factors and multiple sclerosis, *Lancet Neurol* 7, 268-277.
10. Bergamaschi, L., Leone, M. A., Fasano, M. E., Guerini, F. R., Ferrante, D., Bolognesi, E., Barizzone, N., Corrado, L., Naldi, P., Agliardi, C., Dametto, E., Salvetti, M., Visconti, A., Galimberti, D., Scarpini, E., Vercellino, M., Bergamaschi, R., Monaco, F., Caputo, D., Momigliano-Richiardi, P., and D'Alfonso, S. (2010) HLA-class I markers and multiple sclerosis susceptibility in the Italian population, *Genes Immun* 11, 173-180.
11. McElroy, J. P., and Oksenberg, J. R. (2011) Multiple sclerosis genetics 2010, *Neurol Clin* 29, 219-231.
12. Sadovnick, A. D. (2012) Genetic background of multiple sclerosis, *Autoimmun Rev* 11, 163-166.
13. Baranzini, S. E., Mudge, J., van Velkinburgh, J. C., Khankhanian, P., Khrebtukova, I., Miller, N. A., Zhang, L., Farmer, A. D., Bell, C. J., Kim, R. W., May, G. D., Woodward, J. E., Caillier, S. J., McElroy, J. P., Gomez, R., Pando, M. J., Clendenen, L. E., Ganusova, E. E., Schilkey, F. D., Ramaraj, T., Khan, O. A., Huntley, J. J., Luo, S., Kwok, P. Y., Wu, T. D., Schroth, G. P., Oksenberg, J. R., Hauser, S. L., and Kingsmore, S. F. (2010) Genome, epigenome and RNA

- sequences of monozygotic twins discordant for multiple sclerosis, *Nature* 464, 1351-1356.
14. Ascherio, A., and Bar-Or, A. (2010) EBV and brain matter(s)?, *Neurology* 74, 1092-1095.
 15. Lublin, F. D., and Reingold, S. C. (1996) Defining the clinical course of multiple sclerosis: results of an international survey. National Multiple Sclerosis Society (USA) Advisory Committee on Clinical Trials of New Agents in Multiple Sclerosis, *Neurology* 46, 907-911.
 16. Barker, C. F., and Billingham, R. E. (1977) Immunologically privileged sites, *Adv Immunol* 25, 1-54.
 17. Larochelle, C., Alvarez, J. I., and Prat, A. (2011) How do immune cells overcome the blood-brain barrier in multiple sclerosis?, *FEBS letters* 585, 3770-3780.
 18. Ludowyk, P. A., Willenborg, D. O., and Parish, C. R. (1992) Selective localisation of neuro-specific T lymphocytes in the central nervous system, *Journal of neuroimmunology* 37, 237-250.
 19. Engelhardt, B. (2006) Molecular mechanisms involved in T cell migration across the blood-brain barrier, *J Neural Transm* 113, 477-485.
 20. Shrikant, P., and Benveniste, E. N. (1996) The central nervous system as an immunocompetent organ: role of glial cells in antigen presentation, *J Immunol* 157, 1819-1822.
 21. van Noort, J. M., Verbeek, R., Meilof, J. F., Polman, C. H., and Amor, S. (2006) Autoantibodies against alpha B-crystallin, a candidate autoantigen in multiple sclerosis, are part of a normal human immune repertoire, *Multiple sclerosis (Houndmills, Basingstoke, England)* 12, 287-293.
 22. van Noort, J. M., Bsibsi, M., Gerritsen, W. H., van der Valk, P., Bajramovic, J. J., Steinman, L., and Amor, S. (2010) Alphas-crystallin is a target for adaptive immune responses and a trigger of innate responses in preactive multiple sclerosis lesions, *Journal of neuropathology and experimental neurology* 69, 694-703.
 23. Breij, E. C., Brink, B. P., Veerhuis, R., van den Berg, C., Vloet, R., Yan, R., Dijkstra, C. D., van der Valk, P., and Bo, L. (2008) Homogeneity of active demyelinating lesions in established multiple sclerosis, *Annals of neurology* 63, 16-25.
 24. Lucchinetti, C. F., Parisi, J., and Bruck, W. (2005) The pathology of multiple sclerosis, *Neurol Clin* 23, 77-105, vi.
 25. Kipp, M., van der Valk, P., and Amor, S. (2012) Pathology of multiple sclerosis, *CNS & neurological disorders drug targets* 11, 506-517.
 26. Noseworthy, J. H., Lucchinetti, C., Rodriguez, M., and Weinshenker, B. G. (2000) Multiple sclerosis, *N Engl J Med* 343, 938-952.
 27. Alvarez, J. I., Cayrol, R., and Prat, A. (2011) Disruption of central nervous system barriers in multiple sclerosis, *Biochim Biophys Acta* 1812, 252-264.

28. Morandi, B., Bramanti, P., Bonaccorsi, I., Montalto, E., Oliveri, D., Pezzino, G., Navarra, M., and Ferlazzo, G. (2008) Role of natural killer cells in the pathogenesis and progression of multiple sclerosis, *Pharmacol Res* 57, 1-5.
29. Prineas, J. W., and Graham, J. S. (1981) Multiple sclerosis: capping of surface immunoglobulin G on macrophages engaged in myelin breakdown, *Annals of neurology* 10, 149-158.
30. Williams, K. A., and Deber, C. M. (1993) The structure and function of central nervous system myelin, *Crit Rev Clin Lab Sci* 30, 29-64.
31. Sherman, D. L., and Brophy, P. J. (2005) Mechanisms of axon ensheathment and myelin growth, *Nat Rev Neurosci* 6, 683-690.
32. Almeida, R. G., Czopka, T., Ffrench-Constant, C., and Lyons, D. A. (2011) Individual axons regulate the myelinating potential of single oligodendrocytes in vivo, *Development* 138, 4443-4450.
33. Hellings, N., Gelin, G., Medaer, R., Bruckers, L., Palmers, Y., Raus, J., and Stinissen, P. (2002) Longitudinal study of antimyelin T-cell reactivity in relapsing-remitting multiple sclerosis: association with clinical and MRI activity, *Journal of neuroimmunology* 126, 143-160.
34. Jahn, O., Tenzer, S., and Werner, H. B. (2009) Myelin proteomics: molecular anatomy of an insulating sheath, *Molecular neurobiology* 40, 55-72.
35. Derfuss, T., and Meinl, E. (2012) Identifying autoantigens in demyelinating diseases: valuable clues to diagnosis and treatment?, *Current opinion in neurology* 25, 231-238.
36. Steinman, L., and Zamvil, S. S. (2005) Virtues and pitfalls of EAE for the development of therapies for multiple sclerosis, *Trends Immunol* 26, 565-571.
37. Petry, K. G., Boullerne, A. I., Pousset, F., Brochet, B., Caille, J. M., and Dousset, V. (2000) Experimental allergic encephalomyelitis animal models for analyzing features of multiple sclerosis, *Pathol Biol (Paris)* 48, 47-53.
38. Teitelbaum, D., Webb, C., Meshorer, A., Arnon, R., and Sela, M. (1972) Protection against experimental allergic encephalomyelitis, *Nature* 240, 564-566.
39. Johnson, K. P., Brooks, B. R., Cohen, J. A., Ford, C. C., Goldstein, J., Lisak, R. P., Myers, L. W., Panitch, H. S., Rose, J. W., and Schiffer, R. B. (1995) Copolymer 1 reduces relapse rate and improves disability in relapsing-remitting multiple sclerosis: results of a phase III multicenter, double-blind placebo-controlled trial. The Copolymer 1 Multiple Sclerosis Study Group, *Neurology* 45, 1268-1276.
40. Yednock, T. A., Cannon, C., Fritz, L. C., Sanchez-Madrid, F., Steinman, L., and Karin, N. (1992) Prevention of experimental autoimmune encephalomyelitis by antibodies against alpha 4 beta 1 integrin, *Nature* 356, 63-66.
41. Miller, D. H., Khan, O. A., Sheremata, W. A., Blumhardt, L. D., Rice, G. P., Libonati, M. A., Willmer-Hulme, A. J., Dalton, C. M., Miszkiel, K. A., and O'Connor, P. W. (2003) A controlled trial of natalizumab for relapsing multiple sclerosis, *N Engl J Med* 348, 15-23.

42. Steinman, L. (2005) Blocking adhesion molecules as therapy for multiple sclerosis: natalizumab, *Nat Rev Drug Discov* 4, 510-518.
43. Johns, T. G., Kerlero de Rosbo, N., Menon, K. K., Abo, S., Gonzales, M. F., and Bernard, C. C. (1995) Myelin oligodendrocyte glycoprotein induces a demyelinating encephalomyelitis resembling multiple sclerosis, *J Immunol* 154, 5536-5541.
44. Furlan, R., Cuomo, C., and Martino, G. (2009) Animal models of multiple sclerosis, *Methods Mol Biol* 549, 157-173.
45. Croxford, A. L., Kurschus, F. C., and Waisman, A. (2011) Mouse models for multiple sclerosis: historical facts and future implications, *Biochim Biophys Acta* 1812, 177-183.
46. Stohlman, S. A., and Hinton, D. R. (2001) Viral induced demyelination, *Brain Pathol* 11, 92-106.
47. Katz-Levy, Y., Neville, K. L., Padilla, J., Rahbe, S., Begolka, W. S., Girvin, A. M., Olson, J. K., Vanderlugt, C. L., and Miller, S. D. (2000) Temporal development of autoreactive Th1 responses and endogenous presentation of self myelin epitopes by central nervous system-resident APCs in Theiler's virus-infected mice, *J Immunol* 165, 5304-5314.
48. Carbajal, K. S., Miranda, J. L., Tsukamoto, M. R., and Lane, T. E. (2011) CXCR4 signaling regulates remyelination by endogenous oligodendrocyte progenitor cells in a viral model of demyelination, *Glia* 59, 1813-1821.
49. Carbajal, K. S., Schaumburg, C., Strieter, R., Kane, J., and Lane, T. E. (2010) Migration of engrafted neural stem cells is mediated by CXCL12 signaling through CXCR4 in a viral model of multiple sclerosis, *Proceedings of the National Academy of Sciences of the United States of America* 107, 11068-11073.
50. Carbajal, K. S., Weinger, J. G., Whitman, L. M., Schaumburg, C. S., and Lane, T. E. (2011) Surgical transplantation of mouse neural stem cells into the spinal cords of mice infected with neurotropic mouse hepatitis virus, *J Vis Exp*, e2834.
51. Tirota, E., Carbajal, K. S., Schaumburg, C. S., Whitman, L., and Lane, T. E. (2010) Cell replacement therapies to promote remyelination in a viral model of demyelination, *Journal of neuroimmunology* 224, 101-107.
52. Mana, P., Fordham, S. A., Staykova, M. A., Correcha, M., Silva, D., Willenborg, D. O., and Linares, D. (2009) Demyelination caused by the copper chelator cuprizone halts T cell mediated autoimmune neuroinflammation, *Journal of neuroimmunology* 210, 13-21.
53. Wu, G. F., and Alvarez, E. (2011) The immunopathophysiology of multiple sclerosis, *Neurol Clin* 29, 257-278.
54. Henderson, A. P., Barnett, M. H., Parratt, J. D., and Prineas, J. W. (2009) Multiple sclerosis: distribution of inflammatory cells in newly forming lesions, *Annals of neurology* 66, 739-753.

55. Trapp, B. D., Peterson, J., Ransohoff, R. M., Rudick, R., Mork, S., and Bo, L. (1998) Axonal transection in the lesions of multiple sclerosis, *N Engl J Med* 338, 278-285.
56. Raine, C. S. (2008) Multiple sclerosis: classification revisited reveals homogeneity and recapitulation, *Annals of neurology* 63, 1-3.
57. Genain, C. P., Nguyen, M. H., Letvin, N. L., Pearl, R., Davis, R. L., Adelman, M., Lees, M. B., Linington, C., and Hauser, S. L. (1995) Antibody facilitation of multiple sclerosis-like lesions in a nonhuman primate, *The Journal of clinical investigation* 96, 2966-2974.
58. von Budingen, H. C., Hauser, S. L., Ouallet, J. C., Tanuma, N., Menge, T., and Genain, C. P. (2004) Frontline: Epitope recognition on the myelin/oligodendrocyte glycoprotein differentially influences disease phenotype and antibody effector functions in autoimmune demyelination, *Eur J Immunol* 34, 2072-2083.
59. Bitsch, A., Schuchardt, J., Bunkowski, S., Kuhlmann, T., and Bruck, W. (2000) Acute axonal injury in multiple sclerosis. Correlation with demyelination and inflammation, *Brain : a journal of neurology* 123 (Pt 6), 1174-1183.
60. Kornek, B., Storch, M. K., Weissert, R., Wallstroem, E., Stefferl, A., Olsson, T., Linington, C., Schmidbauer, M., and Lassmann, H. (2000) Multiple sclerosis and chronic autoimmune encephalomyelitis: a comparative quantitative study of axonal injury in active, inactive, and remyelinated lesions, *The American journal of pathology* 157, 267-276.
61. Bjartmar, C., Kidd, G., Mork, S., Rudick, R., and Trapp, B. D. (2000) Neurological disability correlates with spinal cord axonal loss and reduced N-acetyl aspartate in chronic multiple sclerosis patients, *Annals of neurology* 48, 893-901.
62. Bjartmar, C., and Trapp, B. D. (2001) Axonal and neuronal degeneration in multiple sclerosis: mechanisms and functional consequences, *Current opinion in neurology* 14, 271-278.
63. Trapp, B. D., and Nave, K. A. (2008) Multiple sclerosis: an immune or neurodegenerative disorder?, *Annu Rev Neurosci* 31, 247-269.
64. Dutta, R., and Trapp, B. D. (2011) Mechanisms of neuronal dysfunction and degeneration in multiple sclerosis, *Prog Neurobiol* 93, 1-12.
65. Ferguson, B., Matyszak, M. K., Esiri, M. M., and Perry, V. H. (1997) Axonal damage in acute multiple sclerosis lesions, *Brain : a journal of neurology* 120 (Pt 3), 393-399.
66. Meuth, S. G., Gobel, K., and Wiendl, H. (2012) Immune therapy of multiple sclerosis--future strategies, *Current pharmaceutical design* 18, 4489-4497.
67. Liu, B. P., Cafferty, W. B., Budel, S. O., and Strittmatter, S. M. (2006) Extracellular regulators of axonal growth in the adult central nervous system, *Philos Trans R Soc Lond B Biol Sci* 361, 1593-1610.
68. McGee, A. W., and Strittmatter, S. M. (2003) The Nogo-66 receptor: focusing myelin inhibition of axon regeneration, *Trends in neurosciences* 26, 193-198.

69. Profyris, C., Cheema, S. S., Zang, D., Azari, M. F., Boyle, K., and Petratos, S. (2004) Degenerative and regenerative mechanisms governing spinal cord injury, *Neurobiol Dis* 15, 415-436.
70. Huber, A. B., and Schwab, M. E. (2000) Nogo-A, a potent inhibitor of neurite outgrowth and regeneration, *Biol Chem* 381, 407-419.
71. Schwab, M. E., and Caroni, P. (1988) Oligodendrocytes and CNS myelin are nonpermissive substrates for neurite growth and fibroblast spreading in vitro, *The Journal of neuroscience : the official journal of the Society for Neuroscience* 8, 2381-2393.
72. Huang, D. W., McKerracher, L., Braun, P. E., and David, S. (1999) A therapeutic vaccine approach to stimulate axon regeneration in the adult mammalian spinal cord, *Neuron* 24, 639-647.
73. McKerracher, L., David, S., Jackson, D. L., Kottis, V., Dunn, R. J., and Braun, P. E. (1994) Identification of myelin-associated glycoprotein as a major myelin-derived inhibitor of neurite growth, *Neuron* 13, 805-811.
74. Mukhopadhyay, G., Doherty, P., Walsh, F. S., Crocker, P. R., and Filbin, M. T. (1994) A novel role for myelin-associated glycoprotein as an inhibitor of axonal regeneration, *Neuron* 13, 757-767.
75. Chen, M. S., Huber, A. B., van der Haar, M. E., Frank, M., Schnell, L., Spillmann, A. A., Christ, F., and Schwab, M. E. (2000) Nogo-A is a myelin-associated neurite outgrowth inhibitor and an antigen for monoclonal antibody IN-1, *Nature* 403, 434-439.
76. Prinjha, R., Moore, S. E., Vinson, M., Blake, S., Morrow, R., Christie, G., Michalovich, D., Simmons, D. L., and Walsh, F. S. (2000) Inhibitor of neurite outgrowth in humans, *Nature* 403, 383-384.
77. GrandPre, T., Nakamura, F., Vartanian, T., and Strittmatter, S. M. (2000) Identification of the Nogo inhibitor of axon regeneration as a Reticulon protein, *Nature* 403, 439-444.
78. Wang, K. C., Koprivica, V., Kim, J. A., Sivasankaran, R., Guo, Y., Neve, R. L., and He, Z. (2002) Oligodendrocyte-myelin glycoprotein is a Nogo receptor ligand that inhibits neurite outgrowth, *Nature* 417, 941-944.
79. Moreau-Fauvarque, C., Kumanogoh, A., Camand, E., Jaillard, C., Barbin, G., Boquet, I., Love, C., Jones, E. Y., Kikutani, H., Lubetzki, C., Dusart, I., and Chedotal, A. (2003) The transmembrane semaphorin Sema4D/CD100, an inhibitor of axonal growth, is expressed on oligodendrocytes and upregulated after CNS lesion, *The Journal of neuroscience : the official journal of the Society for Neuroscience* 23, 9229-9239.
80. Benson, M. D., Romero, M. I., Lush, M. E., Lu, Q. R., Henkemeyer, M., and Parada, L. F. (2005) Ephrin-B3 is a myelin-based inhibitor of neurite outgrowth, *Proceedings of the National Academy of Sciences of the United States of America* 102, 10694-10699.
81. Huang, J. K., Phillips, G. R., Roth, A. D., Pedraza, L., Shan, W., Belkaid, W., Mi, S., Fex-Svenningsen, A., Florens, L., Yates, J. R., 3rd, and Colman, D. R.

- (2005) Glial membranes at the node of Ranvier prevent neurite outgrowth, *Science* 310, 1813-1817.
82. Dou, F., Huang, L., Yu, P., Zhu, H., Wang, X., Zou, J., Lu, P., and Xu, X. M. (2009) Temporospacial expression and cellular localization of oligodendrocyte myelin glycoprotein (OMgp) after traumatic spinal cord injury in adult rats, *J Neurotrauma* 26, 2299-2311.
83. Vourc'h, P., and Andres, C. (2004) Oligodendrocyte myelin glycoprotein (OMgp): evolution, structure and function, *Brain Res Brain Res Rev* 45, 115-124.
84. Hunt, D., Mason, M. R., Campbell, G., Coffin, R., and Anderson, P. N. (2002) Nogo receptor mRNA expression in intact and regenerating CNS neurons, *Molecular and cellular neurosciences* 20, 537-552.
85. Lai, C., Watson, J. B., Bloom, F. E., Sutcliffe, J. G., and Milner, R. J. (1987) Neural protein 1B236/myelin-associated glycoprotein (MAG) defines a subgroup of the immunoglobulin superfamily, *Immunological reviews* 100, 129-151.
86. Salzer, J. L., Holmes, W. P., and Colman, D. R. (1987) The amino acid sequences of the myelin-associated glycoproteins: homology to the immunoglobulin gene superfamily, *The Journal of cell biology* 104, 957-965.
87. Schachner, M., and Bartsch, U. (2000) Multiple functions of the myelin-associated glycoprotein MAG (siglec-4a) in formation and maintenance of myelin, *Glia* 29, 154-165.
88. Domeniconi, M., Cao, Z., Spencer, T., Sivasankaran, R., Wang, K., Nikulina, E., Kimura, N., Cai, H., Deng, K., Gao, Y., He, Z., and Filbin, M. (2002) Myelin-associated glycoprotein interacts with the Nogo66 receptor to inhibit neurite outgrowth, *Neuron* 35, 283-290.
89. Hasegawa, Y., Fujitani, M., Hata, K., Tohyama, M., Yamagishi, S., and Yamashita, T. (2004) Promotion of axon regeneration by myelin-associated glycoprotein and Nogo through divergent signals downstream of Gi/G, *The Journal of neuroscience : the official journal of the Society for Neuroscience* 24, 6826-6832.
90. Mingorance, A., Fontana, X., Soriano, E., and Del Rio, J. A. (2005) Overexpression of myelin-associated glycoprotein after axotomy of the perforant pathway, *Molecular and cellular neurosciences* 29, 471-483.
91. Liu, B. P., Fournier, A., GrandPre, T., and Strittmatter, S. M. (2002) Myelin-associated glycoprotein as a functional ligand for the Nogo-66 receptor, *Science* 297, 1190-1193.
92. Venkatesh, K., Chivatakarn, O., Lee, H., Joshi, P. S., Kantor, D. B., Newman, B. A., Mage, R., Rader, C., and Giger, R. J. (2005) The Nogo-66 receptor homolog NgR2 is a sialic acid-dependent receptor selective for myelin-associated glycoprotein, *The Journal of neuroscience : the official journal of the Society for Neuroscience* 25, 808-822.

93. Sandvig, A., Berry, M., Barrett, L. B., Butt, A., and Logan, A. (2004) Myelin-, reactive glia-, and scar-derived CNS axon growth inhibitors: expression, receptor signaling, and correlation with axon regeneration, *Glia* 46, 225-251.
94. Schweigreiter, R., and Bandtlow, C. E. (2006) Nogo in the injured spinal cord, *J Neurotrauma* 23, 384-396.
95. Josephson, A., Widenfalk, J., Widmer, H. W., Olson, L., and Spenger, C. (2001) NOGO mRNA expression in adult and fetal human and rat nervous tissue and in weight drop injury, *Exp Neurol* 169, 319-328.
96. Gerin, C. G., Madueke, I. C., Perkins, T., Hill, S., Smith, K., Haley, B., Allen, S. A., Garcia, R. P., Paunesku, T., and Woloschak, G. (2011) Combination strategies for repair, plasticity, and regeneration using regulation of gene expression during the chronic phase after spinal cord injury, *Synapse (New York, N.Y.)* 65, 1255-1281.
97. Satoh, J., Onoue, H., Arima, K., and Yamamura, T. (2005) Nogo-A and nogo receptor expression in demyelinating lesions of multiple sclerosis, *Journal of neuropathology and experimental neurology* 64, 129-138.
98. Marklund, N., Fulp, C. T., Shimizu, S., Puri, R., McMillan, A., Strittmatter, S. M., and McIntosh, T. K. (2006) Selective temporal and regional alterations of Nogo-A and small proline-rich repeat protein 1A (SPRR1A) but not Nogo-66 receptor (NgR) occur following traumatic brain injury in the rat, *Exp Neurol* 197, 70-83.
99. Fournier, A. E., GrandPre, T., and Strittmatter, S. M. (2001) Identification of a receptor mediating Nogo-66 inhibition of axonal regeneration, *Nature* 409, 341-346.
100. Wang, X., Chun, S. J., Treloar, H., Vartanian, T., Greer, C. A., and Strittmatter, S. M. (2002) Localization of Nogo-A and Nogo-66 receptor proteins at sites of axon-myelin and synaptic contact, *The Journal of neuroscience : the official journal of the Society for Neuroscience* 22, 5505-5515.
101. Lauren, J., Hu, F., Chin, J., Liao, J., Airaksinen, M. S., and Strittmatter, S. M. (2007) Characterization of myelin ligand complexes with neuronal Nogo-66 receptor family members, *J Biol Chem* 282, 5715-5725.
102. Oertle, T., van der Haar, M. E., Bandtlow, C. E., Robeva, A., Burfeind, P., Buss, A., Huber, A. B., Simonen, M., Schnell, L., Brosamle, C., Kaupmann, K., Vallon, R., and Schwab, M. E. (2003) Nogo-A inhibits neurite outgrowth and cell spreading with three discrete regions, *The Journal of neuroscience : the official journal of the Society for Neuroscience* 23, 5393-5406.
103. Hu, F., and Strittmatter, S. M. (2008) The N-terminal domain of Nogo-A inhibits cell adhesion and axonal outgrowth by an integrin-specific mechanism, *The Journal of neuroscience : the official journal of the Society for Neuroscience* 28, 1262-1269.
104. Karnezis, T., Mandemakers, W., McQualter, J. L., Zheng, B., Ho, P. P., Jordan, K. A., Murray, B. M., Barres, B., Tessier-Lavigne, M., and Bernard, C. C. (2004) The neurite outgrowth inhibitor Nogo A is involved in autoimmune-mediated demyelination, *Nat Neurosci* 7, 736-744.

105. Yang, Y., Liu, Y., Wei, P., Peng, H., Winger, R., Hussain, R. Z., Ben, L. H., Cravens, P. D., Gocke, A. R., Puttaparthi, K., Racke, M. K., McTigue, D. M., and Lovett-Racke, A. E. (2010) Silencing Nogo-A promotes functional recovery in demyelinating disease, *Annals of neurology* 67, 498-507.
106. GrandPre, T., Li, S., and Strittmatter, S. M. (2002) Nogo-66 receptor antagonist peptide promotes axonal regeneration, *Nature* 417, 547-551.
107. Wiessner, C., Bareyre, F. M., Allegrini, P. R., Mir, A. K., Frentzel, S., Zurini, M., Schnell, L., Oertle, T., and Schwab, M. E. (2003) Anti-Nogo-A antibody infusion 24 hours after experimental stroke improved behavioral outcome and corticospinal plasticity in normotensive and spontaneously hypertensive rats, *J Cereb Blood Flow Metab* 23, 154-165.
108. Lee, J. K., Kim, J. E., Sivula, M., and Strittmatter, S. M. (2004) Nogo receptor antagonism promotes stroke recovery by enhancing axonal plasticity, *The Journal of neuroscience : the official journal of the Society for Neuroscience* 24, 6209-6217.
109. Caroni, P., and Schwab, M. E. (1988) Antibody against myelin-associated inhibitor of neurite growth neutralizes nonpermissive substrate properties of CNS white matter, *Neuron* 1, 85-96.
110. Bandtlow, C., Zachleder, T., and Schwab, M. E. (1990) Oligodendrocytes arrest neurite growth by contact inhibition, *The Journal of neuroscience : the official journal of the Society for Neuroscience* 10, 3837-3848.
111. Schnell, L., and Schwab, M. E. (1990) Axonal regeneration in the rat spinal cord produced by an antibody against myelin-associated neurite growth inhibitors, *Nature* 343, 269-272.
112. Bregman, B. S., Kunkel-Bagden, E., Schnell, L., Dai, H. N., Gao, D., and Schwab, M. E. (1995) Recovery from spinal cord injury mediated by antibodies to neurite growth inhibitors, *Nature* 378, 498-501.
113. Merkler, D., Metz, G. A., Raineteau, O., Dietz, V., Schwab, M. E., and Fouad, K. (2001) Locomotor recovery in spinal cord-injured rats treated with an antibody neutralizing the myelin-associated neurite growth inhibitor Nogo-A, *The Journal of neuroscience : the official journal of the Society for Neuroscience* 21, 3665-3673.
114. Raineteau, O., Fouad, K., Noth, P., Thallmair, M., and Schwab, M. E. (2001) Functional switch between motor tracts in the presence of the mAb IN-1 in the adult rat, *Proceedings of the National Academy of Sciences of the United States of America* 98, 6929-6934.
115. Cafferty, W. B., Duffy, P., Huebner, E., and Strittmatter, S. M. (2010) MAG and OMgp synergize with Nogo-A to restrict axonal growth and neurological recovery after spinal cord trauma, *The Journal of neuroscience : the official journal of the Society for Neuroscience* 30, 6825-6837.
116. Lauren, J., Airaksinen, M. S., Saarma, M., and Timmusk, T. (2003) Two novel mammalian Nogo receptor homologs differentially expressed in the central and peripheral nervous systems, *Molecular and cellular neurosciences* 24, 581-594.

117. Pignot, V., Hein, A. E., Barske, C., Wiessner, C., Walmsley, A. R., Kaupmann, K., Mayeur, H., Sommer, B., Mir, A. K., and Frentzel, S. (2003) Characterization of two novel proteins, NgRH1 and NgRH2, structurally and biochemically homologous to the Nogo-66 receptor, *J Neurochem* 85, 717-728.
118. Mi, S., Lee, X., Shao, Z., Thill, G., Ji, B., Relton, J., Levesque, M., Allaire, N., Perrin, S., Sands, B., Crowell, T., Cate, R. L., McCoy, J. M., and Pepinsky, R. B. (2004) LINGO-1 is a component of the Nogo-66 receptor/p75 signaling complex, *Nat Neurosci* 7, 221-228.
119. Park, J. B., Yiu, G., Kaneko, S., Wang, J., Chang, J., He, X. L., Garcia, K. C., and He, Z. (2005) A TNF receptor family member, TROY, is a coreceptor with Nogo receptor in mediating the inhibitory activity of myelin inhibitors, *Neuron* 45, 345-351.
120. Josephson, A., Trifunovski, A., Widmer, H. R., Widenfalk, J., Olson, L., and Spenger, C. (2002) Nogo-receptor gene activity: cellular localization and developmental regulation of mRNA in mice and humans, *J Comp Neurol* 453, 292-304.
121. Fournier, A. E., Gould, G. C., Liu, B. P., and Strittmatter, S. M. (2002) Truncated soluble Nogo receptor binds Nogo-66 and blocks inhibition of axon growth by myelin, *J Neurosci* 22, 8876-8883.
122. Wang, K. C., Kim, J. A., Sivasankaran, R., Segal, R., and He, Z. (2002) P75 interacts with the Nogo receptor as a co-receptor for Nogo, MAG and OMgp, *Nature* 420, 74-78.
123. He, X. L., Bazan, J. F., McDermott, G., Park, J. B., Wang, K., Tessier-Lavigne, M., He, Z., and Garcia, K. C. (2003) Structure of the Nogo receptor ectodomain: a recognition module implicated in myelin inhibition, *Neuron* 38, 177-185.
124. Barton, W. A., Liu, B. P., Tzvetkova, D., Jeffrey, P. D., Fournier, A. E., Sah, D., Cate, R., Strittmatter, S. M., and Nikolov, D. B. (2003) Structure and axon outgrowth inhibitor binding of the Nogo-66 receptor and related proteins, *Embo J* 22, 3291-3302.
125. Mi, S., Miller, R. H., Lee, X., Scott, M. L., Shulag-Morskaya, S., Shao, Z., Chang, J., Thill, G., Levesque, M., Zhang, M., Hession, C., Sah, D., Trapp, B., He, Z., Jung, V., McCoy, J. M., and Pepinsky, R. B. (2005) LINGO-1 negatively regulates myelination by oligodendrocytes, *Nat Neurosci* 8, 745-751.
126. Hunt, D., Coffin, R. S., and Anderson, P. N. (2002) The Nogo receptor, its ligands and axonal regeneration in the spinal cord; a review, *J Neurocytol* 31, 93-120.
127. Mosyak, L., Wood, A., Dwyer, B., Buddha, M., Johnson, M., Aulabaugh, A., Zhong, X., Presman, E., Benard, S., Kelleher, K., Wilhelm, J., Stahl, M. L., Kriz, R., Gao, Y., Cao, Z., Ling, H. P., Pangalos, M. N., Walsh, F. S., and Somers, W. S. (2006) The structure of the Lingo-1 ectodomain, a module implicated in central nervous system repair inhibition, *J Biol Chem* 281, 36378-36390.
128. Liepinsh, E., Ilag, L. L., Otting, G., and Ibanez, C. F. (1997) NMR structure of the death domain of the p75 neurotrophin receptor, *Embo J* 16, 4999-5005.

129. He, X. L., and Garcia, K. C. (2004) Structure of nerve growth factor complexed with the shared neurotrophin receptor p75, *Science* 304, 870-875.
130. Cosgaya, J. M., Chan, J. R., and Shooter, E. M. (2002) The neurotrophin receptor p75NTR as a positive modulator of myelination, *Science* 298, 1245-1248.
131. Yamauchi, J., Chan, J. R., and Shooter, E. M. (2004) Neurotrophins regulate Schwann cell migration by activating divergent signaling pathways dependent on Rho GTPases, *Proc Natl Acad Sci U S A* 101, 8774-8779.
132. Du, Y., Fischer, T. Z., Clinton-Luke, P., Lercher, L. D., and Dreyfus, C. F. (2006) Distinct effects of p75 in mediating actions of neurotrophins on basal forebrain oligodendrocytes, *Mol Cell Neurosci* 31, 366-375.
133. Petratos, S., Gonzales, M. F., Azari, M. F., Marriott, M., Minichiello, R. A., Shipham, K. A., Profyris, C., Nicolaou, A., Boyle, K., Cheema, S. S., and Kilpatrick, T. J. (2004) Expression of the low-affinity neurotrophin receptor, p75(NTR), is upregulated by oligodendroglial progenitors adjacent to the subventricular zone in response to demyelination, *Glia* 48, 64-75.
134. Calza, L., Fernandez, M., Giuliani, A., Aloe, L., and Giardino, L. (2002) Thyroid hormone activates oligodendrocyte precursors and increases a myelin-forming protein and NGF content in the spinal cord during experimental allergic encephalomyelitis, *Proceedings of the National Academy of Sciences of the United States of America* 99, 3258-3263.
135. Madura, T., Yamashita, T., Kubo, T., Fujitani, M., Hosokawa, K., and Tohyama, M. (2004) Activation of Rho in the injured axons following spinal cord injury, *EMBO Rep* 5, 412-417.
136. Bronfman, F. C., and Fainzilber, M. (2004) Multi-tasking by the p75 neurotrophin receptor: sortilin things out?, *EMBO reports* 5, 867-871.
137. Dougherty, K. D., and Milner, T. A. (1999) p75NTR immunoreactivity in the rat dentate gyrus is mostly within presynaptic profiles but is also found in some astrocytic and postsynaptic profiles, *J Comp Neurol* 407, 77-91.
138. Wong, S. T., Henley, J. R., Kanning, K. C., Huang, K. H., Bothwell, M., and Poo, M. M. (2002) A p75(NTR) and Nogo receptor complex mediates repulsive signaling by myelin-associated glycoprotein, *Nat Neurosci* 5, 1302-1308.
139. Yamashita, T., Higuchi, H., and Tohyama, M. (2002) The p75 receptor transduces the signal from myelin-associated glycoprotein to Rho, *The Journal of cell biology* 157, 565-570.
140. Song, X. Y., Zhong, J. H., Wang, X., and Zhou, X. F. (2004) Suppression of p75NTR does not promote regeneration of injured spinal cord in mice, *J Neurosci* 24, 542-546.
141. Shao, Z., Browning, J. L., Lee, X., Scott, M. L., Shulga-Morskaya, S., Allaire, N., Thill, G., Levesque, M., Sah, D., McCoy, J. M., Murray, B., Jung, V., Pepinsky, R. B., and Mi, S. (2005) TAJ/TROY, an orphan TNF receptor family member, binds Nogo-66 receptor 1 and regulates axonal regeneration, *Neuron* 45, 353-359.

142. Hisaoka, T., Morikawa, Y., and Senba, E. (2006) Characterization of TROY/TNFRSF19/TAJ-expressing cells in the adult mouse forebrain, *Brain Res* 1110, 81-94.
143. Mi, S. (2008) Troy/Taj and its role in CNS axon regeneration, *Cytokine Growth Factor Rev* 19, 245-251.
144. Niederost, B., Oertle, T., Fritsche, J., McKinney, R. A., and Bandtlow, C. E. (2002) Nogo-A and myelin-associated glycoprotein mediate neurite growth inhibition by antagonistic regulation of RhoA and Rac1, *The Journal of neuroscience : the official journal of the Society for Neuroscience* 22, 10368-10376.
145. Jalink, K., van Corven, E. J., Hengeveld, T., Morii, N., Narumiya, S., and Moolenaar, W. H. (1994) Inhibition of lysophosphatidate- and thrombin-induced neurite retraction and neuronal cell rounding by ADP ribosylation of the small GTP-binding protein Rho, *The Journal of cell biology* 126, 801-810.
146. Yamashita, T., and Tohyama, M. (2003) The p75 receptor acts as a displacement factor that releases Rho from Rho-GDI, *Nat Neurosci* 6, 461-467.
147. Wang, T., Wang, J., Yin, C., Liu, R., Zhang, J. H., and Qin, X. (2010) Down-regulation of Nogo receptor promotes functional recovery by enhancing axonal connectivity after experimental stroke in rats, *Brain Res* 1360, 147-158.
148. Lee, J. K., Geoffroy, C. G., Chan, A. F., Tolentino, K. E., Crawford, M. J., Leal, M. A., Kang, B., and Zheng, B. (2010) Assessing spinal axon regeneration and sprouting in Nogo-, MAG-, and OMgp-deficient mice, *Neuron* 66, 663-670.
149. Fouad, K., Klusman, I., and Schwab, M. E. (2004) Regenerating corticospinal fibers in the Marmoset (*Callitrix jacchus*) after spinal cord lesion and treatment with the anti-Nogo-A antibody IN-1, *The European journal of neuroscience* 20, 2479-2482.
150. Freund, P., Schmidlin, E., Wannier, T., Bloch, J., Mir, A., Schwab, M. E., and Rouiller, E. M. (2006) Nogo-A-specific antibody treatment enhances sprouting and functional recovery after cervical lesion in adult primates, *Nature medicine* 12, 790-792.
151. Zorner, B., and Schwab, M. E. (2010) Anti-Nogo on the go: from animal models to a clinical trial, *Annals of the New York Academy of Sciences* 1198 Suppl 1, E22-34.
152. Kim, J. E., Li, S., GrandPre, T., Qiu, D., and Strittmatter, S. M. (2003) Axon regeneration in young adult mice lacking Nogo-A/B, *Neuron* 38, 187-199.
153. Simonen, M., Pedersen, V., Weinmann, O., Schnell, L., Buss, A., Ledermann, B., Christ, F., Sansig, G., van der Putten, H., and Schwab, M. E. (2003) Systemic deletion of the myelin-associated outgrowth inhibitor Nogo-A improves regenerative and plastic responses after spinal cord injury, *Neuron* 38, 201-211.
154. Cafferty, W. B., and Strittmatter, S. M. (2006) The Nogo-Nogo receptor pathway limits a spectrum of adult CNS axonal growth, *The Journal of neuroscience : the official journal of the Society for Neuroscience* 26, 12242-12250.

155. Zheng, B., Ho, C., Li, S., Keirstead, H., Steward, O., and Tessier-Lavigne, M. (2003) Lack of enhanced spinal regeneration in Nogo-deficient mice, *Neuron* 38, 213-224.
156. Dimou, L., Schnell, L., Montani, L., Duncan, C., Simonen, M., Schneider, R., Liebscher, T., Gullo, M., and Schwab, M. E. (2006) Nogo-A-deficient mice reveal strain-dependent differences in axonal regeneration, *The Journal of neuroscience : the official journal of the Society for Neuroscience* 26, 5591-5603.
157. Ahmed, Z., Mazibrada, G., Seabright, R. J., Dent, R. G., Berry, M., and Logan, A. (2006) TACE-induced cleavage of NgR and p75NTR in dorsal root ganglion cultures disinhibits outgrowth and promotes branching of neurites in the presence of inhibitory CNS myelin, *Faseb J* 20, 1939-1941.
158. He, Z., and Koprivica, V. (2004) The Nogo signaling pathway for regeneration block, *Annu Rev Neurosci* 27, 341-368.
159. Li, W., Walus, L., Rabacchi, S. A., Jirik, A., Chang, E., Schauer, J., Zheng, B. H., Benedetti, N. J., Liu, B. P., Choi, E., Worley, D., Silvian, L., Mo, W., Mullen, C., Yang, W., Strittmatter, S. M., Sah, D. W., Pepinsky, B., and Lee, D. H. (2004) A neutralizing anti-Nogo66 receptor monoclonal antibody reverses inhibition of neurite outgrowth by central nervous system myelin, *J Biol Chem* 279, 43780-43788.
160. Li, S., Liu, B. P., Budel, S., Li, M., Ji, B., Walus, L., Li, W., Jirik, A., Rabacchi, S., Choi, E., Worley, D., Sah, D. W., Pepinsky, B., Lee, D., Relton, J., and Strittmatter, S. M. (2004) Blockade of Nogo-66, myelin-associated glycoprotein, and oligodendrocyte myelin glycoprotein by soluble Nogo-66 receptor promotes axonal sprouting and recovery after spinal injury, *The Journal of neuroscience : the official journal of the Society for Neuroscience* 24, 10511-10520.
161. Cao, Y., Shumsky, J. S., Sabol, M. A., Kushner, R. A., Strittmatter, S., Hamers, F. P., Lee, D. H., Rabacchi, S. A., and Murray, M. (2008) Nogo-66 receptor antagonist peptide (NEP1-40) administration promotes functional recovery and axonal growth after lateral funiculus injury in the adult rat, *Neurorehabil Neural Repair* 22, 262-278.
162. Li, S., and Strittmatter, S. M. (2003) Delayed systemic Nogo-66 receptor antagonist promotes recovery from spinal cord injury, *The Journal of neuroscience : the official journal of the Society for Neuroscience* 23, 4219-4227.
163. Wang, X., Baughman, K. W., Basso, D. M., and Strittmatter, S. M. (2006) Delayed Nogo receptor therapy improves recovery from spinal cord contusion, *Annals of neurology* 60, 540-549.
164. Ji, B., Li, M., Wu, W. T., Yick, L. W., Lee, X., Shao, Z., Wang, J., So, K. F., McCoy, J. M., Pepinsky, R. B., Mi, S., and Relton, J. K. (2006) LINGO-1 antagonist promotes functional recovery and axonal sprouting after spinal cord injury, *Molecular and cellular neurosciences* 33, 311-320.
165. Fu, Q. L., Hu, B., Wu, W., Pepinsky, R. B., Mi, S., and So, K. F. (2008) Blocking LINGO-1 function promotes retinal ganglion cell survival following ocular

- hypertension and optic nerve transection, *Investigative ophthalmology & visual science* 49, 975-985.
166. Mi, S., Hu, B., Hahm, K., Luo, Y., Kam Hui, E. S., Yuan, Q., Wong, W. M., Wang, L., Su, H., Chu, T. H., Guo, J., Zhang, W., So, K. F., Pepinsky, B., Shao, Z., Graff, C., Garber, E., Jung, V., Wu, E. X., and Wu, W. (2007) LINGO-1 antagonist promotes spinal cord remyelination and axonal integrity in MOG-induced experimental autoimmune encephalomyelitis, *Nature medicine* 13, 1228-1233.
 167. Lv, J., Xu, R. X., Jiang, X. D., Lu, X., Ke, Y. Q., Cai, Y. Q., Du, M. X., Hu, C., Zou, Y. X., Qin, L. S., and Zeng, Y. J. (2010) Passive immunization with LINGO-1 polyclonal antiserum afforded neuroprotection and promoted functional recovery in a rat model of spinal cord injury, *Neuroimmunomodulation* 17, 270-278.
 168. Antoine-Bertrand, J., Villemure, J. F., and Lamarche-Vane, N. (2011) Implication of rho GTPases in neurodegenerative diseases, *Current drug targets* 12, 1202-1215.
 169. Guilluy, C., Garcia-Mata, R., and Burridge, K. (2011) Rho protein crosstalk: another social network?, *Trends Cell Biol* 21, 718-726.
 170. Govek, E. E., Newey, S. E., and Van Aelst, L. (2005) The role of the Rho GTPases in neuronal development, *Genes Dev* 19, 1-49.
 171. Spiering, D., and Hodgson, L. (2011) Dynamics of the Rho-family small GTPases in actin regulation and motility, *Cell adhesion & migration* 5, 170-180.
 172. Hall, A. (1998) Rho GTPases and the actin cytoskeleton, *Science* 279, 509-514.
 173. Mimura, F., Yamagishi, S., Arimura, N., Fujitani, M., Kubo, T., Kaibuchi, K., and Yamashita, T. (2006) Myelin-associated glycoprotein inhibits microtubule assembly by a Rho-kinase-dependent mechanism, *J Biol Chem* 281, 15970-15979.
 174. Dickson, B. J. (2001) Rho GTPases in growth cone guidance, *Curr Opin Neurobiol* 11, 103-110.
 175. Luo, L. (2002) Actin cytoskeleton regulation in neuronal morphogenesis and structural plasticity, *Annu Rev Cell Dev Biol* 18, 601-635.
 176. Luo, L. (2000) Rho GTPases in neuronal morphogenesis, *Nat Rev Neurosci* 1, 173-180.
 177. Arimura, N., Menager, C., Fukata, Y., and Kaibuchi, K. (2004) Role of CRMP-2 in neuronal polarity, *J Neurobiol* 58, 34-47.
 178. Hall, A., and Lalli, G. (2010) Rho and Ras GTPases in axon growth, guidance, and branching, *Cold Spring Harbor perspectives in biology* 2, a001818.
 179. Baas, P. W., and Luo, L. (2001) Signaling at the growth cone: the scientific progeny of Cajal meet in Madrid, *Neuron* 32, 981-984.
 180. Dickson, B. J. (2002) Molecular mechanisms of axon guidance, *Science* 298, 1959-1964.

181. Sabry, J., O'Connor, T. P., and Kirschner, M. W. (1995) Axonal transport of tubulin in Ti1 pioneer neurons in situ, *Neuron* 14, 1247-1256.
182. O'Connor, T. P., Duerr, J. S., and Bentley, D. (1990) Pioneer growth cone steering decisions mediated by single filopodial contacts in situ, *J Neurosci* 10, 3935-3946.
183. Myers, P. Z., and Bastiani, M. J. (1993) Growth cone dynamics during the migration of an identified commissural growth cone, *J Neurosci* 13, 127-143.
184. Tcherkezian, J., and Lamarche-Vane, N. (2007) Current knowledge of the large RhoGAP family of proteins, *Biology of the cell / under the auspices of the European Cell Biology Organization* 99, 67-86.
185. Jaffe, A. B., and Hall, A. (2005) Rho GTPases: biochemistry and biology, *Annu Rev Cell Dev Biol* 21, 247-269.
186. Erschbamer, M. K., Hofstetter, C. P., and Olson, L. (2005) RhoA, RhoB, RhoC, Rac1, Cdc42, and Tc10 mRNA levels in spinal cord, sensory ganglia, and corticospinal tract neurons and long-lasting specific changes following spinal cord injury, *J Comp Neurol* 484, 224-233.
187. Dubreuil, C. I., Winton, M. J., and McKerracher, L. (2003) Rho activation patterns after spinal cord injury and the role of activated Rho in apoptosis in the central nervous system, *J Cell Biol* 162, 233-243.
188. Del Pozo, M. A., Kiosses, W. B., Alderson, N. B., Meller, N., Hahn, K. M., and Schwartz, M. A. (2002) Integrins regulate GTP-Rac localized effector interactions through dissociation of Rho-GDI, *Nat Cell Biol* 4, 232-239.
189. Ahmed, Z., Suggate, E. L., Brown, E. R., Dent, R. G., Armstrong, S. J., Barrett, L. B., Berry, M., and Logan, A. (2006) Schwann cell-derived factor-induced modulation of the NgR/p75NTR/EGFR axis disinhibits axon growth through CNS myelin in vivo and in vitro, *Brain* 129, 1517-1533.
190. Lehmann, M., Fournier, A., Selles-Navarro, I., Dergham, P., Sebok, A., Leclerc, N., Tigyi, G., and McKerracher, L. (1999) Inactivation of Rho signaling pathway promotes CNS axon regeneration, *J Neurosci* 19, 7537-7547.
191. Dergham, P., Ellezam, B., Essagian, C., Avedissian, H., Lubell, W. D., and McKerracher, L. (2002) Rho signaling pathway targeted to promote spinal cord repair, *J Neurosci* 22, 6570-6577.
192. Lord-Fontaine, S., Yang, F., Diep, Q., Dergham, P., Munzer, S., Tremblay, P., and McKerracher, L. (2008) Local inhibition of Rho signaling by cell-permeable recombinant protein BA-210 prevents secondary damage and promotes functional recovery following acute spinal cord injury, *J Neurotrauma* 25, 1309-1322.
193. Fehlings, M. G., Theodore, N., Harrop, J., Maurais, G., Kuntz, C., Shaffrey, C. I., Kwon, B. K., Chapman, J., Yee, A., Tighe, A., and McKerracher, L. (2011) A phase I/IIa clinical trial of a recombinant Rho protein antagonist in acute spinal cord injury, *J Neurotrauma* 28, 787-796.
194. Matsui, T., Amano, M., Yamamoto, T., Chihara, K., Nakafuku, M., Ito, M., Nakano, T., Okawa, K., Iwamatsu, A., and Kaibuchi, K. (1996) Rho-associated

- kinase, a novel serine/threonine kinase, as a putative target for small GTP binding protein Rho, *Embo J* 15, 2208-2216.
195. Ishizaki, T., Maekawa, M., Fujisawa, K., Okawa, K., Iwamatsu, A., Fujita, A., Watanabe, N., Saito, Y., Kakizuka, A., Morii, N., and Narumiya, S. (1996) The small GTP-binding protein Rho binds to and activates a 160 kDa Ser/Thr protein kinase homologous to myotonic dystrophy kinase, *Embo J* 15, 1885-1893.
 196. Kwon, B. K., Borisoff, J. F., and Tetzlaff, W. (2002) Molecular targets for therapeutic intervention after spinal cord injury, *Mol Interv* 2, 244-258.
 197. Zhang, Z., Ottens, A. K., Lerner, S. F., Kobeissy, F. H., Williams, M. L., Hayes, R. L., and Wang, K. K. (2006) Direct Rho-associated kinase inhibition induces cofilin dephosphorylation and neurite outgrowth in PC-12 cells, *Cell Mol Biol Lett* 11, 12-29.
 198. Amano, M., Chihara, K., Nakamura, N., Kaneko, T., Matsuura, Y., and Kaibuchi, K. (1999) The COOH terminus of Rho-kinase negatively regulates rho-kinase activity, *J Biol Chem* 274, 32418-32424.
 199. Hashimoto, R., Nakamura, Y., Kosako, H., Amano, M., Kaibuchi, K., Inagaki, M., and Takeda, M. (1999) Distribution of Rho-kinase in the bovine brain, *Biochem Biophys Res Commun* 263, 575-579.
 200. Mueller, B. K., Mack, H., and Teusch, N. (2005) Rho kinase, a promising drug target for neurological disorders, *Nat Rev Drug Discov* 4, 387-398.
 201. Kimura, K., Ito, M., Amano, M., Chihara, K., Fukata, Y., Nakafuku, M., Yamamori, B., Feng, J., Nakano, T., Okawa, K., Iwamatsu, A., and Kaibuchi, K. (1996) Regulation of myosin phosphatase by Rho and Rho-associated kinase (Rho-kinase), *Science* 273, 245-248.
 202. Riento, K., and Ridley, A. J. (2003) Rocks: multifunctional kinases in cell behaviour, *Nat Rev Mol Cell Biol* 4, 446-456.
 203. Sanders, L. C., Matsumura, F., Bokoch, G. M., and de Lanerolle, P. (1999) Inhibition of myosin light chain kinase by p21-activated kinase, *Science* 283, 2083-2085.
 204. Hashimoto, R., Nakamura, Y., Goto, H., Wada, Y., Sakoda, S., Kaibuchi, K., Inagaki, M., and Takeda, M. (1998) Domain- and site-specific phosphorylation of bovine NF-L by Rho-associated kinase, *Biochem Biophys Res Commun* 245, 407-411.
 205. Greene, L. A., and Tischler, A. S. (1976) Establishment of a noradrenergic clonal line of rat adrenal pheochromocytoma cells which respond to nerve growth factor, *Proc Natl Acad Sci U S A* 73, 2424-2428.
 206. Sebok, A., Nusser, N., Debreceni, B., Guo, Z., Santos, M. F., Szeberenyi, J., and Tigyi, G. (1999) Different roles for RhoA during neurite initiation, elongation, and regeneration in PC12 cells, *J Neurochem* 73, 949-960.
 207. Yang, P., Wen, H. Z., and Zhang, J. H. (2010) Expression of a dominant-negative Rho-kinase promotes neurite outgrowth in a microenvironment mimicking injured central nervous system, *Acta Pharmacol Sin* 31, 531-539.

208. Wu, D., Yang, P., Zhang, X., Luo, J., Haque, M. E., Yeh, J., Richardson, P. M., Zhang, Y., and Bo, X. (2009) Targeting a dominant negative rho kinase to neurons promotes axonal outgrowth and partial functional recovery after rat rubrospinal tract lesion, *Molecular therapy : the journal of the American Society of Gene Therapy* 17, 2020-2030.
209. Duffy, P., Schmandke, A., Sigworth, J., Narumiya, S., Cafferty, W. B., and Strittmatter, S. M. (2009) Rho-associated kinase II (ROCKII) limits axonal growth after trauma within the adult mouse spinal cord, *The Journal of neuroscience : the official journal of the Society for Neuroscience* 29, 15266-15276.
210. Fournier, A. E., Takizawa, B. T., and Strittmatter, S. M. (2003) Rho kinase inhibition enhances axonal regeneration in the injured CNS, *J Neurosci* 23, 1416-1423.
211. Li, M., Huang, Y., Ma, A. A., Lin, E., and Diamond, M. I. (2009) Y-27632 improves rotarod performance and reduces huntingtin levels in R6/2 mice, *Neurobiol Dis* 36, 413-420.
212. Bowerman, M., Beauvais, A., Anderson, C. L., and Kothary, R. (2010) Rho-kinase inactivation prolongs survival of an intermediate SMA mouse model, *Hum Mol Genet* 19, 1468-1478.
213. Boyce-Rustay, J. M., Simler, G. H., McGaraughty, S., Chu, K. L., Wensink, E. J., Vasudevan, A., and Honore, P. (2010) Characterization of Fasudil in preclinical models of pain, *J Pain* 11, 941-949.
214. Furuya, T., Hashimoto, M., Koda, M., Okawa, A., Murata, A., Takahashi, K., Yamashita, T., and Yamazaki, M. (2009) Treatment of rat spinal cord injury with a Rho-kinase inhibitor and bone marrow stromal cell transplantation, *Brain Res* 1295, 192-202.
215. Nishio, Y., Koda, M., Kitajo, K., Seto, M., Hata, K., Taniguchi, J., Moriya, H., Fujitani, M., Kubo, T., and Yamashita, T. (2006) Delayed treatment with Rho-kinase inhibitor does not enhance axonal regeneration or functional recovery after spinal cord injury in rats, *Exp Neurol* 200, 392-397.
216. Sun, X., Minohara, M., Kikuchi, H., Ishizu, T., Tanaka, M., Piao, H., Osoegawa, M., Ohyagi, Y., Shimokawa, H., and Kira, J. (2006) The selective Rho-kinase inhibitor Fasudil is protective and therapeutic in experimental autoimmune encephalomyelitis, *Journal of neuroimmunology* 180, 126-134.
217. Huang, X. N., Fu, J., and Wang, W. Z. (2011) The effects of fasudil on the permeability of the rat blood-brain barrier and blood-spinal cord barrier following experimental autoimmune encephalomyelitis, *Journal of neuroimmunology* 239, 61-67.
218. Yu, J. Z., Ding, J., Ma, C. G., Sun, C. H., Sun, Y. F., Lu, C. Z., and Xiao, B. G. (2010) Therapeutic potential of experimental autoimmune encephalomyelitis by Fasudil, a Rho kinase inhibitor, *Journal of neuroscience research* 88, 1664-1672.

219. Masumoto, A., Mohri, M., Shimokawa, H., Urakami, L., Usui, M., and Takeshita, A. (2002) Suppression of coronary artery spasm by the Rho-kinase inhibitor fasudil in patients with vasospastic angina, *Circulation* 105, 1545-1547.
220. Zhao, J., Zhou, D., Guo, J., Ren, Z., Zhou, L., Wang, S., Xu, B., and Wang, R. (2006) Effect of fasudil hydrochloride, a protein kinase inhibitor, on cerebral vasospasm and delayed cerebral ischemic symptoms after aneurysmal subarachnoid hemorrhage, *Neurol Med Chir (Tokyo)* 46, 421-428.
221. Shibuya, M., Hirai, S., Seto, M., Satoh, S., and Ohtomo, E. (2005) Effects of fasudil in acute ischemic stroke: results of a prospective placebo-controlled double-blind trial, *Journal of the neurological sciences* 238, 31-39.
222. Fukata, Y., Itoh, T. J., Kimura, T., Menager, C., Nishimura, T., Shiromizu, T., Watanabe, H., Inagaki, N., Iwamatsu, A., Hotani, H., and Kaibuchi, K. (2002) CRMP-2 binds to tubulin heterodimers to promote microtubule assembly, *Nat Cell Biol* 4, 583-591.
223. Yoshimura, T., Kawano, Y., Arimura, N., Kawabata, S., Kikuchi, A., and Kaibuchi, K. (2005) GSK-3beta regulates phosphorylation of CRMP-2 and neuronal polarity, *Cell* 120, 137-149.
224. Higurashi, M., Iketani, M., Takei, K., Yamashita, N., Aoki, R., Kawahara, N., and Goshima, Y. (2012) Localized role of CRMP1 and CRMP2 in neurite outgrowth and growth cone steering, *Developmental neurobiology* 72, 1528-1540.
225. Minturn, J. E., Fryer, H. J., Geschwind, D. H., and Hockfield, S. (1995) TOAD-64, a gene expressed early in neuronal differentiation in the rat, is related to unc-33, a *C. elegans* gene involved in axon outgrowth, *The Journal of neuroscience : the official journal of the Society for Neuroscience* 15, 6757-6766.
226. Hamajima, N., Matsuda, K., Sakata, S., Tamaki, N., Sasaki, M., and Nonaka, M. (1996) A novel gene family defined by human dihydropyrimidinase and three related proteins with differential tissue distribution, *Gene* 180, 157-163.
227. Wang, L. H., and Strittmatter, S. M. (1996) A family of rat CRMP genes is differentially expressed in the nervous system, *The Journal of neuroscience : the official journal of the Society for Neuroscience* 16, 6197-6207.
228. Ponnusamy, R., and Lohkamp, B. (2013) Insights into the oligomerization of CRMPs: Crystal structure of human collapsin response mediator protein 5, *J Neurochem*.
229. Charrier, E., Reibel, S., Rogemond, V., Aguera, M., Thomasset, N., and Honnorat, J. (2003) Collapsin response mediator proteins (CRMPs): involvement in nervous system development and adult neurodegenerative disorders, *Molecular neurobiology* 28, 51-64.
230. Goshima, Y., Nakamura, F., Strittmatter, P., and Strittmatter, S. M. (1995) Collapsin-induced growth cone collapse mediated by an intracellular protein related to UNC-33, *Nature* 376, 509-514.
231. Hedgecock, E. M., Culotti, J. G., Thomson, J. N., and Perkins, L. A. (1985) Axonal guidance mutants of *Caenorhabditis elegans* identified by filling sensory neurons with fluorescein dyes, *Dev Biol* 111, 158-170.

232. Byk, T., Ozon, S., and Sobel, A. (1998) The Ulip family phosphoproteins--common and specific properties, *Eur J Biochem* 254, 14-24.
233. Ricard, D., Rogemond, V., Charrier, E., Aguera, M., Bagnard, D., Belin, M. F., Thomasset, N., and Honnorat, J. (2001) Isolation and expression pattern of human Unc-33-like phosphoprotein 6/collapsin response mediator protein 5 (Ulip6/CRMP5): coexistence with Ulip2/CRMP2 in Sema3a- sensitive oligodendrocytes, *The Journal of neuroscience : the official journal of the Society for Neuroscience* 21, 7203-7214.
234. Kamata, T., Subleski, M., Hara, Y., Yuhki, N., Kung, H., Copeland, N. G., Jenkins, N. A., Yoshimura, T., Modi, W., and Copeland, T. D. (1998) Isolation and characterization of a bovine neural specific protein (CRMP-2) cDNA homologous to unc-33, a *C. elegans* gene implicated in axonal outgrowth and guidance, *Brain Res Mol Brain Res* 54, 219-236.
235. Nishimura, T., Fukata, Y., Kato, K., Yamaguchi, T., Matsuura, Y., Kamiguchi, H., and Kaibuchi, K. (2003) CRMP-2 regulates polarized Numb-mediated endocytosis for axon growth, *Nat Cell Biol* 5, 819-826.
236. Arimura, N., Hattori, A., Kimura, T., Nakamuta, S., Funahashi, Y., Hirotsune, S., Furuta, K., Urano, T., Toyoshima, Y. Y., and Kaibuchi, K. (2009) CRMP-2 directly binds to cytoplasmic dynein and interferes with its activity, *J Neurochem* 111, 380-390.
237. Quinn, C. C., Chen, E., Kinjo, T. G., Kelly, G., Bell, A. W., Elliott, R. C., McPherson, P. S., and Hockfield, S. (2003) TUC-4b, a novel TUC family variant, regulates neurite outgrowth and associates with vesicles in the growth cone, *The Journal of neuroscience : the official journal of the Society for Neuroscience* 23, 2815-2823.
238. Kimura, T., Watanabe, H., Iwamatsu, A., and Kaibuchi, K. (2005) Tubulin and CRMP-2 complex is transported via Kinesin-1, *J Neurochem* 93, 1371-1382.
239. Kawano, Y., Yoshimura, T., Tsuboi, D., Kawabata, S., Kaneko-Kawano, T., Shirataki, H., Takenawa, T., and Kaibuchi, K. (2005) CRMP-2 is involved in kinesin-1-dependent transport of the Sra-1/WAVE1 complex and axon formation, *Molecular and cellular biology* 25, 9920-9935.
240. Arimura, N., Inagaki, N., Chihara, K., Menager, C., Nakamura, N., Amano, M., Iwamatsu, A., Goshima, Y., and Kaibuchi, K. (2000) Phosphorylation of collapsin response mediator protein-2 by Rho-kinase. Evidence for two separate signaling pathways for growth cone collapse, *J Biol Chem* 275, 23973-23980.
241. Inagaki, N., Chihara, K., Arimura, N., Menager, C., Kawano, Y., Matsuo, N., Nishimura, T., Amano, M., and Kaibuchi, K. (2001) CRMP-2 induces axons in cultured hippocampal neurons, *Nat Neurosci* 4, 781-782.
242. Cole, A. R., Causeret, F., Yadirgi, G., Hastie, C. J., McLauchlan, H., McManus, E. J., Hernandez, F., Eickholt, B. J., Nikolic, M., and Sutherland, C. (2006) Distinct priming kinases contribute to differential regulation of collapsin response mediator proteins by glycogen synthase kinase-3 in vivo, *J Biol Chem* 281, 16591-16598.

243. Brown, M., Jacobs, T., Eickholt, B., Ferrari, G., Teo, M., Monfries, C., Qi, R. Z., Leung, T., Lim, L., and Hall, C. (2004) Alpha2-chimaerin, cyclin-dependent Kinase 5/p35, and its target collapsin response mediator protein-2 are essential components in semaphorin 3A-induced growth-cone collapse, *The Journal of neuroscience : the official journal of the Society for Neuroscience* 24, 8994-9004.
244. Uchida, Y., Ohshima, T., Sasaki, Y., Suzuki, H., Yanai, S., Yamashita, N., Nakamura, F., Takei, K., Ihara, Y., Mikoshiba, K., Kolattukudy, P., Honnorat, J., and Goshima, Y. (2005) Semaphorin3A signalling is mediated via sequential Cdk5 and GSK3beta phosphorylation of CRMP2: implication of common phosphorylating mechanism underlying axon guidance and Alzheimer's disease, *Genes Cells* 10, 165-179.
245. Hou, S. T., Jiang, S. X., Aylsworth, A., Ferguson, G., Slinn, J., Hu, H., Leung, T., Kappler, J., and Kaibuchi, K. (2009) CaMKII phosphorylates collapsin response mediator protein 2 and modulates axonal damage during glutamate excitotoxicity, *J Neurochem* 111, 870-881.
246. Arimura, N., Menager, C., Kawano, Y., Yoshimura, T., Kawabata, S., Hattori, A., Fukata, Y., Amano, M., Goshima, Y., Inagaki, M., Morone, N., Usukura, J., and Kaibuchi, K. (2005) Phosphorylation by Rho kinase regulates CRMP-2 activity in growth cones, *Mol Cell Biol* 25, 9973-9984.
247. Jiang, S. X., Kappler, J., Zurakowski, B., Desbois, A., Aylsworth, A., and Hou, S. T. (2007) Calpain cleavage of collapsin response mediator proteins in ischemic mouse brain, *The European journal of neuroscience* 26, 801-809.
248. Touma, E., Kato, S., Fukui, K., and Koike, T. (2007) Calpain-mediated cleavage of collapsin response mediator protein(CRMP)-2 during neurite degeneration in mice, *The European journal of neuroscience* 26, 3368-3381.
249. Zhang, Z., Ottens, A. K., Sadasivan, S., Kobeissy, F. H., Fang, T., Hayes, R. L., and Wang, K. K. (2007) Calpain-mediated collapsin response mediator protein-1, -2, and -4 proteolysis after neurotoxic and traumatic brain injury, *J Neurotrauma* 24, 460-472.
250. Zhang, Z., Majava, V., Greffier, A., Hayes, R. L., Kursula, P., and Wang, K. K. (2009) Collapsin response mediator protein-2 is a calmodulin-binding protein, *Cellular and molecular life sciences : CMLS* 66, 526-536.
251. Yuasa-Kawada, J., Suzuki, R., Kano, F., Ohkawara, T., Murata, M., and Noda, M. (2003) Axonal morphogenesis controlled by antagonistic roles of two CRMP subtypes in microtubule organization, *The European journal of neuroscience* 17, 2329-2343.
252. Gu, Y., and Ihara, Y. (2000) Evidence that collapsin response mediator protein-2 is involved in the dynamics of microtubules, *J Biol Chem* 275, 17917-17920.
253. Chae, Y. C., Lee, S., Heo, K., Ha, S. H., Jung, Y., Kim, J. H., Ihara, Y., Suh, P. G., and Ryu, S. H. (2009) Collapsin response mediator protein-2 regulates neurite formation by modulating tubulin GTPase activity, *Cellular signalling* 21, 1818-1826.

254. Desai, A., and Mitchison, T. J. (1997) Microtubule polymerization dynamics, *Annu Rev Cell Dev Biol* 13, 83-117.
255. Cole, A. R., Noble, W., van Aalten, L., Plattner, F., Meimaridou, R., Hogan, D., Taylor, M., LaFrancois, J., Gunn-Moore, F., Verkhratsky, A., Oddo, S., LaFerla, F., Giese, K. P., Dineley, K. T., Duff, K., Richardson, J. C., Yan, S. D., Hanger, D. P., Allan, S. M., and Sutherland, C. (2007) Collapsin response mediator protein-2 hyperphosphorylation is an early event in Alzheimer's disease progression, *J Neurochem* 103, 1132-1144.
256. Yoshida, H., Watanabe, A., and Ihara, Y. (1998) Collapsin response mediator protein-2 is associated with neurofibrillary tangles in Alzheimer's disease, *J Biol Chem* 273, 9761-9768.
257. Hara, M., Takayasu, M., Watanabe, K., Noda, A., Takagi, T., Suzuki, Y., and Yoshida, J. (2000) Protein kinase inhibition by fasudil hydrochloride promotes neurological recovery after spinal cord injury in rats, *J Neurosurg* 93, 94-101.
258. Petratos, S., Li, Q. X., George, A. J., Hou, X., Kerr, M. L., Unabia, S. E., Hatzinisiriou, I., Maksel, D., Aguilar, M. I., and Small, D. H. (2008) The beta-amyloid protein of Alzheimer's disease increases neuronal CRMP-2 phosphorylation by a Rho-GTP mechanism, *Brain : a journal of neurology* 131, 90-108.
259. Kim, J. E., Liu, B. P., Park, J. H., and Strittmatter, S. M. (2004) Nogo-66 receptor prevents raphespinal and rubrospinal axon regeneration and limits functional recovery from spinal cord injury, *Neuron* 44, 439-451.
260. Azari, M. F., Profyris, C., Karnezis, T., Bernard, C. C., Small, D. H., Cheema, S. S., Ozturk, E., Hatzinisiriou, I., and Petratos, S. (2006) Leukemia inhibitory factor arrests oligodendrocyte death and demyelination in spinal cord injury, *Journal of neuropathology and experimental neurology* 65, 914-929.
261. Zang, D. W., and Cheema, S. S. (2003) Leukemia inhibitory factor promotes recovery of locomotor function following spinal cord injury in the mouse, *J Neurotrauma* 20, 1215-1222.
262. Azari, M. F., Galle, A., Lopes, E. C., Kurek, J., and Cheema, S. S. (2001) Leukemia inhibitory factor by systemic administration rescues spinal motor neurons in the SOD1 G93A murine model of familial amyotrophic lateral sclerosis, *Brain Res* 922, 144-147.
263. Basso, D. M., Fisher, L. C., Anderson, A. J., Jakeman, L. B., McTigue, D. M., and Popovich, P. G. (2006) Basso Mouse Scale for locomotion detects differences in recovery after spinal cord injury in five common mouse strains, *J Neurotrauma* 23, 635-659.
264. Barnard, A. L., Chidgey, A. P., Bernard, C. C., and Boyd, R. L. (2009) Androgen depletion increases the efficacy of bone marrow transplantation in ameliorating experimental autoimmune encephalomyelitis, *Blood* 113, 204-213.
265. Short, M. A., Campanale, N., Litwak, S., and Bernard, C. C. (2011) Quantitative and phenotypic analysis of bone marrow-derived cells in the intact and inflamed central nervous system, *Cell adhesion & migration* 5, 373-381.

266. Anderson, J. M., Hampton, D. W., Patani, R., Pryce, G., Crowther, R. A., Reynolds, R., Franklin, R. J., Giovannoni, G., Compston, D. A., Baker, D., Spillantini, M. G., and Chandran, S. (2008) Abnormally phosphorylated tau is associated with neuronal and axonal loss in experimental autoimmune encephalomyelitis and multiple sclerosis, *Brain : a journal of neurology* 131, 1736-1748.
267. Goedert, M., Spillantini, M. G., Cairns, N. J., and Crowther, R. A. (1992) Tau proteins of Alzheimer paired helical filaments: abnormal phosphorylation of all six brain isoforms, *Neuron* 8, 159-168.
268. Ng, W. P., Cartel, N., Roder, J., Roach, A., and Lozano, A. (1996) Human central nervous system myelin inhibits neurite outgrowth, *Brain Res* 720, 17-24.
269. Buffo, A., Zagrebelsky, M., Huber, A. B., Skerra, A., Schwab, M. E., Strata, P., and Rossi, F. (2000) Application of neutralizing antibodies against NI-35/250 myelin-associated neurite growth inhibitory proteins to the adult rat cerebellum induces sprouting of uninjured purkinje cell axons, *The Journal of neuroscience : the official journal of the Society for Neuroscience* 20, 2275-2286.
270. Arber, S., Barbayannis, F. A., Hanser, H., Schneider, C., Stanyon, C. A., Bernard, O., and Caroni, P. (1998) Regulation of actin dynamics through phosphorylation of cofilin by LIM-kinase, *Nature* 393, 805-809.
271. Amano, M., Ito, M., Kimura, K., Fukata, Y., Chihara, K., Nakano, T., Matsuura, Y., and Kaibuchi, K. (1996) Phosphorylation and activation of myosin by Rho-associated kinase (Rho-kinase), *J Biol Chem* 271, 20246-20249.
272. Daniels, R. H., Hall, P. S., and Bokoch, G. M. (1998) Membrane targeting of p21-activated kinase 1 (PAK1) induces neurite outgrowth from PC12 cells, *EMBO J* 17, 754-764.
273. Kozma, R., Sarner, S., Ahmed, S., and Lim, L. (1997) Rho family GTPases and neuronal growth cone remodelling: relationship between increased complexity induced by Cdc42Hs, Rac1, and acetylcholine and collapse induced by RhoA and lysophosphatidic acid, *Molecular and cellular biology* 17, 1201-1211.
274. Beattie, M. S., Hermann, G. E., Rogers, R. C., and Bresnahan, J. C. (2002) Cell death in models of spinal cord injury, *Prog Brain Res* 137, 37-47.
275. Warden, P., Bamber, N. I., Li, H., Esposito, A., Ahmad, K. A., Hsu, C. Y., and Xu, X. M. (2001) Delayed glial cell death following wallerian degeneration in white matter tracts after spinal cord dorsal column cordotomy in adult rats, *Exp Neurol* 168, 213-224.
276. Turnley, A. M., and Bartlett, P. F. (2000) Cytokines that signal through the leukemia inhibitory factor receptor-beta complex in the nervous system, *J Neurochem* 74, 889-899.
277. Stahl, N., Boulton, T. G., Farruggella, T., Ip, N. Y., Davis, S., Witthuhn, B. A., Quelle, F. W., Silvennoinen, O., Barbieri, G., Pellegrini, S., and et al. (1994) Association and activation of Jak-Tyk kinases by CNTF-LIF-OSM-IL-6 beta receptor components, *Science* 263, 92-95.
278. Horvai, A. E., Xu, L., Korzus, E., Brard, G., Kalafus, D., Mullen, T. M., Rose, D. W., Rosenfeld, M. G., and Glass, C. K. (1997) Nuclear integration of JAK/STAT

- and Ras/AP-1 signaling by CBP and p300, *Proceedings of the National Academy of Sciences of the United States of America* 94, 1074-1079.
279. Hendriks, J. J., Slaets, H., Carmans, S., de Vries, H. E., Dijkstra, C. D., Stinissen, P., and Hellings, N. (2008) Leukemia inhibitory factor modulates production of inflammatory mediators and myelin phagocytosis by macrophages, *Journal of neuroimmunology* 204, 52-57.
280. Kerr, B. J., and Patterson, P. H. (2005) Leukemia inhibitory factor promotes oligodendrocyte survival after spinal cord injury, *Glia* 51, 73-79.
281. Curtis, R., Green, D., Lindsay, R. M., and Wilkin, G. P. (1993) Up-regulation of GAP-43 and growth of axons in rat spinal cord after compression injury, *J Neurocytol* 22, 51-64.
282. Butzkueven, H., Emery, B., Cipriani, T., Marriott, M. P., and Kilpatrick, T. J. (2006) Endogenous leukemia inhibitory factor production limits autoimmune demyelination and oligodendrocyte loss, *Glia* 53, 696-703.
283. Mayer, M., Bhakoo, K., and Noble, M. (1994) Ciliary neurotrophic factor and leukemia inhibitory factor promote the generation, maturation and survival of oligodendrocytes in vitro, *Development* 120, 143-153.
284. Martinou, J. C., Martinou, I., and Kato, A. C. (1992) Cholinergic differentiation factor (CDF/LIF) promotes survival of isolated rat embryonic motoneurons in vitro, *Neuron* 8, 737-744.
285. Sendtner, M., Gotz, R., Holtmann, B., Escary, J. L., Masu, Y., Carroll, P., Wolf, E., Brem, G., Brulet, P., and Thoenen, H. (1996) Cryptic physiological trophic support of motoneurons by LIF revealed by double gene targeting of CNTF and LIF, *Curr Biol* 6, 686-694.
286. Cheema, S. S., Richards, L. J., Murphy, M., and Bartlett, P. F. (1994) Leukaemia inhibitory factor rescues motoneurons from axotomy-induced cell death, *Neuroreport* 5, 989-992.
287. Cheema, S. S., Richards, L., Murphy, M., and Bartlett, P. F. (1994) Leukemia inhibitory factor prevents the death of axotomised sensory neurons in the dorsal root ganglia of the neonatal rat, *Journal of neuroscience research* 37, 213-218.
288. Gresle, M. M., Alexandrou, E., Wu, Q., Egan, G., Jokubaitis, V., Ayers, M., Jonas, A., Doherty, W., Friedhuber, A., Shaw, G., Sendtner, M., Emery, B., Kilpatrick, T., and Butzkueven, H. (2012) Leukemia inhibitory factor protects axons in experimental autoimmune encephalomyelitis via an oligodendrocyte-independent mechanism, *PLoS one* 7, e47379.
289. Gresle, M. M., Shaw, G., Jarrott, B., Alexandrou, E. N., Friedhuber, A., Kilpatrick, T. J., and Butzkueven, H. (2008) Validation of a novel biomarker for acute axonal injury in experimental autoimmune encephalomyelitis, *Journal of neuroscience research* 86, 3548-3555.
290. Novotna, I., Slovinska, L., Vanicky, I., Cizek, M., Radonak, J., and Cizkova, D. (2011) IT delivery of ChABC modulates NG2 and promotes GAP-43 axonal regrowth after spinal cord injury, *Cellular and molecular neurobiology* 31, 1129-1139.

291. Wang, D., Ayers, M. M., Catmull, D. V., Hazelwood, L. J., Bernard, C. C., and Orian, J. M. (2005) Astrocyte-associated axonal damage in pre-onset stages of experimental autoimmune encephalomyelitis, *Glia* 51, 235-240.
292. Arimura, N., and Kaibuchi, K. (2005) Key regulators in neuronal polarity, *Neuron* 48, 881-884.
293. Schmidt, H., and Rathjen, F. G. (2010) Signalling mechanisms regulating axonal branching in vivo, *Bioessays* 32, 977-985.
294. Bretin, S., Reibel, S., Charrier, E., Maus-Moatti, M., Auvergnon, N., Thevenoux, A., Glowinski, J., Rogemond, V., Premont, J., Honnorat, J., and Gauchy, C. (2005) Differential expression of CRMP1, CRMP2A, CRMP2B, and CRMP5 in axons or dendrites of distinct neurons in the mouse brain, *J Comp Neurol* 486, 1-17.
295. Taghian, K., Lee, J. Y., and Petratos, S. (2012) Phosphorylation and Cleavage of the Family of Collapsin Response Mediator Proteins May Play a Central Role in Neurodegeneration after CNS Trauma, *J Neurotrauma*.
296. Kwon, B. K., Sekhon, L. H., and Fehlings, M. G. (2010) Emerging repair, regeneration, and translational research advances for spinal cord injury, *Spine (Phila Pa 1976)* 35, S263-270.
297. Jurewicz, A., Matysiak, M., Raine, C. S., and Selmaj, K. (2007) Soluble Nogo-A, an inhibitor of axonal regeneration, as a biomarker for multiple sclerosis, *Neurology* 68, 283-287.
298. French-Constant, C., Colognato, H., and Franklin, R. J. (2004) Neuroscience. The mysteries of myelin unwrapped, *Science* 304, 688-689.
299. Fry, E. J., Ho, C., and David, S. (2007) A role for Nogo receptor in macrophage clearance from injured peripheral nerve, *Neuron* 53, 649-662.
300. Pool, M., Niino, M., Rambaldi, I., Robson, K., Bar-Or, A., and Fournier, A. E. (2009) Myelin regulates immune cell adhesion and motility, *Exp Neurol* 217, 371-377.
301. David, S., Fry, E. J., and Lopez-Vales, R. (2008) Novel roles for Nogo receptor in inflammation and disease, *Trends in neurosciences* 31, 221-226.
302. Lucchinetti, C., Bruck, W., Parisi, J., Scheithauer, B., Rodriguez, M., and Lassmann, H. (2000) Heterogeneity of multiple sclerosis lesions: implications for the pathogenesis of demyelination, *Annals of neurology* 47, 707-717.
303. Petratos, S., Azari, M. F., Ozturk, E., Papadopoulos, R., and Bernard, C. C. (2010) Novel therapeutic targets for axonal degeneration in multiple sclerosis, *Journal of neuropathology and experimental neurology* 69, 323-334.
304. Harrington, E. P., Zhao, C., Fancy, S. P., Kaing, S., Franklin, R. J., and Rowitch, D. H. (2010) Oligodendrocyte PTEN is required for myelin and axonal integrity, not remyelination, *Annals of neurology* 68, 703-716.
305. Lee, B. B., Cripps, R. A., Fitzharris, M., and Wing, P. C. (2013) The global map for traumatic spinal cord injury epidemiology: update 2011, global incidence rate, *Spinal Cord*.

306. Stahel, P. F., VanderHeiden, T., and Finn, M. A. (2012) Management strategies for acute spinal cord injury: current options and future perspectives, *Current opinion in critical care* 18, 651-660.
307. Cole, A. R., Knebel, A., Morrice, N. A., Robertson, L. A., Irving, A. J., Connolly, C. N., and Sutherland, C. (2004) GSK-3 phosphorylation of the Alzheimer epitope within collapsin response mediator proteins regulates axon elongation in primary neurons, *J Biol Chem* 279, 50176-50180.
308. Fouad, K., Dietz, V., and Schwab, M. E. (2001) Improving axonal growth and functional recovery after experimental spinal cord injury by neutralizing myelin associated inhibitors, *Brain Res Brain Res Rev* 36, 204-212.
309. Freund, P., Schmidlin, E., Wannier, T., Bloch, J., Mir, A., Schwab, M. E., and Rouiller, E. M. (2009) Anti-Nogo-A antibody treatment promotes recovery of manual dexterity after unilateral cervical lesion in adult primates--re-examination and extension of behavioral data, *The European journal of neuroscience* 29, 983-996.
310. Freund, P., Wannier, T., Schmidlin, E., Bloch, J., Mir, A., Schwab, M. E., and Rouiller, E. M. (2007) Anti-Nogo-A antibody treatment enhances sprouting of corticospinal axons rostral to a unilateral cervical spinal cord lesion in adult macaque monkey, *J Comp Neurol* 502, 644-659.
311. Weinmann, O., Schnell, L., Ghosh, A., Montani, L., Wiessner, C., Wannier, T., Rouiller, E., Mir, A., and Schwab, M. E. (2006) Intrathecally infused antibodies against Nogo-A penetrate the CNS and downregulate the endogenous neurite growth inhibitor Nogo-A, *Molecular and cellular neurosciences* 32, 161-173.
312. Liebscher, T., Schnell, L., Schnell, D., Scholl, J., Schneider, R., Gullo, M., Fouad, K., Mir, A., Rausch, M., Kindler, D., Hamers, F. P., and Schwab, M. E. (2005) Nogo-A antibody improves regeneration and locomotion of spinal cord-injured rats, *Annals of neurology* 58, 706-719.
313. Zhao, R. R., Andrews, M. R., Wang, D., Warren, P., Gullo, M., Schnell, L., Schwab, M. E., and Fawcett, J. W. (2013) Combination treatment with anti-Nogo-A and chondroitinase ABC is more effective than single treatments at enhancing functional recovery after spinal cord injury, *The European journal of neuroscience*.
314. Hug, A., and Weidner, N. (2012) From bench to bedside to cure spinal cord injury: lost in translation?, *International review of neurobiology* 106, 173-196.
315. Maier, I. C., Ichiyama, R. M., Courtine, G., Schnell, L., Lavrov, I., Edgerton, V. R., and Schwab, M. E. (2009) Differential effects of anti-Nogo-A antibody treatment and treadmill training in rats with incomplete spinal cord injury, *Brain : a journal of neurology* 132, 1426-1440.
316. Rowland, J. W., Hawryluk, G. W., Kwon, B., and Fehlings, M. G. (2008) Current status of acute spinal cord injury pathophysiology and emerging therapies: promise on the horizon, *Neurosurgical focus* 25, E2.
317. Bourquin, C., van der Haar, M. E., Anz, D., Sandholzer, N., Neumaier, I., Endres, S., Skerra, A., Schwab, M. E., and Linington, C. (2008) DNA vaccination efficiently induces antibodies to Nogo-A and does not exacerbate

- experimental autoimmune encephalomyelitis, *European journal of pharmacology* 588, 99-105.
318. Teng, F. Y., and Tang, B. L. (2005) Nogo signaling and non-physical injury-induced nervous system pathology, *Journal of neuroscience research* 79, 273-278.
319. Fontoura, P., Ho, P. P., DeVoss, J., Zheng, B., Lee, B. J., Kidd, B. A., Garren, H., Sobel, R. A., Robinson, W. H., Tessier-Lavigne, M., and Steinman, L. (2004) Immunity to the extracellular domain of Nogo-A modulates experimental autoimmune encephalomyelitis, *J Immunol* 173, 6981-6992.
320. Sicotte, M., Tsatas, O., Jeong, S. Y., Cai, C. Q., He, Z., and David, S. (2003) Immunization with myelin or recombinant Nogo-66/MAG in alum promotes axon regeneration and sprouting after corticospinal tract lesions in the spinal cord, *Molecular and cellular neurosciences* 23, 251-263.
321. Reindl, M., Khantane, S., Ehling, R., Schanda, K., Lutterotti, A., Brinkhoff, C., Oertle, T., Schwab, M. E., Deisenhammer, F., Berger, T., and Bandtlow, C. E. (2003) Serum and cerebrospinal fluid antibodies to Nogo-A in patients with multiple sclerosis and acute neurological disorders, *Journal of neuroimmunology* 145, 139-147.
322. Merkler, D., Oertle, T., Buss, A., Pinschewer, D. D., Schnell, L., Bareyre, F. M., Kerschensteiner, M., Buddeberg, B. S., and Schwab, M. E. (2003) Rapid induction of autoantibodies against Nogo-A and MOG in the absence of an encephalitogenic T cell response: implication for immunotherapeutic approaches in neurological diseases, *FASEB journal : official publication of the Federation of American Societies for Experimental Biology* 17, 2275-2277.
323. Corboy, J. R., Goodin, D. S., and Frohman, E. M. (2003) Disease-modifying Therapies for Multiple Sclerosis, *Curr Treat Options Neurol* 5, 35-54.
324. Frohman, E. M., Racke, M. K., and Raine, C. S. (2006) Multiple sclerosis--the plaque and its pathogenesis, *N Engl J Med* 354, 942-955.
325. Trapp, B. D., Ransohoff, R., and Rudick, R. (1999) Axonal pathology in multiple sclerosis: relationship to neurologic disability, *Current opinion in neurology* 12, 295-302.
326. De Stefano, N., Narayanan, S., Francis, G. S., Arnaoutelis, R., Tartaglia, M. C., Antel, J. P., Matthews, P. M., and Arnold, D. L. (2001) Evidence of axonal damage in the early stages of multiple sclerosis and its relevance to disability, *Archives of neurology* 58, 65-70.
327. Bjartmar, C., Kinkel, R. P., Kidd, G., Rudick, R. A., and Trapp, B. D. (2001) Axonal loss in normal-appearing white matter in a patient with acute MS, *Neurology* 57, 1248-1252.
328. Bjartmar, C., and Trapp, B. D. (2003) Axonal degeneration and progressive neurologic disability in multiple sclerosis, *Neurotox Res* 5, 157-164.
329. Bjartmar, C., Wujek, J. R., and Trapp, B. D. (2003) Axonal loss in the pathology of MS: consequences for understanding the progressive phase of the disease, *Journal of the neurological sciences* 206, 165-171.

330. O'Donnell, M., R. K. Chance, et al. (2009). "Axon growth and guidance: receptor regulation and signal transduction." Annu Rev Neurosci **32**: 383-412.

APPENDICES

APPENDIX I

APPENDIX II

APPENDIX III

APPENDIX IV

APPENDIX VI

ADDENDUM

